2022

Investigating the antibacterial activity of novel metal complexes against antimicrobial resistant pathogens

Megan O'Shaughnessy
Technological University Dublin, megan.oshaughnessy@tudublin.ie

Funder: The Fiosraigh Dean of Graduate Students Scholarship

Investigating the antibacterial activity of novel metal complexes against antimicrobial resistant pathogens

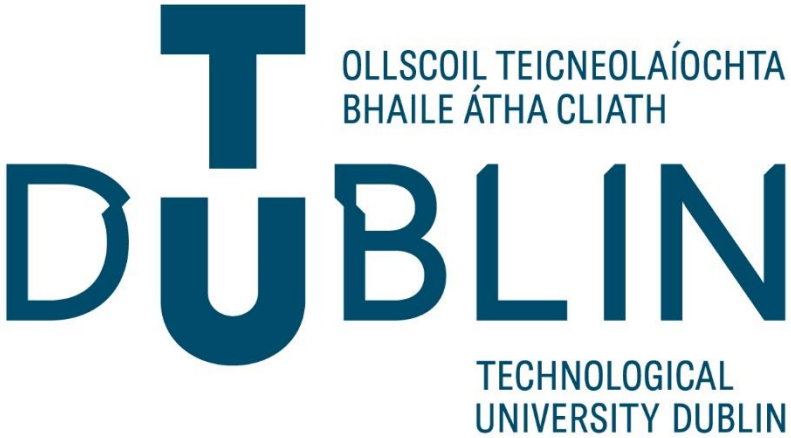

A thesis submitted to Technological University Dublin – City Campus for the degree of

Doctor of Philosophy

Submitted by:

Megan O'Shaughnessy, B.Sc. (Hons.)

School of Biological and Health Science

Technological University Dublin

Grangegorman

Dublin 7

Supervisors:

Professor Orla Howe

Professor Michael Devereux

Abstract

Antimicrobial resistance (AMR) is one of the serious global health challenges of our time. There is an urgent need to develop novel therapeutic agents to overcome AMR, preferably through alternative mechanistic pathways from conventional treatments. Interdisciplinary research in inorganic medicinal chemistry with biology is advancing the knowledge and implementation of transition metal complexes for therapy and is offering a realistic alternative to traditional antibiotics. Metal complexes with 1,10-phenanthroline (phen) ligands have demonstrated promising therapeutic capabilities with diverse biological activity. Consequently, there has been a resurgence in research of these complexes as possible alternatives or adjuvants to established antimicrobial clinical therapeutics. The antibacterial activity of novel metal complexes (metal = Cu(II), Mn(II), and Ag(I)) incorporating phen and various dicarboxylate ligands was the focus of this research.

The first objective of this study was to screen all metal complexes and their phen derivatives against common Gram-positive and Gram-negative resistant clinical isolates. Overall, superior toxicity was evident in complexes that incorporate the phen ligand compared to the activities of their simple salt and dicarboxylate precursors. The chelates incorporating 3,6,9-trioxaundecanedioate (tdda) were the most effective, and the varied toxicity depended on the metal centre. Whole-genome sequencing was carried out on reference Gram-positive and Gram-negative strains, *Staphylococcus aureus* (ATCC 29213), and *Pseudomonas aeruginosa* (PAO1). The strains were exposed to sub-lethal doses of lead metal-tdda-phen complexes to form mutants with induced resistance properties. Various mutations were detected in the mutant *P. aeruginosa* genome, causing amino acid changes to proteins involved in cellular respiration, the polyamine biosynthetic pathway, and virulence mechanisms.

To further investigate the anti-pseudomonal potential of the novel metal complexes, clinical *P. aeruginosa* isolates from cystic fibrosis (CF) lungs of Irish patients were obtained since inherited CF is prevalent in Ireland. The bacteria's capacity to form a biofilm in its pathogenesis is highly virulent and leads to decreased susceptibility to most antibiotic treatments.

The second objective was to investigate the activity profiles of the Cu(II), Mn(II), and Ag(I) complexes $\{[Cu(3,6,9\text{-tdda})(phen)_2].3H_2O.EtOH\}_n$ (**Cu-tdda-phen**), $\{[Mn(3,6,9\text{-tdda})(phen)_2].3H_2O.EtOH\}_n$ (**Mn-tdda-phen**) and $[Ag_2(3,6,9\text{-tdda})(phen)_4].EtOH$ (**Ag-tdda-phen**) towards clinical isolates of *P. aeruginosa* derived from Irish CF patients compared to two reference laboratory strains (ATCC 27853 and PAO1). The effects of the metal-tdda-phen complexes and established antibiotic gentamicin on planktonic growth, biofilm formation (pre-treatment), and mature biofilm (post-treatment) alone and in combination with gentamicin were investigated. The effects of the metal-tdda-phen complexes on the individual biofilm components; exopolysaccharide, extracellular DNA (eDNA), pyocyanin, and pyoverdine are also presented. All three metal-tdda-phen complexes showed comparable and often superior activity to gentamicin in the CF strains compared to their activities in the laboratory strains concerning biofilm formation and established biofilms. Combination studies presented synergistic activity between all three complexes and gentamicin, particularly for the post-treatment of established mature biofilms, and were supported by the reduction of the individual biofilm components examined.

The ability of metal-tdda-phen complexes to act on *P. aeruginosa* clinical isolates synergistically with gentamicin prompted *in vivo* studies. Therefore, the final objective was to assess the efficacy of individual treatments of Cu-tdda-phen, Mn-tdda-phen, and Ag-tdda-phen and in combination with gentamicin in larvae of *Galleria mellonella* infected with clinical isolates and laboratory strains of *P. aeruginosa*. All test complexes were tolerated by *G. mellonella* in concentrations up to 10 µg/larva and affected the host's immune response by

stimulating immune cells (hemocytes) and enhancing the expression of genes that encode for immune-related peptides, specifically *transferrin* and *inducible metalloproteinase inhibitor* (IMPI). Combining the metal-tdda-phen complexes with gentamicin further intensified this response at lower concentrations, clearing a *P. aeruginosa* infection previously resistant to gentamicin alone. Therefore, this work highlights the anti-pseudomonal capabilities of metal-tdda-phen complexes alone and combined with gentamicin in a valuable pre-clinical *in vivo* model.

In summary, this research demonstrates the potential of novel metal complexes incorporating dicarboxylate and 1,10-phenanthroline ligands with low toxicity and high efficacy that could become part of the therapeutic arsenal in the battle against multidrug-resistant bacteria, particularly for strong biofilm formers such as *P. aeruginosa*.

Declaration

I certify that this thesis which I now submit for examination for the award of PhD, is entirely my own work and has not been taken from the work of others, save and to the extent that such work has been cited and acknowledged within the text of my work.

This thesis was prepared according to the regulations for postgraduate study by research of the Technological University Dublin and has not been submitted in whole or in part for another award in any other third level institution.

The work reported on in this thesis conforms to the principles and requirements of the TU Dublin's guidelines for ethics in research.

TU Dublin has permission to keep, lend or copy this thesis in whole or in part, on condition that any such use of the material of the thesis be duly acknowledged.

Signature: 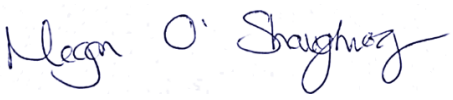

Date: 13/05/2022

Acknowledgements

This has been the most challenging but rewarding experience of my life, and you do not make it this far without standing on the shoulders of a mountain of people. First and foremost, I would like to thank my supervisors. Prof Orla Howe has been a mentor to me for most of my academic journey, a constant source of guidance and support. Thank you for talking me off many a ledge, always making me see the bigger picture, never letting me coast, and introducing me to your innovative way of using the BSC. Prof Michael Devereux, thank you for your patience in bringing out the chemist in me. It was no easy task, especially with 8 am meetings. I also thank Dr Livia Viganor; although our time working together was short, I appreciate the kindness you showed me as I found my PhD feet. The Fiosraigh Dean of Graduate Students Scholarship from TU Dublin is gratefully acknowledged.

Many fantastic researchers helped and guided me along the way, and I would not have made it this far without them. Thank you to Dr Celine Herra, Dr Gordon Chambers, and Mr Mitchel Moody in TU – Dublin for providing the clinical isolates and being so gracious with your time. A massive thank you to Prof Kevin Kavanagh, Ms Magdalena Piatek, and all in the Medical Mycology Lab Maynooth; your knowledge and patience are unparalleled. Prof Malachy McCann, thank you for allowing me to continue researching your metal-phen complexes and Dr Pauraic McCarron, thank you for synthesising them for me. To Dr Garret Rochford and Dr Aisling Crowley, thank you for always having the time to answer my questions and providing immense moral support. To the OGs of Lab 233, Tadhg, Alex, Conor, Shaui, Jamie, TJ, and Brian, and the ESHI newbies, Rory, Aaron, and Kate. There is no getting rid of you, is there? Thank you for the laughter, the discussions, the problem solving, the friendships, and the many, many pints. I would not have made it through this without you, although I might have done it

in half the time. To all the fantastic people of Focas Research Institute I m*et al*ong the way, you are all such amazing people and possibly insane.

There are too many family and friends to mention here but thank you all for your unfailing love and support over the years. As the first in my family afforded the opportunity to finish secondary school, never mind progress to third-level education, I have never taken that for granted. I cannot thank my parents enough for their sacrifices and continuous encouragement. I hope I have made you proud! Lastly, I would like to dedicate this thesis to my dad. Although he would not have a clue what a PhD was, I know he would have been my biggest cheerleader, along with Jack. I miss you both every day, but I carry you with me always!

Glossary of terms

6-APA	6-aminopenicillianic acid
ABC	ATP-binding cassette superfamily
Ag	Silver
$AgNO_3$	Silver nitrate
AgNPs	Silver nanoparticles
AIDS	Acquired immunodeficiency syndrome
AME	Aminoglycosides modifying enzyme
AMR	Antimicrobial resistance
ANOVA	One-way analysis variance
ASL	Airway surface liquid
ATCC	American Type Culture Collection
ATP	Adenosine triphosphate
Au	Gold
$BdaH_2$	Butanedioic acid
BEAS-2B	Normal bronchial epithelium cells
Bpy	2,2'-bipyridine
BSA	Bovine serum albumin
BSI	Bloodstream infection
c-di-GMP	bis-(3′,5′)-cyclic dimeric guanosine monophosphate
Ca	Calcium
CAMHB	Cation-adjusted Mueller-Hinton broth
CAT	Chloramphenicol acetyltransferases
CDC	The Centers for Disease Control and Prevention
CF	Cystic fibrosis
CFBE41o-	Cystic Fibrosis Bronchial Epithelial Cells
CFTR	Cystic fibrosis transmembrane conductance regulator
CFU	Colony-forming unit
Co	Cobalt

CO-ADD	The Community for Open Antimicrobial Drug Discovery
COPD	Chronic obstructive pulmonary disease
COVID-19	Coronavirus Disease 2019
CRE	Carbapenem-resistant *Enterobacterales*
CPA	*N*-carbamoylputrescine amidase
CPE	Carbapenem-producing *Enterobacterales*
CTAB	Cetyltrimethylammonium bromide
Cu	Copper
$CuCl_2$	Copper chloride
DMSO	Dimethyl sulfoxide
DSB	Double-stranded break
D-Ala-D-Ala	D-Alanine-D-Alanine
D-Ala-D-Lac	D-Alanine-D-lactate
D-Ala-D-Ser	D-Alanine-D-serine
eDNA	Extracellular DNA
ECDC	The European Centre for Disease Prevention and Control
ECM	Extracellular matrix
EDTA	Ethylenediaminetetraacetic acid
EPS	Extracellular polymeric substances
ESBL	Extended spectrum β-lactamase
EU	European Union
EUCAST	European Committee on Antimicrobial Susceptibility Testing
FBS	Foetal bovine serum
FDA	The US Food and Drug Administration
Fe	Iron
Fe-S	Iron-sulphur
FIC	Fractional inhibitory concentration
FIC_I	FIC index
Ga	Gallium
GLASS	Global Antimicrobial Resistance Surveillance System
H_2O_2	Hydrogen peroxide

HCAI	Healthcare-associated infection
HGT	Horizontal gene transfer
HIV	Human immunodeficiency virus
$HpdaH_2$	Heptanedioic acid
HPSC	Health Protection Surveillance Centre
$HxdaH_2$	Hexanedioic acid
IC_{50}	Half-maximal inhibitory concentration
IDSA	Infectious Diseases Society of America
IF	Initiation factors
KPC	*Klebsiella pneumoniae* carbapenemase-producer
LPS	Lipopolysaccharides
MATE	Multidrug and toxic compound extrusion family
MBC	Minimum bactericidal concentration
MBEC	Minimum biofilm eradication concentration
MBIC	Minimum biofilm inhibitory concentration
MBL	Metallo-β-lactamase-producer
MCR	Mobile colistin resistance
MDR	Multidrug-resistance
MEM	Minimum essential medium
MeOH	Methanol
MFS	Major facilitator superfamily
Mg	Magnesium
MHA	Mueller-Hinton agar
MHB	Mueller-Hinton broth
MIC	Minimum inhibitory concentration
Mn	Manganese
$MnCl_2$	Manganese chloride
MRSA	Methicillin-resistant *Staphylococcus aureus*
MTT	Methylthiazolyldiphenyl-tetrazolium bromide
NaCl	Saline
Ni	Nickel

mRNA	Messenger RNA
NAG	*N*-acetylglucosamine
NAM	*N*-acetylmuramic acid
OECD	Organisation for Economic Co-operation and Development
$OdaH_2$	Octanedioic acid
PABA	Para-aminobenzoic acid
PBP	Penicillin-binding proteins
PBP2a	Penicillin-binding protein 2a
PCR	Polymerase chain reaction
$PdaH_2$	Pentanedioic acid
Phen	1,10-phenanthroline
phH_2	Phthalic acid
Pd	Palladium
PDR	Pan-drug resistance
PDT	Photodynamic therapy
PG	Phosphatidylglycerol
PMQR	Plasmid-mediated quinolone resistance
Pt	Platinum
QRDR	Quinolone-resistance determining region
qRT-PCR	quantitative real-time PCR
QS	Quorum sensing
RND	Resistance-nodulation-division family
ROS	Reactive oxygen species
rRNA	Ribosomal RNA
Ru	Ruthenium
SARS-CoV-2	Severe acute respiratory syndrome coronavirus 2
SCC	Staphylococcal chromosomal cassette
SMR	Small multidrug-resistance family
SNP	Single nucleotide polymorphisms
SOD	Superoxide dismutase
T2SS	Type II secretion system

TB	Tuberculosis
$TddaH_2$	3,6,9-trioxaundecanedioate
TI	Therapeutic index
tRNA	Transfer RNA
TSA	Tryptic soy agar
TSB	Tryptic soy broth
UN	United Nations
VRE	Vancomycin-resistant *Enterococci*
VRSA	Vancomycin-resistant *Staphylococcus aureus*
XDR	Extensive drug resistance
WGS	Whole-genome sequencing
WHO	World Health Organization
Zn	Zinc

Table of Contents

List of Tables

List of Figures

Publications

- **O'Shaughnessy M**, Hurley J, Dillon SC, Herra C, McCarron P, McCann M, Devereux M, Howe O. Antibacterial activity of metal-phenanthroline complexes against multidrug-resistant Irish clinical isolates: A whole genome sequencing approach. **Accepted to the Journal of Biological Inorganic Chemistry, 2022**
- **O'Shaughnessy M**, McCarron P, Viganor L, McCann M, Devereux M, Howe O. The antibacterial and anti-biofilm activity of metal complexes incorporating 3,6,9-trioxaundecanedioate and 1,10-phenanthroline ligands in clinical isolates of *Pseudomonas aeruginosa* from Irish Cystic Fibrosis patients. **Antibiotics. 2020; 9(10):674.**
- **O'Shaughnessy M**, Piatek M, McCarron P, McCann M, Devereux M, Kavanagh K, Howe O. In vivo activity of metal complexes containing 1,10-phenanthroline and 3,6,9-trioxaundecanedioate ligands against *Pseudomonas aeruginosa* infection in *Galleria mellonella* larvae. **Biomedicines. 2022; 10(2):222.**

Additional relevant publications

- Howe O, **O'Shaughnessy M**, O'Shea D, Pereira M, Rochford G, Kavanagh K, McCann M, Devereux M. Novel water-soluble and photo-stable cytotoxic silver(I) complexes containing dicarboxylate and 1,10-phenanthroline ligands: induction of *in vivo* antioxidant, inflammatory and innate immune responses in *Saccharomyces cerevisiae* and *Galleria mellonella* models. **In preparation, 2022.**
- O'Loughlin J, Napolitano S, Alkhathami F, O'Beirne C, Marhöfer D, **O'Shaughnessy M**, Howe O, Tacke M, Rubini M. The antibacterial drug candidate SBC3 is a potent inhibitor of bacterial thioredoxin reductase. **ChemBioChem. 2020; 22(6):3**

- Galdino A, Viganor L, de Castro A, da Cunha E, Mello T, Mattos L, Pereira M, Hunt M, **O'Shaughnessy M**, Howe O, Devereux M, McCann M, Ramalho TC, Branquinha M and Santos ALS. Disarming *Pseudomonas aeruginosa* virulence by the inhibitory action of 1,10-phenanthroline-5,6-dione-based compounds: Elastase B (LasB) as a chemotherapeutic target. **Frontiers in Microbiology. 2019; 10:1701**

Conference participation

National

- *In vivo activity of metal complexes containing 1,10-phenanthroline and 3,6,9-trioxaundecanedioate ligands against Pseudomonas aeruginosa infection in Galleria mellonella larvae.* **Poster presentation** at the Microbiology Society Annual Conference, Online, April 2021
- 4th Irish Biological Inorganic Chemistry Society (IBICS) symposium, Virtual, November 2020. **Awarded 'Highly Commended' Postgraduate Award**
- *The anti-biofilm activity of metal complexes with 1,10-phenanthroline against Pseudomonas aeruginosa isolated from Irish Cystic Fibrosis patients*. **Oral presentation** at 3rd Irish Biological Inorganic Chemistry Society (IBICS) symposium, Royal College of Surgeons Ireland, November 2019. **Awarded 'Best Oral Presentation'**.
- *The potential of metal complexes with 1,10-phenanthroline and dicarboxylate ligands as anti-biofilm agents against Pseudomonas aeruginosa*. **Oral presentation** at 2nd Irish Biological Inorganic Chemistry Society (IBICS) Symposium, National University of Ireland Galway, November 2018
- *The potential of metal complexes with 1,10-phenanthroline and dicarboxylate ligands as anti-biofilm agents against Pseudomonas aeruginosa isolated from Irish Cystic*

Fibrosis patients. **Oral presentation** at the 9th Annual Postgraduate Research Symposium, Dublin Institute of Technology, November 2018

- *The antibacterial activity of metal complexes incorporating 1,10-phenanthroline and dicarboxylate ligands: activity against WHO problematic pathogens*. **Poster presentation** at Focused meeting 2018 – Microbes and mucosal surfaces. Microbiology Society, University College Dublin, June 2018
- *A screen of metal-phenanthroline complexes against problematic human pathogens*. **Poster presentation** at the 1st Irish Biological Inorganic Chemistry Society Symposium, Maynooth University, November 2017
- *A proteomics approach to identify the mechanism of action of 1,10-phenanthroline-based drugs against resistant clinical isolates***. Poster presentation** at the 8th Annual Graduate Research Symposium, Dublin Institute of Technology, December 2017.
- *The anti-inflammatory and antimicrobial effects of novel metal-based complexes.* **Poster presentation** at the Irish Institute of Metal-Based Drugs (IIMBD) 7th meeting, Dublin Institute of Technology, Grangegorman, November 2016
- *The anti-inflammatory and antimicrobial effects of novel metal-based complexes.* **Poster presentation** at the 7th Annual Graduate Research Symposium, Dublin Institute of Technology, May 2016

International

- The Merck Proteomics Core Partnership Meeting held by Sigma-Aldrich, Malta, March 2019. **Won a travel grant from Merck Life Sciences to attend the meeting**
- *Antibacterial activity of metal complexes incorporating 1,10-phenanthroline and dicarboxylate ligands: activity against problematic resistant clinical isolates*. **Poster**

presentation at 14th European Biological Inorganic Chemistry Conference (EuroBIC), Birmingham, August 2018

- *A proteomics approach to identify the mechanism of action of 1,10-phenanthroline-based drugs against resistant clinical isolates*. **Oral presentation** at Sao Paulo School of Advanced Science on Mass Spectrometry-based Proteomics (SPSAS-MS), Brazil, September 2017. **Received a scholarship to attend the SPSAS-MS, funded by Sao Paulo Research Foundation [grant #2016/18802-4, FAPESP]**

TU Dublin Structured PhD Modules Completed

Discipline-specific

- Bacterial Interactions with host epithelial (ITT-ENEH1002) – 5 ECTS
- Introduction to Genomic Technologies (Coursera-John Hopkins University) – 4 ECTS
- Algorithms for DNA Sequencing (Coursera-John Hopkins University) – 4 ECTS
- Command Line Tools for Genomic Data Science (Coursera-John Hopkins University) – 4 ECTS
- Statistics for Genomic Data Science (Coursera-John Hopkins University) – 4 ECTS

Employability skills

- Research Methods (DIT-GRSO1001) – 5 ECTS
- Data mining for biomedical sciences (DIT-ENEH1004) – 5 ECTS
- Genomic Data Science with Galaxy (Coursera-John Hopkins University) – 4 ECTS
- Python for Genomic Data Science (Coursera-John Hopkins University) – 4 ECTS
- Bioconductor for Genomic Data Science (Coursera-John Hopkins University) – 4 ECTS

Chapter 1.

General Introduction

1.1. Antimicrobial resistance – A global crisis

Sir Alexander Fleming warned us of the rise of antimicrobial resistance in his Nobel Prize speech (11th December 1945) for discovering the world's first antibiotic, penicillin. In his remarks, he included a hypothetical situation of the negligent use of non-lethal doses, changing the nature of the microbe and conferring resistance to the drug (Fleming, 1945). Since then, the multidrug-resistance (MDR) of microorganisms to antibiotics as the now therapeutic mainstream medicines has become a global crisis. The consequences of antimicrobial resistance (AMR) are widespread. It threatens the effective prevention and treatment of an increasing range of infections caused by bacteria, parasites, fungi, and viruses that are no longer susceptible to the standard medicines used to treat them. AMR also contributes to different complications in vulnerable patients undergoing chemotherapy, organ transplantation, surgeries, dialysis, intensive care for a pre-term newborn, and many other activities (Nanayakkara *et al*., 2021; Turner, 2021). Furthermore, growing resistance will heavily affect people with chronic conditions like diabetes, asthma, and rheumatoid arthritis.

As seen with the global pandemic of the Coronavirus Disease 2019 (COVID-19) caused by severe acute respiratory syndrome coronavirus 2 (SARS-CoV-2), the global monitoring of infectious agents with the research and development of new therapeutics to deal with them is paramount. Moreover, this outbreak has exacerbated the existing AMR crisis due to the pre-emptive use of antimicrobials to incorrectly treat SARS-CoV-2-infected patients (Pelfrene *et al.*, 2021). The Achilles heel of antibacterial agents is the proficiency at which target pathogenic bacteria can develop resistance, and this has been rapidly accelerated due to increased use and misuse of antibiotics in human and veterinary medicine worldwide, along with other global issues including poor sanitation systems, overpopulation and high international migration (Chokshi *et al*., 2019; Hernando-Amado

et al., 2020). This is further perpetuated by evidence that research on novel antibiotics is slowing down, and there is an apparent lack of novel drug development by the pharmaceutical sector.

The problem of AMR is especially urgent due to antibiotic resistance in bacteria and has been a long-time concern for government and health agencies, including the United Nations (UN) and the World Health Organization (WHO). The European Centre for Disease Prevention and Control (ECDC) and Organisation for Economic Co-operation and Development (OECD) published a report on bacterial resistance in the European Union (EU). They stated that the health burden of infections due to bacteria with AMR in the EU/EEA population is comparable to that of influenza, tuberculosis, and HIV/AIDS combined (ECDC, 2019). Due to resistant bacteria, approximately 670,000 infections occur in the EU/EEA each year, with 33,000 directly attributable deaths and costing €1.1 billion in extra healthcare costs (ECDC, 2020). The Centers for Disease Control and Prevention (CDC) reported that more than 2.8 million antibiotic-resistant infections occur annually in the USA, resulting in 35,000 deaths (CDC, 2019). A recent systemic analysis estimates 4.95 million fatalities worldwide associated with bacterial AMR in 2019, including 1.27 million deaths directly attributable to bacterial resistance alone (Murray *et al*., 2022), which is expected to increase to 10 million by the year 2050 (Neill, 2014).

In addition to the ongoing struggle of rising AMR, it is well-documented that there is a limited pipeline of new antimicrobials under development to compete with this increasing resistance (Tacconelli *et al*., 2018; Theuretzbacher *et al*., 2019; Theuretzbacher, 2020; Butler *et al*., 2022). The WHO established the Global Antimicrobial Resistance Surveillance System (GLASS), an operational framework for resistance surveillance. They also published a list of antibiotic-resistant priority pathogens to promote and expand research on these highly resistant microorganisms and produce new technologies and

drugs (WHO, 2017). Infections caused by these microorganisms pose a severe worldwide hazard, and the 2020 WHO clinical antibacterial pipeline analysis report stated that the demand had not been met. In addition, the WHO highlighted that of the 12 antibiotics approved by the FDA and EMA since 2017, over 80% are derivatives of existing antibiotics where resistance mechanisms are well established, and rapid emergence of resistance is predicted (WHO, 2021). Therefore the report also included a comprehensive overview of non-traditional antibacterial medicines in the pipeline to encourage more research on novel medicinal approaches (WHO, 2021). It is recognised that there is a critical urgency to develop novel therapeutic agents to overcome antibiotic resistance for selected pathogenic organisms of concern preferably through novel classes, targets or modes of action and without known cross-resistance (Miethke *et al*., 2021).

1.2. Antibacterial agents

1.2.1 The history of antibacterial agents

It is commonly stated that antibiotics were not discovered until 1928 however, evidence of antibacterial use can be traced back for centuries. Many ancient cultures, for example, China, Egypt, Greece, and Serbia, used the crusts of mouldy bread and applied them to open wounds to prevent infection (Lemire *et al*., 2013). In the middle ages, the warriors would apply honey to arrow wounds for the same reason. Nonetheless, weapons against bacterial ailments were tenuous until the latter half of the 19th century, when the 'germ theory of disease' was proposed (Kong *et al*., 2010). Scientists such as Lister, Pasteur, and Koch suggested that microorganisms were responsible for various infections plaguing humanity, transforming the understanding and treatment of these diseases. By 1910, the first synthetic antimicrobial agent had been successfully established. It was a 3-ammino-4-hydroxyphenyl-As(III) chemical dye, as seen in **Figure 1.1**, called Arsphenamine and

later salvarsan, developed by Paul Ehrlich (Ehrlich 1912; Ehrlich & Bertheim 1912). Heralded as the father of chemotherapy, his principle was that a chemical agent should have a specific affinity for pathogens and directly affect its proliferation at a tolerable concentration by its host. He deemed this the 'magic bullet' that is now described as selective toxicity. To uncover a magic bullet, large-scale synthesis of organoarsenic derivatives and systemic screening was initiated with colleagues Bertheim and Hata (Ehrlich & Hata 1910). The 606th preparation of the arsenobenzene compound was tested in syphilis-infected rabbits and was highly effective at clearing the infection.

Following Erhlich's approach, Bayer laboratories in Germany discovered and developed sulfonamides. More specifically, the red dye known by its commercial name of Prontosil (as seen in **Figure 1.1**) was tested for its antimicrobial potential in a murine model of *Streptococcus pyogenes* systemic infection (Domagk, 1935). Further studies established that the sulfonamide was a prodrug and that the active component, sulfanilamide (**Figure 1.1**), was already utilized in the dye industry, and the patent had expired for many years. This, along with the cheap production cost, enabled many laboratories to synthesize and mass-produce derivatives of the drug within quick succession. Despite the many benefits of sulfonamides, there were also usage impediments due to the toxic products formed when it is metabolized. An additional legacy of sulfanilamide was a significant modification with diethylene glycol in 1937. The drug was released without any toxicology analysis and caused the death of 105 people in the United States, prompting the introduction of a legislative framework for drug release (Wax, 1995). This set of laws, the Federal Food, Drug, and Cosmetic Act of 1938, was the first of its kind. It is still the drug regulatory authority of America today, although now called the US Food and Drug Administration (FDA, 2018).

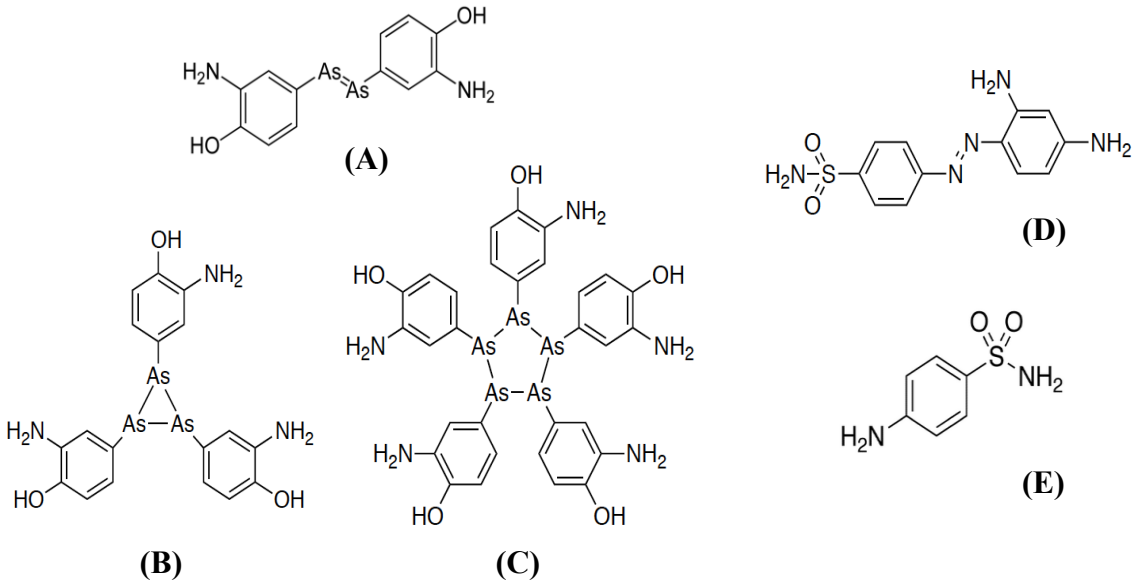

Figure 1.1 The chemical structure of Salvarsan (**A-C**) with the initially proposed structure (**A**), the known structure derived from a mixture of (**B**) and (**C**), and the prodrug Prontosil (**D**) that is metabolised into its active form sulphanilamide (**E**). Diagram adapted from (Li *et al*., 2015)

1.2.2 The golden age to the discovery void of antimicrobial agents

Fleming made his vital medical breakthrough in 1928 by serendipitously discovering penicillin in a *Staphylococcus aureus* plate contaminated by *Penicillium chrysogenums* that inhibited bacterial growth (Fleming, 1929). However, the toxic fungal metabolite application as a therapeutic agent was not brought into existence until the 1940s, when Florey and Chain overcame the problems of purifying the active ingredient in sufficient quantities for clinical trials (Chain *et al*., 1940). Later 6-aminopenicillianic acid (6-APA) was identified as the bioactive intermediate of penicillin, and this discovery revolutionized drug development by providing the starting material for semi-synthetic penicillin. This set up the paradigm for drug discovery for the subsequent three decades leading to the 'Golden Age' of antibiotic pioneering and deployment in the clinic, as presented in **Figure 1.2** below. The ensuing years saw a surge in antibacterial discovery

in which several new classes of antibiotics originated from soil bacteria and moulds (β-lactams, aminoglycosides, tetracycline, macrolides, and chloramphenicol) or were chemically synthesized (quinolones and sulfonamide) (Silver, 2011; Gould, 2016). As screening for natural bioactive products became less fruitful and repeat discoveries were more commonplace, the pharmaceutical companies backing the research of novel antibiotics withdrew support (Silver, 2011). From 1986 until the present day, only a handful of new antibiotics have been registered, and this period is referred to as the 'discovery void' within the scientific community. The escalating resistance difficulties during this period have forced researchers to modify the already existing arsenal to enhance activity, increasing sensitivity toward resistance while reducing toxicity (Chopra *et al*., 2002; Fair and Tor, 2014).

Nonetheless, this approach has not halted the evolution of bacterial resistance to antimicrobial agents (**Figure 1.2**). With the advent of bacterial genomics in the early 1990s came the potential for target-based antibacterial drug discovery and the pharmaceutical sector's renewed interest in developing novel antibiotics (Hutchings *et al*., 2019). Intense efforts to discover new antibacterial compounds were performed using high-throughput screens, and hundreds of novel bacterial targets were identified. However, no successful drug candidates emerged from these screens, and the larger pharmaceutical companies abandoned the mission to discover novel antibacterial compounds (Baker *et al*., 2018).

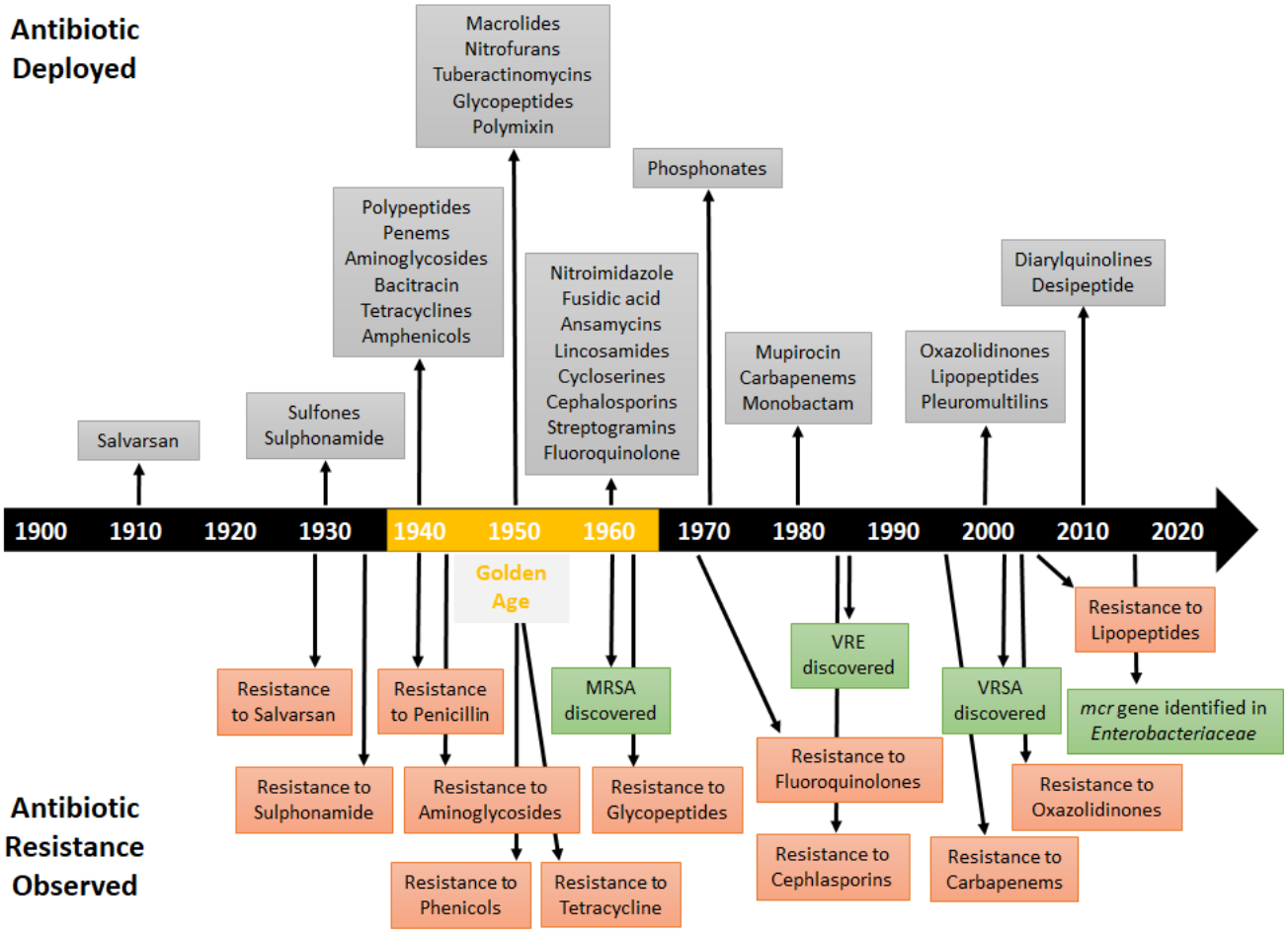

Figure 1.2 A timeline displaying antibiotic deployment into the clinic (on top) and the subsequent discovery of resistance (on the bottom). The first discovery of methicillin-resistant *Staphylococcus aureus* (MRSA), vancomycin-resistant *Enterococci* (VRE), vancomycin-resistant *Staphylococcus aureus* (VRSA), and the mobile colistin resistance (*mcr*) gene, enabling bacteria to be highly resistant to polymixins such as colistin, are also highlighted, adapted from (Hutchings, Truman and Wilkinson, 2019).

1.2.3 Classification of antibacterial agents

The central success of antibacterial agents is their selective nature for pathogens without adversely affecting the host. Such selective toxicity depends on identifying differences between the invading organism and the host that can be exploited. There are several ways that antibacterial drugs can be classified, including the following criteria; source, the spectrum of activity, effect on the target pathogen, chemical or molecular structure, and mechanism of action (Etebu and Arikekpar, 2016; Pancu *et al*., 2021). While the route at

which the drug is administered, such as injectable, oral, and topical treatment, represents an alternative classification.

Depending on the range of microorganisms susceptible to these drugs, antibacterial agents can be categorized as a broad- or narrow-spectrum (Acar, 1997; Najafpour, 2007). As the name suggests, broad-spectrum antibiotics exert their toxicity against various pathogens, including Gram-positive and Gram-negative bacteria. The narrow-spectrum antibacterial agents are considered effective against a specific pathogen, for instance, Gram-positive or Gram-negative bacteria. Narrow-spectrum antibiotics are generally preferred over broad-spectrum toxic drugs due to their specificity and reduced bacterial resistance (Ullah and Ali, 2017).

Due to the differences by which antibacterial agents eradicate the infection, they can also be classified as bactericidal or bacteriostatic. Bactericidal compounds trigger cell death via inhibiting cell wall synthesis, cell membrane function, or protein synthesis (Ullah and Ali, 2017), while bacteriostatic agents affect bacterial cellular activity and growth without triggering death. In clinical practice, however, these two categories are much more fluid. A bactericidal agent is unlikely to kill every bacterium within a host, and a bacteriostatic agent may destroy a high proportion but not all of the disease-causing bacteria within the host.

Antibacterial activity can also be classified into five different mechanisms, including; (i) interfering with bacterial cell wall synthesis, (ii) disruption of bacterial plasma membrane, (iii) inhibition of bacterial protein synthesis, (iv) inhibition of bacterial nucleic acid transcription and replication, and (iv) antimetabolite activity (Fair and Tor, 2014; Kapoor *et al*., 2017; Peterson and Kaur, 2018). These antibacterial mechanisms are demonstrated as cellular targets depicted in **Figure 1.3** below. Furthermore, the classes

of antibiotics according to their chemical structure, acting on these specific cellular targets, and elucidating their mechanism of action are presented in **Table 1.1**.

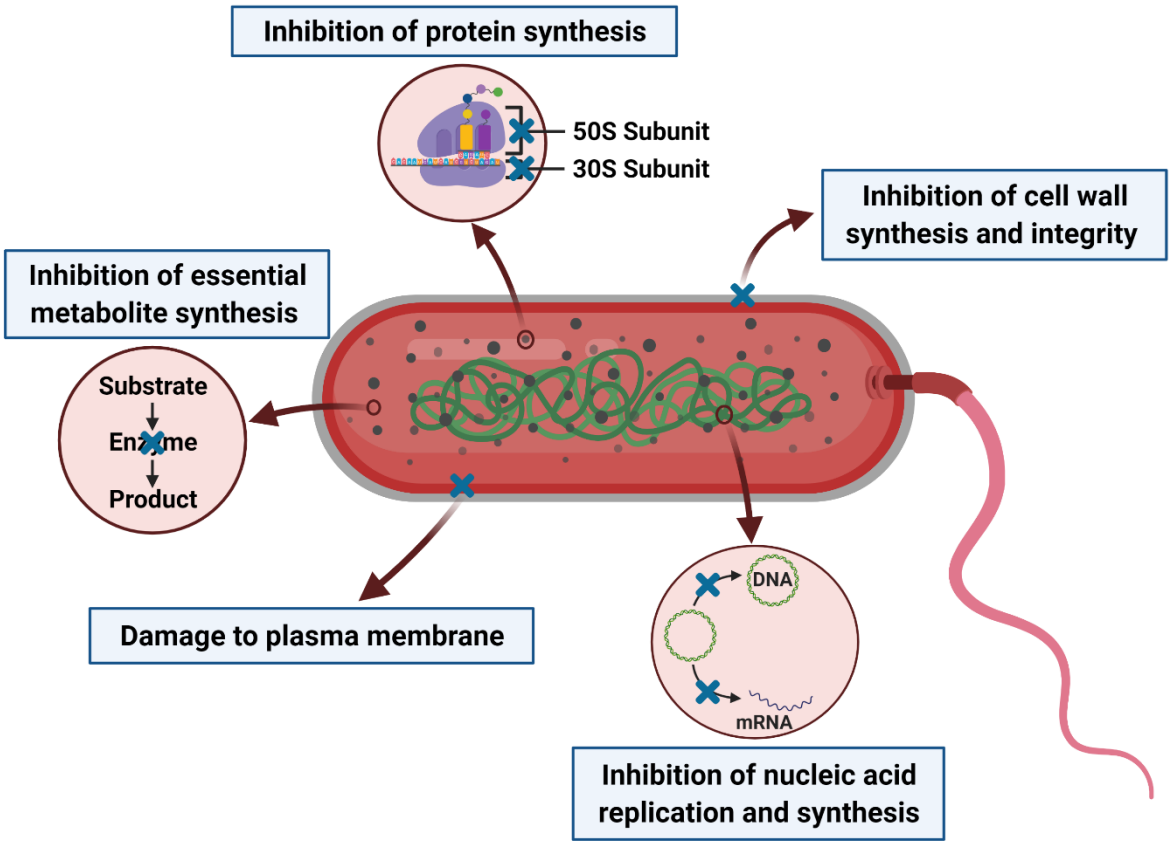

Figure 1.3 Cellular targets of established antibacterial agents; (**i**) Cell wall inhibitors – blocking synthesis and repair, (**ii**) Damage to plasma membrane – causing loss of selective permeability, (**iii**) Protein synthesis inhibitors acting on ribosomes – 30S subunit and 50S subunits, (**iv**) DNA/RNA inhibitors – inhibiting DNA gyrase and RNA polymerase, and (**v**) Block pathways and inhibit metabolism

Major target	Antibacterial class	Mechanism of action
Cell wall synthesis	β-lactam	Bind cell wall cross-linking enzyme (PBPs, transpeptidases)
	Glycopeptide	Block cell wall glycosyltransferases by binding D-Alanine-D-Alanine (D-Ala-D-Ala)
	Bacitracin	Blocks lipid carrier of cell wall precursors
Protein synthesis	Aminoglycoside	Bind 30S ribosomal subunit Block translocation of peptide chain Cause misreading of mRNA
	Tetracycline	Bind 30S ribosomal subunit Inhibit peptide elongation
	Oxazolidinone	Bind 50S ribosomal subunit Inhibit initiation of peptide synthase
	Mupirocin	Blocks isoleucyl tRNA synthesis
	Chloramphenicol	Bind 50S ribosomal subunit Block aminoacyl tRNA positioning
	Lincosamides	Bind 50S ribosomal subunit Block peptide bond formation
	Macrolides	Bind 50S ribosomal subunit Block peptide chain exit
	Streptogramins	Bind 50S ribosomal subunit Block peptide chain exit
Nucleic Acid Synthesis	Fluoroquinolones	Inhibit DNA enzymes, gyrase and topoisomerase IV, creating enzymes-DNA-drug complex inhibiting DNA replication
	Rifamycins	Inhibit RNA polymerase
Folate synthesis	Sulfonamides	Inhibit dihydropteroate synthetase
	Trimethoprim	Inhibits dihydrofolate reductase
Plasma membrane	Polymyxin	Bind LPS and disrupt outer and cytoplasmic membranes
	Lipopeptide	Produces membrane channel and membrane leakage

Table 1.1 Mode of action of different classes of antibacterial agents. Key; penicillin-binding protein (PBPs), lipopolysaccharide (LPS).

1.2.3.1 Antibacterial drugs inhibiting cell wall synthesis

The cell wall is the main osmotic pressure bearing and shape-maintaining element, preventing mechanical, chemical, or enzymatic damage. A significant cell wall component is peptidoglycan, and Gram-positive (50-100 peptidoglycan layers) bacteria have a thicker layer than Gram-negative bacteria (2 peptidoglycan layers). Peptidoglycan is assembled from alternating units of *N*-acetylmuramic acid (NAM), and *N*-acetylglucosamine (NAG) cross-linked through pentapeptides at the lactic acid residue of NAM, and this is important for the shape and physical strength of the bacterium (Irazoki *et al*., 2019). The lactic acid of NAM is further linked to four amino acids in the series L-Alanine, D-Glutamate, L-Lysine, and D-Alanine by peptide bonds. This cell wall is not found in eukaryotes; therefore, drugs that target this entity are selectively toxic, creating extraordinary clinical efficacy and safety in controlling bacterial infection.

The β-lactam antibiotic family encompasses penicillin, cephalosporin, carbapenem, and monobactam subfamilies and their derivatives. Each structure within these subfamilies possesses the characteristic β-lactam core structure and varies by side chain attached or additional cycles. The biosynthesis of the peptidoglycan polymer is an intricate three-stage process where β-lactams target the final stage of development. More succinctly, they interfere with transpeptidation by binding to penicillin-binding proteins (PBPs), preventing the cross-linking of muramic acid residues and glycan chains in peptidoglycan, altering its structural integrity and promoting death (Rice, 2012; Dik *et al*., 2018).

Similarly, glycopeptides such as vancomycin inhibit peptidoglycan synthesis in Gram-positive bacteria by binding to the substrate of transpeptidases and forming a complex with D-Alanine-D-Alanine (D-Ala-D-Ala) of peptidoglycan precursors (Périchon and Courvalin, 2009; Olademehin *et al*., 2021).

1.2.3.1 Antibacterial drugs targeting protein synthesis

Protein biosynthesis (also known as translation) occurs on ribosomes, macromolecular enzymatic complexes, that catalyse the formation of polypeptide chains based on the genetic code of messenger RNA (mRNA) (Polikanov *et al.*, 2018). This complex process involves multiple steps; initiation and elongation comprise the entry of aminoacyl tRNA with anticodon reading of the mRNA codon leading to the peptidyl transfer of each amino acid to a growing polypeptide chain, the translocation of the ribosomes for each mRNA codon and then termination of the process. The prokaryotic 70S ribosome is composed of a small subunit (30S), which consists of the 16S ribosomal RNA (rRNA) chain and 21 proteins, and a large subunit (50S) that contains the 5S and 23S rRNA chains and 34 proteins (Steitz and Moore, 2003). Initiation of protein synthesis begins with the accurate positioning of the start codon (AUG) of mRNA to the decoding centre of 16S rRNA in the 30S subunit, which facilitates interactions with the anticodons of transfer RNA (tRNA) (Rodnina, 2018). This assembles the initiation complex, which also encompasses the binding of initiator tRNA with a UAC anticodon loop and carrying a methionine amino acid at the 3' end and three initiation factors (IF1, IF2, and IF3). Subsequently, the 50S subunit, which contains the peptidyl transferase centre (PTC) of the 23S rRNA for peptide-bond formation, combines with this complex forming the now active 70S ribosome. The ribosome has three tRNA binding sites designated the aminoacyl (A), peptidyl (P), and exit (E) sites found in the larger subunit. (Rodnina, 2018). During the elongation phase, the A-site and P-site bind corresponding tRNA, whereby incoming tRNA carrying the amino acid enters the aminoacyl site (A-site), and the amino acid is transferred to the growing polypeptide chain held in the peptidyl site (P-site). At the same time, the E-site removes the deacylated tRNAs from the ribosome (Bennison *et al.*, 2019). Termination of protein synthesis occurs when a stop codon (UAA, UAG, UGA) in the

mRNA is reached at the A-site and recognized by protein release factors resulting in the dissociation of the translational apparatus. The ribosomes of eukaryotic cells cytoplasmic are bigger (80S) and structurally distinct from those found in prokaryotes, consisting of a larger 60S subunit and a smaller 40S subunit. Classes of antibiotics that target protein synthesis are therefore selective and can be further divided into protein synthesis inhibitors that target the small 30S or the large 50S ribosomal subunit.

Aminoglycosides are used as bactericidal agents for the treatment of Gram-negative infections. Their primary target is the 16S rRNA A-site of the 30S small ribosomal subunit. The binding of the antibacterial agent here leads to disruption of the decoding process and misreading of mRNA, interfering with codon recognition and translocation (Borovinskaya *et al*., 2007; Polikanov *et al*., 2018). Tetracyclines passively diffuse into the bacterial cell and bind close to the A-site, blocking the association of aminoacyl-tRNAs with the 30S small ribosomal subunit, thus preventing the polypeptide chain from growing (Mccoy *et al*., 2011; Chukwudi, 2016).

Chloramphenicol is lipid-soluble and therefore passes through bacterial cell membranes. It binds reversibly to the A-site of the 50S subunit of bacterial ribosomes, inhibiting peptide bond formation and resulting in protein synthesis by preventing amino acid transfer to expand peptide chains, potentially by suppressing peptidyl transferase activity (Dinos *et al*., 2016). Oxazolidinones exhibit their antibacterial effects through binding to the A-site of 23S rRNA of the 50S subunit of the ribosome blocking the incoming aminoacyl-tRNA complex from binding to the A-site. This prevents the translation of bacterial proteins required for critical processes such as DNA replication and cell division, preventing bacteria from multiplying (Zhanel *et al*., 2015). Macrolides also bind to the 23S rRNA of bacterial 50S ribosomal subunits. They inhibit the transpeptidation or translocation process of protein synthesis, blocking it and interfering with the emerging

polypeptide as it is being synthesized, resulting in the premature separation of incomplete peptide chains, preventing bacterial protein synthesis (Parnham *et al*., 2014).

1.2.3.2 Antibacterial drugs targeting nucleic acids

Genetic material must be replicated for the survival and posterity of bacterial cells. Therefore, the metabolic pathways that result in synthesising nucleic acids are essential. Most bacterial species encode two distinct type II topoisomerases, DNA gyrase (topoisomerase II) and DNA topoisomerase IV. These enzymes play essential roles in nucleic acid processes, which modulate the chromosomal supercoiling required for DNA synthesis, transcription, and cell division (Cebrián *et al*., 2021). DNA Gyrase and topoisomerase IV preserve genomic integrity during the unwinding of DNA by attaching to each DNA strand of the intact double helix and passing it through a transient double-stranded break (DSB) generated in a separate segment the of DNA (Vos *et al*., 2011). Subsequently, the enzymes form covalent bonds between the 5′-terminus of each DNA strand, generating topoisomerase-DNA cleavage complexes (D'Atanasio *et al*., 2020). Both enzymes are in an A_2B_2 heterotetramer with gyrase composed of GyrA and GyrB subunits, and topoisomerase IV has ParC and ParE subunits (Forterre *et al*., 2007). Although they have similar homology, they differ in physiological action. Gyrase is uniquely responsible for introducing negative supercoils into DNA, thereby relaxing the helix (Gubaev *et al*., 2016), while topoisomerase IV removes knots that accumulate in the bacterial chromosome and the decatenation of the interlocked daughter chromosomes at the end of replication (López *et al*., 2012). Antibiotics that interfere with this process target the specific topoisomerases of bacterial cells and have been successfully exploited as molecular targets.

Quinolones are quinine-derived structural units that are potent synthetic antibacterial agents, and the addition of fluorine at position 6 is called fluoroquinolone. Gyrase and

topoisomerase IV function to generate DSBs in the bacterial chromosome. As described above, quinolone and fluoroquinolones avail of this process as the DNA is weakened and binds to the cleavage complexes noncovalently (Correia *et al.*, 2017). When DNA tracking systems, such as the replication fork or transcription complexes, collide with the newly formed quinolone–topoisomerase–DNA ternary complex, the DSBs are converted to permanent ones promoting cell death (Millanao *et al.*, 2021). Rifamycin is a semi-synthetic bactericidal agent of the rifampicin class and non-covalently binds to the β-subunit of the DNA-dependent RNA polymerase. This directly blocks the elongation of RNA, thus inhibiting transcription and causing cellular death (Mosaei and Zenkin, 2020). The DNA-dependent RNA polymerase in eukaryotes is unaffected as the drug binds to a peptide chain not present in the mammalian RNA polymerase.

1.2.3.3 Antibacterial drugs damaging plasma membrane

The bacterial cell membrane is a crucial structural and functional component that regulates most cell processes required for the stability of the bacterial cell. However, mammalian cells also possess a plasma membrane, so this is not a selective target. Therefore, antibacterial agents that target the plasma membrane exert toxicity towards the host but have been revisited recently as a last resort due to mounting resistance.

Daptomycin is a lipopeptide that performs in a calcium-dependent manner on Gram-positive bacteria by inserting into phosphatidylglycerol (PG) rich regions of the cell membrane, causing it to be permeabilised and disrupting membrane function leading to the loss of bacterial cell stability and subsequent death (Hachmann *et al.*, 2011). Polymixins also target the cell membrane, but they are specific to Gram-negative infections as they interact with lipid A of the bacterial lipopolysaccharides, concentrating on the outer membrane followed by penetration into the inner membrane leading to loss of cell membrane integrity and then cellular lysis (Epand *et al.*, 2016). The cationic

polypeptides consist of a lipid tail that is paramount to its toxicity in causing membrane damage through a detergent-like mode of action.

1.2.3.4 Antibacterial drugs targeting metabolic pathways

Antibacterial agents express antimetabolite activity by targeting folate metabolism. Tetrahydrofolate is imperative in both prokaryotes and eukaryotes as it is an enzyme cofactor involved in synthesising pyrimidine nucleotides by providing a carbon unit. Pyrimidine nucleotides are bases for DNA replication, repair, and other vital cellular processes.

The sulfonamides are a group of synthetic antimicrobial agents that are structural analogues of para-aminobenzoic acid (PABA). They act as competitive inhibitors of dihydropteroate synthase. This enzyme converts PABA as a substrate to dihydrofolic acid (folic acid) and blocks the biosynthesis of tetrahydrofolate in bacterial cells (Fernández-Villa *et al*., 2019). Another enzyme, dihydrofolate reductase, sequentially converts dihydrofolate to tetrahydrofolate (folinic acid). Diaminopyrimidines such as trimethoprim inhibit dihydrofolate reductase further into the folic acid synthesis pathway (DeJarnette *et al*., 2020).

1.3. Bacterial resistance to antibiotics

The resistance of microorganisms to a harmful agent is a natural process required for the survival of the species. However, the increased misuse and overuse of antibacterial agents across the globe have significantly accelerated this process and contributed to the emergence of highly resistant strains, severely limiting effective treatment options (Chokshi *et al*., 2019; Hernando-Amado *et al*., 2020). The primary forms of resistance are intrinsic, acquired, or phenotypic.

Intrinsic antibiotic resistance is a trait within the genome of bacterial species, independent of previous antibiotic exposure and not related to horizontal gene transfer (Cox and Wright, 2013; Reygaert, 2018). The mechanisms are typically chromosome-encoded and include the overexpression of non-specific efflux pumps, limited outer membrane permeability and drug inactivating enzymes (Chetri *et al*., 2019). Acquired resistance mainly occurs through the transfer of antibiotic resistance genes between bacterial populations by genetic exchange mechanisms. These mechanisms include transformation with free DNA, transduction by bacteriophages, or bacterial conjugation involving resistance plasmids (F plasmids), collectively referred to as the horizontal gene transfer mechanisms (Arnold *et al*., 2022). Phenotypic resistance can be achieved without genetic variation and occurs when susceptible bacteria become transiently resistant by either developing persistence or growth in biofilms. Persister cells are a subpopulation that enters a metabolically dormant state and effectively stops growing (Fernandes *et al*., 2022). A microbe formation of biofilms by a homogeneous or heterogeneous bacterial population is another mechanism to form protective resistance measures against antibiotics and other harmful substances (Sharma *et al*., 2019).

1.3.1 Mechanisms of antibiotic resistance

Resistance mechanisms exploit every possible way of preventing a drug from hitting its target. They typically occur by one or more of the following processes: (i) limiting drug uptake, (ii) modification of drug target, (iii) inactivation of drug, or (iv) increase in active drug efflux (Munita and Arias, 2016; Reygaert, 2018; Peterson and Kaur, 2018). These resistance mechanisms are presented in **Table 1.2** below and are separated by their primary bacterial cell target (as described previously in **Section 1.3.2**).

Major target	Antibacterial class	Mechanism of resistance
Cell wall synthesis	β-lactams	- Alteration of PBP target - Drug inactivation by β-lactamases - Reduced diffusion through porin channels
	Glycopeptides	- Alteration of the target from D-Ala-D-Ala to D-Ala-D-Lactate or D-Ala-D-Serine
	Bacitracin	- Active efflux
Protein synthesis	Aminoglycosides	- Drug modifying enzymes – AMEs - Methylation at ribosome binding site - Decreased permeation at target due to active efflux
	Tetracyclines	- Active drug efflux - Ribosomal protection proteins
	Oxazolidinones	- Altered rRNA binding site - Methylation of ribosome binding site
	Mupirocin	- Acquired resistant tRNA synthetase - Altered native tRNA synthetase target
	Chloramphenicol	- Drug modifying enzymes - CAT
	Lincosamides	- Methylation at ribosome binding site
	Macrolides	- Target modification through methylation at the ribosome binding site - Active drug efflux
	Streptogramins	- Target modification through methylation at the ribosome binding site - Active drug efflux
Nucleic acid synthesis	Quinolones	- Alteration of target - QRDR - Active efflux - Protection of target from drugs
	Rifamycins	- Altered target
Folate synthesis	Sulfonamides	- Acquired resistant dihydropteroate synthetase (drug bypass)
	Trimethoprim	- Acquired resistant dihydrofolate reductase
Cell membrane	Polymixin	- Altered cell membrane charge with reduced drug binding
	Daptomycin	- Altered cell membrane with reduced drug binding

Table 1.2 Resistance mechanisms to currently used antibacterial agents. Key: Aminoglycosides modifying enzymes (AMEs), penicillin-binding protein (PBPs), Chloramphenicol acetyltransferases (CAT), Quinolone-resistance determining region (QRDR), Lipopolysaccharide (LPS)

1.3.1.1 Limiting drug uptake

The distinction between Gram-positive and Gram-negative bacteria lies in the composition of their cell envelope, as illustrated in **Figure 1.4**. Gram-negative bacteria are naturally less permeable to specific antibacterial agents due to their outer membrane. This layer is effectively a second highly hydrophobic lipid bilayer composed with the addition of an amphiphilic lipopolysaccharide (LPS), lipoprotein and β-barrel transmembrane protein (Okuda *et al*., 2016). LPS consists of three structural components: hydrophobic lipid A (endotoxin), hydrophilic core oligosaccharide, and O-polysaccharide. The core oligosaccharide of LPS is negatively charged, resulting in a strong affinity for divalent cations such as calcium and magnesium. Porins are β-barrel structures that form channels to orchestrate the movement of small hydrophilic molecules across the outer membrane. The threshold size of transportable molecules depends on the porin and bacterial strain but is generally restricted to 600 Daltons (Choi and Lee, 2019). This size-exclusion makes the outer membrane a very effective and selective permeability barrier impeding the accessibility of antibacterial agents to their intracellular targets. This is notably highlighted when compared to the size exclusion of a Gram-positive cell wall, >10,000 Daltons. Hydrophilic glycopeptide antibiotics (such as vancomycin) are ineffective against Gram-negative bacteria, resulting from the permeability barrier imposed by the outer membrane (Antonoplis *et al*., 2019). Alterations of the outer membrane permeability influence the diffusion of hydrophobic antibiotics, resulting in poor uptake. For instance, in *P. aeruginosa*, mutations in the LPS transport pathway decrease membrane permeability, resulting in increased tobramycin resistance (Van den Bossche *et al*., 2021).

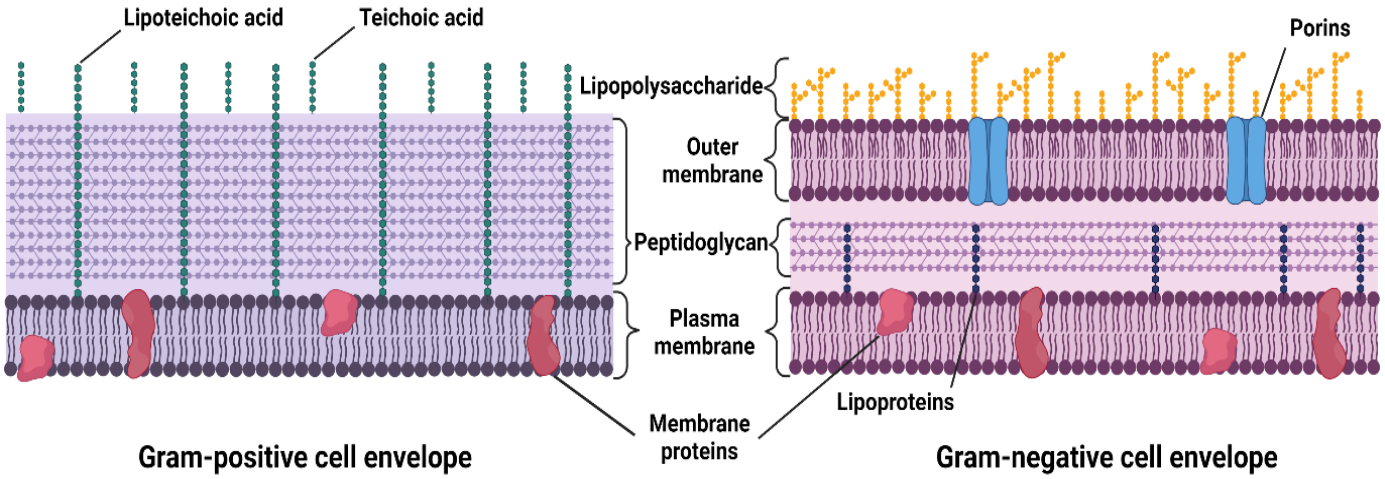

Figure 1.4 General comparison of Gram-positive (left) and Gram-negative (right) bacterial cell wall structure.

1.3.1.2 Modification of drug target

The alteration of the drug target is a common mechanism by which microbes develop resistance to antibacterial agents (Reygaert, 2018). Gram-positive bacteria primarily develop resistance to β-lactam drugs via alterations in the structure and the amount of PBPs. The *mecA* gene mediates methicillin resistance in *S. aureus*, which is harboured on the mobile genetic element staphylococcal chromosomal cassette (SCC) and encodes the penicillin-binding protein 2a (PBP2a) (Rolo *et al*., 2017). The alternative transpeptidase has reduced binding affinity to virtually all β-lactams, enabling cell wall synthesis to continue even in the presence of typically inhibitory concentrations of the antibiotic (Belluzo *et al.*, 2019). Resistance to glycopeptide antibiotics is acquired by reprogramming peptidoglycan precursor biosynthesis, replacing the terminal D-Ala with D-lactate (D-Ala-D-Lac) or D-serine (D-Ala-D-Ser), thus reducing the antibiotic affinity for its molecular target (Ahmed and Baptiste, 2018). The most clinically relevant operons related to resistance in Enterococci and Staphylococci are the *vanA* gene, conferring resistance to vancomycin and teicoplanin (glycopeptide) antibiotics, and enterococci containing *vanB* gene that demonstrate high resistance to vancomycin and susceptibility

to teicoplanin (Yushchuk *et al*., 2020). Resistance to fluoroquinolones occurs through spontaneous mutations in the quinolone resistance determining regions (QRDR) of *gyrA* and *parC* genes within DNA gyrase and topoisomerase IV, respectively (Rice, 2012), and more recently through plasmid-mediated quinolone resistance (PMQR) (Tao *et al*., 2020). Mutations in QRDR and PMQR genes result in amino acid substitutions that structurally change the target protein, reducing the drug-binding affinity of the enzyme (Shaheen *et al*., 2021).

1.3.1.3 Inactivation of drug

One of the most common mechanisms bacteria employ to evade antibiotics involves the production of enzymes that irreversibly destroy or neutralize them. Such enzymes are particularly prevalent among Gram-negative pathogens. They comprise those that destroy the active antibiotic site (such as β-lactamases) (Tooke *et al*., 2019) or that modify vital structural elements of the drug that hinder its interaction with the target site (such as aminoglycoside modifying enzymes) (Ramirez and Tolmasky, 2010). β-lactamases remain the most critical resistance mechanism among Gram-negative pathogens. They spread through horizontal gene transfer and concentrate within the periplasm, hydrolysing the β-lactam ring formation before reaching its PBP target (De Oliveira *et al*., 2020). There are two major classification systems for β-lactamase enzymes, the Ambler molecular classification (Ambler, 1980) and the Bush-Jacoby-Medeiros functional classification (Bush *et al*., 1995). There are four classes (A to D) of β-lactamases in the Ambler system that are grouped according to primary amino acid sequence homology. Class A, C, and D are serine hydrolases, whereas class B are zinc metalloenzymes. In the functional classification of Bush-Jacoby-Medeiros, β-lactamases are classified into groups 1 to 3 depending on the degradation of β-lactam substrates and the active-site serine β-lactamases (classes A, C and D) and the zinc-dependent β-lactamases (class B)

(Tooke *et al*., 2019). Resistance to the clinically essential aminoglycoside antibiotics results from the procurement of mobile genetic elements encoding for aminoglycoside modifying enzymes (nucleotidyltransferase, phosphotransferases, or acetyltransferases) that deactivate the drug preventing its interaction with the ribosomal subunit (Werner *et al*., 2013).

1.3.1.4 Increase in active drug efflux

Many antibiotics are transported out of the cell by bacterial efflux pumps, frequently seen in Gram-positive and -negative clinical isolates (Reygaert, 2018). Various efflux pumps are categorised by their structure and energy supply. The five primary families are (i) the adenosine triphosphate (ATP)-binding cassette (ABC) superfamily (Orelle *et al*., 2019), (ii) the major facilitator superfamily (MFS) (Lee *et al*., 2016), (iii) the small multidrug-resistance family (SMR) (Kermani *et al*., 2020), (iv) the multidrug and toxic compound extrusion family (MATE) (Kusakizako *et al*., 2020), and (v) the resistance-nodulation-division family (RND) (Colclough *et al*., 2020). The ABC family requires ATP as an energy source to remove antibiotics, whereas the other families utilize the proton motive force as the energy source. The MFS superfamily, primarily present in Gram-positive bacteria and the RND family, are characteristic of Gram-negative bacteria and is mainly associated with antibiotic resistance (De Oliveira *et al*., 2020).

1.3.1.5 Biofilms

In addition to the aforementioned resistance mechanisms, it is recognised that growth within biofilms can further impede antibacterial activity (Høiby *et al*., 2011; Høiby, 2017; Gebreyohannes *et al*., 2019). The nature of biofilm structure and the physiological attributes of organisms within the biofilm can confer an inherent resistance to antimicrobial agents. In addition, the biofilm organisms have higher horizontal gene

transmission than their planktonic counterparts (Ciofu and Tolker-Nielsen, 2019; De Oliveira *et al*., 2020).

Biofilms are structured multi-cellular sessile communities, organized as micro-colonies, encased within a self-produced extracellular matrix (ECM) that forms the scaffold for its three-dimensional architecture (Christophersen *et al*., 2020). This porous and complex structure is composed of water and extracellular polymeric substances which possess bacterial secreted biopolymers such as polysaccharides, extracellular DNA (eDNA), proteins, lipids, and metabolites (Seviour *et al*., 2019). Over several decades, biofilms have been extensively studied as they are a critical factor in the persistence of varied infections, reported to cause 65–80% of human infections (Rasamiravaka *et al*., 2015). They are particularly prevalent with tissue-related infections, such as chronic wounds, endocarditis, urinary tract infections and lung infections in cystic fibrosis patients (Høiby *et al*., 2011).

Figure 1.5 presents an example of a biofilm formed by *P. aeruginosa* strain PAO1 on respiratory epithelial cells and its structured ECM. Due to the protective and altered nature of the matrix, pathogenic biofilms from infected patients demonstrate up to 1,000-fold reduced susceptibility compared to their planktonic form (Hughes and Webber, 2017; Ciofu and Tolker-Nielsen, 2019). The formation of these aggregated communities with their resistance to antibiotics and host immune attacks are at the root of many persistent and chronic bacterial infections. For instance, for patients with CF infected with *P. aeruginosa*, antibiotic treatment often relieves the symptoms but does not necessarily cure the infection (Stefani *et al*., 2017). The acquisition of chronic *P. aeruginosa* infection is associated with worsened disease progression and increased mortality.

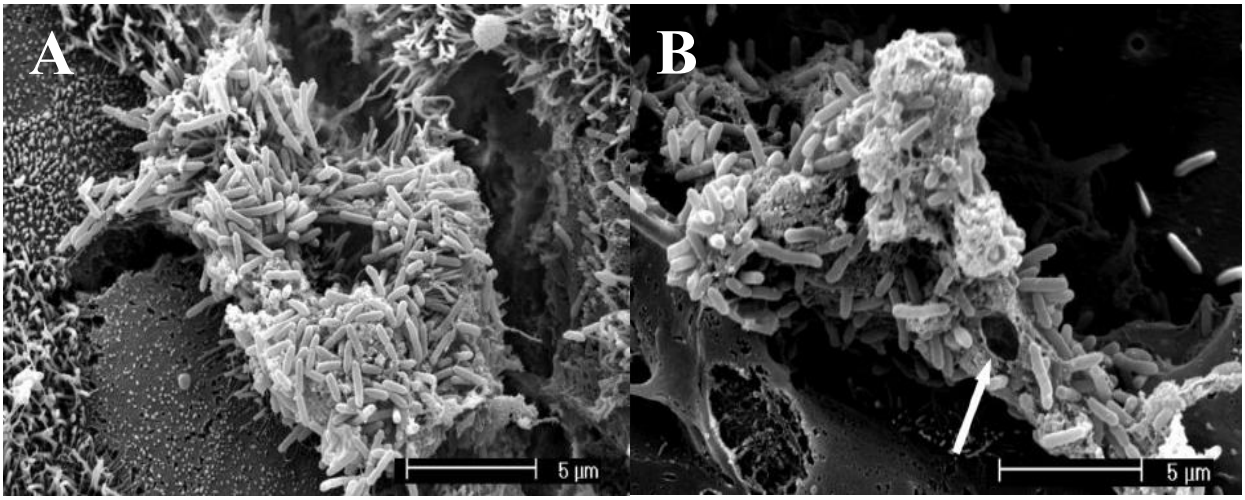

Figure 1.5 An SEM photomicrograph of PAO1 biofilm structure (**A**) within and on the underlying cilia of a respiratory epithelium showing exopolysaccharide matrix and (**B**) water channels (white arrow). Pictures are taken from (Woodworth *et al*., 2008)

The formation of a biofilm is a well-regulated, multi-step, endless cycle (as displayed in **Figure 1.6**), including (i) initial reversible attachment of bacterial cells with biotic or abiotic surfaces, followed by (ii) irreversible attachment within quick succession leading to (iii) the development of the immature biofilm architecture as the bacteria undergoes numerous physiological and phenotypic changes. The aggregation and accumulation of adherent bacteria lead to (iv) the formation of multiple cell layers to form a mature biofilm with water channels (**Figure 1.5.B**) responsible for distributing nutrients and signalling molecules within the biofilm. Finally, due to extrinsic or intrinsic factors, the bacteria (v) convert back to a planktonic state to allow dispersal of the cells and colonization in a new cycle of biofilm formation (De la Fuente-Núñez *et al*., 2013; Rabin *et al*., 2015; Sharma *et al*., 2019).

Upon sensing a stress signal, planktonic cells initiate interaction with a surface and produce extracellular polymers that facilitate attachment and matrix formation, resulting in an alteration in the phenotype of the organisms for growth rate and gene transcription.

Cell attachment is mediated by fimbriae, pili, flagella and extracellular proteins, which irreversibly trigger an alteration in gene expression, favouring the maturation from a motile to a sessile state (Veerachamy *et al*., 2014). Quorum sensing (QS) is a cell density-based communication mechanism within bacteria that allows for a coordinated response to environmental cues across the entire population (Yan and Wu, 2019). These chemical signals encourage further aggregation of cells resulting in multiple layers of bacteria starting to grow on top of each other, producing microcolonies maturing the formation of a matrix. The microcolonies are encased in a self-secreted matrix consisting of proteins, nucleic acids, polysaccharides, and water (Tuon *et al*., 2022). This process is carried on as cells in the biofilm reform to a planktonic state and break away from the biofilm to initiate a new cycle, enabling spread and colonization.

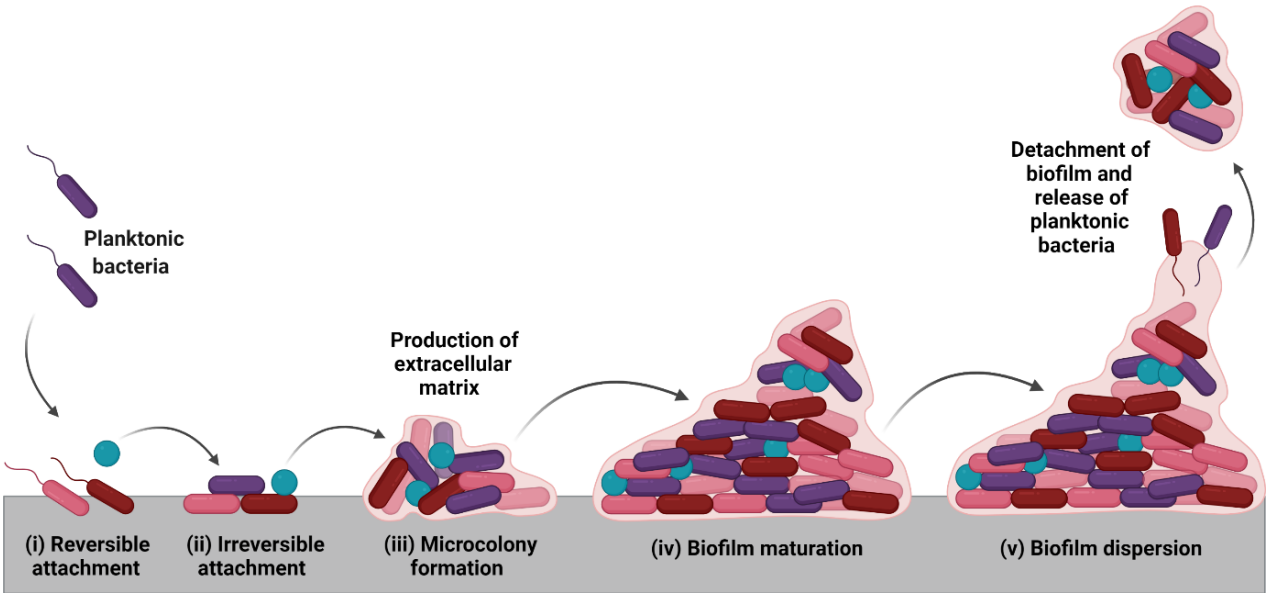

Figure 1.6 This diagram depicts the processes involved in forming a biofilm, including cell attachment, colonization and growth, development and active dispersal.

1.4. Antibacterial agents under clinical development

Although many antibiotics are available to clinicians, many have similar if not the same cellular target or process, leading to cross-resistance (Dewachter *et al*., 2019). Despite this, the number of new antibiotics developed and released onto the market has diminished steadily over the past few decades (Silver, 2011). WHO published a report in 2021 on antibacterial agents in the clinical and preclinical development pipeline for 2020 to assess which ones might potentially reach patients over the coming decade. The review highlighted that there are currently 43 traditional antibiotics and combinations with a new therapeutic entity in the clinical antibacterial pipeline. The 43 traditional antibiotics comprised 12 agents under development to act against *M. tuberculosis*, 5 agents against *Clostridioides difficile*, and 26 against WHO priority pathogens (**Table 1.3**). Of these 26, 13 are active against at least one of the Gram-negative pathogens on the WHO critical priority list, but most of these are still in phase 1 trials (WHO, 2021). While these traditional antibiotics represent a viable short-term solution, a new approach is required for more prosperous longevity. This was captured in the WHO report, as 27 non-traditional antibacterial agents were added for the first time. They are described as agents that are not small-molecule drugs and do not act by directly targeting bacterial components necessary for bacterial growth, and include microbiome-modulating drugs, antibodies, immunomodulation agents, and phage-derived enzymes. Another promising strategy involves the development of inorganic complexes for the antimicrobial treatment of bacteria by a mechanism that can inhibit growth or suppress virulence in a multi-modal fashion (Viganor *et al*., 2016a; Frei *et al*., 2020).

Priority category	Pathogen	Antibiotic resistance
Critical	*Acinetobacter baumannii*	Carbapenem-resistant
	Pseudomonas aeruginosa	Carbapenem-resistant
	Enterobacterales	Carbapenem-resistant
	Klebsiella pneumoniae, Escherichia coli, Enterobacter spp., Serratia spp., Proteus spp., Providencia spp., Morganella spp.	Third-generation cephalosporin-resistant
High	*Enterococcus faecium*	Vancomycin-resistant
	Staphylococcus aureus	Methicillin-resistant Vancomycin intermediate and resistant
	Helicobacter pylori	Clarithromycin-resistant
	Campylobacter	Fluoroquinolone-resistant
	Salmonella spp.,	Fluoroquinolone-resistant
	Neisseria gonorrhoeae	Third-generation cephalosporin-resistant Fluoroquinolone-resistant
Medium	*Streptococcus pneumoniae*	Penicillin-non-susceptible
	Haemophilus influenzae	Ampicillin-resistant
	Shigella spp.	Fluoroquinolone-resistant

Table 1.3 World Health Organisation (WHO) global priority pathogens list – pathogen and their resistance pattern. Pathogens are colour coded in relation to their gram stain; pink denotes Gram-negative and purple for Gram-positive pathogenic microorganisms.

1.4.1 Novel antimicrobial approaches using inorganic chemistry

Metal-based remedies have played a crucial role in medicine throughout history. Ancient Egyptians discovered the therapeutic potential of gold salts (Nobili *et al*., 2009), Chinese medicine has long established the antiseptic competence of arsenic (Dilda and Hogg, 2007), and the use of silver in wound management can be traced back to the 17th century, during which silver nitrate was administered to treat ulcers (Klasen, 2000). Paul Ehrlich and his co-workers developed the first successful metalloid complex in the 1900s, an arsenic-based therapeutic agent named salvarsan (**Figure 1.1**). This effectively cleared a syphilis infection for which no prior treatment was available (Ehrlich 1912; Ehrlich & Bertheim 1912). Nevertheless, research into metal-based coordination complexes was not

stimulated until the fortuitous discovery of a platinum complex known as cisplatin by Barnett Rosenberg. In 1960 Rosenberg observed that certain electrolysis products of platinum mesh electrodes could inhibit cell division in *E. coli* (Rosenberg *et al*., 1965). The team subsequently discovered cis-[$Pt(NH_3)_2Cl_2$] demonstrated superior antitumor activity both *in vitro* (Rosenberg *et al*., 1967) and in S180 murine sarcomas with a single dose (8 mg/kg), resulting in successful regression of the tumours after 8 days (Rosenberg *et al*., 1969). Cisplatin entered clinical trials in 1971 and became the first FDA-approved platinum compound for cancer treatment in 1978 (Mukherjee and Sadler, 2009). This landmark study brought metal-bearing compounds to the cornerstone of medicinal chemistry.

Since then, cisplatin has been extensively studied as a chemotherapeutic drug and is broadly administered to various cancers, including ovarian, lung, head and neck, testicular and bladder (Dasari and Tchounwou, 2014; Aldossary, 2019). It has been decidedly competent against testicular germ cell tumours leading to complete remission in approximately 70-80% of treated patients (Makovník *et al*., 2021), and combination treatment with radiotherapy is more successful than radiotherapy alone in non-small cell lung carcinomas (Nieder *et al*., 2013). Cisplatin is structurally a coordination compound with square planar geometry and exerts its antitumor activity via intra-cellular hydrolysis and subsequent covalent binding to DNA-forming adducts, triggering apoptosis (Tchounwou *et al*., 2021). Despite its triumph, cisplatin has several disadvantages and has been associated with mild to severe nephrotoxicity, neurotoxicity, ototoxicity, nausea and vomiting (Dasari *et al*., 2022). These toxic effects and solubility issues limit the dose applied to patients. Chemoresistance is a multifactorial phenomenon and accredits the most eminent disincentive in using the platinum drug. The mechanisms involved in its resistance are vast and numerous. Still, they are thought to be the repercussion of

intracellular changes that prevent cisplatin from interacting with DNA or interfere with DNA damage signals from activating the apoptotic machinery (Cocetta *et al*., 2019; Kryczka *et al*., 2021). These issues with cisplatin prompted further research into alternative Pt complexes. There are now three Pt(II) compounds approved for clinical use worldwide, Cisplatin (1), Carboplatin (2), Oxaliplatin (3) and three others, Nedaplatin (4), Heptaplatin (5) and Lobaplatin (6) are used in Japan, South Korea and China respectively (as seen in **Figure 1.7**) (Johnstone *et al*., 2015; Reece and Marimon, 2019).

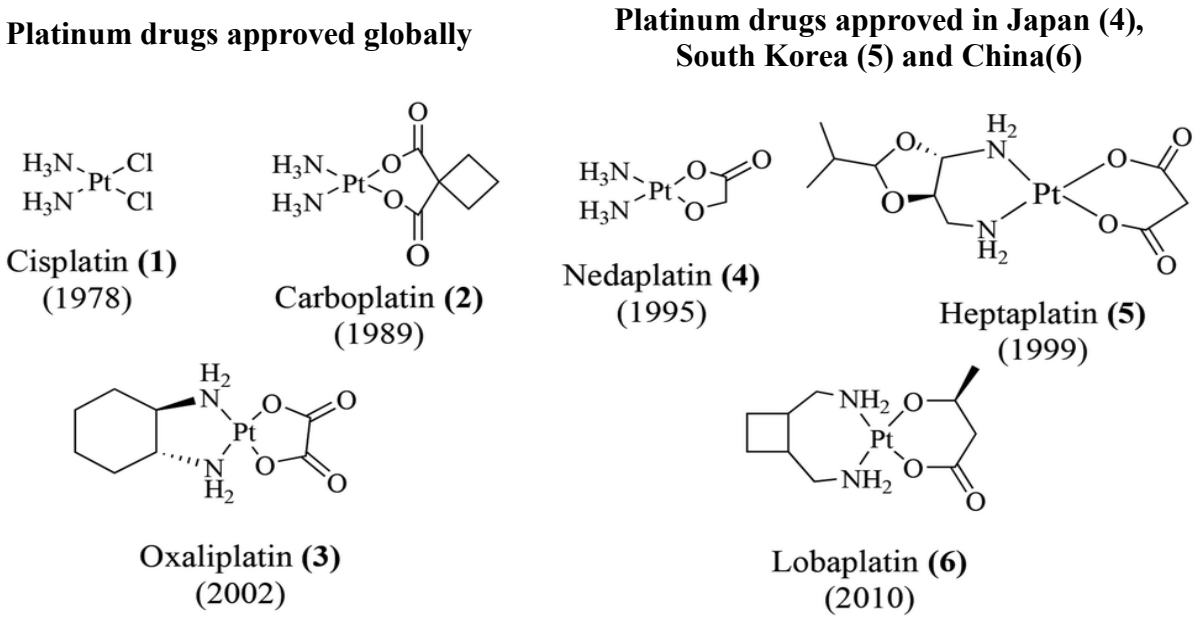

Figure 1.7 Platinum drugs in clinical use (**1–6**) with the years they received regulatory approval (Reece and Marimon, 2019).

Several more metal complexes have been introduced into the clinic in the last two decades, including gold for treating rheumatoid arthritis (Messori and Marcon, 2004), lithium for bipolar disorder (Gitlin, 2016), aluminium and zinc were used as antiulcer agents (Hunt, 1991) and arsenic, bismuth and silver as antimicrobial agents (Mjos and Orvig, 2014). More precisely, bismuth is co-administered with other antibiotics to treat

Helicobacter pylori infections, and silver sulphadiazine is used as a topical treatment for some burn wounds (Mégraud, 2012). A palladium-based photodynamic therapy (PDT) agent was also approved in 2019 for the treatment of prostate cancer by the European Medicines Agency (EMA) (Gunaydin *et al*., 2021).

Metal complexes can adopt a range of coordination geometries and redox states, allowing for more significant chemical variations when compared with purely organic antibiotics, with a different and potentially multi-modal mechanism of action that may target antimicrobial resistance (Boros *et al*., 2020; Claudel *et al*., 2020; Nasiri Sovari and Zobi, 2020). For instance, a recent study by the Community for Open Antimicrobial Drug Discovery (CO-ADD), a global free open-access screening initiative, discussed metal-bearing complexes enhanced activity profile (Frei *et al*., 2020). The group evaluated 906 individual metal compounds within their database (as presented in **Figure 1.8**), from d-block elements, against critical ESKAPE bacteria and fungi and found an impressive success rate of the metal compounds (9.9%) in comparison to solely organic molecules (0.87%). From this panel of metal complexes, 88 demonstrated activity (MIC ≤ 16 µg/mL or 10 µM) against one of their tested strains (58 against fungi and 30 against bacteria) while also being tolerated by mammalian cells (CC_{50} > 32 µg/mL or > 20 µM against human embryonic kidney cell line) and not demonstrating haemolytic activity (HC_{10} > 32 µg/mL or > 20 µM). Only 14 of these metal complexes showed activity (MIC ≤ 32 µg/mL) against Gram-negative bacteria, 8 of which also maintained toxicity towards Gram-positive bacteria. The paper highlighted gallium, palladium, silver, cadmium, iridium, and platinum as having the highest overall success rate and mentioned two manganese complexes for their specific activity against *E.coli* and MRSA. Overall, the group emphasized the potential antibiotic capabilities of metal compounds due to the

extent of possible modes of action with broader coverage of three-dimensional chemical space than their organic counterparts.

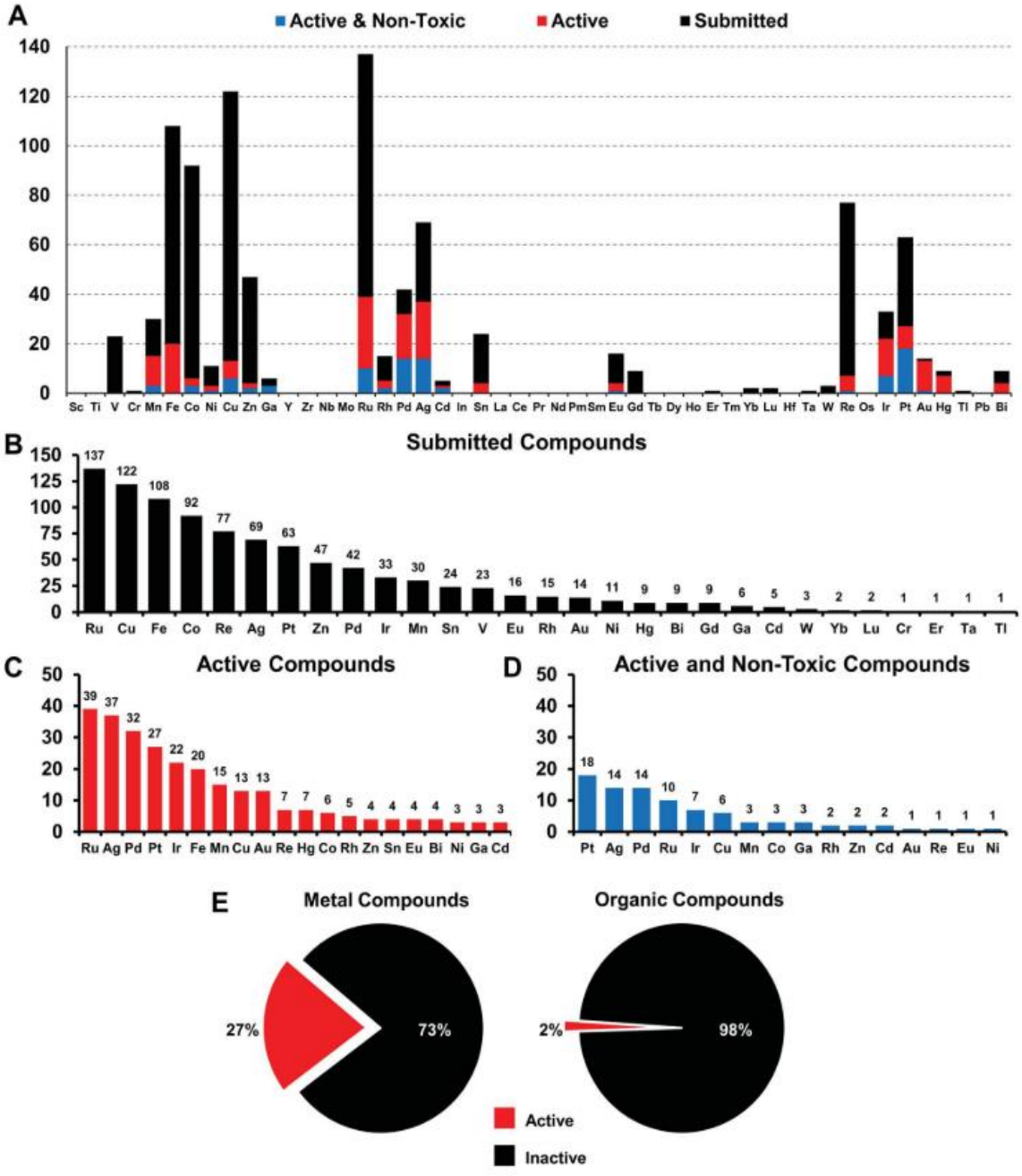

Figure 1.8 A diagram from CO-ADD demonstrating (**A**) the range of metal complexes submitted to the study. (**B**) The metal frequency across the 906 metal-containing compounds received. (**C**) The metal frequency among the 246 metal complexes that had activity against one tested ESKAPE pathogens or fungi. (**D**) The metal frequency among the 88 compounds that are active with low toxicity towards mammalian cells. (**E**) The percentage of submitted metal-containing compounds with antimicrobial activity compared to the overall hit rate for organic compounds within the CO-ADD collection (Frei *et al*., 2020).

1.4.2 1,10-phenanthroline and its metal complexes

The coordination of a metal ion to a biologically active ligand can serve to facilitate the uptake of the non-lipophilic metal across the lipophilic cell envelope and/or to act synergistically with the metal, such that the combined toxic effects of the metal and the active ligand will exert an enhanced and targeted activity in the problematic cell (Lemire *et al*., 2013; Frei *et al*., 2020). 1,10-phenanthroline (phen) is a heterocyclic and chelating bidentate ligand for metal ions which has played an important role in advancing coordination chemistry. The ideally placed nitrogen atoms, as seen in **Figure 1.9.A**, have rigid planar structure, hydrophobic, π-electron-deficient heteroaromatic, and acidic properties allowing the ligand to assist in the stabilisation of a variety of metal complexes in various oxidation states (Sammes and Yahioglu, 1994; Bencini and Lippolis, 2010). Phen has long shown antibacterial effects in an *in vitro* setting, demonstrating excellent bacteriostatic activity on Gram-positive and Gram-negative species of pathogenic bacteria (Turian, 1951; Kilah and Meggers, 2012). This antimicrobial action has been attributed to the chelating capabilities of phen and its sequestering nature of metal ions (McCann *et al.*, 2012). Thus, it selectively disturbs the essential metal cellular metabolism interference with metal acquisition and bioavailability for crucial reactions impeding the microbial nutrition, growth, virulence, and pathogenesis of a variety of microorganisms, including *Leishmania* spp., *Aspergillus* spp., *Candida albicans*, *Fonsecaea pedrosoi* and *Streptococcus agalactiae* (Santos *et al.*, 2012; Dos Santos *et al*., 2009). Accordingly, metal chelators such as phen have been investigated for their therapeutic potential against microbial infections as metals such as iron, copper, and zinc play an important role in cellular homeostasis. Moreover, it was shown that the sequestered metals produce a metal-phen complex, and the emerging complex is driving the toxic effects demonstrated in previous studies (Husseini and Stretton, 1980). Investigations into the *in vitro*

antibacterial activity of phen derivatives (displayed in **Figure 1.9**), such as 3,4,7,8-tetramethyl-1,10-phenanthroline, 5-nitro-1,10-phenanthroline, 1,10-phenanthroline-5,6-dione, 2,9-dimethyl-1,10-phenanthroline, and various others have also been undertaken (Zoroddu *et al*., 1996). A significant increase in biocidal activity was achieved when the various ligands were coordinated with copper(II) ions, with the 2,9-dimethyl derivative being the most active against *S. aureus* and *E. coli.*

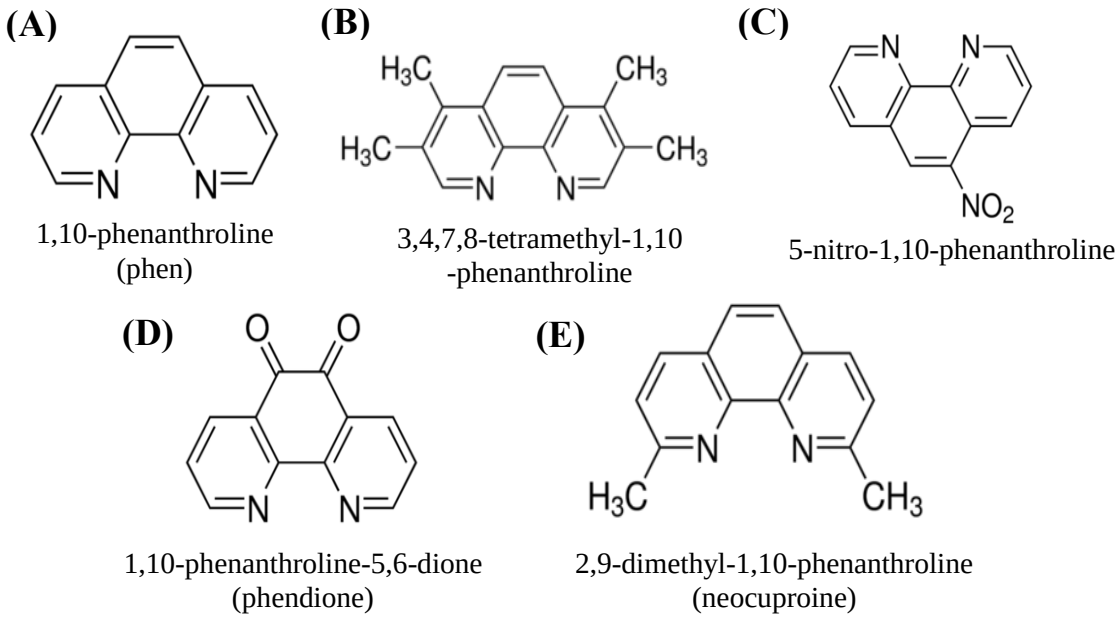

Figure 1.9 Structure of 1,10-phenanthroline (phen) and examples of its derivatives

To date, metal complexes containing phen, and its derivatives, have been reported in the literature for their anticancer (Kellett *et al*., 2012; Thornton *et al*., 2016; Rochford *et al*., 2018, 2020), antifungal (Santos *et al.*, 2012; Gandra *et al.*, 2017, 2020; Granato *et al.*, 2017, 2021), antiparasitic (Vargas Rigo *et al*., 2019; Lima *et al*., 2021), antibacterial (Viganor *et al*., 2016a; McCarron *et al*., 2018; Ahmed *et al*., 2019; Ventura *et al*., 2020; Vianez Peregrino *et al*., 2021) and antiviral (Shulman and White, 1973; Mazumder *et al*., 1995; Papadia *et al*., 2005; Chang *et al*., 2010) competence. The work of polypyridyl

metal complexes was pioneered by Francis Dwyer and co-workers when they published a landmark study outlining the biological activity of dicationic ruthenium (Ru), iron (Fe), nickel (Ni), cobalt (Co), copper (Cu), zinc (Zn), calcium (Ca) and manganese (Mn) chelates containing phen and its derivatives (Dwyer *et al*., 1969). Their work established the *in vitro* toxicity of the metal-phen chelates against *M. tuberculosis, S. aureus, S. pneumoniae, Clostridium perfringens, E. coli, and Proteus vulgaris* (presented in descending order of activity), while the metal-free phen demonstrated dampened effects. Furthermore, the toxicity exerted was independent of the metal present, except for *M. tuberculosis*. They also identified that the bacteria and fungi did not develop resistance of any significance to the selected chelates. *In vivo* bacterial infection treatment studies using mice and guinea pig models showed that metal-phen chelates were clinically useful as topical antimicrobials. However, selected compounds were chemotherapeutically ineffective when administered intravenously due to rapid clearance from the bloodstream.

Although the results were promising, the interest in polypyridyl metal complexes as potential antibacterial chemotherapeutics was void in the pharmaceutical sector, possibly due to the vast array of antibiotics in the pipeline or the immensely lower incidence of antibacterial resistance at the time. In modern times, transition metal-based compounds have had a revival of interest as possible alternatives or adjuvants to the current armamentarium of antibacterial agents that cannot contend with the rapid emergence of resistant bacteria worldwide (Lemire *et al*., 2013). Metal complexes incorporating phen as a ligand are at the forefront of that research. However, it is necessary to establish their mechanism of action and ensure there is a substantial difference from the resistance-prone antibiotics.

Our research group has been developing and investigating 1,10-phenanthroline (phen), its derivatives and their metal complexes as potential therapeutic agents for several

decades. 1,10-phenanthroline-5,6-dione (phendione; **Figure 1.9**) is a phenanthrene-based ligand and a derivative of the classical chelating agent phen. The free ligand and its coordinated copper(II) and silver(I) complexes, $[Ag(phendione)_2]ClO_4$ (Ag-phendione) and $[Cu(phendione)_3](ClO_4)4H_2O$ (Cu-phendione) have been extensively studied by our research group across a variety of microbial cells. The metal-free phendione and its metal complexes were able to inhibit the growth of the *Candida albicans* (McCann *et al*., 2004), *Phialophora verrucosa* (Granato *et al*., 2017, 2021), *Pseudallescheria boydii* (Santos *et al*., 2012) and *Trichomonas vaginalis* (Vargas Rigo *et al*., 2019). Gandra *et al.* (2017) tested a range of Mn(II), Cu(II) and Ag(I) dicarboxylate complexes containing phen and phendione ligands against nine clinical isolates of three species that make up the highly resistant *Candida haemulonii* species complex, an emerging opportunistic pathogen resistant to most antifungal drugs currently used in clinical practice. From this study, the Ag(I) chelates were the most effective drugs when assessed against planktonic cells (overall geometric mean of the minimum inhibitory concentration (GM-MIC) ranged from 0.26 to 2.16 µM), followed by the Mn(II) (overall GM-MIC ranged from 0.87 to 10.71 µM) and Cu(II) (overall GM-MIC ranged from 3.37 to >72 µM) chelates. Although the same activity was not maintained when testing the strains during a biofilm lifecycle. The *in vivo* potential of the chelates to clear *C. haemulonii* infections utilising *Galleria mellonella* larvae was also investigated. Mn(II)- and Ag(I)-phen chelates could conserve antifungal activity at concentrations that were reasonably non-toxic toward *G. mellonella*. Most notable was the $\{[Mn(3,6,9\text{-tdda})(phen)_2]3H_2O.EtOH\}_n$ complex as it induced the lowest mortality rate while reducing the fungal burden on infected larvae and also could affect the virulence of *C. haemulonii* (Gandra *et al*., 2020).

McCarron *et al.* (2018) reported on a range of manganese(II)- and copper(II)-phen complexes that inhibited the viability of *M. tuberculosis* laboratory reference strain H37Rv and clinically derived CDC1551 strain. The Mn(II) complexes were highly tolerated by A549 mammalian cells culminating in high selectivity index values. Ahmed *et al.* (2019) aimed to enhance this toxicity by synthesizing a new Schiff base ligand, combining the anti-tuberculosis drug isoniazid (INH) with phendione creating a hydrazide ligand ((Z)-*N*'-(6-oxo-1,10- phenanthroline-5(6H)-ylidene)isonicotinohydrazide; **Figure 1.10**), and further complexed the ligand to Ag(I) and Mn(II) metal ions. The antimycobacterial activity of this ligand was comparable to INH alone, and its metal complexes were four times more potent than INH when assessed against a drug-susceptible and three drug-resistant *M. tuberculosis* strains. Ahmed *et al.* (2022) also synthesized a series of phenanthroline-oxazine ligands (**Figure 1.10**) by reacting L-tyrosine amino acid esters and phendione and subsequently formed metal complexes $[Ag(1)_2]ClO_4$, $[Mn(1)_3](ClO_4)_2$ and $[Cu(1)_3](ClO_4)_2$ (where 1 = phenanthroline-oxazine ligand). All metal complexes had enhanced toxicity in comparison to the starting ligand. However, due to their lipophilicity, both complexes and ligands were only active against S. aureus, not E. coli.

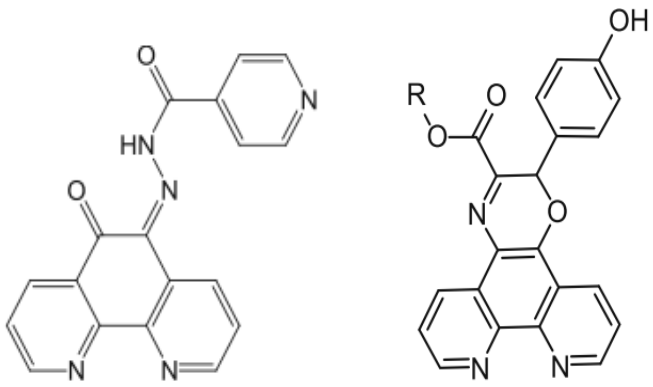

Figure 1.10 Structure of hydrazine ligand (left) and phenanthroline-oxazine ligand (right) (Ahmed *et al*., 2019, 2022)

1.4.3 Mechanisms of metal-phen complexes

Research into the possible mechanisms by which promising phen-based complexes exert their toxic effects has been carried out by our research group within *in vitro* models, including mammalian, fungal, and bacterial cells and in a range of *in vivo* biological models. **Figure 1.11** gives a visual synopsis of the proposed modes of antifungal action by phen and its derivatives. (**1**) depicts the dysfunction and disruption of the cell membrane along with the withdrawal of the cytoplasmic membrane, (**2**) shows drug-induced circumvention on the action of cell division (budding), (**3**) displays damage to the functional mechanisms of the mitochondria, (**4**) exhibits chelation and/or sequestering of trace metal ions which inhibits glycosylphosphatidylinositol (GPI) biosynthesis, (**5**) illustrates the rupturing of internal organelles along with the enlargement of the nucleus and (**6**) the degrading of nuclear DNA (McCann *et al.*, 2012).

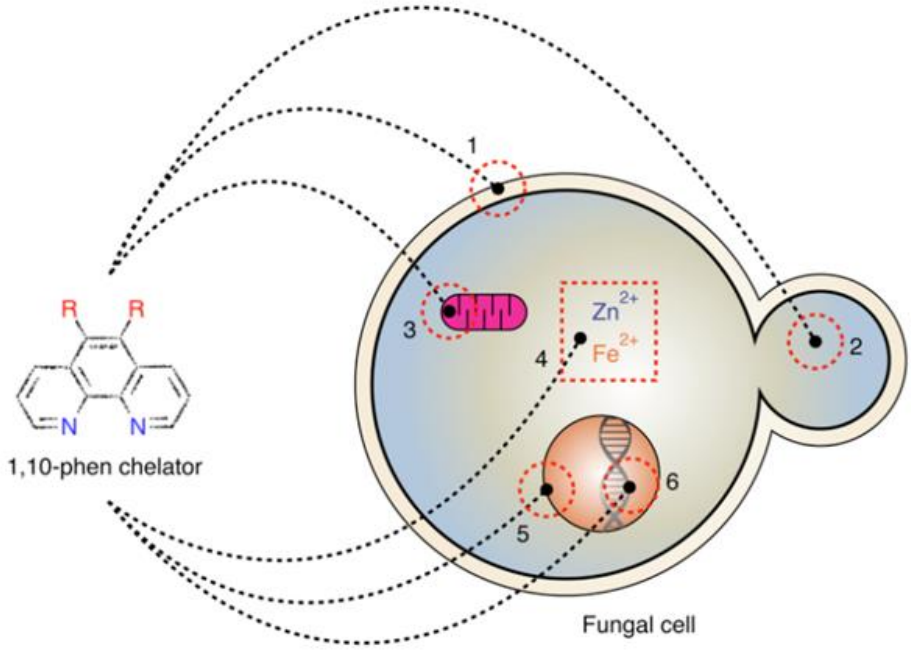

Figure 1.11 Summary of the current potential modes of antifungal action by phen and derivatives as reported by McCann *et al.*, 2012.

Our group have also investigated the potential antibacterial capability of metal-phen complexes and their mechanism of action (Viganor *et al*., 2016). These findings are summarized in the following sub-sections, and this thesis aims to further broaden the current understanding of the antibacterial capabilities and mechanisms of a range of metal-phen complexes used for the research described.

1.4.3.1 The bacterial cell envelope and activity of metal-phen complexes

The cell wall and outer cell membrane are considered a significant obstacle in developing novel antibacterial agents that are effective against Gram-negative bacteria as they must be lipophilic and able to penetrate the outer membrane (**Figure 1.4**). Contradictory to this, silver (Ag) has well-documented bactericidal properties. In its cationic form Ag(I), it is oligodynamic. It displays a broad spectrum of activity dependent upon the slow release of biologically active ions thought to bind to the bacterial cell surface and interfere with growth by inhibiting transport across the cell wall and membrane (Lemire *et al*., 2013; Domínguez *et al*., 2020). As charged entities, free metal ions require protein- or ionophore-mediated transport to cross a lipid bilayer as these transporter proteins encase the cations in a hydrophobic sleeve to pass. The complexation of metals to a hydrophobic chelating ligand such as phen can enact the same process allowing their penetration through the bacterial cell envelope, presenting the chelate to its target biomolecule to inhibit cell growth or initiate cell death (Raman *et al*., 2007). Cationic metal-phen chelates can be bacteriostatic (Dwyer *et al*., 1969) or bactericidal (Butler *et al*., 1969) towards Gram-positive bacteria, including *S. aureus* and *S. pyogenes* and *C. perfringens*. However, they do not exhibit the same potency against Gram-negative bacteria. The lipophilicity of a complex is taken as a good measure of its ability to pass into the cell by diffusion, and in some cases increased lipophilicity correlates with antimicrobial potency (Wang *et al*., 2021b). Almost 70 years ago, Dwyer *et al*. identified this relationship when

working with mononuclear ruthenium and phen complex, $[Ru(phen)_3]^{2+}$. Initially, this complex was inactive against all tested bacterial strains however, when methyl substituents were incorporated into the phenanthroline ligand, $[Ru(3,4,7,8\text{-}Me_4phen)_3]^{2+}$, the non-polar surface interaction was increased. This corresponded to increased activity against all examined bacteria, especially Gram-positive and acid-fast bacteria (Dwyer *et al*., 1952).

Over the past decade, there has been renewed interest in the antimicrobial activity of polypyridylruthenium(II) complexes. Crowley *et al*. (2016) have used a series of 2-(1-R-1*H*-1,2,3-triazol-4-yl)pyridine "click" ligands (R-pytri) as functionalised analogues of 2,2'-bipyridine (bpy) and phen chelators to synthesise a diverse range of ruthenium complexes ($[Ru(R\text{-}pytri)_3](PF_6)_2$), and examined their antimicrobial activities. Some of the Ru(II) R-pytri complexes showed good activity against Gram-positive bacteria but were significantly less active against Gram-negative species. The mode of action was determined to disrupt the cell wall and the cytoplasmic membrane. As the ruthenium complexes displayed low cytotoxicity against human dermal keratinocytes, they may also be helpful as a topical treatment of recalcitrant infections for slow-growing bacteria (Kumar *et al*., 2016).

Keene, Grant Collins and co-workers have extensively researched ruthenium(II) complexes and their potential as antimicrobials. They developed kinetically inert mono-, di-, tri-, and tetra-nuclear polypyridylruthenium(II) complexes, whereby the Ru(II) metal centres are bridged by a flexible and lipophilic bis[4(4'-methyl-2,2'-bipyridyl)]-1),*n*-alkane ligand (bb_n) and are collectively termed '$Rubb_n$' complexes, where n = the number of methyl groups in the bb_n linker chain (n = 2, 5, 7, 10, 12, 14 or 16). The antibacterial activity of this series of complexes is correlated with increasing lipophilicity through increased length of the bb_n chain, and only slight differences were observed with

enantiomeric forms of the complexes (Li *et al*., 2012). The dinuclear ruthenium complexes 'Rubb$_n$' has been the most extensively studied and has produced exciting results. The Rubb$_n$ complexes enter bacteria energy-dependent as they significantly depolarise and permeabilise the cellular membrane (Li *et al*., 2013). There was preferential uptake of Rubb$_n$ in microbes compared to cancerous cells, which was suggested to result from the greater presence of negatively charged components in the bacterial envelope (Weber *et al*., 2016). Rubb$_{16}$ was found to be the most active with selective toxicity towards bacteria. This complex condensed ribosomes when they existed as polysomes by preferentially binding to RNA over DNA *in vivo*, offering the interruption of protein synthesis in actively growing bacterial cells as a potential mode of action (Li *et al*., 2014).

The corresponding tri- and tetra-nuclear complexes 'Rubb$_n$-tri' and 'Rubb$_n$-tetra' were the more active, demonstrating MICs four times their dinuclear analogues (Gorle *et al*., 2014). Although the level of cellular uptake in Gram-negative bacteria was similar to that of Gram-positive bacteria, there was significantly less activity in the former species, which was an interesting observation. The authors suggested that this was a result of the inherent resistance of Gram-negative bacteria to inert polpyridylruthenium(II) complexes, particularly *P. aeruginosa*, in which the outer membrane permeability is 10- to 100-fold lower than, for example, that of *E. coli* (Li *et al*., 2015). However, while the antibacterial activity increased as the ruthenium centres and the length of the alkyl chain in the bb$_n$ ligand increased the toxicity toward eukaryotic cells reduced selectivity (Gorle *et al*., 2016).

1.4.3.2 DNA as an antibacterial target for metal-phen complexes

The design of agents capable of controlled nucleic acid cleavage is of great importance, and since the initial work of Sigman *et al.* (1979) there has been a considerable attraction to artificial metallonucleases. The copper-bis-phenanthroline complex, $[Cu(phen)_2]^{2+}$, induced oxidative cleavage of DNA in the presence of a reductant, which is unusual for complexes containing phen as this compound as a singular agent usually intercalates with DNA. DNA as a target offers a fresh avenue for potential antibacterial agents as it has been relatively unexplored thus far (Bolhuis and Aldrich-Wright, 2014). A variety of publications have reported the enhanced antibacterial activity of quinolone/fluoroquinolone antibiotics containing metal(II)-phen complexes (metal = Cu(II), Ni(II), Co(II), Mn(II)) (Psomas and Kessissoglou, 2013). One example is the combination of Levofloxacin (lvx) with Cu(II) forming the binary complex, $[Cu(lvx)]^{2+}$, that significantly increases DNA binding but is not stable at a physiological pH. However, the addition of phen as an *N*-donor form a very stable ternary complex $[Cu(lvx)(phen)]^{2+}$ (Sousa *et al*., 2012). Cu(II)/phenanthroline/fluoroquinolone complexes have demonstrated intercalation with DNA, exhibiting nuclease activity, and are taken into the cell differently from the free fluoroquinolone drug (Fernandes *et al*., 2014). Furthermore, when tested against a mutant strain of *E. coli* lacking porins, it was identified that the higher the hydrophobicity of the complexes, the higher the need for porins for their uptake (Gameiro *et al*., 2007). Marmion *et al*. rationally developed a family of metallo-antibiotics with the general formula [Cu(N,N)(CipA)Cl], where N,N represents a phenanthrene ligand, and CipA is a derivative of fluoroquinolone antibiotic ciprofloxacin (Ude *et al*., 2019). The complexes were active against sensitive and resistant *S. aureus* bacteria. They appeared to intercalate DNA via minor groove interactions and mediate DNA damage by generating ROS with superoxide and hydroxyl free radicals playing

crucial roles in DNA strand scission. Molecular docking analysis prompted the synthesis of derivatives [Cu(N,N)(CipHA)]NO_3 where CipHA represents a hydroxamic acid of ciprofloxacin. Proteomic analysis of *S. aureus* exposed to two lead complexes [Cu(phen)(CipHA)]NO_3 and [Cu(DPPZ)(CipHA)]NO_3 (where DPPZ = dipyridophenazine) suggests that proteins involved in virulence, pathogenesis and the synthesis of nucleotides and DNA repair mechanisms are most affected (Ude *et al*., 2021). Metal-phen complexes without adding the quinolone ligand have also demonstrated moderate antibacterial activity with DNA binding and/or nuclease activity as the proposed antibacterial mechanism of action. The metals include Ag(I) (Smoleński *et al*., 2013), Cu(I) (Chetana *et al*., 2016), Cu(II) (Raman and Raja, 2007), Zn(II) (Tabassum *et al*., 2012), Pt(II) (Ng *et al*., 2013), Mn(II) (Shivakumar *et al*., 2013), and Fe(III) (Dimitrakopoulou *et al*., 2007).

1.4.3.3 Induction of oxidative stress by metal-phen complexes

Bactericidal antibiotics have been proposed to contribute to bacterial death by inducing oxidative stress executed by reactive oxygen species (ROS) (Kohanski *et al*., 2007). In this proposed model the agitation of metabolism and respiration stimulated by an antibacterial agent leads to increased superoxide production, thereby releasing ferrous iron from damaged iron-sulphur (Fe-S) clusters (Kohanski *et al*., 2008). Elevated intracellular concentrations of ferrous iron interact with endogenous hydrogen peroxide and, through the Fenton reaction, generates lethal hydroxyl radicals, which can directly damage cellular DNA, lipids and proteins (Dwyer *et al*., 2007). This action alone as a mechanism of cell death has been challenged (Imlay, 2015). However, as part of a multi-modal effect may be plausible. Although sub-lethal concentrations of antibiotics have been reported to induce mutagenesis by stimulating the production of ROS, thus promoting antibiotic resistance (Kohanski *et al*., 2010). To defend against the increase in

ROS, bacteria enhance the production of antioxidant enzymes, such as superoxide dismutase (SOD) and catalase (Imlay, 2008), and antioxidant molecules such as ascorbic acid and glutathione (Cabiscol *et al*., 2000) that can detoxify ROS through regulatory mechanisms (SoxRS, OxyRS, and SOS regulons) to counter the damage (Wang and Zhao, 2009).

Metal-free phen significantly enhances its activity against *E. coli* after adding hydrogen peroxide (H_2O_2) (Asad and Leitao, 1991). This was proposed to result from the reaction kinetics of Fe scavenging by phen, forming adducts with ferrous iron (Fe^{2+}) and ferric iron (Fe^{3+}), catalyzing the Fenton reaction and generation of free radicals. It was later supported by Furtado *et al.* (1997) by exposing *E. coli* to both phen and H_2O_2 preceded by treatments with metal chelators, bipyridine for Fe^{2+} and desferal for Fe^{3+} separately in the presence of free-radical scavengers, thiourea. They observed that protection was achieved for radical and Fe^{2+} scavengers but not Fe^{3+}. The authors also noted that a known Cu^{+1} scavenger, neocuproine (2,9-dimethyl-phen; **Figure 1.9**), offered sufficient protection supporting the hypothesis that metallonuclease $[Cu(phen)_2]^{1+}$ can play a role in bacterial cytotoxicity. Metal-phen complexes such as $[Cr(phen)_3]^{3+}$ have been reported to generate ROS in bacteria, which contributes to its antibacterial capabilities (Páez *et al*., 2013).

1.4.3.4 The activity of metal-phen complexes on biofilms

Bacterial biofilm communities differ from planktonic bacteria in various ways, such as growth rate, gene expression, and protein expression (Sharma *et al*., 2019). This is due to biofilms creating an altered microenvironment with higher osmolarity, nutrient scarcity and increased cell density of heterogeneous bacterial communities (Flemming and Wingender, 2010; Flemming *et al*., 2016). Bacteria usually reside in biofilms, and biofilm-residing bacteria can be resilient to the immune system, antibiotics, and other

treatments (Fenker *et al*., 2018; Sharma *et al*., 2019; Vestby *et al*., 2020). Therefore, agents that can navigate the difficult terrain of a biofilm to the bacteria embedded within or dissociate the extracellular matrix to expose the bacteria are important.

Although there are few reports of metal-phen complexes with anti-biofilm activity, some advances have been made in developing novel compounds. A range of Cu(II) complexes, $[Cu(I_L)(A_L)]^{2+}$ (where I_L represents functionalized 1,10-phenanthrolines and A_L represents 1S,2S- 1,2-diaminoethane or 1R,2R-diaminocyclohexane) were tested on a number bacterial strains (Beeton *et al*., 2014). Although the metal complexes generated higher MICs (2-32 µg/mL) than the control antibiotic vancomycin (MIC = 0.25 µg/mL), they showed significant activity against *S. aureus* biofilms and were better in the removal of biofilms than vancomycin. For example, 100 µg/mL of vancomycin, which is 400 fold the MIC, reduced biofilm biomass by just 44%, whereas 25 µg/mL of [Cu(5,6-dimethyl-phen)(*SS*-dach)]$^{2+}$ (equivalent to 3-fold the MIC) reduced the biofilm by 68% in only 2 h. This decrease in biomass was similar in all Cu complexes and is metal-dependent as replacing the centre with Pt(II), or Pd(II) removed both the antibacterial and anti-biofilm action. Therefore suggests that the potential mechanism of action in both planktonic and biofilm cells is related to the nuclease activity of Cu, as neither Pt nor Pd possesses this capability, particularly given that the extracellular matrix contains a considerable quantity of nucleic acids. A series of complexes incorporating phen and cyanoguanidine (cnge) have been reported with the general formula M(II)/phen/cnge (where M = Cd, Cu or Zn) (Falkievich *et al*., 2022). The cadmium complex, $[Cd(phen)_2(SO_4)H_2O]cnge•5H_2O$, possessed enhanced activity across the assessed bacterial and fungal pathogen in comparison to its metal derivatives. This prompted subsequent antibiofilm analysis against *P. aeruginosa* laboratory strain ATCC 27853, in which 0.5 x MIC (93.5 µg/mL) of the metal complex inhibited approximately 40% of the biofilm formation. Moreover,

there was a reduction in the acute toxicity of the phen ligand when it was incorporated into the Cd(II)/phen/cnge complex within a crustacean model, *Artemia salina*.

A derivative of phen, 1,10-phenanthroline-5,6-dione (phendione, **Figure 1.9**), has also been investigated for its antibacterial and anti-biofilm capabilities. This compound contains an o-quinoid moiety and forms strong complexes with transition metal ions at the *N-N* terminal with predominance toward Zn(II) and to a lesser extent for Fe(II), Ca(II), Cu(II), Co(II), and Mn(II) (McCann *et al*., 2012a). Tay *et al.* (2015) reported the MIC and MBC values of phendione for *Enterococcus faecalis* as 2 μg/mL and 16 μg/mL, respectively, relating their activity to the ability to sequester the Zn(II) from metalloenzymes. In order to kill *E. faecalis* cells embedded in a biofilm structure, a MIC four times that required to kill planktonic bacteria was required. However, the biofilm was eradicated at this concentration. Although the authors could not explain the mechanism of phendione eradicating *E. faecalis* biofilm, they speculate that it may weaken the biofilm's extracellular polymeric substances by disrupting Zn(II) balance.

Viganor *et al.* (2016) also investigated the effect of phen, phendione and metal complexes Cu-phendione and Ag-phendione (**Figure 1.12**) on planktonic and biofilm growing *P. aeruginosa*. The compounds presented the following potency against susceptible and resistant planktonic cells, Cu-phendione (7.76 μM) > Ag-phendione (14.05 μM) > phendione (31.15 μM) > phen (579.28 μM). It was also identified that the compounds could disrupt a mature biofilm in a dose-dependent manner, especially Ag-phendione (IC_{50} = 9.39 μM) and Cu-phendione (IC_{50} = 10.16 μM). Further investigation demonstrated that Cu-phendione was an effective inhibitor of the metalloenzyme Elastase B (lasB), mitigating the toxic effect of lasB-containing bacterial secretions in the in *vivo* model, increasing the survival time of *G. mellonella* larvae (Galdino *et al*., 2019), therefore suggesting this as a potential therapeutic target. Metal-phendione complexes

could interact with double-stranded DNA and promote oxidative damage suggesting multiple mechanisms of action in *P. aeruginosa* (Galdino *et al*., 2022). The same activity sequence of the test complexes (Cu-phendione > Ag-phendione > phendione) was maintained when assessed in both planktonic- and biofilm-forming cells of MDR *A. baumannii* (Ventura *et al*., 2020) and *K. pneumoniae* (Vianez Peregrino *et al*., 2021) clinical isolates. The combination of either Cu-phendione or Ag-phendione with meropenem had synergistic activities, according to their fractional inhibitory concentration, against *K. pneumoniae* carbapenemase (KPC)-producing clinical isolates. Moreover, the combination of the metal complex and meropenem restored the efficacy of the antibiotic (in terms of MIC) in 87% of phenotypically resistant strains (Vianez Peregrino *et al*., 2021). The metal-phendione complexes also had low toxicity in *G. mellonella* larvae (Gandra *et al*., 2020; Granato *et al*., 2021) and mice (McCann *et al*., 2012b), reinforcing that these compounds may represent a novel antimicrobial agent with potential therapeutic applications across a variety of pathogens.

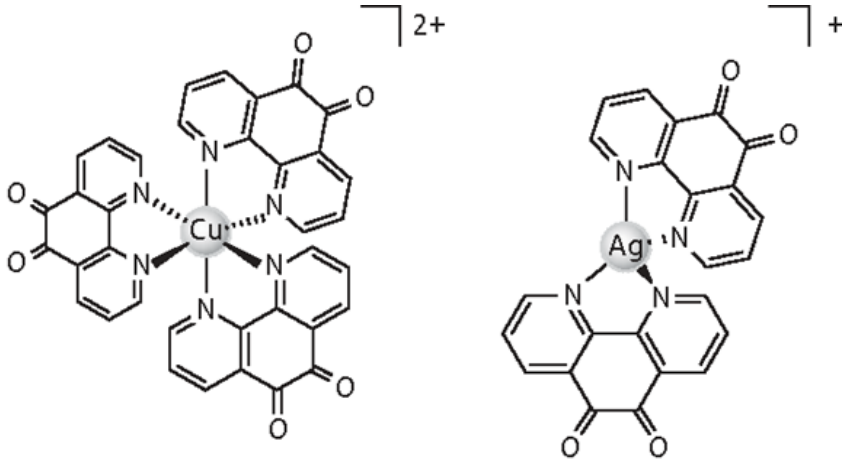

Figure 1.12 Structure of phendione containing metal complexes $[Cu(phendione)_3]^{2+}$ (left) and $[Ag(phendione)_2]^{+}$ (right)

These findings against three Gram-negative bacteria that are on both the WHO priority pathogen list (**Table 1.3**) and a part of the ESKAPE pathogens (discussed in the next section) are of great significance due to their ability to rapidly develop and acquire resistance to multiple classes of antibiotics severely limiting the currently available drugs still affective at clearing their infections.

1.5. Problematic multidrug-resistant bacteria

Bacterial infections are becoming more challenging to treat due to increasing numbers of resistant infections to the current arsenal of antimicrobial therapies (Piddock, 2016). This has given rise to the potential return of many diseases worldwide that were previously controlled (Sabin *et al*., 2020). For example, previously controlled tuberculosis (TB) has re-emerged to become the second leading cause of morbidity and mortality from an infectious disease worldwide (WHO, 2019). TB is curable and preventable, but there is an increasing prevalence of multidrug-resistant strains of TB (MDR-TB) with high-level resistance to the two most potent anti-TB drugs, isoniazid and rifampicin. This resulted in nearly half a million cases of drug-resistant TB occurring annually, of which 78% had MDR-TB, with extensively drug-resistant TB (XDR-TB) making up 6.2% of this (WHO, 2019). Our research group has reviewed the growing concern of MDR-TB and the potential application of metal complexes to address this growing worldwide threat (Viganor *et al*., 2015). More recently, Mn(II) complexes containing 1,10-phenanthroline and dicarboxylate ligands (McCarron *et al*., 2018) and Ag(I) and Mn(II) complexes with hydrazide ligands (Ahmed *et al*., 2019) have been reported for their anti-TB activity in addition to high mammalian cell tolerance, culminating in high selectivity index (SI) values.

In addition to the WHO global priority pathogens list (**Table 1.3**), reports using data from hospital-based surveillance studies as well as from the Infectious Diseases Society of America (IDSA) have established a group of nosocomial pathogens referred to as 'ESKAPE bugs' of current global concern (Bassetti *et al*., 2013). This acronym encompasses the most worrisome microorganisms in current clinical practice; *E. faecium, S. aureus, K. pneumoniae, A. baumannii, P. aeruginosa*, and *Enterobacter* species, that require rapid development of new drugs due to their ability to 'escape' the effects of many commonly prescribed antibiotics (Rice, 2008; Boucher *et al*., 2009). *Enterococci, Staphylococci* and *Enterobacterales*, especially *E. coli* and *K. pneumoniae*, are a part of the normal microbiome preventing their complete removal from hospital settings, while the other opportunistic pathogens are environmental contaminants. However, these microbe's ability to acquire multidrug resistance (MDR) and extensive drug resistance (XDR) through the promiscuous nature of horizontal gene transfer and, on a lesser scale, through chromosomal mutations solidify them as a significant threat to public health. The discovery of the mobile colistin resistance (*mcr*) gene, enabling bacteria to be highly resistant to polymixins such as colistin, attracted recent global attention.

Carbapenem resistance is a pivotal event in generating XDR pathogens, creating havoc in the clinic due to the exhaustion of therapeutic options. The majority of acquired carbapenemases belong to either Ambler class A, class B (metallo-β-lactamases, MBLs), or class D (oxacillinases, OXAs) (Karaiskos *et al*., 2019). Although not conferring resistance to carbapenems, extended-spectrum β-lactamases (ESBLs) are also problematic as ESBL- and carbapenemase-encoding plasmids are frequently vectors of resistance determinants for other antimicrobial classes, such as aminoglycosides and fluoroquinolones (Ruh *et al*., 2019; Fournier *et al*., 2022). Colistin was largely abandoned as a treatment for bacterial infections in the early 1980s due to toxicity and low renal

clearance concerns. Now with limitations of current therapeutics and the widespread emergence of Carbapenem-Resistant *Enterobacterales* (CRE), clinicians have revisited colistin as a 'last resort' against MDR pathogens and have significantly increased their dependence on it (Lim *et al*., 2010; Ahmed *et al*., 2020a; Gogry *et al*., 2021). The recent escalation in the use of colistin in clinical practice, accompanied by its unrestricted use in agriculture, has contributed to the rapid dissemination of resistance across species and the usefulness of colistin as the last resort antibacterial is now compromised by the presence of an increasing number of the transferable plasmid-mediated colistin resistance gene, *mcr*, and its variants. For instance, the first *mcr* gene, *mcr*-1 was reported in China in November 2015 (Liu *et al*., 2016) and has since been identified in several species of bacteria in 72 countries across 6 continents (Wang *et al*., 2018a; Mmatlia *et al*., 2022). To date, nine additional variants (*mcr*-2 to *mcr*-10) have been identified in different bacteria isolated from animals, foods, farms, humans, and the environment (Xavier *et al*., 2016; AbuOun *et al*., 2017; Borowiak *et al*., 2017; Carattoli *et al*., 2017; Yin *et al*., 2017; Wang *et al*., 2018b; Yang *et al*., 2018; Carroll *et al*., 2019). More worrisome is the presence of *mcr* in *Enterobacterales* carrying carbapenem resistance genes such as MBL, ESBL, and New Delhi metallo-β-lactamase (NDM), progressing them from extensive drug resistance (XDR) to pan-drug resistance (PDR) (Wang *et al*., 2017; Hussein *et al*., 2021).

In addition to *Enterobacterales* recent years have also witnessed an increasing prevalence of MDR and XDR *P. aeruginosa* strains, with rates of between 15% and 30% in some parts of the world (Walkty *et al*., 2017; Sader *et al*., 2018). The European Centers for Disease Prevention and Control (ECDC) reported that 30.1% of the *P. aeruginosa* isolates in 2020 were resistant to at least one of the examined antimicrobial groups, and 9.8% were resistant to three or more (ECDC, 2022). Although this has significantly decreased

since 2015, the report emphasized that *P. aeruginosa* remains one of the major causes of healthcare-associated infection (HCAI) in Europe. The bacterium is a biofilm-forming opportunistic pathogen that causes life-threatening chronic infections in immunocompromised individuals with diseases like burn wounds, urinary tract infections, and respiratory infections (Vestby *et al*., 2020). In fact, *P. aeruginosa* was one of the most common co-infecting bacteria in COVID-19 patients (Lansbury *et al*., 2020; Qu *et al*., 2021). *P. aeruginosa* is also a critical pulmonary pathogen and the predominant cause of morbidity and mortality in people with cystic fibrosis.

1.6. Cystic fibrosis and *Pseudomonas aeruginosa*

Cystic fibrosis (CF) remains one of the most prevalent, life-limiting hereditary disorders in the Caucasian population and affects more than 70,000 individuals worldwide (CFF, 2021). Ireland has one of the highest global incidences of CF, with almost 1,400 individuals registered as living with the disease (Farrell, 2008; CF Registry of Ireland, 2017). Although it manifests in multiple organs, including the pancreas, liver, intestines, sweat glands and reproductive organs, a progressive pulmonary disease marked by a severe dysregulated inflammatory response and recurrent bacterial infections is a significant contributor to morbidity and mortality (Fonseca *et al*., 2020). Despite the substantial advances in early diagnosis and treatment, the median life expectancy for people with CF is 40-50 years in developed countries (Elborn *et al*., 2016). CF is an autosomal recessive disorder caused by a mutation in the gene, expressed on chromosome 7 (7q31.2), encoding the cystic fibrosis transmembrane conductance regulator (CFTR) anion channel (Rommens *et al*., 1989). More than 2000 gene variants have been identified and classified into six groups depending on their consequences on the CFTR protein (Elborn, 2016). Deletion of phenylalanine at position 508 (Phe508del or ΔF508) of the CFTR protein (Group II) is the most common mutation associated with CF, 91.7% of

individuals with CF are carriers of a single mutation in Ireland, while 55.5% are homozygous (CF Registry of Ireland, 2019). Defects caused by Phe508del lead to misfolding of CFTR and subsequent proteasome-mediated degradation (Fonseca *et al*., 2020), preventing the protein from reaching the cell surface and functioning optimally.

As presented in **Figure 1.13**, *CFTR* encodes a cAMP-dependent channel that transports chloride (Cl^-) and bicarbonate (HCO_3-) across the apical plasma membrane of epithelial cells while also modulating the sodium (Na^+) channel (ENaC) (Elborn *et al*., 2016). The absence of HCO_3- causes an imbalance in the function and viscosity of mucus so that it becomes thick and compromises mucociliary clearance. The hyperabsorption of Na^+ via ENaC will lead to insufficient water secretion to the pulmonary epithelial surface, contributing to mucus hyperviscosity and dehydration. Therefore, the lack of functional CFTR protein results in an ion imbalance leading to viscous mucus secretions impairing mucociliary clearance, creating an ideal environment for microbial colonisation. The most commonly isolated pathogens from CF airway samples are *S. aureus* (including MRSA), *Haemophilus influenzae, P. aeruginosa*, *Burkholderia cepacia* complex, non-tuberculous mycobacteria and *Aspergillus fumigatus* (CF Registry of Ireland, 2019). However, *S. aureus* and *P. aeruginosa* tend to dominate in this harsh landscape. Subsequently, *S. aureus* is the most prevalent pathogen detected during exacerbations of CF patients in childhood (CF Registry of Ireland, 2019), while *P. aeruginosa* dominantly colonizes the airways from adolescence and becomes the most abundant by adulthood, with approximately 80% of CF patients chronically colonised with the bacterium by the age of 20 (Beswick *et al*., 2020). Chronic infection with *P. aeruginosa* is associated with a rapid decline in pulmonary function, more frequent exacerbations, and higher mortality rates (Malhotra *et al*., 2019), thus treatments aiming to eradicate or dampen the effects of initial infections are highly sought after.

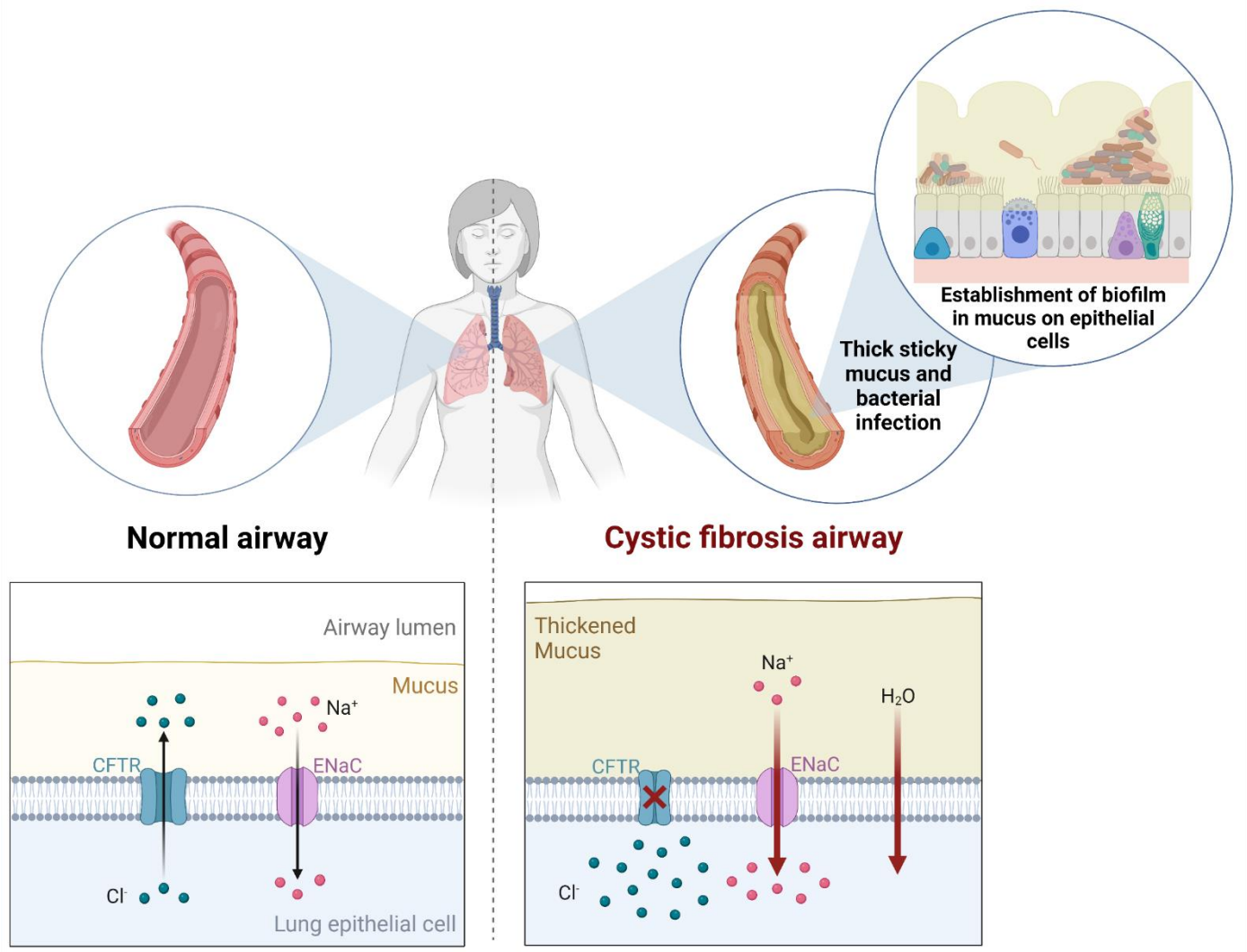

Figure 1.13 Cystic fibrosis transmembrane conductance regulator (CFTR) in a normal airway and CF airway. Imbalance at the pulmonary epithelium due to mutations in the CFTR channel compromising the flow of chloride (Cl^-) and bicarbonate (HCO_3-) by epithelial cells to the extracellular space while also modulating sodium (Na^+) via epithelial sodium channel (ENaC) leading to thick mucus which is optimal for bacterial growth.

P. aeruginosa is a ubiquitous and opportunistic Gram-negative human pathogen that is highly successful in colonising a diversity of sites (Gellatly and Hancock, 2013; Jurado-Martín *et al*., 2021). The bacterium is metabolically versatile with an extensive repertoire of virulence factors, antibiotic resistance determinants and the ability to form robust biofilms, allowing it to adapt to conditions in the airway and evade antibiotics and host

immune attacks (Ciofu and Tolker-Nielsen, 2019; Jurado-Martín *et al*., 2021; Van den Bossche *et al*., 2021). The attributes of *P. aeruginosa* that aid with colonisation and inflammation within the lung include lipopolysaccharide (LPS) (Di Lorenzo *et al*., 2015), the type III secretion system (T3SS) (Anantharajah *et al*., 2016), proteases (Galdino *et al*., 2017), pyocyanin (Hall *et al*., 2016) and pyoverdine (Minandri *et al*., 2016). A *P. aeruginosa* cell possesses a single polar flagellum and several type IV pili that facilitate motility, bacterial chemotaxis, and attachment of the bacteria to a common assialyated glycolipid (Asialo-GM1) on host cells. Shared by several Gram-negative bacteria species, the type III secretion system (T3SS) is one of the most clinically relevant virulence determinants in *P. aeruginosa* (Sarges *et al*., 2020), which acts through the translocation of up to four exotoxins (ExoS, ExoT, ExoU, ExoY) to the host cell by the needle appendage (Jurado-Martín *et al*., 2021). ExoU and ExoS are considered the significant cytotoxins as they have the greatest impact on disease severity, while ExoT and ExoY play a minor role in virulence. The irreversible attachment of the bacterial cell to the host cell triggers an alteration in gene expression favouring the maturation from a motile to sessile state, producing microcolonies and creating a biofilm. As previously discussed (**Section 1.3.1.5**), a biofilm is a structured community of bacterial cells enclosed in an extracellular matrix (ECM) that provides exceptional protection (Ciofu and Tolker-Nielsen, 2019; De Oliveira *et al*., 2020). *P. aeruginosa* produce three exopolysaccharides, alginate, Psl, and Pel, which play an essential role in forming biofilm and stabilizing its structure. While planktonic cells are readily cleared, once a biofilm has formed the effectiveness of both polymorphonuclear neutrophils and macrophages are superfluous. In addition, biofilms are associated with a high level of tolerance or resistance to antimicrobials (Billings *et al*., 2013; Ciofu *et al*., 2015; Ciofu and Tolker-Nielsen, 2019).

Quorum sensing (QS) is a cell density-based communication mechanism within bacteria that allows for a coordinated response to environmental cues across the entire population. As population density increases, so does the chemical signal molecules, autoinducers, which in Gram-negative bacteria are *N*-acyl homoserine lactones (AHL) and alkyl quinolone (AQ). *P. aeruginosa* has three main interlinked hierarchical networks consisting of the Pseudomonas quinolone signal (PQS) and two LuxR/LuxI-type systems, LasR/LasI and RhlR/RhlI, comprised of a transcriptional regulator (R) and synthase (I) (Kostylev *et al*., 2019). The Las system is at the top of the hierarchy, positively controlling the expression of the other networks. These systems are highly interconnected, and QS has been reported to regulate motility, EPS production, virulence production such as proteases, pyocyanin and rhamnolipids, and biofilm formation and is thus highly influential (Lee and Zhang, 2014).

1.7. Research rationale

The emergence of antimicrobial drug resistance necessitates new approaches to challenge bacterial pathogens, and novel therapeutic strategies are required to compensate for the diminishing availability of effective antibiotics. Concurrently, transition metal complexes have had a revival of interest as possible alternatives or adjuvants to the current arsenal of antimicrobial agents, with complexes containing polypyridyl ligands playing a notable role. The metal complexes described in this report represent a rationally designed series of copper(II), manganese(II) and silver(I) complexes incorporating various dicarboxylate anions as bridging ligands. These metal-dicarboxylate complexes were also derivatised with 1,10-phenanthroline (phen), yielding an additional set of phen-bearing chelates to enhance their toxicity.

1.7.1 Research objectives

Each research objective 1-3 for this project described below resulted in the production of an article for publication, all three of which were based on the experimental work described in chapters 2, 3 and 4 of this thesis.

Objective 1 – Paper 1 (Chapter 2)

The first objective of this project was to assess the antibacterial activity of a range of metal complexes (where metal = Cu(II), Mn(II), and Ag(I)) incorporating phen and a range of dicarboxylate ligands against a panel of Gram-positive and Gram-negative WHO priority pathogens that are also problematic within Irish clinical settings. Whole-genome sequencing was carried out on *S. aureus*, and *P. aeruginosa* cells made resistant to sub-optimal concentrations of the lead metal-tdda-phen complexes to identify resistance mutations.

O'Shaughnessy M, Hurley J, Dillon SC, Herra C, McCarron P, McCann M, Devereux M, Howe O. Antibacterial activity of metal-phenanthroline complexes against multidrug-resistant Irish clinical isolates: A whole genome sequencing approach. **Accepted to the Journal of Biological Inorganic Chemistry, 2022.**

Objective 2 – Paper 2 (Chapter 3)

The next objective was to further investigate selected metal complexes incorporating 3,6,9-trioxaundecanedioate and 1,10-phenanthroline ligands within a cystic fibrosis (CF) disease model, utilising clinical isolates of *P. aeruginosa* derived from Irish CF patients, both alone and in combination with gentamicin, a prescription antibiotic. The effects on planktonic growth and the inhibition of biofilm formation and disarticulation were assessed in terms of biofilm biomass and cell viability once treated. In addition, the selectivity of these metal complexes to the pathogens over potential host, mammalian cell

lines Cystic Fibrosis Bronchial Epithelial Cells (CFBE41o-) and BEAS-2B (SV40/adenovirus 12 transformed normal bronchial epithelium) cells were also assessed to establish the toxicity of the complexes towards them.

O'Shaughnessy M, McCarron P, Viganor L, McCann M, Devereux M, Howe O. The antibacterial and anti-biofilm activity of metal complexes incorporating 3,6,9-trioxaundecanedioate and 1,10-phenanthroline ligands in clinical isolates of *Pseudomonas aeruginosa* from Irish Cystic Fibrosis patients. **Antibiotics. 2020; 9(10):674.**

Objective 3 – Paper 3 (Chapter 4)

The final objective was to test the therapeutic potential of the three selected metal complexes alone and in combination with gentamicin in an *in vivo* model using *Galleria mellonella*.

O'Shaughnessy M, Piatek M, McCarron P, McCann M, Devereux M, Kavanagh K, Howe O. *In vivo* activity of metal complexes containing 1,10-phenanthroline and 3,6,9-trioxaundecanedioate ligands against *Pseudomonas aeruginosa* infection in *Galleria mellonella* larvae. **Biomedicines. 2022; 10(2):222**.

Chapter 2.

The antibacterial activity of novel metal complexes against multidrug-resistant clinical isolates

Chapter 2 (objective 1) is based on the following paper: ***O'Shaughnessy M****, Hurley J, Dillon SC, Herra C, McCarron P, McCann M, Devereux M, Howe O. Antibacterial activity of metal-phenanthroline complexes against multidrug-resistant Irish clinical isolates: A whole genome sequencing approach. Accepted to the Journal of Biological Inorganic Chemistry, 2022.*

2.1. Introduction

Copper(II), manganese(II), and silver(I) complexes incorporating phen and dicarboxylate ligands were the focus of this study, specifically on WHO priority pathogens (WHO, 2017) that are also problematic within Irish clinical settings (HPSC, 2019). The panel comprised Gram-positive bacteria methicillin-resistant *Staphylococcus aureus* (MRSA) and vancomycin-resistant *Enterococci* (VRE), Gram-negative bacteria carbapenem-resistant and ESBL-producing *Enterobacterales* and *Pseudomonas aeruginosa*, derived from patients in Irish hospitals.

S. aureus is a significant bacterial human pathogen that causes a wide variety of clinical manifestations, ranging from sub-acute skin infection to life-threatening septicaemia (Tong *et al*., 2015) and is one of the most common causes of hospital-acquired infections (Lee *et al*., 2018). MRSA has been endemic in Ireland since the 1980s, but as a result of national surveillance and an effective infection control policy and practices, we have seen the lowest proportion of MRSA specific bloodstream infections in 2020 (11.5%), despite this Ireland still has one of the highest proportions of MRSA in northern and western Europe (HPSC, 2022). *Enterococci* spp. are common inhabitants of the human microbiota but have adapted to colonizing and persisting in a hospital environment causing invasive infections (Krawczyk *et al*., 2021). *Enterococcus faecium* and *Enterococcus faecalis* are the most frequently isolated species in nosocomial settings and display both intrinsic and acquired resistance to several antibiotic classes, of which vancomycin-resistant *Enterococci* (VRE) has become the most alarming (McDermott *et al*., 2018; Ayobami *et al*., 2020). The number of bloodstream infections caused by VRE are continuously increasing, and since 2008 Ireland, the Health Protection Surveillance Centre (HPSC), as part of the EARS-Net, has reported the highest percentage of VRE-associated infections in Europe, with rates in 2020 at 35.1% (HPSC, 2022). The emergence of VRE strains

resistant to all established antimicrobial agents is now recognized as a public health priority in Ireland. *Enterobacterales* (such as *Klebsiella pneumoniae* and *Escherichia coli*) are a family of Gram-negative bacteria and the most common cause of healthcare-associated infections (HCAI) in Ireland, associated with mortality rates of 50% (HSPC 2016). Due to the successful nature in which they harbour and transmit antimicrobial-resistance plasmids on an intra- and inter-species level, they are becoming challenging to treat. Initially, *Enterobacterales* that produced extended-spectrum β-lactamases (ESBLs) posed the most prominent health concern (Dangelo *et al*., 2016), forcing clinicians to prescribe carbapenems as first-line empirical treatments, which resulted in carbapenem-resistant *Enterobacterales* (CRE) (Suay-García and Pérez-Gracia, 2019). HPSC figures indicate that the number of ESBL-positive isolates of *K. pneumoniae* was 14.3%, increasing yearly since 2013, while ESBL-producing *E. coli* accounted for 9.9% of isolates (HPSC, 2022). The emergence of carbapenemase-producing strains of *K. pneumoniae* and *E. coli* was declared a national public health emergency in Ireland in 2017. *P. aeruginosa* is a highly versatile bacterium associated with a wide range of infections. The opportunistic human pathogen is frequently isolated from nosocomial infections, and the increasing occurrence of multidrug-resistant (MDR) strains, in addition to its adaptive resistance during chronic infections, is causing high levels of morbidity and mortality (Pang *et al*., 2019). Invasive *P. aeruginosa* infections increased by 54% between 2015 and 2020, and in that time, MDR-isolates accounted for 2.5-9% (HPSC, 2022).

In this chapter, the antibacterial activity of copper(II), manganese(II), and silver(I) complexes incorporating 1,10-phenanthroline (phen) and dicarboxylate ligands against WHO priority pathogens that are also problematic within Irish clinical settings are presented. The panel comprised Gram-positive bacteria methicillin-resistant *S. aureus*

(MRSA) and vancomycin-resistant *Enterococci* (VRE), Gram-negative bacteria carbapenem-resistant and ESBL-producing *Enterobacterales* and *P. aeruginosa*, derived from patients in Irish hospitals. For the microbiological screening of the complexes, European Committee on Antimicrobial Susceptibility Testing (EUCAST) standardised susceptibility testing methods were utilised as currently, these guidelines are used in all diagnostic laboratories throughout Ireland. One representative Gram-positive, *S. aureus*, and Gram-negative, *P. aeruginosa*, organism were selected for subsequent acquired resistance studies to selected metal-phen complexes and were dosed with sub-lethal concentrations of the complexes. Whole-genome sequencing (WGS) was then performed on the mutant strains to unveil any genome changes leading to an alteration in the amino acid sequence of a protein and, therefore, indicative of acquired resistance mechanisms by the microorganisms.

2.2. Materials and Methods

2.2.1 Test complexes

The formulae, solubility, and respective codes of the metal complexes examined in this chapter are shown in **Table 2.1,** and the structures are presented in **Figure 2.1.** In order to illustrate that any observed effects were due to the complexes rather than the attached ligands or free metal ions that may be produced within the cellular environment, the activity of simple metal salts and the metal-free dicarboxylic acids were also included in the study as direct comparators. These included the following: copper(II) chloride (**$CuCl_2$**), manganese(II) chloride (**$MnCl_2$**) and silver(I) nitrate (**$AgNO_3$**), and the free ligands; 1,10-phenanthroline (**phen**), butanedioic acid (**$bdaH_2$**), pentanedioic acid (**$pdaH_2$**), hexanedioic acid (**$hxdaH_2$**), heptanedioic acid (**$hpdaH_2$**), octanedioic acid (**$odaH_2$**), undecanoic acid (**$uddaH_2$**), phthalic acid (**phH_2**) and 3,6,9-trioxaundecanedioic acid (**$tddaH_2$**). All of the complexes were dissolved in their corresponding diluent at a concentration of 10 mg/mL. Complexes which were only soluble in dimethyl sulfoxide (DMSO) were made in a 0.1% (DMSO/H2O) solution, while phen and the dicarboxylate ligands were dissolved in methanol (MeOH) and diluted down to a 1% (MeOH/H_2O) solution. The remaining complexes were fully water-soluble. Working solutions (512 µg/mL) for the bacterial screen were made up in Mueller Hinton Broth (MHB; Cruinn).

Code	Complex Formula	Solubility	Reference
	Cu(II) complexes		
Cu-ph-phen	$[Cu(ph)(phen)(H_2O)_2]$	DMSO	(Kellett *et al*., 2012)
Cu-oda	$[Cu(oda)]H_2O$	DMSO	(McCann *et al*., 1995)
Cu-oda-phen	$[Cu(oda)(phen)_2]8H_2O$	DMSO	(McCann *et al*., 1995)
Cu_2-oda-phen	$[Cu_2(oda)(phen)_4](ClO_4)_2 2.76H_2O.EtOH$	H_2O	(Devereux *et al*., 1999)
Cu-tdda	$[Cu(3,6,9\text{-}tdda)]H_2O$	H_2O	(Gandra *et al*., 2017)
Cu-tdda-phen	$[Cu(3,6,9\text{-}tdda)(phen)_2]3H_2O.EtOH$	H_2O	(Gandra *et al*., 2017)
	Mn(II) complexes		
Mn-bda	$[Mn(bda)].2H_2O$	H_2O	(McCann *et al.*, 1997a)
Mn-bda-phen	$[Mn_2(bda)_2(phen)_2(H_2O)_4].4H_2O$	H_2O	(McCann *et al.*, 1997a)
Mn-pda	$[Mn(pda)].H_2O$	H_2O	(Geraghty *et al*., 1998)
Mn-pda-phen	$[Mn(pda)(phen)]$	H_2O	(Geraghty *et al*., 1998)
Mn-hxda	$[Mn(hxda)].H_2O$	H_2O	(McCann *et al*., 1997b)
Mn-hxda-phen	$[Mn(hxda)(phen)_2(H_2O)].7H_20$	H_2O	(McCann *et al*., 1997b)
Mn-hpda	$[Mn(hpda)]$	H_2O	(McCann *et al*., 1997b)
Mn-hpda-phen	$[Mn(phen)_2(H_2O)_2][Mn(hpda)(phen)_2(H_2O)]hpda.12.5H_2O$	H_2O	(McCann *et al*., 1997b)
Mn-oda	$[Mn(oda)]H_2O$	H_2O	(Casey *et al*., 1994)
Mn-oda-phen	$[Mn_2(oda)(phen)_4(H_2O)_2][Mn_2(oda)(phen)_4(oda)_2].4H_2O$	H_2O	(Casey *et al*., 1994)
Mn-tdda	$[Mn(3,6,9\text{-}tdda)]H_2O$	H_2O	(McCann *et al.*, 1997c)
Mn-tdda-phen	$\{[Mn(3,6,9\text{-}tdda)(phen)_2]3H_2O.EtOH\}_n$	H_2O	(McCann *et al.*, 1997c)
	Ag(I) complexes		
Ag-udda	$[Ag_2(udda)]$	H_2O	(Thornton *et al*., 2016)
Ag-udda-phen	$[Ag_2(phen)_3(udda)].{}_3H_2O$	H_2O	(Thornton *et al*., 2016)
Ag-tdda	$[Ag_2(3,6,9\text{-}tdda)]_2H_2O$	H_2O	(Gandra *et al*., 2017)
Ag-tdda-phen	$[Ag_2(3,6,9\text{-}tdda)(phen)_4]EtOH$	H_2O	(Gandra *et al*., 2017)
	Controls		
	Copper chloride	H_2O	
	Manganese chloride	H_2O	
	Silver nitrate	H_2O	
	1,10-phenanthroline	MeOH	

Table 2.1 Metal complexes assessed in this study. phen = 1,10-phenanthroline, $bdaH_2$ = butanedioic acid, $pdaH_2$ = pentanedioic acid, $hxdaH_2$ = hexanedioic acid, $hpdaH_2$ = heptanedioic acid, $odaH_2$ = octanedioic acid, $uddaH_2$ = undecanoic acid, phH_2 = phthalic acid, $tddaH_2$ = 3,6,9-trioxaundecanedioic acid

Cu(II) complexes

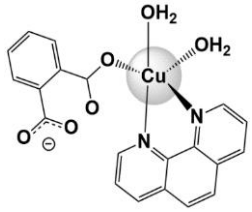

Cu-ph-phen

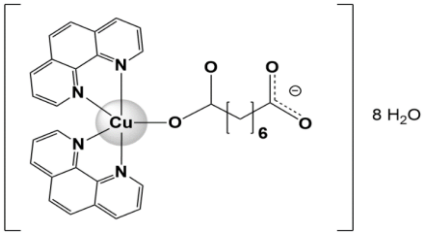

Cu-oda-phen

Mn(II) complexes

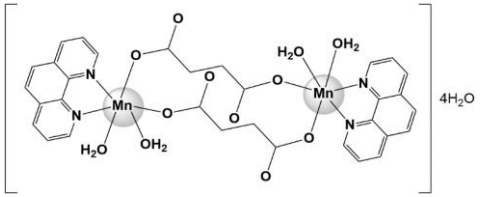

Mn-bda-phen

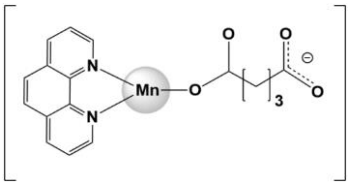

Mn-pda-phen

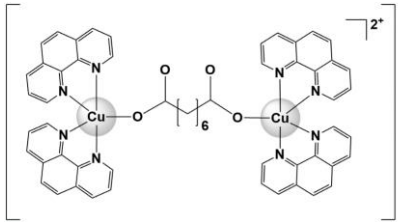

Cu2-oda-phen

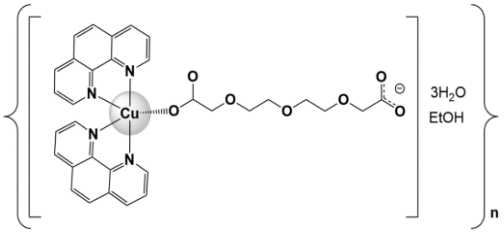

Cu-tdda-phen

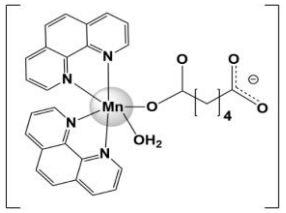

Mn-hxda-phen

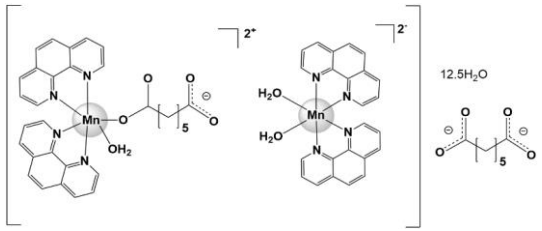

Mn-hpda-phen

Ag(I) complexes

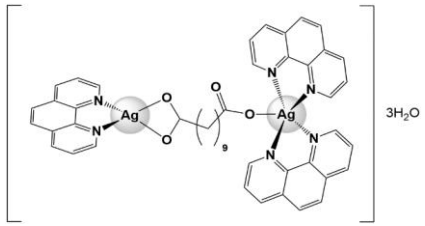

Ag-udda-phen

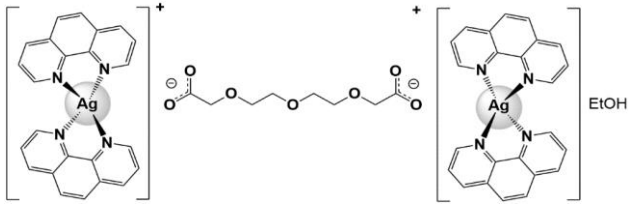

Ag-tdda-phen

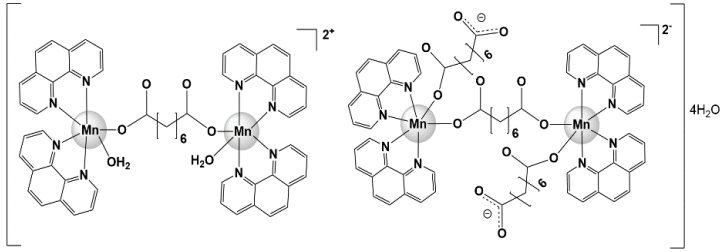

Mn-oda-phen

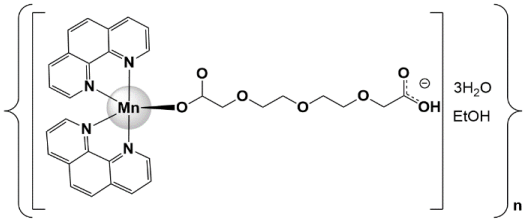

Mn-tdda-phen

Figure 2.1 Structure of metal-phen complexes examined in this study

2.2.2 Clinical isolates and control strains

The clinical isolates assessed were Gram-positive methicillin-resistant *S. aureus* (*n* = 5; MRSA1-MRSA5) and vancomycin-resistant *Enterococci* (*n* = 6; VRE1-VRE6) and Gram-negative *Enterobacterales*, including extended-spectrum β-lactamase-producer (*n* = 1; ESBL1), metallo-β-lactamase-producer (*n* = 1; MBL1) and *K. pneumoniae* carbapenemase-producer (*n* = 1; KPC1), and *P. aeruginosa* (*n* = 4; PA1-PA4) collected from a range of hospitals throughout Ireland. In addition to the clinical isolates, reference Gram-positive and Gram-negative strains obtained from the American Type Culture Collection (ATCC) were included as quality control strains. Gram-positive bacteria included *S. aureus* (ATCC 29213) and *E. faecalis* (ATCC 29212), and Gram-negative bacteria included *E. coli* (ATCC 25922), *K. pneumoniae* (ATCC 10031), and *P. aeruginosa* (ATCC 27853 and PAO1). *K. pneumoniae* (ATCC 700603 and ATCC BAA-1705) were also included in the Gram-negative panel as resistant controls of an ESBL-producer and a KPC-producer, respectively. All isolates were obtained from the School of Biological and Health Sciences TU Dublin-City campus. Under GDPR compliance, clinical isolates were provided anonymously to the researcher, and no patient data was processed.

2.2.3 Antimicrobial susceptibility testing by disc diffusion

Antimicrobial susceptibility profiles of clinical isolates were established through the qualitative Kirby-Bauer disc-diffusion method, performed according to European Committee on Antimicrobial Susceptibility Testing (EUCAST) guidelines (EUCAST, 2017a). Selections of antimicrobial agents were chosen according to EUCAST recommendations for quality control and are displayed in **Table 2.2** below**.** All antimicrobial discs were obtained from Oxoid™ Ltd (Thermo Fisher Scientific). Bacteria were stored on beads in cryogenic vials (Microbank™Cryovials) at -80 ºC and

resuscitated on 5% blood agar 24 h before experiments. Three to five colonies were transferred from the agar plate to 5 mL of sterile saline (NaCl) solution and adjusted until the turbidity matched that of a 0.5 McFarland standard (equivalent to a 1.5 $x10^8$ CFU/mL). This was carried out for each strain. When the inoculum matched the 0.5 McFarland standard, a cotton swab was used to spread it on Mueller-Hinton agar (MHA) plate. The plate was allowed to dry for 3-5 min before the corresponding antimicrobial disc (**Table 2.2**) was added to the plate with sterile forceps. After incubation for 16-18 h at 37 ºC, the zone of inhibition was determined by measuring the inhibition of growth around the disc at 3 points using a digital calliper. Studies were performed in triplicate, three independent times, and results are expressed as the mean measurement.

Strains	Antibiotic (Antibiotic class)	Disc content (µg)
Gram-positive panel		
-*S. aureus* (ATCC 29213) -Clinical isolates MRSA1-MRSA5	Cefoxitin (Cephalosporin)	30
	Ciprofloxacin (Fluoroquinolone)	5
	Gentamicin (Aminoglycosides)	10
	Linezolid (Oxazolidinones)	10
	Rifampicin (Ansamycin)	5
-*E. faecalis* (ATCC 29212) -Clinical isolates VRE1-VRE6	Ampicillin (Penicillin)	2
	Ciprofloxacin (Fluoroquinolone)	5
	Gentamicin (Aminoglycosides)	30
	Vancomycin (Glycopeptide)	5
	Linezolid (Oxazolidinone)	10
Gram-negative panel		
-*E. coli* (ATCC 25922) -*K. pneumoniae* (ATCC 10031) -*K. pneumoniae* (ATCC 700603 - ESBL, ATCC BAA1705 - KPC) -Clinical isolates ESBL1, MBL1 and KPC1	Ampicillin (Penicillin)	10
	Cefotaxime (Cephalosporin)	5
	Ceftazidime (Cephalosporin)	10
	Erthapenem (Carbapenem)	10
	Gentamicin (Aminoglycosides)	10
-*P. aeruginosa* (ATCC 27853, PAO1) -Clinical isolates PA1-PA4	Piperacillin-tazobactam (Penicillin-β-lactamase inhibitor)	36 (30-6)
	Ceftazidime (Cephalosporin)	10
	Meropenem (Carbapenem)	10
	Ciprofloxacin (Fluoroquinolone)	5
	Gentamicin (Aminoglycosides)	10

Table 2.2 Antibiotic controls used for disc diffusion assay, chosen per EUCAST guidelines

2.2.4 Minimum Inhibitory Concentration (MIC)

The minimum inhibitory concentration (MIC) was determined against clinical isolates and reference strains using the broth micro-dilution method in a 96 well-plate as specified by EUCAST (2017b). The test complexes were serially diluted two-fold in cation-adjusted Mueller-Hinton broth (CAMHB) and mixed with equal volumes (50 µL) of diluted bacteria in 96-well plates (Cruinn), thus making a final concentration range of the complexes tested between 0.25 and 256 µg/mL. Each plate contained a positive control (bacteria and broth) and a negative control (just broth). In addition to the metal

complexes, vehicle control (0.1% DMSO, 1% MeOH), starting materials (simple metal salts, phen and bridging ligands) and common antibiotics (**Table 2.2**) were assessed in the same way. The MIC was defined as the lowest concentration to prevent microorganism growth after incubation at 37 ºC for 16-18 h. Studies were performed in triplicate, three independent times, and results are expressed as the mean measurement.

2.2.5 Minimum Bactericidal Concentration (MBC)

The minimum bactericidal concentration (MBC) of the metal complexes against test isolates was determined by sub-culturing 5 μL of test dilution from each well in the MIC assay, which failed to show turbidity growth, onto antibiotic-free MHA plates. Plates were incubated for a further 16-18 h at 37 ºC. The MBCs were recorded as the lowest concentration of agent that prevented the growth (no growth observed) of an organism after subculture. Studies were performed in triplicate, three independent times, and results are expressed as the mean MBC value.

2.2.6 Fractional Inhibitory Concentration (FIC)

The antibacterial activity of Cu-tdda-phen, Mn-tdda-phen and Ag-tdda-phen complexes (**Table 2.1**) in combination with antibiotics were evaluated using the broth micro-dilution checkerboard assay (Odds, 2003). Plates were prepared as described in **Section 2.2.4.** After incubation at 37 ºC for 16-18 h, the fractional inhibitory concentration (FIC) index (FIC_I) for combinations of metal complexes with antibiotics was calculated according to the equation: $FIC_I = FIC_{(metal\ complex)} + FIC_{(antibiotic)}$. Where, $FIC_{(metal\ complex)}$ = (MIC of metal complex in combination with antibiotic)/(MIC of metal complex alone) and $FIC_{(antibiotic)}$ = (MIC of antibiotic in combination with metal complex)/(MIC of antibiotic alone). With this method, FIC_I was interpreted as synergy at a FIC index ≤0.5; additive at a FIC index >0.5 to 1; indifference at a FIC index >1 – <2; and antagonism at a FIC index ≥2

(EUCAST, 2000). Studies were performed in triplicate, three independent times, and results were expressed as mean measurement.

2.2.7 Mutant selection

Mutants with decreased susceptibility to lead metal-tdda-phen complexes, Mn(II), Cu(II), and Ag(I), were generated by serial passage of *S. aureus* ATCC 29213 and *P. aeruginosa* PAO1 to increasing concentrations of the relative complex. See **Figure 2.2** for a schematic overview of mutants.

Briefly, conical flasks containing 2 mL of MHB with two-fold increasing concentrations of either Mn-tdda-phen, Cu-tdda-phen, or Ag-tdda-phen were inoculated with 1×10^7 CFU/mL of ATCC 29213 or PAO1. Following overnight incubation at 37 °C aerated at 200 rpm, the MIC was determined by the micro-dilution method as the lowest drug concentration to inhibit bacterial growth. The conical flasks with the highest drug concentration that permitted growth were used to inoculate a series of tubes containing fresh MHB with two-fold increasing concentrations of Mn-tdda-phen, Cu-tdda-phen, or Ag-tdda-phen adjusted to a starting concentration of 1×10^7 CFU/mL. These inoculums were incubated overnight at 37 °C aerated at 200 rpm. Again, the lowest drug concentration that inhibited growth was determined by the microdilution method to be the MIC, and the inoculum growing at the highest drug concentration was used to prepare the inoculum for the following passage. In total, there were 3 passages carried out to produce mutant strains of ATCC 29213 exposed to metal-tdda-phen complexes (with a final MIC of 8 µg/mL) and 8 passages to produce mutant strains of PAO1 exposed to metal-tdda-phen complexes (with a final MIC of 256 µg/mL).

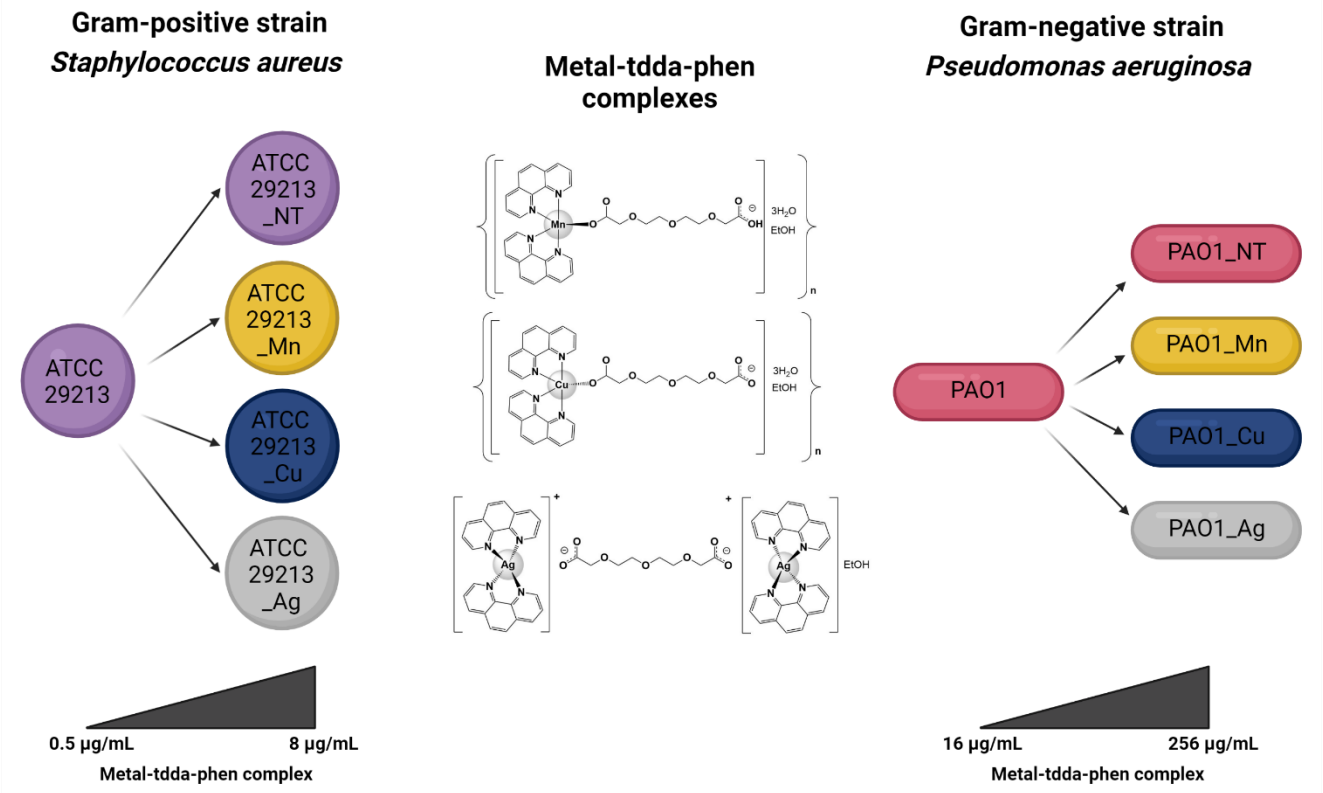

Figure 2.2 Schematic overview of reducing drug susceptibility of lead metal-tdda-phen complexes, Mn-tdda-phen, Cu-tdda-phen, and Ag-tdda-phen in reference strains *S. aureus* ATCC 29213 (ATCC 29213_Mn, ATCC 29213_Cu, ATCC 29213_Ag, respectively) and *P. aeruginosa* PAO1 (PAO1_Mn, PAO1_Cu, PAO1_Ag, respectively). ATCC 29213_NT and PAO1_NT refer to the control strains that did not receive any treatment.

2.2.8 Whole-genome sequencing and analysis

The whole-genome sequencing (WGS) of mutant strains *S. aureus* ATCC 29213 (ATCC 29213_NT, ATCC 29213_Mn, ATCC 29213_Cu, ATCC 29213_Ag, respectively) and *P. aeruginosa* PAO1 (PAO1_NT, PAO1_Mn, PAO1_Cu, PAO1_Ag, respectively) were performed by MicrobesNG (http://www.microbesng.com). The sequence files for this study have been deposited in the European Nucleotide Archive (ENA) at EMBL-EBI under accession number PRJEB52838.

Ms Jasmine Hurley, as a part of her TU Dublin undergraduate research project, carried out the analysis of WGS data. Briefly, FASTQ files received from MicrobesNG were imported into Geneious Prime and mapped against reference genomes from the NCBI Nucleotide database. 'PAO1, complete genome' (Accession no. NC_002516) was used as the reference genome for the *P. aeruginosa* files. There was no reference genome available for ATCC 29213 in the NCBI Nucleotide database; instead, 'NCTC 8325, complete genome' (Accession no. CP000253) was used as the reference genome for the *S. aureus* files. Variants were detected within Geneious Prime and exported. The settings used were taken from the WGS guide created by Gautam *et al.* (2019).

Variants in resistant strains of *P. aeruginosa* were compared to each other, and the *P. aeruginosa* control using Ablebits add-in in Microsoft Excel. Any variants that were shared between at least two resistant strains and were not present in the control were noted. BLAST searches were conducted to identify the possible function of any variant-containing hypothetical proteins.

2.3. Results

2.3.1 Susceptibility profile of all clinical isolates

Clinical isolates were first assessed against various commercial antibacterial agents commonly used within the clinic. The susceptibility profile of Gram-positive bacteria represented by *S. aureus* and *Enterococcus* species (*E. faecium* and *E. faecalis*) and Gram-negative bacteria, *Enterobacterales* (*E. coli and K. pneumoniae*) and *P. aeruginosa* are presented in **Table 2.3**. Each representative bacterial group consists of an ATCC control strain and clinical strains isolated from patients with bloodstream infections (BSI's) in Irish hospitals. These microorganism's susceptibility profiles were assessed per the EUCAST guidelines (EUCAST, 2017a, 2017c). The zones of inhibition for the ATCC control strains fell within the accepted ranges (EUCAST, 2017b).

All five clinical MRSA strains (MRSA1-MRSA5) were resistant to cefoxitin and ciprofloxacin, while two (MRSA1 and MRSA2) isolates were also resistant to gentamicin (**Table 2.3**). The clinical, vancomycin-resistant *Enterococci* strains (VRE1-VRE6) demonstrated resistance to all standard antibacterial agents. Representative Gram-negative sub-panels included the *Enterobacterales* panel encompassed by extended-spectrum β-lactamase (ESBL)-producing strains, ATCC 700603 (*K. pneumoniae)* and clinical isolate ESBL1, metallo-β-lactamase (MBL)-producing clinical isolate MBL1, and *K. pneumoniae* carbapenemase (KPC)-producing strain ATCC BAA1705 and clinical isolate KPC1. As expected, the ESBL+ strain demonstrated resistance to all β-lactams tested but remained susceptible to the carbapenem. Similarly, both MBL+ and KPC+ CRE test strains also demonstrated the expected antimicrobial susceptibility testing (AST) profiles with resistance expressed to all β-lactams, including the carbapenem, a last resort drug. The *P. aeruginosa* group incorporated four clinical isolates (PA1-PA4).

PA1 was susceptible to all test antibiotics except gentamicin, while PA2, PA3 and PA4 were resistant to all examined agents.

Based on the criteria released by the European Centre for Disease Prevention and Control (ECDC) and the Centres for Disease Control and Prevention (CDC), the bacterial panel is comprised of several multidrug-resistant (MDR) isolates which are defined as non-susceptibility to at least one agent in three or more antimicrobial classes (Magiorakos *et al*., 2012).

Species	Strain	Antibiotic (zone of inhibition as nm)				
Gram-positive panel						
		Cefoxitin	**Ciprofloxacin**	**Gentamicin**	**Linezolid**	**Rifampicin**
Staphylococcus aureus	**ATCC 29213**	27 (S)	24 (S)	21 (S)	24 (S)	33 (S)
	MRSA1	10 (R)	0 (R)	8 (R)	23 (S)	27 (S)
	MRSA2	13 (R)	0 (R)	8 (R)	22 (S)	28 (S)
	MRSA3	11 (R)	0 (R)	19 (S)	24 (S)	27 (S)
	MRSA4	15 (R)	0 (R)	21 (S)	24 (S)	27 (S)
	MRSA5	13 (R)	0 (R)	20 (S)	24 (S)	28 (S)
		Vancomycin	**Ciprofloxacin**	**Gentamicin**	**Linezolid**	**Ampicillin**
Enterococcus faecalis, Enterococcus faecium	**ATCC 29212**	24 (S)	25 (S)	20 (S)	23 (S)	24 (S)
	VRE1	0 (R)	0 (R)	0 (R)	0 (R)	0 (R)
	VRE2	0 (R)	0 (R)	0 (R)	13 (R)	0 (R)
	VRE3	0 (R)	0 (R)	0 (R)	11 (R)	0 (R)
	VRE4	0 (R)	0 (R)	0 (R)	13 (R)	0 (R)
	VRE5	0 (R)	0 (R)	0 (R)	11 (R)	0 (R)
	VRE6	0 (R)	0 (R)	0 (R)	10 (R)	0 (R)
Gram-negative panel						
		Ertapenem	**Ceftazidime**	**Cefotaxime**	**Gentamicin**	**Ampicillin**
Escherichia coli, Klebsiella pneumoniae	**ATCC 25922**	32 (S)	26 (S)	27 (S)	21 (S)	20 (S)
	ATCC 10031	27 (S)	13 (R)	14 (R)	13 (R)	10 (R)
	ATCC 700603	26 (S)	8 (R)	15 (R)	12 (R)	0 (R)
	ESBL1	25 (S)	0 (R)	0 (R)	0 (R)	0 (R)
	MBL1	0 (R)	0 (R)	0 (R)	0 (R)	0 (R)
	ATCC BAA1705	0 (R)	0 (R)	0 (R)	17 (S)	0 (R)
	KPC1	0 (R)	0 (R)	0 (R)	0 (R)	0 (R)
		Ceftazidime	**Ciprofloxacin**	**Gentamicin**	**Meropenem**	**Piperacillin-Tazobactam**
Pseudomonas aeruginosa	**ATCC 27853**	25 (S)	29 (S)	20 (S)	27 (S)	25 (S)
	PAO1	15 (S)	25 (S)	18 (S)	18 (S)	25 (S)
	PA1	20 (S)	24 (S)	13 (R)	25 (S)	21 (S)
	PA2	16 (R)	0 (R)	0 (R)	0 (R)	0 (R)
	PA3	0 (R)	0 (R)	0 (R)	17 (R)	0 (R)
	PA4	0 (R)	0 (R)	0 (R)	9 (R)	0 (R)

Table 2.3 Susceptibility profile of control strains and clinical isolates as determined by disc diffusion and classified according to EUCAST guidelines. Zones of inhibition are presented in mm. Resistant (R; Red); Susceptible (S; Green).

2.3.2 Antibacterial testing of metal complexes

Once the susceptibility profiles of the clinical isolates were established, *in vitro* studies were carried out to determine the antibacterial activity of the metal-dicarboxylate-phen complexes against the Gram-positive and Gram-negative panels (**Figure 2.3** and **2.4,** respectively). Quantitative serial broth dilutions of each complex were performed to establish the MIC and MBC values. In addition, the simple metal salts, metal-free ligands and prescription antibacterial agents were included. Ciprofloxacin and gentamicin were used as controls for the Gram-positive panel as they are well-known broad-spectrum antibiotics with different activity mechanisms and inhibition of DNA synthesis (ciprofloxacin) and protein synthesis (gentamicin). Gentamicin and meropenem (inhibition of cell wall synthesis) were utilised for the Gram-negative panel.

2.3.2.1 Gram-positive panel

Staphylococcus aureus

The MIC values (µg/mL) of the metal complexes and commonly used antibiotics against *S. aureus* strains are displayed in **Figure 2.3.A** below. Except for Mn-hpda-phen, metal complexes containing the phen ligand demonstrated a higher level of antibacterial activity against both the control strain (ATCC 29213) and the clinical isolates (MRSA1-MRSA5) in comparison to their non-phen precursors. The MIC value for gentamicin was 1 µg/mL (1.74 µM) for ATCC 29213 (*S. aureus*) and MRSA3-MRSA5 isolates which interprets them as susceptible to the antibiotic according to EUCAST breakpoints. Ciprofloxacin also had a MIC value of 1 µg/mL (3.02 µM) against ATCC 29213, whilst all of the clinical isolates were resistant to the antibiotic (>256 µg/mL) (>772 µM). The Cu(II)-phen complexes, Cu-ph-phen (2.25 µM), Cu-oda-phen (1.35 µM), Cu_2-oda-phen (0.76 µM) and Cu-tdda-phen (1.34 µM), and Mn(II) complex Mn-tdda-phen (1.36 µM) also produced a MIC of 1 µg/mL against ATCC 29213. The simple salts, $CuCl_2$ and $MnCl_2$,

had no appreciable effects against the strain (**Table A.1**), and although phen alone was able to inhibit growth, it was not as effective as the Cu(II) and Mn(I)-phen complexes. Moreover, none of the dicarboxylic acid ligands demonstrated any inhibitory effects (data not shown), and this is in agreement with previously reported data (Devereux *et al*., 2000). This suggests that the activity of metal-phen complexes are a consequence of the whole complex rather than its separate constituent parts. However, activity is not necessarily dependent on the number of coordinated phen ligands present per complex. For instance, Cu-oda-phen, Cu-tdda-phen and Mn-tdda-phen contain two phen ligands, and Cu_2-oda-phen contains four ligands. Mn-oda-phen has the greatest amount of phen ligands attached (eight) but had a MIC value of 32 µg/mL (104 µM) against ATCC 29213. A sub-set of these complexes (Mn-oda-phen, Mn-tdda-phen and Cu_2-oda-phen) was previously examined against *Mycobacterium tuberculosis*, and a similar observation was made (McCarron *et al*., 2018).

Cu-tdda-phen had an MBC value of 4 µg/mL (5.38 µM), which matched the MBC of gentamicin (6.95 µM). Antibiotics are usually regarded as bactericidal if the MBC is no more than four times the MIC value (Levison and Levison, 2009), so in this regard, the majority of Cu-tdda-phen MBCs are four times the established MIC value (**Table A.1**). Strains resistant to gentamicin had a MIC value of 64 µg/mL (100 µM) (MRSA1) and 128 µg/mL (500 µM) (MRSA2), while Mn-tdda-phen (MIC of 1 µg/mL/1.36 µM and 8 µg/mL/10.9 µM against MRSA1 and MRSA2, respectively) and Cu-tdda-phen required a lower concentration to inhibit the growth of the isolates (MIC of 8 µg/mL/10.8 µM against both). The similar activities of Cu-tdda-phen and Mn-tdda-phen suggest that, in these particular cases, antimicrobial activity is independent of the nature of the central transition metal dication. This supports previous observations that, in certain instances, activity can be independent of the metal present (Frei *et al*., 2020). However, the metal

complexes that contain an Ag(I) nucleus behaved differently from their counterparts. Ag-tdda-phen (6.65-13.3 µM) and Ag-udda-phen (7.81-15.6 µM) had a MIC range of 8-16 µg/mL across all of the test isolates. Their non-phen precursors, Ag-tdda (67 µM) and Ag-udda (74 µM) maintained activity across all strains at the administered concentration of 32 µg/mL. It was postulated that these complexes exerted their toxicity by releasing Ag(I) ions from the complex into the growth medium. This is substantiated by the observation that the simple metal salt, $AgNO_3$, exerted similar activity (MIC value 4-64 µg/mL) (**Table A.1**). This is not surprising as silver is widely reported to have strong antibacterial properties, particularly against *S. aureus*, with a multi-target mode of action and the ability to overcome antibiotic resistance (Wang *et al*., 2021a).

Enterococcus faecium* and *Enterococcus faecalis

The MIC values of the metal complexes and commonly used antibiotics against *Enteroccous* spp are displayed in **Figure 2.3.B**. The control antibiotics ciprofloxacin and gentamicin had a MIC of 1 µg/mL (3.02 µM) and 8 µg/mL (18.3 µM), respectively, against the control strain ATCC 29212, which fell within the recommended values provided by EUCAST. In contrast, all the clinical isolates had MICs greater than the highest concentration of antibiotics used (256 µg/mL), thus classifying them as resistant to the antibacterial agents. Fewer metal complexes exercised antibacterial action against the *Enterococci* group of isolates. Although the Cu(II)-phen complexes inhibited the growth of all strains, considerably higher concentrations were required (16-256 µg/mL) (12.2-443 µM). Of the Cu(II) and Mn(II) panels, Cu-tdda-phen and Mn-tdda-phen were the most active. Both complexes established MICs of 16-64 µg/mL (21.5-87 µM) across the bacterial strains and were superior to the control antibiotics, ciprofloxacin and gentamicin (>256 µg/mL). Moreover, the MBCs for Cu-tdda-phen ranged from 32 µg/mL (43 µM) to 128 µg/mL (172 µM) (**Table A.2**), demonstrating that not only was the

complex able to inhibit the growth of highly resistant microorganisms at lower concentrations than the control antibiotics but was also able to kill them at concentrations below the MICs of the antibiotics. As with the MRSA isolates, the Ag(I) complexes behaved differently from the other metal complexes. Ag-tdda-phen (6.65-13.3 µM) and Ag-udda-phen (7.81-15.6 µM) had a MIC range of 8-16 µg/mL across all strains, whilst their non-phen precursors, Ag-tdda (67 µM) and Ag-udda (74 µM), respectively, required 32 µg/mL to inhibit the growth of the bacterial isolates. The MBCs of the phen-containing complexes, Ag-tdda-phen (26.6-53.2 µM) and Ag-udda-phen (31.2-62.5 µM), were 32-64 µg/mL and their non-phen complexes had an MBC value of 128 µg/mL (271-297 µM). The simple metal salt, $AgNO_3$, inhibited all bacterial isolates at a concentration of 4 µg/mL, outperforming the Ag(I) complexes. However, the Ag(I) complexes were able to kill the same bacteria at lower concentrations. Metal-free phen and the dicarboxylic acids did not have MBC values within the test concentration range, and therefore it is postulated that coordination of the ligands to the metal enhances the bactericidal effect.

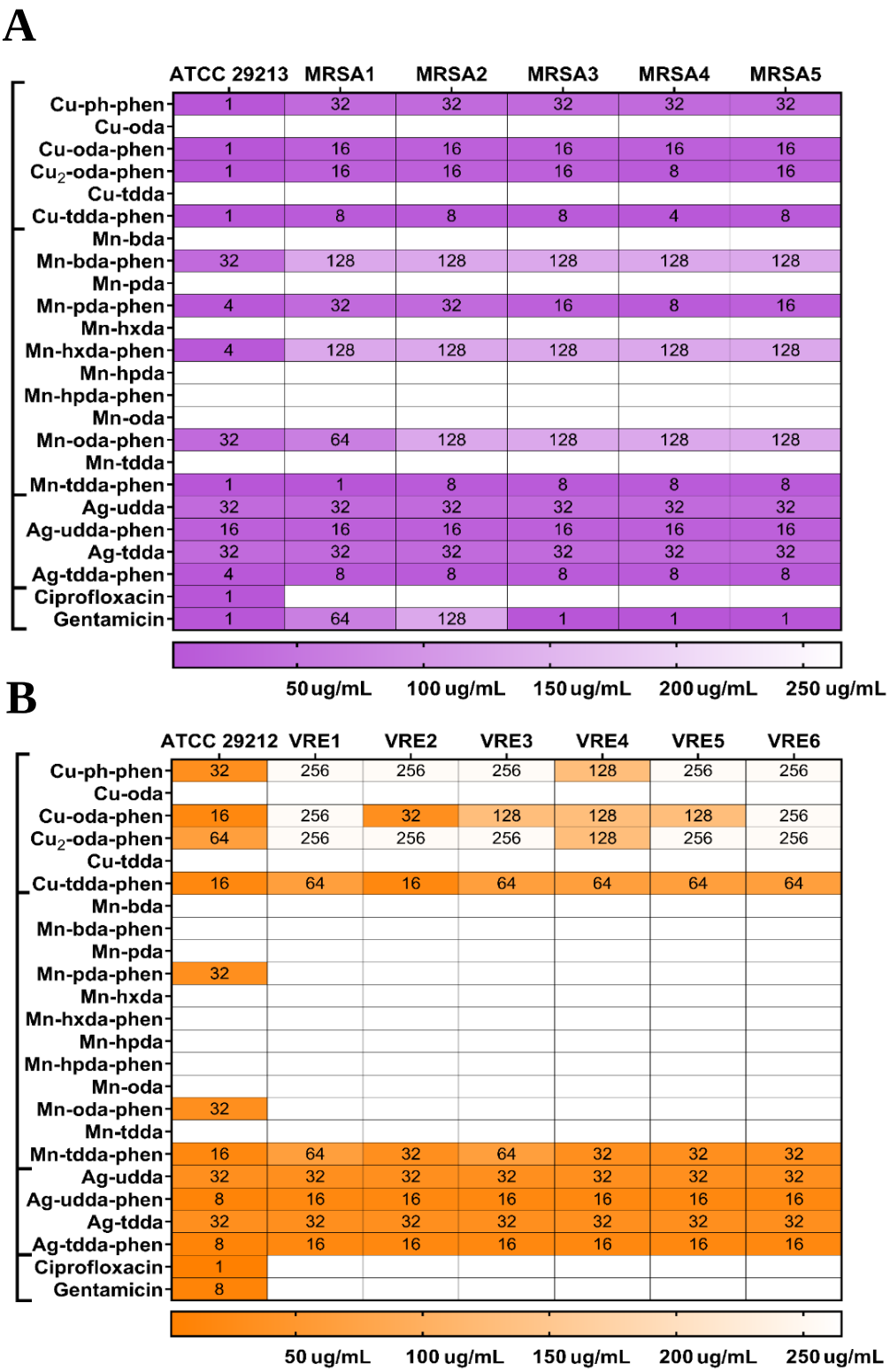

Figure 2.3 Gram-positive panel. Heat map displaying the mean MIC of metal complexes, grouped according to their metal centre and antibiotic controls (ciprofloxacin and gentamicin) for (**A**) *Staphylococcus aureus*, control strain ATCC 29213, and clinical isolates, MRSA1-MRSA5, and (**B**) *Enterococcus* spp, control strain ATCC 29212 (*E. faecalis*) and clinical isolates, VRE1-VRE6. Graph tiles that are white without a value did not have a MIC that fell within the tested range (>256 µg/mL). Detail of the concentration range, and its relation to colour, is displayed in the figure legend

2.3.2.2 Gram-negative panel

Escherichia coli* and *Klebsiella pneumoniae

The *Enterobacterales* panel are represented by susceptible control strains ATCC 25922 (*E. coli*) and ATCC 10031 (*K. pneumoniae*), resistant control strains ATCC 700603 (*K. pneumoniae* extended-spectrum β-lactamase (ESBL)-producer) and ATCC BAA1705 (*K. pneumoniae* carbapenemase (KPC)-producer), and clinical isolates ESBL producer (ESBL1) a metallo-β-lactamase (MBL)-producer (MBL1) and a KPC producer (KPC1). **Figure 2.4.A** highlights that a reduced selection of complexes retained activity when screened against Gram-negative bacteria and, overall, complexes containing a phen ligand had heightened activity. Of the Cu(II) complexes, Cu_2-oda-phen (48.7-194 µM) and Cu-oda-phen (80.5-345 µM) had a MIC value in the range of 64-256 µg/mL, while Cu-ph-phen was essentially inactive against the Gram-negative panel. Gram-negative bacteria, unlike Gram-positive bacteria, possess a protective outer membrane (OM) which can impede access to some antibacterial agents, which can be a limiting factor in a chemotherapeutic treatment protocol (Impey *et al*., 2020). Cu-tdda-phen (MICs = 16-64 µg/mL) (21.5-86 µM), Mn-tdda-phen (MIC = 16-128 µg/mL) (21.8-174 µM) and Ag-tdda-phen (MIC = 8-64 µg/mL) (6.7-53.2 µM) were the most active agents from within each representative group. The Ag(I) complexes, Ag-udda, Ag-udda-phen and Ag-tdda, produced a similar toxicity profile as the silver salt, $AgNO_3$ (**Table A.3**), across all strains, again suggesting that the binuclear silver complexes may be exerting activity by releasing Ag(I) ions into solution. Ag-tdda-phen generated an MBC value (64-128 µg/mL) twice that of its MIC value (32-64 µg/mL) across the clinical isolates apart from ESBL1, which required 4 times the MIC value (16 µg/mL) to eliminate the isolate. Transmission electron microscopy observation of $AgNO_3$ treated *E. coli* identified morphological and structural changes and enhanced permeability in the bacterial cell envelope (RubenMorones-

Ramirez *et al*., 2013), suggesting that the Ag(I) complexes are exerting their antibacterial activity in this manner.

Pseudomonas aeruginosa

When investigating the MIC of the metal complexes (**Figure 2.4.B**), Cu-tdda-phen (21.5-86 µM) and Mn-tdda-phen (21.8-87 µM) were decidedly the most active complexes from those that harbour a Cu(II) or Mn(II) nucleus. A related activity pattern was observed through the test strains, with ATCC 27853 having a MIC value of 16 µg/mL (21.5 µM and 21.8 µM, respectively) for both chelates and an MBC value of 32 µg/mL (43 µM and 43.5 µM, respectively). For the Cu(II) and Mn(II) tdda-phen complexes to inhibit the growth of the clinical isolates PA2 and PA4, a MIC value of 16 µg/mL was necessary, whereas both of these bacterial strains were resistant to the control antibiotics, meropenem (MIC = >256 µg/mL, >585 µM) and gentamicin (MIC = >256 µg/mL, 444 µM). Ag-tdda-phen presented with an MIC value of 8 µg/mL (6.6 µM) for ATCC 27853 and PA1, and 32-64 µg/mL (26.6-53.2 µM) across the remaining strains. The non-phen derivative, Ag-tdda, had a MIC value of 128-256 µg/mL (106-213 µM) for all clinical strains, indicating that the inclusion of the phen ligand caused a more potent effect.

.

A

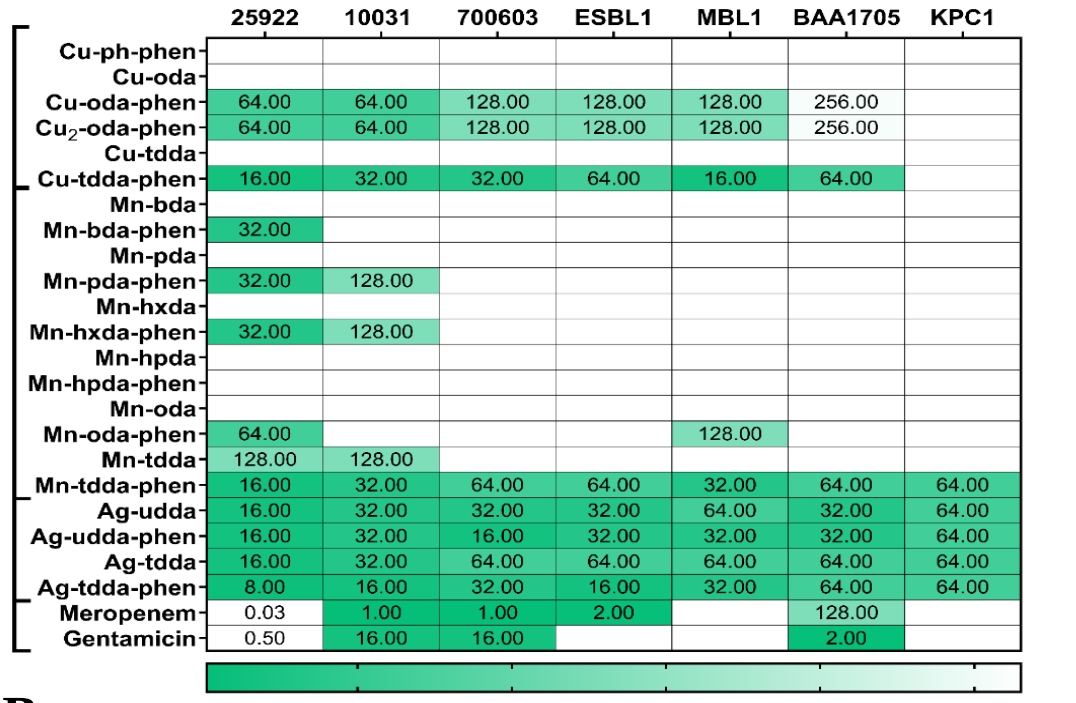

B

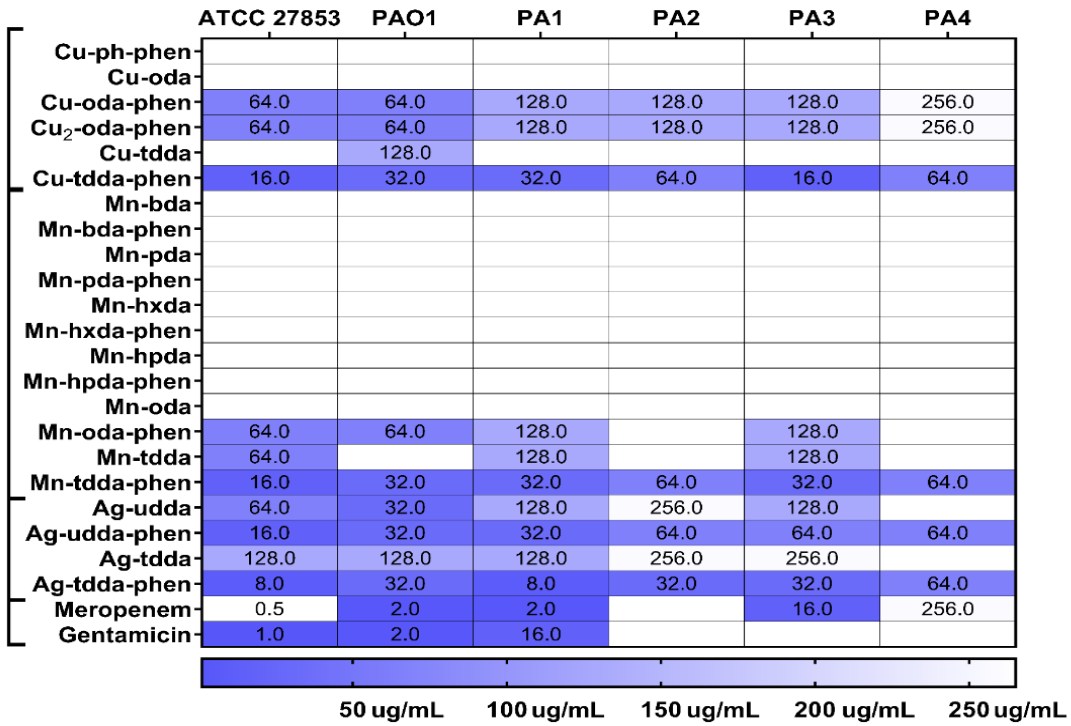

Figure 2.4 Gram-negative panel. Heat map displaying the mean MIC of metal complexes, grouped according to their metal centre and antibiotic controls (meropenem and gentamicin) for (**A**) Enterobacterales, control strain ATCC 29213 (*E. coli*), ATCC 10031 (*K. pneumoniae*), ATCC 700603 (ESBL+), ATCC BAA1705 (KPC+) and clinical isolates ESBL1, MBL1 and KPC1, and (**B**) *Pseudomonas aeruginosa*, control strain ATCC 27853, PAO1 and clinical isolates PA1-PA4. Graph tiles that are white without a value did not have a MIC that fell within the tested range (>256 µg/mL). Detail of the concentration range, and its relation to colour, is displayed in the figure legend.

2.3.3 Combination effects of selected clinical isolates with lead metal-tdda-phen complexes and antibiotics

Combination therapy is a method for restoring the clinical efficacy of antibiotics and avoiding the development of drug resistance in the clinic. Although a single agent antimicrobial therapy is generally preferred, combining two or more antibacterial agents is recommended under certain circumstances. This approach would be selected for polymicrobial infections (Stacy *et al*., 2016), to delay the evolution of drug resistance (Angst *et al*., 2021), to reduce the dosage of individual drugs, and in turn potentially reduce adverse effects (Niederman *et al*., 2021), or to potentially eliminate resistant strains (Coates *et al*., 2020). However, the selection of appropriate combinatorial treatment is critical for the successful elimination of infections. Metal-tdda-phen complexes and control antibiotics were used to determine the interaction and potency of the combined treatments compared to their individual activities on the selected clinical isolates. Representative isolates were chosen from each genus, particularly strains with a more extensive resistance profile (**Table 2.3**). They were as follows: *S. aureus* clinical isolates, MRSA1 and MRSA2, *Enterococci* isolates, VRE1 and VRE6, *Enterobacterales*, ATCC 700603, ESBL1, MBL1, ATCC BAA1705 and KPC1, and *P. aeruginosa* isolates PA2 and PA4. Selected antibacterial agents were unique to the group of bacteria, for instance, antibiotics chosen for VRE isolates were vancomycin and linezolid. Finally, a representative metal complex from each different metal-containing series was selected including the very active tdda-phen family, Cu-tdda-phen, Mn-tdda-phen and Ag-tdda-phen. When drugs are combined, their effects on bacterial cells may be amplified, slightly enhanced, weakened, or have no effect at all, so the drugs may show synergistic, additive, indifferent or antagonistic interactions, respectively. On the basis of their FIC index, each combination was categorized as synergistic (≤0.5), additive (>0.5 to 1), indifferent (>1 to

<2) or antagonistic (≥2), according to the EUCAST guidelines (EUCAST, 2000). Ideally, for the combination of metal complex with antibiotic, a synergistic effect was desired.

2.3.3.1 Combination effects in selected Gram-positive isolates

Methicillin-resistant *Staphylococcus aureus* (MRSA)

Ciprofloxacin is a bactericidal antibiotic of the fluoroquinolone class that targets DNA replication (Correia *et al*., 2017), and gentamicin is a clinically significant aminoglycoside antibiotic that inhibits protein synthesis (Magnet and Blanchard, 2005). Results for the combinations of the antibiotics, ciprofloxacin and gentamicin, with Cu-tdda-phen, Mn-tdda-phen and Ag-tdda-phen against the clinical isolates, MRSA1 and MRSA2, are presented in **Table 2.4**. All three metal-tdda-phen complexes in combination with ciprofloxacin produced an indifferent effect. This means that the inhibitory effect of the combined agents is the same as that of the more active drug alone, this being the metal-tdda-phen complexes. When the complexes were co-administered with gentamicin, the combination was synergistic in terms of the FIC_I value. In this context, the inhibitory effect against the bacterium in the combination was more potent than that of the individual agents alone.

Antibiotic	Test complexes	Isolate	FIC Index	Interpretation
Ciprofloxacin	Cu-tdda-phen	MRSA1	1.5	Indifferent
		MRSA2	1.5	Indifferent
	Mn-tdda-phen	MRSA1	1.5	Indifferent
		MRSA2	1.5	Indifferent
	Ag-tdda-phen	MRSA1	1.3	Indifferent
		MRSA2	1.5	Indifferent
Gentamicin	Cu-tdda-phen	MRSA1	0.05	Synergistic
		MRSA2	0.13	Synergistic
	Mn-tdda-phen	MRSA1	0.27	Synergistic
		MRSA2	0.07	Synergistic
	Ag-tdda-phen	MRSA1	0.02	Synergistic
		MRSA2	0.04	Synergistic

Table 2.4 The fractional inhibitory concentration (FIC) index of metal-tdda-phen analogues Cu-tdda-phen, Mn-tdda-phen and Ag-tdda-phen in MRSA clinical isolates, MRSA1 and MRSA2 with antibiotics ciprofloxacin and gentamicin. FIC_I is the sum of the FIC (**Table A.5**) of the two agents used in the combination**.**

Vancomycin-resistant *Enterococci* (VRE)

Vancomycin, a glycopeptide, exerts its bactericidal effect by binding to D-alanyl-D-alanine residues of the bacterial cell wall and preventing the polymerization of peptidoglycans (Lee *et al*., 2019). Linezolid is the first synthetic oxazolidinone antibiotic with a unique mechanism of action as it appears to block the initiation of protein production (Chen *et al*., 2020). All combinations of vancomycin or linezolid with the three metal-tdda-phen complexes against the clinical isolates, VRE1 and VRE6, produced indifferent effects (**Table 2.5**)

Antibiotic	Test complexes	Isolate	FIC Index	Interpretation
Vancomycin	Cu-tdda-phen	VRE1	1.5	Indifferent
		VRE6	1.25	Indifferent
	Mn-tdda-phen	VRE1	1.5	Indifferent
		VRE6	1.5	Indifferent
	Ag-tdda-phen	VRE1	1.03	Indifferent
		VRE6	1.06	Indifferent
Linezolid	Cu-tdda-phen	VRE1	1.5	Indifferent
		VRE6	1.5	Indifferent
	Mn-tdda-phen	VRE1	1.5	Indifferent
		VRE6	1.5	Indifferent
	Ag-tdda-phen	VRE1	1.25	Indifferent
		VRE6	1.25	Indifferent

Table 2.5 The fractional inhibitory concentration (FIC) index of metal-tdda-phen analogues Cu-tdda-phen, Mn-tdda-phen and Ag-tdda-phen in VRE clinical isolates, VER1 and VRE6 with antibiotics vancomycin and linezolid. FIC_I is the sum of the FIC (**Table A.6**) of the two agents used in the combination.

2.3.3.2 Combination effects in Gram-negative strains

Enterobacterales isolates

Ceftazidime is a third-generation cephalosporin antibiotic that exerts its bactericidal action by inhibiting enzymes responsible for cell wall synthesis primarily through penicillin-binding protein 3 (PBP3) (Testa *et al*., 2015). Meropenem is a broad-spectrum antibacterial agent of the carbapenem class that inhibits cell wall synthesis also through binding to PBP targets. Its strongest affinities are toward PBPs 2, 3 and 4 of Gram-negative bacteria and PBPs 1, 2 and 4 of Gram-positive bacteria (Zandi and Townsend, 2021). The strains representing the test *Enterobacterales* group were ATCC 700603, ATCC BAA1705, ESBL1, MBL1 and KPC1 isolates (**Table 2.6**). Co-exposure of ceftazidime with Cu-tdda-phen or Mn-tdda-phen, and the combinations of all of the metal-tdda-phen complexes with meropenem, caused an indifferent effect with all strains (the inhibitory rate of the combined agents was the same as that of the more active drug alone, that being the metal-tdda-phen complex). The addition of Ag-tdda-phen to

ceftazidime also had an indifferent effect against ESBL1 and KPC1 strains. However, the same combination against ATCC 700603, MBL1 and ATCC BAA1705 produced an additive effect (the combination of agents did not increase the inhibitory effect to the extent that was better than administering the concentration of the more active single drug alone). The same effect was observed with the combinations of Cu-tdda-phen, Mn-tdda-phen and Ag-tdda-phen with gentamicin against ESBL1. There have been numerous reports of simple silver or silver nanoparticles (AgNPs) restoring the activity of ineffective antibiotics against multidrug-resistant strains (Liang *et al*., 2018; Zou *et al*., 2018; She *et al*., 2019). One report stated that the combination of AgNPs with ceftazidime were synergistic against 62.50% of examined ESBL+ *K. pneumoniae* isolates, confirming the inhibition of β-lactamase enzymes in isolates exposed to AgNPs (Panáček *et al*., 2016).

Antibiotic	Test complexes	Isolate	FIC Index	Interpretation
Ceftazidime	Cu-tdda-phen	ATCC 700603	1.13	Indifferent
		ESBL1	1.13	Indifferent
		MBL1	1.03	Indifferent
		ATCC BAA1705	1.13	Indifferent
		KPC1	1.50	Indifferent
	Mn-tdda-phen	ATCC 700603	1.25	Indifferent
		ESBL1	1.13	Indifferent
		MBL1	1.06	Indifferent
		ATCC BAA1705	1.13	Indifferent
		KPC1	1.13	Indifferent
	Ag-tdda-phen	ATCC 700603	0.56	Additive
		ESBL1	1.03	Indifferent
		MBL1	0.53	Additive
		ATCC BAA1705	0.56	Additive
		KPC1	1.13	Indifferent
Meropenem	Cu-tdda-phen	MBL1	1.03	Indifferent
		ATCC BAA1705	1.50	Indifferent
		KPC1	1.50	Indifferent
	Mn-tdda-phen	MBL1	1.06	Indifferent
		ATCC BAA1705	1.50	Indifferent
		KPC1	1.13	Indifferent
	Ag-tdda-phen	MBL1	1.06	Indifferent
		ATCC BAA1705	1.50	Indifferent
		KPC1	1.13	Indifferent
Gentamicin	Cu-tdda-phen	ATCC 700603	1.50	Indifferent
		ESBL1	0.56	Additive
	Mn-tdda-phen	ATCC 700603	1.25	Indifferent
		ESBL1	0.56	Additive
	Ag-tdda-phen	ATCC 700603	1.50	Indifferent
		ESBL1	0.52	Additive

Table 2.6 The fractional inhibitory concentration (FIC) index of metal-tdda-phen analogues Cu-tdda-phen, Mn-tdda-phen and Ag-tdda-phen in *Enterobacterales* clinical isolates with antibiotics ceftazidime, meropenem and gentamicin. FIC_I is the sum of the FIC (**Table A.7**) of the two agents used in the combination.

Pseudomonas aeruginosa

When the clinical isolates PA2 and PA4 were tested with the metal-tdda-phen complexes in tandem with meropenem and gentamicin, the results were indifferent and synergistic, respectively (**Table 2.7**).

Antibiotic	Test complexes	Isolate	FIC Index	Interpretation
Meropenem	Cu-tdda-phen	PA2	1.13	Indifferent
		PA4	1.25	Indifferent
	Mn-tdda-phen	PA2	1.13	Indifferent
		PA4	1.25	Indifferent
	Ag-tdda-phen	PA2	1.06	Indifferent
		PA4	1.25	Indifferent
Gentamicin	Cu-tdda-phen	PA2	0.07	Synergistic
		PA4	0.07	Synergistic
	Mn-tdda-phen	PA2	0.07	Synergistic
		PA4	0.07	Synergistic
	Ag-tdda-phen	PA2	0.01	Synergistic
		PA4	0.00	Synergistic

Table 2.7 The fractional inhibitory concentration (FIC) index of metal-tdda-phen analogues Cu-tdda-phen, Mn-tdda-phen and Ag-tdda-phen in *P. aeruginosa* clinical isolates, PA2 and PA4 with antibiotics meropenem and gentamicin. FIC_I is the sum of the FIC (**Table A.7**) of the two agents used in the combination.

2.3.4 Whole-genome sequencing of Gram-positive *Staphylococcus aureus* and Gram-negative *Pseudomonas aeruginosa* for resistance properties to lead metal-tdda-phen complexes

Wild type *S. aureus* strain ATCC 29213 and *P. aeruginosa* strain PAO1 were exposed to sub-lethal concentrations of lead metal-tdda-phen complexes to induce resistance properties (**Figure 2.2**). This generated distinct strains denoted as ATCC 29213_Mn and PAO1_Mn, ATCC 29213_Cu and PAO1_Cu, and ATCC 29213_Ag and PAO1_Ag that were exposed to Mn-tdda-phen, Cu-tdda-phen and Ag-tdda-phen, respectively. Whole-genome sequencing (WGS) was performed on all strains, and the genomes were subsequently analyzed using the bioinformatics programme 'Geneious Prime'. The

genomes of the strains that received metal-tdda-phen complexes were compared to those that received no treatment (denoted as ATCC 29213_NT and PAO1_NT).

2.3.4.1 Gram-positive *Staphylococcus aureus* ATCC 29213

Only one mutation was shared between the metal-tdda-phen *S. aureus* treated strains (ATCC29213_Cu and ATCC29213_Ag) while concurrently absent from the non-treated control (ATCC29213_NT). This mutation results in the replacement of threonine with isoleucine in a conserved hypothetical protein encoded by an unnamed gene (SAOUHSC_01873). A BLAST search revealed that this gene matched the *ebh* gene in '*Staphylococcus aureus* strain NCTC8325 genome assembly chromosome 1', which encodes a surface protein known as Ebh. The protein Ebh promotes cell growth and envelope assembly and is a known fibronectin-binding protein (Speziale *et al*., 2019).

The sub-lethal exposure of *Staphylococcus aureus* strain NCTC8325 to metal-tdda-phen complexes and mutant strains WGS will have to be carried out as the varying genomes may account for the limited mutations identified.

2.3.4.2 Gram-negative *Pseudomonas aeruginosa* PAO1

Various mutations were identified when comparing the untreated control strain (PAO1_NT) to the metal-tdda-phen treated strains (PAO1_Cu, PAO1_Mn and PAO1_Ag strains) as presented in **Table 2.8**. One variant was identified between all metal-tdda-phen exposed strains and was situated in an unnamed gene that encodes for a hypothetical protein linked to a carbon-nitrogen hydrolase containing protein. A BLAST search and computational predictions suggest that the protein exhibits *N*-carbamoylputresceine amidase activity (UniProt, 2021). The protein is a crucial component in the polyamine biosynthetic pathway, indicating that resistance to the metal-tdda-phen complexes may be acquired through alterations in the activity levels of this pathway. Mutations in

agmatine deiminase and *N*-carbamoylputrescine amidase can directly influence the rate at which polyamines are produced. Arginine deiminase, GatB of the aspartyl/glutamyl-tRNA amidotransferase complex and ɣ-glutamyl phosphate reductase can all indirectly contribute to an altered polyamine biosynthetic rate (Sekula and Dauter, 2019). The remaining mutations (**Table 2.8**) were aligned to specific pathways and mechanisms discussed below.

2.3.4.3 Mutations associated with cellular respiration

Genome analysis suggests that alterations to energy metabolism pathways contributed to the development of bacterial resistance. Amino acid altering single nucleotide polymorphisms (SNPs) occurred in various unspecified oxidoreductases and known oxidases and dehydrogenases in metal-tdda-phen-treated strains. These enzymes are heavily involved in cellular respiration (Alford *et al*., 2020; Lee *et al*., 2021). In situations where electron acceptors in oxidative phosphorylation are unavailable, the protein D-lactate dehydrogenase may act as a temporary electron sink (Kasai *et al*., 2019). Additionally, recent studies have demonstrated the ability of D-lactate dehydrogenase to act as an electron transferring agent, transporting electrons from NADH to quinones present in the plasma membrane (Lin *et al*., 2018). A mutation in the gene encoding for D-lactate dehydrogenase, *ldhA*, was identified in the analysis. In addition, a SNP was identified in an unspecified cytochrome *c* oxidase which acts as a terminal electron acceptor but also has other functions in bacteria, such as promoting virulence and biofilm growth (Jo *et al*., 2017). Both of these mutations indicate that cellular respiration was affected by the metal-tdda-phen complexes.

2.3.4.4 Mutations associated with polyamine biosynthetic pathway

Amino acid substitutions were identified in agmatine deiminase and *N*-carbamoylputrescine amidase (CPA). An inhibitory mutation in agmatine deiminase

would prevent the formation of *N*-carbamoylputrescine, and therefore no mutation would be required in CPA as it would not have a substrate on which to act. Similarly, the arginine biosynthetic pathway involves the conversion of glutamate into arginine through a series of consecutive enzymatic reactions (Majumdar *et al*., 2016). Mutations were identified in arginine deiminase, GatB of the aspartyl/glutamyl-tRNA amidotransferase complex and ɣ-glutamyl phosphate reductase. Arginine deiminase and ɣ-glutamyl phosphate reductase catalyse the conversion of arginine to citrulline and *N*-acetyl-glutamyl-5-phosphate to *N*–acetyl-glutamyl-5-semialdehyde, respectively (Majumdar *et al*., 2016). These reactions are essential steps in the arginine biosynthetic pathway. GatB is involved in synthesising glutamine, a precursor to glutamate (Friederich *et al*., 2018). Amino acid substitutions in each of these enzymes further support the previous postulation that an enhanced rate of polyamine biosynthesis could contribute to the resistance of the PAO1 strain to the three metal-tdda-phen complexes.

2.3.4.5 Mutations associated with virulence factors

Bis-(3′-5′)-cyclic dimeric guanosine monophosphate (c-di-GMP) is the principle second messenger involved in the regulation of cell cycle, differentiation, virulence, motility, biofilm formation and dispersion (Valentini and Filloux, 2016; Valentini *et al*., 2018). It is synthesized from two GTP molecules by diguanylate cyclases (DGC) and is degraded by phosphodiesterases (PDE). Variants in PDE, PprA, WspC, RhlA and alginate lyases were identified in metal-tdda-phen-treated strains, suggesting that changes occurred in the biofilm life cycle. Additionally, WspC is a methyltransferase that promotes the activation of the Wsp pathway. This pathway is involved in regulating c-di-GMP concentration (Maunders and Welch, 2017; Cai and Webb, 2020). Similarly, the gene *pprA* encodes the histidine kinase sensor, PprA, for the two-component system PprA-PprB. This system is associated with biofilm formation during high-stress conditions.

PprA is responsible for the activation of the two-component system, and a mutation in *pprA* could indicate that the activity status of the system was altered as a resistance strategy toward the metal-tdda-phen complexes (Bhagirath *et al*., 2019; Wang *et al*., 2019a). A mutation in *rhlA* was identified, a gene that codes for rhamnosyltransferase subunit A that acts as a critical enzyme in the biosynthesis of rhamnolipid, a secondary metabolite that is important for the maintenance of mature biofilms (Thi *et al*., 2020). A SNP in an alginate lyase domain-containing protein was also observed in both PAO1_Cu and PAO1_Mn strains. This mutation resulted in an arginine residue being substituted for a glutamine residue. Alginate is a critical component of biofilms, providing the thick mucoid consistency that facilitates protection against the environment and stressors. Alginate lyase proteins degrade alginate, and this mutation may reduce the enzyme's efficiency, allowing alginate levels to rise and promoting biofilm formation (Moradali *et al*., 2017; Blanco-Cabra *et al*., 2020).

SNPs were identified in other virulence factors, such as *nalC*, which is a transcriptional regulator responsible for the control of the *mexAB-oprM* operon (Braz *et al*., 2016), encoding the primary efflux pump of *P. aeruginosa*, MexAB-OprM (Barbosa *et al*., 2021). The MexAB-OprM system is responsible for the resistance to quinolones, macrolides, chloramphenicol, tetracyclines, lincomycin, and β-lactam antibiotics (Scoffone *et al*., 2021). A mutation in this protein resulted in an arginine residue replacing a serine residue. Another notable variant was XqhA, a protein that increases the specificity of the type II secretion system (T2SS) (Michel *et al*., 2007). T2SS is known to secrete PlcH, a hemolytic toxin in which another mutation was identified, causing the substitution of serine with an alanine (Pena *et al*., 2019). Finally, a mutation resulting in the replacement of asparagine with a lysine occurred in the highly conserved bacterial protein, ClpB. This protein is vital in the disaggregation of proteins during high-stress

conditions (Alam *et al*., 2021), suggesting that the metal-tdda-phen complexes may have triggered protein aggregation within the bacterial cell.

Variants shared between PAO1_Cu, PAO1_Mn and PAO1_Ag strains						
Genomic location	**Locus tag**	**Gene**	**Product**	**Amino acid change**	**Polymorphism type**	**Protein effect**
3473819	PA3093	-	Carbon-nitrogen hydrolase domain-containing protein	G → R	SNP (transversion)	Substitution
Variants shared between PAO1_Cu and PAO1_Mn strains						
Genomic location	**Locus tag**	**Gene**	**Product**	**Amino acid change**	**Polymorphism type**	**Protein effect**
12145	PA0008	*glyS*	Glycine-tRNA ligase subunit beta	I → S	SNP (transversion)	Substitution
328965	PA0292	*aguA*	Agmatine deiminase	I → V	SNP (transversion)	Substitution
919457	PA0844	*plcH*	Hemolytic phospholipase C	R → Q	SNP (transition)	Substitution
1044192	PA0958	*oprD*	Porin OprD	N → D	SNP (transition)	Substitution
1442789	PA1330	-	Short-chain dehydrogenase	Q → E	SNP (transition)	Substitution
1709846	PA1569	-	Major facilitator superfamily transporter	A → G	SNP (transition)	Substitution
1743146	PA1600	-	Cytochrome *c*	A → G	SNP (transversion)	Substitution
1743297	PA1601	-	Aldehyde dehydrogenase	R → Q	SNP (transversion)	Substitution
1932730	PA1784	-	Alginate lyase domain-containing protein	R → Q	SNP (transition)	Substitution
2683088	PA2402	-	Peptide synthase	A → D	SNP (transition)	Substitution
2703112	PA2420	-	Porin	I → L	SNP (transversion)	Substitution
3665586	PA3272	-	ATP-dependent DNA helicase	N → S	SNP (transversion)	Substitution
3871062	PA3462	-	Sensor/response regulator hybrid protein	A → T	SNP (transition)	Substitution

4149515	PA3706	*wspC*	Methyltransferase	P → S	SNP (transition)	Substitution
4167142	PA3721	*nalC*	Transcriptional regulator	S → R	SNP (transition)	Substitution
4356981	PA3891	-	ATP-binding cassette transporters transporter	V → I	SNP (transversion)	Substitution
4475825	PA3994	-	Epoxide hydrolase	T → A	SNP (transition)	Substitution
4803257	PA4284	*recB*	Exodeoxyribo-nuclease V subunit beta	A → T	SNP (transition)	Substitution
4818942	PA4293	*pprA*	Two-component sensor	S → N	SNP (transition)	Substitution
5145714	PA4593	-	ATP-binding cassette transporters transporter permease	A → S	SNP (transition)	Substitution
5179615	PA4621	-	Oxidoreductase	S → N	SNP (transversion)	Substitution
5525871	PA4926	-	TGc domain-containing protein	Q → P	SNP (transition)	Substitution
5807024	PA5158	-	Outer membrane protein	A → T	SNP (transversion)	Substitution
5863513	PA5208	-	Hypothetical protein	H → N	SNP (transition)	Substitution

Variants shared between PAO1_Cu and PAO1_Ag strains

Genomic location	Locus tag	Gene	Product	Amino acid change	Polymorphism type	Protein effect
172340	PA0151	-	TonB-dependent receptor	T → A	SNP (transition)	Substitution
520509	PA0459	-	Chaperone protein ClpB	N → K	SNP (transversion)	Substitution
579718	PA0519	*nirS*	Nitrite reductase	T → S	SNP (transversion)	Substitution
1012950	PA0927	*ldhA*	D-lactate dehydrogenase	S → T	SNP (transversion)	Substitution
1882855	PA1738	-	Transcriptional regulator	M → V	SNP (transition)	Substitution
2176433	PA1990	*pqqH*	Peptidase	W → R	SNP (transition)	Substitution
2214540	PA2022	-	UDP-glucose 6-dehydrogenase	Y → F	SNP (transversion)	Substitution
3020368	PA2672	-	Type II secretion system	N → S	SNP (transition)	Substitution

3193266	PA2839	-	LigB domain-containing protein	R → H	SNP (transition)	Substitution
3892506	PA3479	*rhlA*	Rhamnosyl-transferase subunit A	Q → P	SNP (transversion)	Substitution
4487286	PA4007	*proA*	Ɣ- glutamyl phosphate reductase	V → A	SNP (transition)	Substitution
5193272	PA4626	*hrpA*	Glycerate dehydrogenase	R → H	SNP (transition)	Substitution
6047419	PA5372	*betA*	Choline dehydrogenase	A → V	SNP (transition)	Substitution
6165065	PA5474	-	Metalloproteinase	D → G	SNP (transition)	Substitution
Variants shared between PAO1_Mn and PAO1_Ag strains						
Genomic location	**Locus tag**	**Gene**	**Product**	**Amino acid change**	**Polymorphism type**	**Protein effect**
31334	PA0029	-	Sulfate transporter	S → N	SNP (transition)	Substitution
1228628	PA1137	-	Oxidoreductase	D → N	SNP (transition)	Substitution
1228637	PA1137	-	Oxidoreductase	V → L	SNP (transversion)	Substitution
1238899	PA1147	-	Amino acid permease	V → L	SNP (transversion)	Substitution
1710229	PA1569	-	Major facilitator superfamily transporter	M → I	SNP (transition)	Substitution
1800632	PA1654	-	Aminotransferase	P → A	SNP (transversion)	Substitution
2029517	PA1868	*xqhA*	Secretion protein	S → A	SNP (transversion)	Substitution
3823531	PA3417	-	Pyruvate dehydrogenase E1 component subunit alpha	R → Q	SNP (transition)	Substitution
4591824	PA4108	-	c-di-GMP phospho-diesterase	P → Q	SNP (transversion)	Substitution
5016474	PA4484	*gatB*	Aspartyl/glutamyl -tRNA Amidotransferase subunit B	A → T	SNP (transition)	Substitution
5823613	PA5171	*arcA*	Arginine deiminase	V → I	SNP (transition)	Substitution
6254544	PA5561	*atpI*	ATP synthase subunit I	A → T	SNP (transition)	Substitution

Table 2.8 Variants of interest in *P. aeruginosa* PAO1 treated with sub-lethal doses of Cu-tdda-phen (PAO1_Cu), Mn-tdda-phen (PAO1_Mn) and Cu-tdda-phen (PAO1_Cu) when compared to the untreated strain (PAO1_NT). – denotes an unnamed gene while → refers to the change in amino acid.

2.4. Discussion

The rise of antimicrobial resistance (AMR) is well established and constitutes an increasingly severe threat to public health worldwide (Destoumieux-Garzón *et al*., 2018; Cassini *et al*., 2019). Consequently, the efficacy of conventional antimicrobial agents is rapidly declining, leaving healthcare professionals unpropitious to treat common infections, and hence the development of new antibacterial compounds with novel mechanisms of action to overcome AMR represents a global challenge. A recent systemic analysis estimates 4.95 million deaths associated with bacterial AMR in 2019, including 1.27 million deaths directly attributable to bacterial AMR alone (Murray *et al*., 2022). Moreover, it is widely reported that the pipeline for new antibacterial agents is dwindling due to a lack of funding and interest from pharmaceutical companies (Tacconelli *et al*., 2018; Theuretzbacher *et al*., 2019; Theuretzbacher, 2020; Butler *et al*., 2022).

In this chapter, the antibacterial capabilities of novel copper(II), manganese(II), and silver(I) complexes containing dicarboxylate ligands and phen in panels of clinical isolates derived from Irish hospitals. Further investigation into the potential resistance mechanisms by whole genome sequencing (WGS) of the lead complexes in representative Gram-positive organism, *S. aureus*, and Gram-negative organism, *P. aeruginosa*, were also carried out. With Gram-positive and -negative bacteria, their distinction lies in the cell envelope composition. The scaffold of the Gram-positive cell wall consists of a thick layer of peptidoglycan polymer embedded with teichoic and lipoteichoic acids anchored to the cell membrane. Teichoic acids are long anionic glycopolymers that bind cations contributing to bacterial cell surface charge and hydrophobicity, which in turn affects the interaction of antibiotics and host defences (Brown *et al*., 2013). In contrast, and in the absence of teichoic acid, the Gram-negative cell wall consists of a thin layer of peptidoglycan. However, the outer membrane encloses this. This layer is effectively a

second lipid bilayer containing amphiphilic lipopolysaccharide (LPS), phospholipids and outer membrane proteins (Okuda *et al*., 2016). Porins are β-barrel structures that form channels to orchestrate the movement of small hydrophilic molecules across the outer membrane (Silhavy *et al*., 2010), and efflux pumps are membrane-bound proteins responsible for the extrusion of a variety of solutes. Therefore, the outer membrane is a very effective and selective permeability barrier and a significant obstacle in developing antibacterial agents that are effective against Gram-negative bacteria (Zgurskaya *et al*., 2016; Impey *et al*., 2020). In addition to this intrinsic resistance, acquired resistance is developing rapidly, creating a further impediment in the treatment of diseases caused by these pathogens (Peterson and Kaur, 2018; Pang *et al*., 2019; Khan *et al*., 2020).

Overall, the metal complexes incorporating the phen ligand demonstrated superior antibacterial toxicity compared to their non-phen precursors, metal-free phen, metal-free dicarboxylic acids or simple metal salts. The greater activity profiles of metal-phen complexes or metal-phendione complexes (phendione is a derivative of phen), in comparison to their non-phen analogues, have previously been reported against a range of microorganisms (Viganor *et al*., 2016a; Gandra *et al*., 2017; Granato *et al*., 2017; McCarron *et al*., 2018; Ventura *et al*., 2020). Moreover, the metal-phen complexes containing the 3,6,9-trioxaundecanedioate (tdda) bridging dianionic ligand maintained their potency in varying degrees across the Gram-positive and Gram-negative panels (**Figure 2.3** and **Figure 2.4**). The tdda ligand enhances the water solubility of the metal complexes, strengthening their hydrophilicity and potentially increasing their uptake into the bacterial cell and thus their subsequent antibacterial action (Ng *et al*., 2013, 2016). Although generally, the inclusion of the phen ligand in the complex formulations is key to their antibacterial action, the general exception to this was the Ag(I) complexes which were found to be active in both their phen and non-phen containing forms. Ag(I)

compounds have well-documented multi-modal bactericidal properties, displaying a broad spectrum of activity across both classes of bacteria (Domínguez *et al*., 2020; Wang *et al*., 2021a). Ag(I) ions interact with the bacterial cell envelope and destabilize the membrane (Jung *et al*., 2008; McQuillan *et al*., 2012), coupled with nucleic acids and proteins (Arakawa *et al*., 2001), and inhibit metabolic pathways (Gordon *et al*., 2010; Wang *et al*., 2019b). Although the Ag(I) ion is generally not regarded as being redox-active, the generation of reactive oxygen species (ROS) is also attributed to its antibacterial activity (Lemire *et al*., 2013; Domínguez *et al*., 2020). However, it is thought that the production of ROS indirectly occurs through the perturbation of the respiratory electron transfer chain (Gu and Imlay, 2011), Fenton chemistry following destabilization of Fe-S clusters or displacement of iron (Barras *et al*., 2018) and inhibition of anti-ROS defences by thiol–silver bond formation (Saulou-Bérion *et al*., 2015). The composition of the cell wall influences the antibacterial potential of Ag(I). The thick negatively charged peptidoglycan layer in Gram-positive bacteria attracts/binds the metal cations and retards their entry (Dakal *et al*., 2016; Domínguez *et al*., 2020). The complexation of metal ions to a hydrophobic chelating ligand, such as phen, encases the cations in a hydrophobic sleeve and enables their penetration through the cell wall and membrane of a bacterium, thus presenting the complex to internal target biomolecules, which ultimately inhibits cell growth or even triggers cell death (Viganor *et al*., 2016b). The heightened activity of phen-containing Ag(I) complexes, compared to their non-phen precursors, was evident in the present work with both the Gram-positive (**Figure 2.3**) and Gram-negative panels (**Figure 2.4**). Ag(I) complexed to phen or a phen-type ligand (e.g. phendione) have presented with additional routes in which they exert their toxicity against microorganisms such as interacting with double-stranded DNA (Galdino *et al*., 2022) or suppressing virulence (Galdino *et al*., 2019). Cu(II) and Mn(II)-phen complexes have

been reported to be avid producers of ROS (Kellett *et al*., 2011a), which is thought to cause cell membrane damage and thiol depletion. Oxidative and thiol stress promotes the release of metal ions (Fe, Zn and Cu) from metalloproteins, increasing their intracellular concentration and initiating Fenton-type chemistry, which then stimulates further ROS generation (Schramm *et al*., 2019). This, coupled with the intercalation of the complexes with bacterial DNA, would cause deformation and cleavage of the nucleic acid (Kellett *et al*., 2011a; McCarron *et al*., 2018; Ng *et al*., 2018), producing cascade effects that would eventually lead to bacterial cell death. These previous observations substantiate the hypothesis that the current metal-tdda-phen complexes, producing high intracellular levels of ROS, affect cellular respiration (**Table 2.8**). Various mutations were detected in the mutant genome of the metal-tdda-phen-treated *P. aeruginosa* representative strain, PAO1, causing amino acid changes within proteins involved in the polyamine biosynthetic pathway. Polyamines have demonstrated the ability to reduce oxidative damage caused by ROS (Seo *et al*., 2019). As previously mentioned, Cu(II), Mn(II) and Ag(I)-phen complexes generate free radicals, which are highly reactive and unstable. Polyamines act as ROS scavengers, stabilizing ROS and preventing ROS-induced damage to DNA, lipids and proteins. Recent findings suggest that these organic cations may also upregulate genes associated with the enzymatic degradation of ROS, such as catalases and superoxide dismutases. Superoxide dismutases can degrade superoxide radicals, while catalases can degrade hydrogen peroxide (Van Acker and Coenye, 2017; Guillouzo and Guguen-Guillouzo, 2020).

Due to the increasing rate of AMR, metals and metal complexes have not only been investigated as alternatives to antibiotics but also as adjuvants. There have been numerous reports on the capacity of metals or metal-bearing compounds to synergise and potentiate antibiotics within both *in vitro* and *in vivo* models (Kim *et al*., 2008; RubenMorones-

Ramirez *et al*., 2013; Garza-Cervantes *et al*., 2017; Herisse *et al*., 2017; Chen *et al*., 2018). Within the present study, all three metal-tdda-phen complexes potentiated gentamicin (an aminoglycoside) activity in clinical isolates of MRSA, EBSL and *P. aeruginosa* in terms of their fractional inhibitory concentration (FIC) index. Aminoglycosides are bactericidal antibiotics that inhibit protein synthesis by binding with a high affinity to the aminoacyl-tRNA site (A site) within the 30S ribosomal subunit, thereby inhibiting the translation process and producing truncated proteins and affecting the cell wall composition. This increases membrane permeability and subsequently heightens drug uptake (Kohanski *et al*., 2008). In studies using strains of *E. coli*, Herisse *et al.* (2017) reported a 10-fold increase in antimicrobial activity of aminoglycosides (gentamicin, tobramycin, kanamycin, and streptomycin) when co-administered with $AgNO_3$. Aminoglycosides cross the cell membrane via proton motive forces, and the Ag(I) ion enhances their toxicity by acting independently of this process. Morones-Ramirez *et al.* (2013) also reported the synergistic combination of $AgNO_3$ with β-lactams, aminoglycosides, and quinolones against *E. coli*, and they suggested that this was due to intensified ROS production. One or both of the mechanisms mentioned above could also be why the present metal-tdda-phen complexes enhanced the activity of gentamicin, which warrants further investigation.

To summarise, of the metal complexes assessed, those incorporating the phen ligand had superior activity to their non-phen derivatives. In addition, the three metal-phen complexes incorporating the 3,6,9-trioxaundecanedioate as their bridging ligand broadly maintained activity across the bacterial panel of both classes. Therefore, it was decided to select them for further study and examination. In addition, the synergistic capabilities with gentamicin were also further investigated, particularly within a *P. aeruginosa* disease model.

Chapter 3.

Antibacterial and anti-biofilm examination of selected metal complexes against *Pseudomonas aeruginosa* isolated from Irish Cystic Fibrosis patients

Chapter 3 (objective 2) is based on the following paper: ***O'Shaughnessy M****, McCarron P, Viganor L, McCann M, Devereux M, Howe O. The antibacterial and anti-biofilm activity of metal complexes incorporating 3,6,9-trioxaundecanedioate and 1,10-phenanthroline ligands in clinical isolates of Pseudomonas aeruginosa from Irish Cystic Fibrosis patients. Antibiotics. 2020; 9(10):674*

3.1. Introduction

Pseudomonas aeruginosa is a ubiquitous Gram-negative bacterium that can colonise a diversity of sites with severe clinical consequences. Isolates of *P. aeruginosa* are found in nosocomial infections within immunocompromised patients, ranging from burn sepsis (Brandenburg *et al*., 2019) to ventilator-associated pneumonia (Ramírez-Estrada *et al*., 2016) to pulmonary infections of patients with lung afflictions such as cystic fibrosis (CF) and chronic obstructive pulmonary disease (COPD) (Fenker *et al*., 2018). CF is an inherited autosomal recessive disorder characterised by mutations in the cystic fibrosis transmembrane conductance regulator (CFTR) gene located on chromosome 7, primarily affecting the lungs. Of particular concern in Ireland is the Phe508del mutation, of which 1 in 19 Irish people are asymptomatic carriers (Farrell, 2008). Individuals with this mutated gene suffer from a defective chloride channel protein on the epithelial cells of the lungs, causing an imbalance of chloride ions and fluid, and therefore the production of thick mucus and impaired mucociliary clearance of inhaled microbes resulting in recurrent chronic respiratory infections and inflammation. *P. aeruginosa* is the leading cause of infection in patients with CF, and it is more prevalent in adults (Reece *et al*., 2017).

The prosperity of this microorganism is attributed to its biofilm-forming capability and its vast repertoire of cell-associated and extracellular virulence factors controlled by transcriptional regulators, which enables its swift adaptation to environmental changes and host defences. Biofilms are structured multi-cellular sessile communities, organized as micro-colonies, encased within a self-produced extracellular matrix (ECM) that forms the scaffold for its three-dimensional architecture (Christophersen *et al*., 2020). Conventional antibiotics are active against planktonic cells of *P. aeruginosa* that cause acute infection but often fail to completely eradicate their biofilms, leading to persistent

infections. It is well documented that pathogenic biofilms from patients demonstrate up to 1000-fold reduced susceptibility compared to their planktonic counterparts due to the protective and altered nature of the biofilm (Hughes and Webber, 2017). The formation of these aggregated communities with their inherent resistance to antibiotics and host immune attacks are at the root of many persistent and chronic bacterial infections. Antibiotic treatment for patients with CF who are infected with P. aeruginosa often relieves the symptoms but does not necessarily cure the infection (Stefani *et al*., 2017). The acquisition of chronic *P. aeruginosa* infection is associated with worsened disease progression and increased mortality. Moreover, the effectiveness of the antibacterial agents to treat these pathogens is also compromised by the emergence of multidrug-resistant (MDR) strains which highlight the urgent need for novel drugs that can eradicate the robust biofilms of *P. aeruginosa* by acting either alone or in tandem with other clinical therapeutic interventions.

In this chapter, selected metal complexes metal-tdda and metal-tdda-phen complexes were tested on three clinical isolates of *P. aeruginosa* (CF1-CF3) derived from Irish hospital patients with CF, both alone and in combination with gentamicin, as they demonstrated synergistic interactions in **Chapter 2**. The results were compared to two established laboratory strains (ATCC 27853 and PAO1). The effects on planktonic growth as well as inhibition of biofilm formation and biofilm disarticulation were assessed in terms of biofilm biomass and cell viability once treated. The anti-biofilm effects were further probed through analysis of individual biofilm components, including polysaccharides, eDNA and the virulence factors pyocyanin and pyoverdine that help establish and maintain the biofilm. Finally, the toxicity of these complexes was assessed using a CF cell model (CFBE41o-) and a well-characterised ‘healthy’ cell line (BEAS-2B) to establish the selectivity of complexes to the bacteria.

3.2. Materials and Methods

3.2.1 Test complexes

The selected metal complexes (**Table 2.1**) used for this chapter were [Cu(3,6,9-tdda)].H_2O (**Cu-tdda**) and {[Cu(3,6,9-tdda)$(phen)_2$].$3H_2O$.EtOH}$_n$ (**Cu-tdda-phen**), [Mn(3,6,9-tdda)$(H_2O)_2$].$2H_2O$ (**Mn-tdda**) and {[Mn(3,6,9-tdda)$(phen)_2$].$3H_2O$.EtOH}$_n$ (**Mn-tdda-phen**), and [Ag_2(3,6,9-tdda].$2H_2O$ (**Ag-tdda**) and [Ag_2(3,6,9-tdda)$(phen)_4$].EtOH (**Ag-tdda-phen**). In order to establish that the observed biological effects were due to the discrete complexes rather than their free ligands, 1,10-phenathroline (**phen**) and 3,6,9-trioxaundecanedioate (**tdda**), and metal salts, manganese(II) chloride (**$MnCl_2$**), copper(II) chloride (**$CuCl_2$**), and silver(I) nitrate (**$AgNO_3$**) were also assessed (all chemicals were purchased from the Sigma-Aldrich company and used without further purification). The aminoglycoside antibiotic, gentamicin (Sigma-Aldrich), was also incorporated into the study. All stock complexes (10 mg/mL) were diluted in Tryptic Soy broth (TSB) media for desired test concentrations.

3.2.2 Bacterial strains and culture conditions

Clinical isolates of *P. aeruginosa* (CF1, CF2 and CF3) from cystic fibrosis patients at local Irish hospitals were obtained from the Department of Science TU Dublin-Tallaght campus. Under GDPR compliance, clinical isolates were provided anonymously to the researcher, and no patient data was processed. Standard laboratory strains ATCC 27853 and PAO1 were also included. Stock frozen cultures were maintained at −80 °C in 20% (v/v) glycerol solutions in tryptic soy broth (TSB; Lab M). Frozen cultures were streaked onto plates of tryptic soy agar (TSA; Lab M) and incubated overnight at 37 °C. A single

colony of bacteria was then inoculated into TSB (50 mL) to prepare the bacterial inoculate for the experiments (37 °C at 200 rpm).

3.2.3 Antibacterial and anti-biofilm testing of complexes on *Pseudomonas aeruginosa* strains

3.2.3.1 Effects of test compounds on planktonic bacteria

All metal complexes and controls were tested for their activity on the clinical isolates (CF1-CF3) and laboratory strains (ATCC 27853 and PAO1) of *P. aeruginosa* using the standard broth microdilution method to establish their minimum inhibitory concentration (MIC). The test complexes were two-fold serially diluted and mixed with equal volumes (100 µL) of diluted bacteria in 96-well plates (Cruinn), thus making a final concentration range of the complexes tested and including the antibiotic control gentamicin of between 0.5 and 256 µg/mL. The MIC measurements were recorded based on turbidity according to EUCAST guidelines (EUCAST, 2017b) after 24 h of incubation at 37 °C with agitation.

3.2.3.2 Effects of test complexes on biofilm formation (pre-treatment)

The activity of Cu-tdda-phen, Mn-tdda-phen and Ag-tdda-phen complexes (**Table 2.1**) and controls on biofilm formation of all *P. aeruginosa* strains were tested by measuring cellular viability and the total biomass in the cell culture wells. For both assays, 100 µL of the bacterial culture (made up in TSB medium) was distributed into each well of flat-bottomed 96–well polystyrene microtitre plates (Cruinn) and incubated for 48 h at 37 °C in the presence of all test compounds (100 µL), administered at a concentration range of 0.5–256 µg/mL. The supernatants from each well were removed, and the wells were then washed three times with phosphate-buffered saline (PBS). Viable cells in the biofilm were assessed by a fluorometric assay that measures the metabolic capacity of cells (Peeters *et al*., 2008). TSB (250 µL) containing 5% (v/v) resazurin (Sigma-Aldrich) was added to

the plates and incubated for 20 min at 37 °C. Fluorescence was measured at λexcitation = 560 nm and λemission = 590 nm with a Varioskan LUX (Thermo Scientific) microplate reader. Then, the resazurin stain was removed and replaced by 250 µL of 0.1% (w/v) crystal violet solution on the same plate (Skogman *et al.*, 2012) to evaluate biofilm biomass. After 20 min, the crystal violet stain was removed, and the wells were washed three times. The wells were dried, and 250 µL of 30% acetic acid (Sigma–Aldrich) was added to release the bound crystal violet. Absorbance was measured on a Multiskan GO (Thermo Scientific) microplate reader at 590 nm.

3.2.3.3 Effects of test complexes on the mature biofilm (post-treatment)

In addition to testing the effects of the Cu-tdda-phen, Mn-tdda-phen and Ag-tdda-phen complexes (**Table 2.1**) on biofilm formation (pre-treatment) of the *P. aeruginosa* strains, their ability to weaken an established biofilm was also assessed with the post-treatment of mature biofilms. Moreover, 100 µL of the bacteria culture (in TSB) was added to each well of flat bottomed 96–well polystyrene microtitre plates (Cruinn) and incubated for 48 h at 37 °C to allow for biofilm formation. After 48 h incubation, the test complexes and control were added over a range of concentrations (0.5–256 µg/mL) to mature biofilms and incubated for an additional 24 h. To the untreated control, 100 µL of fresh media was added to the wells. Cellular viability and biofilm biomass were measured using resazurin staining and crystal violet staining, as previously described in **Section 3.2.3.2**

3.2.3.4 Checkerboard assay for mature biofilms

The anti-biofilm activity of individual Cu-tdda-phen, Mn-tdda-phen and Ag-tdda-phen complexes (**Table 2.1**) alone and in combination with gentamicin were evaluated against the *P. aeruginosa* strains using the broth micro-dilution checkerboard technique (Odds, 2003). Mature biofilms were prepared as previously described in **Section 3.2.3.2**. The preformed biofilms in the wells of separate 96-well microtitre plates were rinsed with

PBS and 100 µL of the metal-tdda-phen complexes and gentamicin (two-fold serial dilutions); each was added to the wells containing the biofilms. Following incubation for 24 h at 37 °C, the biofilm biomass and cell viability were measured as previously described.

The fractional inhibitory concentration (FIC) index (FIC_I) for combinations of testing agents was calculated for selected *P. aeruginosa* strains PAO1 and CF3, according to the equation: $FIC_I = FIC_{(metal\text{-}tdda\text{-}phen\ complex)} + FIC_{(gentamicin).}$ Where, $FIC_{(metal\text{-}tdda\text{-}phen\ complex)}$ = (MBEC* of metal-tdda-phen complex in combination with gentamicin)/(MBEC* of metal-tdda-phen complex alone) and $FIC_{(gentamicin)}$ = (MBEC* of gentamicin in combination with metal-tdda-phen complex)/(MBEC* of gentamicin alone). The following criteria were used to interpret the FIC_I: ≤0.5 synergy; 0.5–4.0 indifferent; >4.0 antagonism. *The minimum biofilm eradication concentration (MBEC) was defined as the minimal concentration of the compound required to eradicate the biofilm.

3.2.4 Effects of test complexes on individual components of the biofilm

Selected *P. aeruginosa* strains, PAO1 and CF3, were incubated in the presence and absence of Cu-tdda-phen, Mn-tdda-phen and Ag-tdda-phen complexes (**Table 2.1**), alone and in combination with gentamicin. To assess the effects of biofilm formation (pre-treatment), experiments were set up according to **Section 3.2.3.2** with strains pre-treated to 0.5 × minimum biofilm inhibitory concentration (MBIC). To assess the effects on established mature biofilms (post-treatment), experiments were set up according to **Section 3.2.3.3**, with biofilms grown to 48 h, then treated with 0.5 × minimum biofilm eradication concentration (MBEC) for a further 24 h. The biofilms were harvested, and the following components, including exopolysaccharide, extracellular DNA (eDNA), pyocyanin and pyoverdine, were analysed using the methods described below.

3.2.4.1 Extraction and quantification of exopolysaccharide

Extraction and quantification of exopolysaccharides were performed using a modified protocol of Tribedi and Sil (Tribedi and Sil, 2014). Biofilms were grown on a glass surface and extracted by gentle dislodgment using a cell scraper (25 cm, Sarstedt) and PBS. The biofilm suspension was centrifuged at 4500 g for 15 min, and the supernatant was collected. The resulting pellet was treated with 10 mM/L EDTA, vortexed and centrifuged again to extract cell-bound polysaccharide. The supernatant was harvested and mixed with the first harvested supernatant. An equal volume of chilled absolute ethanol was added to the pooled supernatant and incubated at −20 °C for 1 h. After centrifugation at 10,000 g for 10 min, the pellet was re-suspended in sterile water and measured by the phenol-sulphuric acid extraction method (Dubois *et al*., 1951). Briefly, 1 mL of the precipitated exopolysaccharide solution was mixed with an equal amount of chilled phenol (5%) and 5 mL of concentrated sulphuric acid. The resulting red colour was measured at 490 nm on a spectrophotometer (Hach, Bio-Sciences).

3.2.4.2 Extraction and quantification of extracellular DNA (eDNA)

Extracellular DNA (eDNA), a vital component of the biofilm, was extracted from the matrix using a modified enzymatic method, as reported by Wu and Xi (Wu and Xi, 2009). To release the eDNA from the matrix, the biofilms were first exposed to cellulase (10 µg/mL, Novozymes) and α-amylase (10 µg/mL, Sigma-Aldrich) to hydrolyse the polysaccharides and incubated at 50 °C for 30 min (Loiselle and Anderson, 2003; Fleming *et al*., 2017). Proteinase K (5 µg/mL, Sigma-Aldrich) was then added to the mixture for a further 30 min to degrade proteins, and the supernatant was sequentially filtered through a 0.45 µm and then a 0.20 µm filter to remove residual bacteria. The eDNA was precipitated by 1 volume of cetyltrimethylammonium bromide (CTAB, Sigma-Aldrich) solution (1% CTAB in 50 mM Tris–10 mM EDTA, pH 8.0), incubated at 65 °C for 30

min, followed by centrifugation at 5000 g for 10 min. Each pellet was re-suspended in high-salt TE buffer (10 mM Tris-HCL, 0.1 mM EDTA, 1 M NaCl, pH 8.0) and 0.7 volume of cold isopropanol, and incubated at −20 °C for 3 h. After centrifugation at 10,000 g for 15 min, pellets were suspended in TE buffer (10 mM Tris-HCL, 0.1 mM EDTA, pH 8.0) and an equal volume of equilibrated phenol:chloroform:isoamyl alcohol (25:24:1) and centrifuged again. The upper aqueous layer was transferred to a tube with an equal volume of chloroform:isoamyl alcohol (24:1) and centrifuged again. The supernatant was then precipitated with 2 volumes of cold ethanol (70%) and one tenth the final volume of sodium acetate (0.3 M), incubated at −20 °C for 1 h and centrifuged at 10,000 g for 15 min. The pellets were finally washed twice with ethanol and re-suspended in MilliQ water. The purity of the DNA was checked by determining the ratio of absorbance at 260 nm and 280 nm (A260/280) using a MultiskanTM GO (Thermo Scientific) UV spectrophotometer with the µDrop plate, and the DNA was quantified fluorometrically (Qubit 3.0 Fluorometer, Invitrogen) by using SYBR Green I (Molecular Probes), as described by Zipper (Zipper, 2003). The size of extracellular DNA was analysed on a 1% (w/v) agarose gel in a Tris-Borate-EDTA (TBE) buffer.

3.2.4.3 Quantification of pyocyanin

Pyocyanin is a toxic, QS-controlled metabolite produced by *P. aeruginosa*, enabling biofilm formation. After a 24 h treatment, the bacterial strains were centrifuged at 4500 g for 20 min, and the cell-free supernatant was used. Pyocyanin from the supernatant was extracted and measured by the methods of Essar *et al.* (Essar *et al*., 1990). Then, 5 mL of filtered culture supernatant was extracted with chloroform (3 mL), vortexed and centrifuged at 4500 g for 15 min. The chloroform phase was transferred to a fresh tube with 1 mL of 0.2 M hydrochloric acid (HCL). After centrifugation at 4500 g for 4 min, the top layer was collected, and its absorption was measured on a spectrophotometer

(Hach, Bio-Sciences) at 520 nm. Pyocyanin concentrations expressed as micrograms per millilitre (μg/mL) of culture supernatant were determined by multiplying the OD at 520 nm by 17.072 (extinction coefficient).

3.2.4.4 Quantification of pyoverdine

Pyoverdine is the main siderophore of *P. aeruginosa*, deployed in severely iron-limited environments to assure sufficient supply of this essential nutrient, and is found at increased concentrations in biofilms. After a 24 h treatment, the bacterial strains were centrifuged at 4500 g for 20 min, and the cell-free supernatant was used to measure pyoverdine. The relative concentration of pyoverdine in all treated supernatant with respect to control was measured through fluorescence at an excitation wavelength of 405 nm and an emission wavelength of 465 nm (Adonizio *et al*., 2008) with a Varioskan LUX (Thermo Scientific) microplate reader.

3.2.4.5 Quantification of bacteria

In addition to the biofilm components, the liquid medium with bacteria was collected and centrifuged (4500 g for 20 min), after which the supernatant was discarded, and the pellet was re-suspended in 1 mL PBS. Ten-fold serial dilutions of the re-suspended bacteria were then prepared and plated on nutrient agar utilising the Miles and Misra (20 μL drop) method. Agar plates were incubated at 37 °C for 16–18 h, after which colony-forming unit (CFU) per mL was calculated using the formula: CFU/mL = average number of colonies for a dilution × 50 × dilution factor.

3.2.5 Toxicity of selected test complexes toward mammalian cell model

3.2.5.1 Cell lines

Cystic Fibrosis Bronchial Epithelial Cells (CFBE41o-) cells are transformed bronchial epithelial cells isolated from a CF patient with the Phe508/Phe508 deletion (Gruenert *et al*., 2004). BEAS-2B (SV40/adenovirus 12 transformed normal bronchial epithelium) cells were used to represent a well-characterised 'healthy' cell line (Reddel *et al*., 1993). Dr Gordon Cooke, Department of Science, TU Dublin-Tallaght campus, kindly donated both cell lines.

3.2.5.2 Routine maintenance and culturing

CFBE and BEAS-2B cell lines were revived from liquid nitrogen storage and placed in minimum essential medium (MEM, Gibco) that had been supplemented with 10% foetal bovine serum (FBS) (Gibco) and 1% of L-Glutamine (Gibco). CFBE cells require coated flasks and plates, while BEAS-2B cells naturally adhere to the plastic. The coating solution for the CFBE cell line consisted of bovine serum albumin (BSA, 1 mL, Sigma-Aldrich), fibronectin (100 µL, Sigma-Aldrich), collagen (100 µL, Sigma-Aldrich) and MEM (8.8 mL, Gibco), which was made fresh every two weeks and stored at 4 ºC. To coat flasks, 3-4 mL was added to a T75 cell culture flasks (Sarstedt) and left for 1 min. Afterwards, the coating solution was removed, and the flask was air-dried for 1 h. Both cell lines were cultured in T75 cell culture flasks (Sarstedt) and incubated at 37 °C with 5% CO_2 and 95% O_2 to mimic conditions in the human body. Cells were monitored each day until 85-90 % cell confluence was reached, and they were then sub-cultured for routine maintenance or experimentation.

Sub-culturing involved removing the cell culture media from the monolayer of cells and washing with PBS (Sigma-Aldrich) to remove any dead or detached cells from the

population. 3-4 mL of trypsin/EDTA solution was added to the T75 flask, and the cells were incubated at 37 °C for 1-2 min approximately to remove cells from their monolayer on the base of the flask. Cells were placed in 3-4 mL of fresh culture media to deactivate the trypsin enzyme and produce the single cell stock suspension. The stock cell solution was used for toxicity assays and to seed different cell densities in T75 stock flasks to maintain the cells in culture.

3.2.5.3 MTT viability assay

The cytotoxic properties of metal-tdda-phen complexes Cu-tdda-phen, Mn-tdda-phen and Ag-tdda-phen (**Table 2.1**) and antibiotic control gentamicin were assessed utilising the methylthiazolyldiphenyl-tetrazolium bromide (MTT) assay. This method is based on reducing the yellow MTT, by the mitochondrial enzyme succinate dehydrogenase of metabolically active cells, to an insoluble dark purple formazan crystal (Mossman, 1983). Therefore, the resultant product formation is directly proportional to the number of viable cells. Hence, dead cells will be metabolically inactive and will not reduce the MTT.

Cells were seeded ($1x10^4$ cells/100 µL) in 96-well flat-bottomed clear plates and allowed to acclimatise (37 °C with 5% CO_2) overnight before exposure to the metal-phen complexes or antibiotic control. The test complexes and control stocks (10 mg/mL) were further diluted in MEM to desired concentrations (1-500 µg/mL) and added to the seeded 96-well plates. After 24 h, a working solution of MTT (5 mg/mL in 0.1 M PBS) (Sigma, Ireland) was prepared and 100 µL of the solution was added to each well of the 96-well plates after the exposed cell culture media was then removed. All plates were incubated for 3 h, and afterwards, each well was washed with sterilised PBS (Sigma, Ireland). After the final wash, 100 µL of DMSO (ACS grade) was added to each well, and the plates were placed on a plate shaker for 15 min to allow the coloured formazan crystals to

develop. The plate was then read on the MultiskanTM GO (Thermo Scientific) spectrophotometer at 595 nm.

To establish the toxicity of the test complexes, IC_{50} (inhibitory concentration) values were calculated, defined as the drug concentration that caused a 50 % reduction in the number of viable cells (Cheng & Prusoff, 1973). In addition, the selectivity index (SI) was calculated as follows: IC_{50} (mammalian cells)/MIC_{50} (*P. aeruginosa* cells).

3.3. Results

3.3.1 The inhibition of planktonic bacterial growth

Antimicrobial susceptibility testing of {[Cu(3,6,9-tdda)(phen)$_2$].3H$_2$O.EtOH}$_n$ (**Cu-tdda-phen**), {[Mn(3,6,9-tdda)(phen)$_2$].3H$_2$O.EtOH}$_n$ (**Mn-tdda-phen**) and [Ag$_2$(3,6,9-tdda)(phen)$_4$].EtOH (**Ag-tdda-phen**), along with their phen-free precursors, [Cu(3,6,9-tdda)].H$_2$O (**Cu-tdda**), [Mn(3,6,9-tdda)(H$_2$O)$_2$].2H$_2$O (**Mn-tdda**) and [Ag$_2$(3,6,9-tdda].2H$_2$O (**Ag-tdda**), and their component synthetic starting materials, 3,6,9-trioxaundecanedioate (**tdda**), phen, the simple salts $MnCl_2$, $CuCl_2$ and $AgNO_3$, and the antibiotic gentamicin were evaluated through establishing their minimum inhibitory concentration (MIC), in accordance with the European Committee on Antimicrobial Susceptibility Testing (EUCAST) guidelines (EUCAST, 2017c), and the results are summarised in **Table 3.1.** In accordance with the EUCAST breakpoints, control strains ATCC 27853 and PAO1 were susceptible to the aminoglycoside antibiotic gentamicin with MICs of 1 µg/mL (1.7 µM) and 2 µg/mL (3.5 µM), respectively, while all the clinical isolates were deemed resistant to the antibiotic. When all of the strains were incubated in the presence of the Cu(II), Mn(II) and Ag(I) simple salts (effectively the free metal ions) or in the presence of the metal-free phen ligand, no clinically relevant effects against either control strains (ATCC 27853 and PAO1) or clinical isolates (CF1-CF3) were observed. A similar inactivity profile was witnessed for the phen-free precursor complexes, Cu-tdda, Mn-tdda and Ag-tdda.

The metal-tdda-phen complexes were the most active against all of the *P. aeruginosa* strains compared to their non-phen precursors, simple metal salts and metal-free phen. The three metal-tdda-phen complexes all had different activity profiles across the strains. Of the control strains (ATCC 27853 and PAO1), gentamicin had the greatest inhibitory

action (1–2 µg/mL) (1.7–3.5 µM), followed by Ag-tdda-phen (8–32 µg/mL) (6.6–26.6 µM), with the least active being Cu-tdda-phen, and Mn-tdda-phen (both had the same activity of ca. 16 and 32 µg/mL) (ca. 21 and 43 µM). In contrast to these control strains, the metal-tdda-phen complexes were active against all CF clinical isolates. Against CF1, these three metal complexes had activity (8–16 µg/mL) (10.9–13.3 µM) comparable to that of gentamicin and were more active than this antibiotic against CF2 (8–16 µg/mL) (10.9–13.3 µM) and CF3 (64–128 µg/mL) (53.2–174 µM). Following the MIC measurement, only the three metal-tdda-phen complexes and gentamicin were used in further biological assays.

Test Compound	MIC µg/mL and (µM)				
	ATCC 27853	PAO1	CF1	CF2	CF3
Mn-tdda	>256 (737)	>256 (737)	>256 (737)	>256 (737)	>256 (737)
Cu-tdda	>256 (848)	128 (424)	>256 (848)	>256 (848)	256 (848)
Ag-tdda	>256 (542)	>256 (542)	>256 (542)	>256 (542)	>256 (542)
Mn-tdda-phen	16 (21.7)	32 (43.5)	8 (10.9)	8 (10.9)	128 (174)
Cu-tdda-phen	16 (21.5)	32 (43)	8 (10.7)	8 (10.7)	64 (86)
Ag-tdda-phen	8 (6.6)	32 (26.6)	16(13.3)	16 (13.3)	64 (53.2)
Phen	128 (710)	>256 (1420)	128 (710)	128 (710)	>256 (1420)
tddaH$_2$	>256 (1152)	>256 (1152)	>256 (1152)	>256 (1152)	>256 (1152)
MnCl$_2$	>256 (1294)	>256 (1294)	>256 (1294)	>256 (1294)	>256 (1294)
CuCl$_2$	>256 (1502)	>256 (1502)	>256 (1502)	>256 (1502)	>256 (1502)
AgNO$_3$	128 (753)	256 (1507)	>256 (1507)	>256 (1507)	256 (1507)
Gentamicin	1 (1.7)	2 (3.5)	8 (13.9)	128 (222)	>256 (445)

Table 3.1 Effects of test compounds on planktonic growth of *P. aeruginosa* laboratory strains (ATCC 27853 and PAO1) and clinical isolates (CF1–CF3).

3.3.2 The inhibition and disruption of biofilm

Although bacteria are unicellular organisms, they exist in natural and clinical settings, predominately within biofilms. To determine the capacity of the test complexes to prevent the formation of biofilms by *P. aeruginosa* isolates, bacterial cells were pre-treated with the three metal-tdda-phen complexes or gentamicin for 48 h. Similarly, the post-treatment of established mature biofilms (at 48 h) was also carried out to compare the effect of the compounds on developing or developed biofilms. For both pre- and post-treatment

studies, cellular viability (resazurin stain) and biofilm biomass (crystal violet stain) were measured. Both stains could be used sequentially on the same treated biofilm sample, as resazurin measures only viable cells, whereby crystal violet binds to the extracellular matrix of biofilms and stains all cells present in the biomass, with no discrimination between live or dead cells. However, one limitation of the resazurin method is that it does not allow for the detection of persister cells that may be present in the biofilm and therefore was measured just to accompany biofilm biomass data.

The pre-treatment of potential biofilm-forming bacterial cells with the metal-tdda-phen complexes and gentamicin was dose-dependent for both cellular viability (**Figure 3.1** and **Figure 3.2**) and biofilm biomass (**Figure 3.3** and **Figure 3.4**), inhibiting biofilm formation at concentrations lower than the concentration required to restrict planktonic bacterial growth, as previously outlined (**Table 3.1**), and with contrasting activity between the laboratory strains and CF clinical isolates. Gentamicin was found to inhibit biofilm formation in strains ATCC 27853 and PAO1, upwards of 50% at a concentration of 1.7 µg/mL (2.9 µM) and 1.9 µg/mL (3.3 µM), respectively, while it required 8.6–39.2 µg/mL (7.2–53.3 µM) of the metal-tdda-phen complexes to elicit the same response. The activity of Mn-tdda-phen, Cu-tdda-phen and Ag-tdda-phen varied across the clinical isolates and were either comparable (CF1) or superior to gentamicin (CF2 and CF3). For CF1, the biomass was inhibited 50% by Mn-tdda-phen at a concentration of 4 µg/mL (5.4 µM), followed by gentamicin (4.2 µg/mL, 7.3 µM), Ag-tdda-phen (6.1 µg/mL, 5.1 µM) and Cu-tdda-phen (8.4 µg/mL, 11.3 µM). To inhibit biofilm formation by 50% in CF2, 2.5 µg/mL (3.4 µM) of Mn-tdda-phen, 4.4 µg/mL (5.9 µM) of Cu-tdda-phen, 6.2 µg/mL (5.2 µM) of Ag-tdda-phen and 81.3 µg/mL (141.2 µM) of gentamicin were required, respectively, while for CF3, which formed the strongest biofilm, 26.5 µg/mL (35.6 µM) of Cu-tdda-phen, 29.7 µg/mL (40.4 µM) of Mn-tdda-phen, 33.4 µg/mL (27.8 µM) of Ag-

tdda-phen and 116.5 µg/mL (202.4 µM) of gentamicin were required to inhibit the biofilm formation by 50%. Interestingly, pre-treatment of the clinical isolates with sub-MICs of gentamicin increased the biomass relative to the untreated sample, which has previously been observed (Hoffman *et al*., 2005).

As antibiotics are predominantly administered in clinical practice to counteract an existing infection, evaluating the effects on established mature biofilms (post-treatment) provided a more pragmatic insight into the anti-biofilm activity of the test complexes. None of the test complexes caused the complete eradication of *P. aeruginosa* biofilms at the concentrations presented by cellular viability (**Figure 3.1** and **Figure 3.2**) and biofilm biomass (**Figure 3.3** and **Figure 3.4**). The activity of gentamicin diminished considerably across all strains when administered to established biofilms, a feature commonly reported (Ciofu and Tolker-Nielsen, 2019). While gentamicin maintained moderate activity against ATCC 27853, with the minimum biofilm eradication concentration (MBEC) removing 50% of the biomass ($MBEC_{50}$) being 19.6 µg/mL (34.1 µM), the $MBEC_{50}$ for PAO1 was considerable larger (181 µg/mL, 314 µM). At the highest concentration of gentamicin examined (256 µg/mL, 445 µM) against the clinical isolates CF1, CF2 and CF3, there was still approximately 52%, 67% and 98% biofilm remaining, respectively, relative to the untreated samples. It is well known that, as a mature biofilm is established, the extracellular matrix slows or prevents the penetration of antibiotics into the microbial communities embedded in it. Surprisingly, against the clinical isolates, the metal-tdda-phen complexes all showed similar activity ($MBEC_{50}$ range ca. 12–51 µg/mL, 14–70 µM) and were superior to gentamicin.

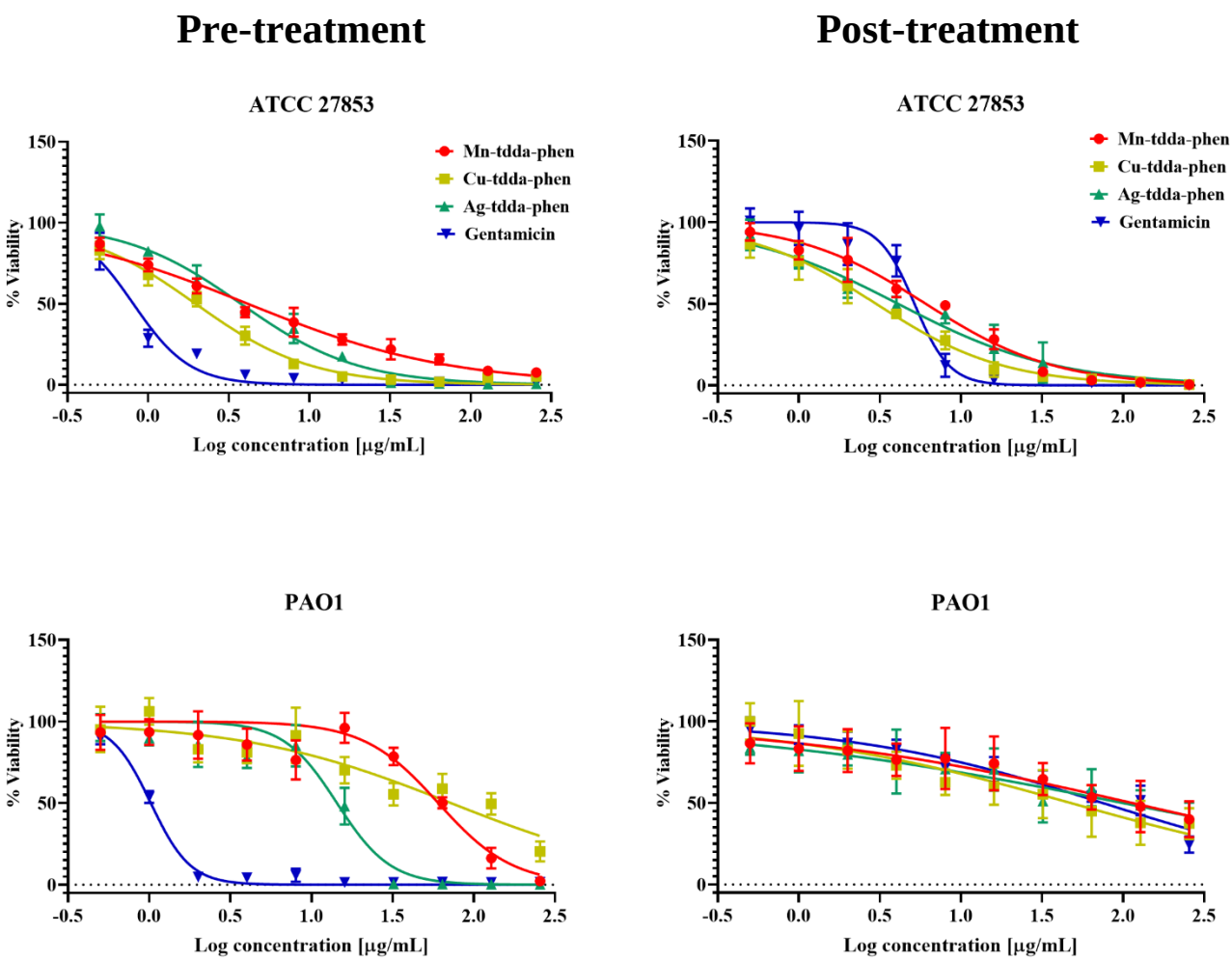

Figure 3.1 Cell viability – Laboratory strains. Effect of metal-tdda-phen complexes (Mn-tdda-phen, Cu-tdda-phen and Ag-tdda-phen) and gentamicin on both inhibiting biofilm formation (pre-treatment) and dismantling established biofilms (post-treatment) of laboratory strains (ATCC 27853 and PAO1)

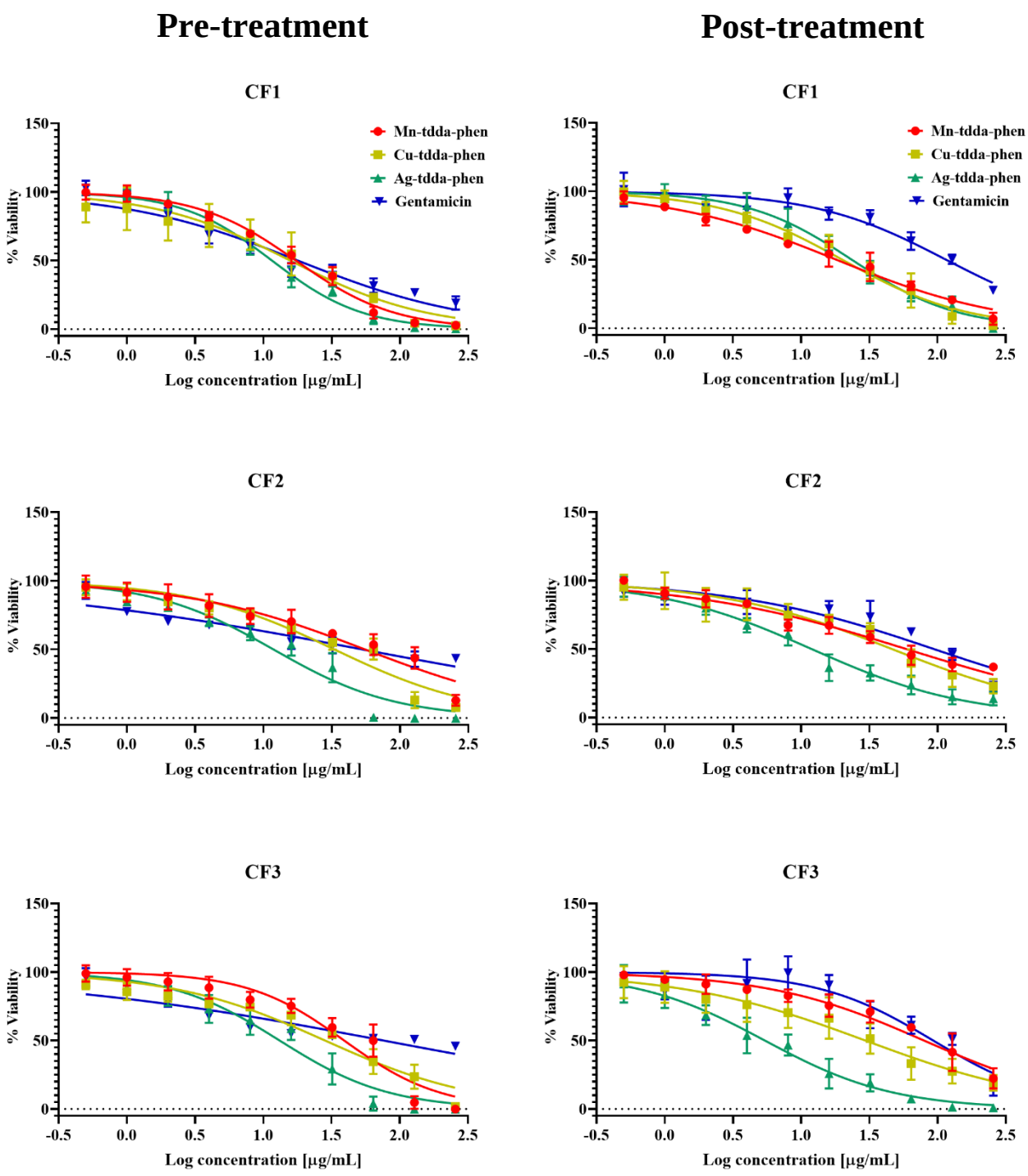

Figure 3.2 Cell viability – Clinical isolates. Effect of metal-tdda-phen complexes (Mn-tdda-phen, Cu-tdda-phen and Ag-tdda-phen) and gentamicin on both inhibiting biofilm formation (pre-treatment) and dismantling established biofilms (post-treatment) of clinical isolates (CF1-CF3).

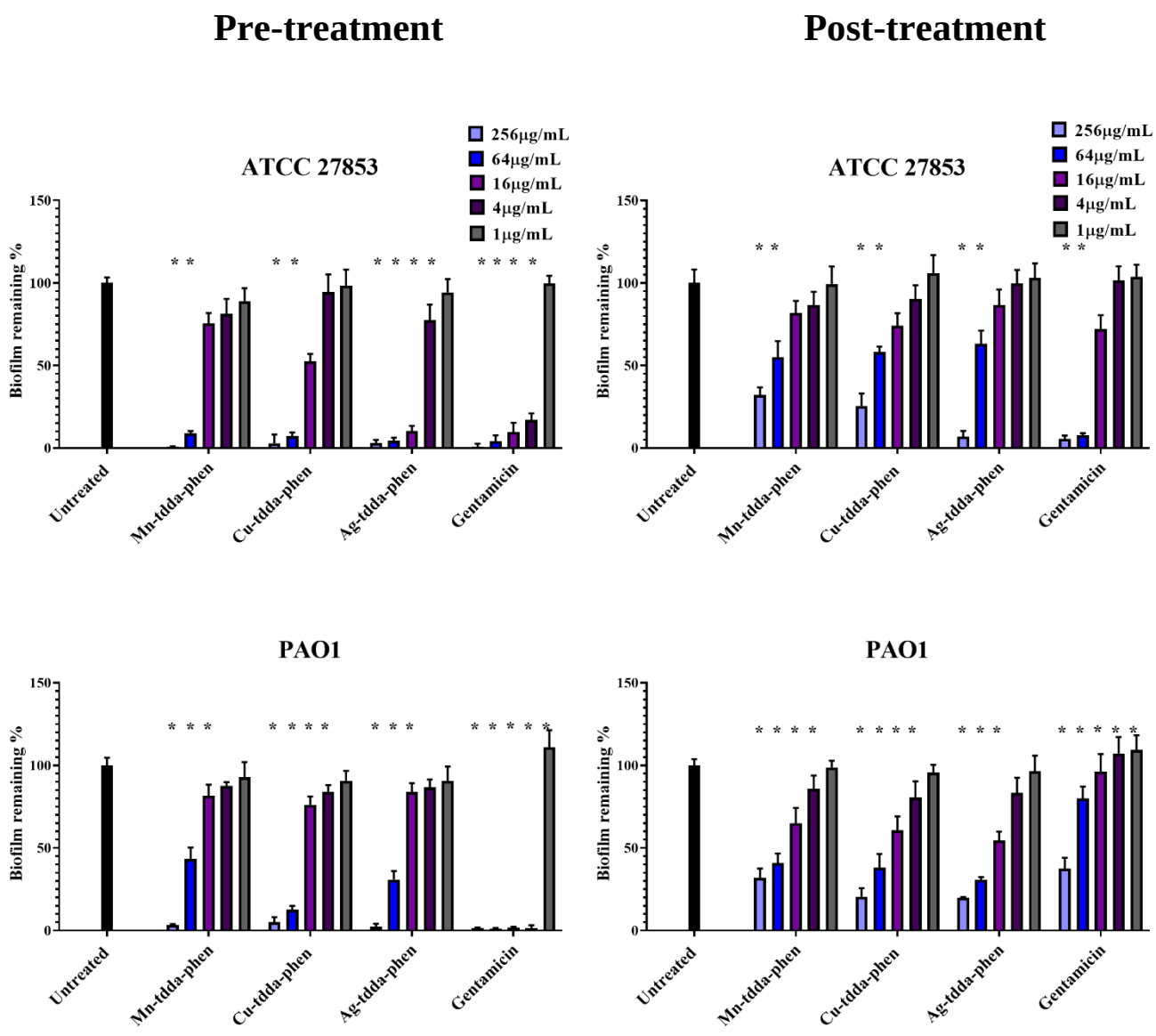

Figure 3.3 Biofilm biomass – Laboratory strains. Effect of metal-phen complexes (Mn-tdda-phen, Cu-tdda-phen and Ag-tdda-phen) and gentamicin on both inhibiting biofilm formation (pre-treatment) and dismantling established biofilms (post-treatment) of laboratory strains (ATCC 27853 and PAO1). Asterisks indicate significance ($p > 0.05$) relative to the untreated control.

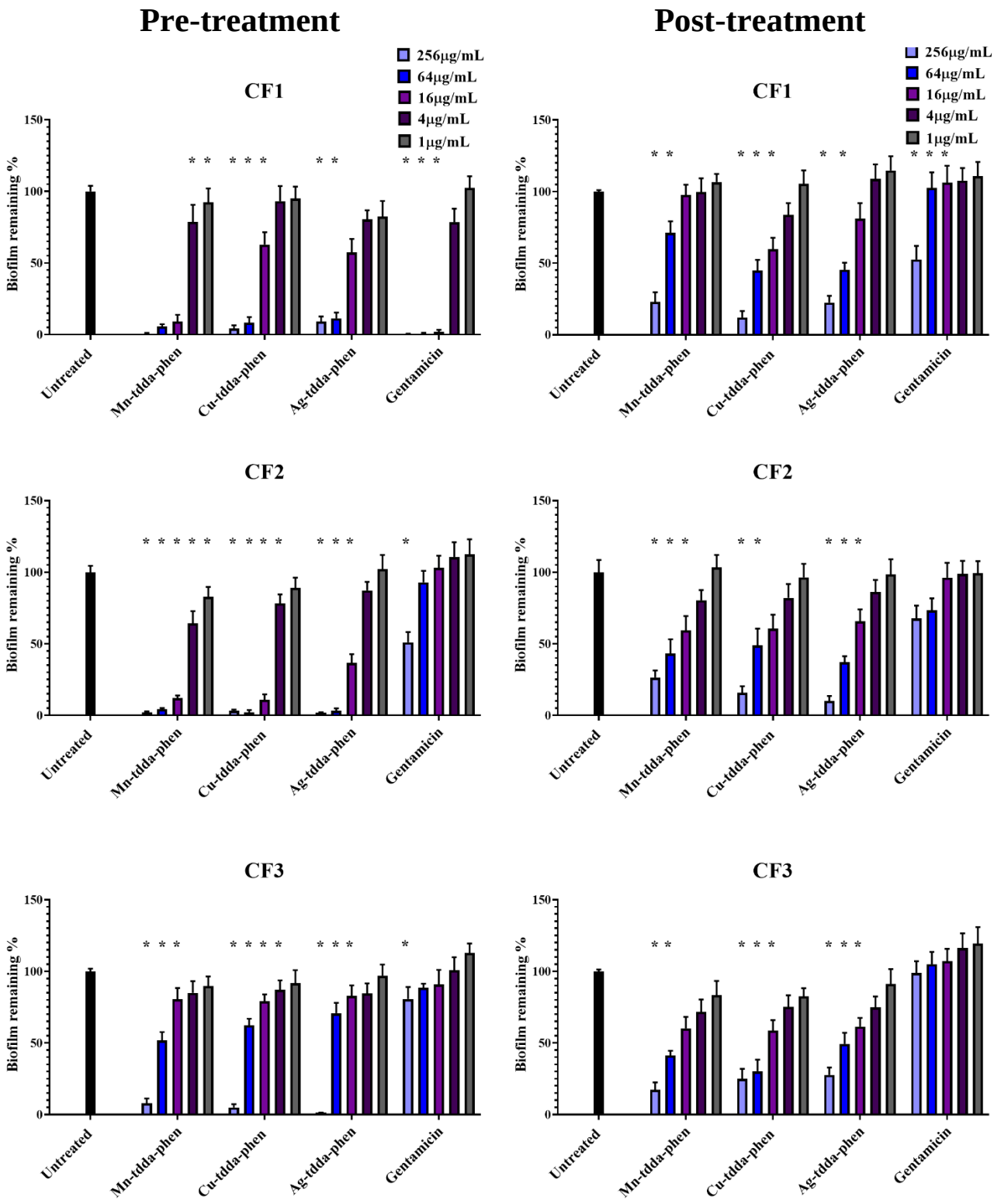

Figure 3.4 Biofilm biomass – Clinical isolates. Effect of metal-phen complexes (Mn-tdda-phen, Cu-tdda-phen and Ag-tdda-phen) and gentamicin on both inhibiting biofilm formation (pre-treatment) and dismantling established biofilms (post-treatment) of clinical isolates (CF1-CF3). Asterisks indicate significance ($p > 0.05$) relative to the untreated control.

3.3.3 Metal-tdda-phen complexes enhanced the anti-biofilm activity of gentamicin

Biofilm-associated tolerance is multifactorial and is attributed to the restricted penetration of the antimicrobial agent and the different metabolic states and virulence factors of the microbial community within the biofilm. Current research approaches aimed at increasing the likelihood of biofilm eradication include the use of non-antibiotic complexes, either alone or in combination with conventional antibiotics (Lebeaux *et al*., 2014; Kadam *et al*., 2019; Cao *et al*., 2020; Thi *et al*., 2020; Zhang *et al*., 2020). The combination of metal-tdda-phen complexes (0–64 µg/mL) with gentamicin (0–32 µg/mL) was tested on established mature (48 h) biofilms of *P. aeruginosa* using the checkerboard assay, and the results are presented in **Figure 3.5** for strains ATCC 27853 (A–C) and PAO1 (D–F), **Figure 3.6** for strains CF1 (G–I) and CF2 (J–L) and **Figure 3.7** for CF3 (M–O). To varying degrees, adding the metal-tdda-phen complexes enhanced the anti-biofilm activity of gentamicin across all strains. At the highest concentration of gentamicin alone (32 µg/mL, 55.5 µM), ca. 19–37% of the biofilm was removed from reference strains ATCC 27853 and PAO1, whilst the same concentration of gentamicin, combined with 4 µg/mL (3.3–5.4 µM) of the metal-tdda-phen complexes, was able to degrade over 50% of the biofilm. Increasing the concentration of the added metal-tdda-phen complexes prompted the further disintegration of the established biofilm. Most noteworthy is the combination of the antibiotic with Mn-tdda-phen and Ag-tdda-phen at 64 µg/mL (53.2 and 87 µM, respectively), which removed 99.6% and 99.1% of PAO1 biofilm, respectively. The enhanced activity was also maintained across the clinical isolates, with the combined metal-tdda-phen/gentamicin combinations presenting a dose-dependent response. At the highest test concentration, the combination of metal-tdda-phen complexes (64 µg/mL, 53.2–87 µM) with gentamicin (32 µg/mL, 55.5 µM) dismantled

over 90% of the mature biofilm for all three metal-tdda-phen complexes in CF2 (93.5–96.5% dismantled) and CF3 (93.9–99.6%), while in CF1, the combination results were: Ag-tdda-phen (92.8%), Cu-tdda-phen (86.1%), Mn-tdda-phen (83.1%).

A

ATCC 27853

Mn-tdda-phen (µg/mL)

Gentamicin (µg/mL)	64	32	16	8	4	2	1	0
32	80.7	76.6	65.8	60.1	55.4	47.7	42.9	34.6
16	78.4	75.4	60.1	56.3	49.8	41.9	34.5	28.9
8	75.2	69.2	55.6	54.9	45.3	33.6	28.8	13.5
4	69.8	66.4	50.2	46.5	38.8	26.1	22.3	6.0
2	67.0	62.1	47.9	41.1	35.7	19.4	11.2	3.6
0	58.9	35.5	24.0	20.5	17.5	13.7	9.4	0.0

B

ATCC 27853

Cu-tdda-phen (µg/mL)

Gentamicin (µg/mL)	64	32	16	8	4	2	1	0
32	82.8	75.5	68.1	58.4	48.5	47.3	36.0	34.6
16	75.8	71.9	61.3	57.4	43.3	43.4	38.3	28.9
8	72.8	68.7	52.5	51.0	41.4	34.3	31.4	13.5
4	68.7	61.6	48.3	42.6	39.5	28.3	22.4	6.0
2	61.6	52.7	45.2	36.7	30.2	22.9	14.1	3.6
0	51.8	43.7	39.0	31.3	19.8	11.0	6.0	0.0

C

ATCC 27853

Ag-tdda-phen (µg/mL)

Gentamicin (µg/mL)	64	32	16	8	4	2	1	0
32	93.5	84.7	70.6	63.5	52.5	44.7	36.9	34.6
16	81.9	79.1	67.0	56.7	46.6	34.9	30.8	28.9
8	74.0	77.7	52.4	47.9	40.9	32.2	23.3	13.5
4	69.0	68.0	49.0	44.1	37.8	23.4	20.7	6.0
2	67.6	62.6	44.8	40.4	28.2	22.8	13.6	3.6
0	53.1	45.3	43.3	39.3	24.1	21.2	7.8	0.0

D

PAO1

Mn-tdda-phen (µg/mL)

Gentamicin (µg/mL)	64	32	16	8	4	2	1	0
32	99.6	89.7	81.7	67.6	54.4	43.0	33.8	20.0
16	95.9	84.9	74.4	59.5	53.4	41.9	31.7	14.9
8	89.8	75.9	62.2	55.4	49.0	35.5	30.9	8.8
4	71.1	62.6	59.0	54.1	32.2	32.0	29.3	4.9
2	59.0	53.0	42.6	32.1	27.6	25.6	26.7	3.1
0	49.1	32.2	24.5	17.9	22.0	19.5	14.9	0.0

E

PAO1

Cu-tdda-phen (µg/mL)

Gentamicin (µg/mL)	64	32	16	8	4	2	1	0
32	82.9	80.7	71.0	58.7	51.9	42.0	41.3	20.0
16	75.4	73.8	68.5	51.2	48.0	39.5	33.2	14.9
8	73.5	67.6	67.9	46.7	45.0	31.4	29.0	8.8
4	63.1	59.6	57.3	42.2	39.7	24.4	27.9	4.9
2	58.0	52.7	52.3	37.4	32.6	23.5	21.9	3.1
0	55.5	46.8	36.2	24.1	22.7	13.0	11.7	0.0

F

PAO1

Ag-tdda-phen (µg/mL)

Gentamicin (µg/mL)	64	32	16	8	4	2	1	0
32	99.1	93.6	87.4	77.0	68.0	55.7	51.1	20.0
16	92.4	88.1	71.9	69.5	64.4	50.6	41.6	14.9
8	87.2	76.7	70.7	60.9	56.7	44.6	36.3	8.8
4	72.2	69.8	63.3	53.7	47.4	40.9	25.1	4.9
2	65.8	65.3	59.7	50.1	45.5	37.7	22.9	3.1
0	61.0	53.6	40.7	33.3	15.6	12.0	5.7	0.0

Figure 3.5 Laboratory strains - Heat map representation of the percentage of biofilm removal of 48 h established biofilms of laboratory strains, ATCC 27853 and PAO1 by combinations of metal-tdda-phen complexes with gentamicin. Mn-tdda-phen and gentamicin (**A, D**); Cu-tdda-phen and gentamicin (**B, E**); Ag-tdda-phen and gentamicin (**C, F**). The heat map shows the percentage of biofilm removed with respect to the untreated sample.

G

		CF1 Mn-tdda-phen (µg/mL)							
		64	32	16	8	4	2	1	0
Gentamicin (µg/mL)	32	83.1	73.9	67.1	53.5	42.5	32.8	30.6	8.1
	16	73.3	65.9	62.5	51.3	35.3	29.2	25.5	5.6
	8	71.1	61.3	56.4	46.9	34.7	24.2	14.8	3.5
	4	61.0	48.0	44.0	37.3	26.9	19.2	11.1	2.1
	2	45.2	38.6	34.6	32.0	22.5	16.8	9.6	0.7
	0	33.3	25.5	24.1	18.1	13.3	5.5	3.4	0.0

J

		CF2 Mn-tdda-phen (µg/mL)							
		64	32	16	8	4	2	1	0
Gentamicin (µg/mL)	32	93.5	83.2	71.5	62.5	54.3	42.8	35.2	23.8
	16	90.1	78.1	66.4	56.2	50.1	37.9	29.5	9.4
	8	81.9	65.3	58.9	53.0	45.3	34.1	26.7	4.8
	4	71.8	63.3	48.6	43.8	34.7	26.0	23.5	3.1
	2	61.4	51.0	42.1	36.5	26.4	19.8	13.9	1.6
	0	52.5	41.8	35.7	26.3	21.7	13.4	2.4	0.0

H

		CF1 Cu-tdda-phen (µg/mL)							
		64	32	16	8	4	2	1	0
Gentamicin (µg/mL)	32	86.1	81.7	70.6	65.8	50.3	49.0	32.0	8.1
	16	80.7	81.2	68.1	60.2	47.2	43.4	26.4	5.6
	8	73.4	71.0	62.3	52.1	44.1	41.5	22.9	3.5
	4	67.3	67.1	54.9	51.2	39.5	29.8	19.5	2.1
	2	62.7	61.1	50.8	46.7	35.8	28.5	16.8	0.7
	0	59.5	53.9	44.1	34.8	24.3	6.6	1.1	0.0

K

		CF2 Cu-tdda-phen (µg/mL)							
		64	32	16	8	4	2	1	0
Gentamicin (µg/mL)	32	96.5	89.9	74.8	63.3	58.7	48.0	39.6	23.8
	16	87.0	78.7	66.0	59.9	52.5	41.7	38.4	9.4
	8	76.4	70.2	65.3	52.1	48.4	35.1	30.5	4.8
	4	74.2	59.5	55.7	45.9	39.7	33.2	22.8	3.1
	2	64.0	55.6	47.0	34.7	27.6	23.9	12.6	1.6
	0	41.3	40.8	34.7	28.6	18.2	11.1	1.7	0.0

I

		CF1 Ag-tdda-phen (µg/mL)							
		64	32	16	8	4	2	1	0
Gentamicin (µg/mL)	32	92.8	86.9	75.5	63.4	57.0	37.3	34.4	8.1
	16	85.9	85.3	74.5	60.7	55.5	36.1	29.4	5.6
	8	79.8	81.9	69.0	55.4	52.2	33.0	26.1	3.5
	4	75.4	72.1	64.5	53.9	49.7	27.7	21.0	2.1
	2	66.4	64.8	61.4	48.5	45.2	21.0	15.5	0.7
	0	57.2	52.4	45.0	29.3	9.7	6.7	1.0	0.0

L

		CF2 Ag-tdda-phen (µg/mL)							
		64	32	16	8	4	2	1	0
Gentamicin (µg/mL)	32	95.9	90.4	82.7	72.6	70.4	38.1	28.5	23.8
	16	90.8	78.1	78.8	67.5	64.5	35.6	25.5	9.4
	8	79.8	74.7	65.2	62.7	53.8	34.2	21.7	4.8
	4	70.9	61.1	51.0	42.6	37.4	31.7	17.4	3.1
	2	64.4	53.9	46.7	37.1	33.8	30.0	14.0	1.6
	0	53.2	46.6	32.1	26.6	13.4	5.6	3.5	0.0

Figure 3.6 Clinical isolates - Heat map representation of the percentage of biofilm removal of 48 h established biofilms of clinical isolates, CF1 and CF2 by combinations of metal-tdda-phen complexes with gentamicin. Mn-tdda-phen and gentamicin (**G, J**); Cu-tdda-phen and gentamicin (**H, K**); Ag-tdda-phen and gentamicin (**I, L**). The heat map shows the percentage of biofilm removed with respect to the untreated sample.

M		CF3							
		Mn-tdda-phen (µg/mL)							
		64	32	16	8	4	2	1	0
Gentamicin (µg/mL)	32	99.5	89.4	82.4	64.7	59.0	44.6	29.4	8.5
	16	92.1	83.4	80.4	61.9	56.1	42.8	27.8	7.6
	8	84.6	73.1	72.2	52.5	50.8	37.8	24.6	6.2
	4	76.3	70.5	66.3	48.0	46.8	31.3	19.4	4.3
	2	75.0	61.5	52.7	47.5	42.5	24.3	17.5	2.0
	0	54.7	44.9	42.7	39.5	36.4	14.4	10.5	0.0
N		CF3							
		Cu-tdda-phen (µg/mL)							
		64	32	16	8	4	2	1	0
Gentamicin (µg/mL)	32	93.9	85.7	75.2	69.5	58.8	37.8	33.9	8.5
	16	88.1	72.3	68.8	66.1	50.4	33.8	32.5	7.6
	8	77.1	66.1	65.0	57.9	49.2	32.4	29.7	6.2
	4	70.4	62.7	57.3	53.4	40.4	30.4	27.6	4.3
	2	64.4	58.5	55.1	47.3	39.6	27.0	24.7	2.0
	0	60.6	50.3	45.8	33.3	30.7	23.9	19.2	0.0
O		CF3							
		Ag-tdda-phen (µg/mL)							
		64	32	16	8	4	2	1	0
Gentamicin (µg/mL)	32	99.6	92.7	85.5	66.7	56.3	49.0	44.4	8.5
	16	91.9	86.3	74.6	58.1	46.6	43.2	32.8	7.6
	8	78.4	75.3	62.9	55.0	43.2	32.8	31.6	6.2
	4	68.1	58.4	54.3	46.7	39.9	31.3	27.6	4.3
	2	60.7	54.5	52.2	42.6	37.2	27.2	25.0	2.0
	0	45.5	43.2	38.0	30.2	24.3	15.9	10.8	0.0

Figure 3.7 Clinical isolates continued - Heat map representation of the percentage of biofilm removal of 48 h established biofilms of clinical isolate CF3 by combinations of metal-tdda-phen complexes with gentamicin. Mn-tdda-phen and gentamicin (**M**); Cu-tdda-phen and gentamicin (**N**); Ag-tdda-phen and gentamicin (**O**). The heat map shows the percentage of biofilm removed with respect to the untreated sample.

The fractional inhibitory concentration (FIC) index (FIC_I) for combinations of metal-tdda-phen complexes with gentamicin was calculated according to the equation: $FIC_I = FIC_{(metal\text{-}tdda\text{-}phen\ complex)} + FIC_{(gentamicin).}$ Results for the interactions between the metal-tdda-phen complexes and gentamicin combinations in the selected *P. aeruginosa* strains, PAO1 and CF3, are given in **Table 3.2.** The data revealed synergistic activity ($FIC \leq 0.5$) against the established mature biofilms for all metal-tdda-phen/gentamicin combinations.

Test complexes	Organism	FIC Index	Interpretation
Mn-tdda-phen + Gentamicin	PAO1	0.141	Synergistic
	CF3	0.133	Synergistic
Cu-tdda-phen + Gentamicin	PAO1	0.313	Synergistic
	CF3	0.156	Synergistic
Ag-tdda-phen + Gentamicin	PAO1	0.141	Synergistic
	CF3	0.133	Synergistic

Table 3.2 Results of interaction studies for metal-tdda-phen/gentamicin combinations against PAO1 (reference strain) and CF3 (clinical isolate) in established biofilms.

3.3.4 Toxicity of metal-tdda-phen complexes against mammalian cells

In vitro growth inhibitory data (IC_{50} values) for the metal-tdda-phen complexes against mammalian CFBE and BEAS-2B epithelial cells are listed in **Table 3.3.** Both cell lines were more tolerant of gentamicin (CFBE IC_{50} = 335 µg/mL, 617 µM; BEAS-2B IC_{50} = 320 µg/mL, 556 µM) and metal-tdda-phen complexes Mn-tdda-phen (CFBE IC_{50} = 306 µg/mL, 416 µM; BEAS-2B IC_{50} = 257 µg/mL, 350 µM) and Ag-tdda-phen (CFBE IC_{50} = 264 µg/mL, 219 µM; BEAS-2B IC_{50} = 233 µg/mL, 194 µM). Cu-tdda-phen was remarkably more toxic to the CFBE (IC_{50} = 8 µg/mL, 11 µM) and BEAS-2B (IC_{50} = 6 µg/mL, 8 µM) cells. This toxicity profile has also been reported by Gandra *et al.*, (2017)

and McCarron *et al.*, (2018). There was no significant differences between the CF and normal cell lines.

The selectivity of compounds to microbial cells is an essential criterion for evaluating the cytotoxic action of an antibacterial agent. This parameter is characterized by a selectivity index (SI) value, calculated as the ratio between the IC_{50} for mammalian cells and the MIC_{50} value for bacterial cells. The greater the SI value, the higher the selectivity of the compound to bacteria. The SI for metal-tdda-phen complexes and gentamicin are in **Table 3.3** for the CF cell line (CFBE) and healthy cell line (BEAS-2B). Aside from prescription antibiotic gentamicin, which is known to be selective for prokaryotes by inhibiting bacterial protein synthesis by binding to 30S ribosomes, the overall mean SI present as Mn-tdda-phen >Ag-tdda-phen > Cu-tdda-phen. Observing the clinical isolates individually, gentamicin's SI drops considerably compared to the reference strains. For instance, the SI of gentamicin for ATCC 27853 was 710 for the CFBE cell line and 640 BEAS-2B cell line; however it was 1 for CF3 for both cell lines. This was to be expected as the activity of gentamicin declined considerably against this isolate. The SI for metal-tdda-phen complexes Mn-tdda-phen and Ag-tdda-phen were 5-4 and 8-7 for CFBE and BEAS-2B, respectively. This is due to the heightened activity of these complexes towards CF3.

Test Compounds	IC_{50} µg/mL and (µM)	Selectivity Index (SI)					Overall mean SI
	CFBE	ATCC 27853	PAO1	CF1	CF2	CF3	
Mn-tdda-phen	306 (416)	38	19	77	77	5	43
Cu-tdda-phen	8 (11)	1	1	2	2	0	1
Ag-tdda-phen	264 (219)	66	17	33	33	8	31
Gentamicin	355 (617)	710	355	89	6	1	232
Test Compounds	**IC_{50} µg/mL and (µM)**	**Selectivity Index (SI)**					**Overall mean SI**
	BEAS-2B	**ATCC 27853**	**PAO1**	**CF1**	**CF2**	**CF3**	
Mn-tdda-phen	257 (350)	32	16	64	64	4	36
Cu-tdda-phen	6 (8)	1	0	2	2	0	1
Ag-tdda-phen	233 (194)	58	15	29	29	7	28
Gentamicin	320 (556)	640	320	80	5	1	209

Table 3.3 *In vitro* IC_{50} values presented as µg/mL and (µM) for CFBE (CF cell line) and BEAS-2B (healthy cell line) epithelial cells and calculated selectivity values (SI) values for the metal-tdda-phen complexes and gentamicin control. Larger SI values indicate greater cell selectivity

3.3.5 Metal-tdda-phen complexes affect individual components of a biofilm

In biofilms, microbes are held together by a protective polymeric extracellular matrix (ECM) comprised of polysaccharides, extracellular DNA (eDNA), and virulence factors such as pyocyanin and pyoverdine. To understand how the metal-tdda-phen complexes affect both the formation of biofilms (pre-treatment) and the reduction of established mature biofilms (post-treatment), $MBIC_{50}$ and $MBEC_{50}$ doses were applied to *P. aeruginosa* strains PAO1 and CF3, alone and in the presence of gentamicin, and the results are presented in **Figure 3.8** and **3.9.**

Exopolysaccharide is an important component of the ECM for the formation and stabilisation of the biofilm structure, and therefore the reduction of this component would

be a beneficial target for antimicrobial agents. The pre-treatment of PAO1 and CF3 with metal-tdda-phen complexes caused an attenuation in exopolysaccharides. Exposure to Mn-tdda-phen caused the greatest reduction of exopolysaccharide in PAO1 (74% ± 4), followed by Cu-tdda-phen (67% ± 1), Ag-tdda-phen (49% ± 6) and gentamicin (47% ± 9). Combined pre-treatment of Mn-tdda-phen, Cu-tdda-phen and Ag-tdda-phen with gentamicin reduced exopolysaccharides in PAO1 by 64% ± 6, 72% ± 5 and 81% ± 5, respectively, reducing the efficacy of Mn-tdda-phen as a single agent, but enhancing the effect of the other two metal-tdda-phen complexes. Pre-treatment of the clinical isolate CF3 with the test agents saw a reduction in the activity of metal-tdda-phen complexes (52–55% ± 7) and gentamicin (38% ± 6) against the exopolysaccharides, compared to that seen for PAO1. However, in contrast to PAO1, the Mn-tdda-phen/gentamicin combination was the most effective (77% ± 1) at reducing exopolysaccharides in the clinical isolate. For the post-treatment studies, the biofilms were allowed to grow for 48 h and then exposed to the test complexes for a further 24 h. For PAO1, the reduction of exopolysaccharides by the metal-tdda-phen complexes (41–46% ± 9) was similar to that observed for gentamicin (44% ± 9), while the combined treatment again intensified the activity, prompting a 73–78% reduction in exopolysaccharide. For the treatment of CF3, gentamicin was the least effective and Ag-tdda-phen the most when used singularly (the latter complex reduced the exopolysaccharide in the biofilm by 61% ± 9). For the metal-tdda-phen/gentamicin combinations, activity increased somewhat uniformly (72–77% reduction).

Extracellular DNA (eDNA) is an essential constituent of the ECM. It facilitates biofilm formation and enhances biofilm strength and stability by bridging divalent ions to other components in the matrix. It has also been observed that eDNA increases the tolerance of *P. aeruginosa* biofilms toward cationic antibiotics, such as aminoglycosides, by binding

directly to the antibiotic and preventing penetration (Chiang *et al*., 2013). The pre-treatment of PAO1 and CF3 with metal-tdda-phen complexes or gentamicin singly did not cause any appreciable difference in eDNA content compared to the untreated sample. The combination treatments were unilaterally more effective, with Ag-tdda-phen/gentamicin inhibiting eDNA in PAO1 by 50% ± 11, Cu-tdda-phen/gentamicin by 49% ± 4 and Mn-tdda-phen/gentamicin 34% ± 6. A similar trend was observed for CF3. Except for gentamicin, the post-treatment of established biofilms of both strains with single metal-tdda-phen complexes was more effective than pre-treatment. A dramatic improvement in eDNA inhibition was witnessed when both of the established biofilms were exposed to all of the metal-tdda-phen/gentamicin combinations (66–75% reduction), with Cu-tdda-phen/gentamicin being the most aggressive.

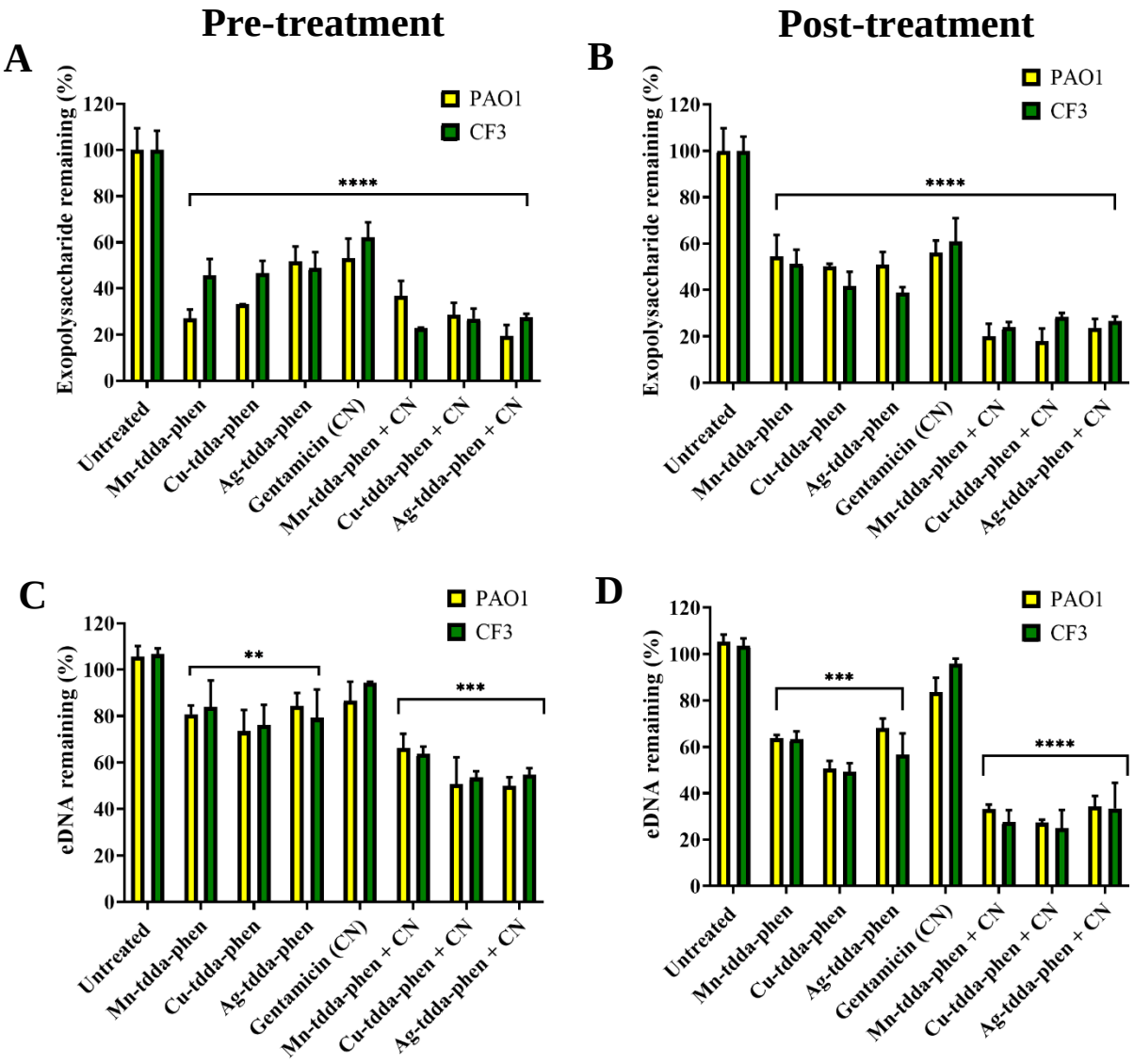

Figure 3.8 Effects of metal-tdda-phen complexes alone, gentamicin alone, and metal-tdda-phen complexes with gentamicin on both the formation of biofilm (pre-treatment) and reduction of established biofilm (post-treatment) of PAO1 and CF3: The percentages of exopolysaccharide (**A**, **B**) and eDNA (**C**, **D**) remaining after treatment (relative to untreated biofilms) are given. (*: $P < 0.05$, **: $P < 0.01$, ***: $P < 0.001$)

The prevalence and progression of infection by *P. aeruginosa* in the host is dependent upon the secretion of numerous extracellular molecules, such as the virulent factors, pyocyanin and pyoverdine. Pyocyanin is one of the major components dictating the advancement of infection and biofilm formation, especially in CF patients, and is under quorum sensing (QS) control. It is redox-active and promotes eDNA release in *P.*

aeruginosa by inducing cell lysis mediated via hydrogen peroxide production. The extent of pyocyanin production varied amongst the strains of *P. aeruginosa* tested. Untreated PAO1 manufactured about 10 µM of pyocyanin, while the untreated CF clinical isolate, CF3, produced upwards of 80 µM. The results of the pyocyanin assay are presented as a percentage of production relative to the untreated sample for comparison (**Figure 3.9**). Pre-treatment with the Ag-tdda-phen/gentamicin combination significantly reduced pyocyanin in both PAO1 (80% ± 9) and CF3 (65% ± 6). The manganese and copper metal-tdda-phen/gentamicin combinations also reduced pyocyanin production compared to their treatment as a single agent. Surprisingly, the pre-treatment of PAO1 with Cu-tdda-phen alone actually enhanced the production of pyocyanin (106% ± 8), and gentamicin also had a similar positive influence on CF3 (116% ± 13). In general, the single test compounds and their gentamicin combinations were much less effective at reducing pyocyanin production by the two mature biofilms. Although Ag-tdda-phen alone increased pyocyanin in PAO1 (134%), the Ag-tdda-phen/gentamicin combination caused the greatest reduction of pyocyanin (35% ± 9 in PAO1 and 49% ± 7 in CF3).

Pyoverdine, the main siderophore of *P. aeruginosa*, has a high affinity for ferric (Fe^{3+}) iron and thus is responsible for obtaining extracellular iron, an essential nutrient for biofilm formation (Kang *et al*., 2018). In addition, pyoverdine can regulate the production of multiple bacterial virulence factors. In the pre-treatment studies (**Figure 3.9**), it was found that only the Ag-tdda-phen/gentamicin caused a notable reduction in pyoverdine production (by 16% ± 5 in PAO1 and 49% ± 6 in CF3), with most of the remaining test substances enhancing production (by up to 134%). Post-treatment of the two established biofilms with the single metal-tdda-phen compounds had little or no effect on pyoverdine production with respect to the control. Whilst gentamicin singly and the Mn-tdda-phen/gentamicin combination caused a sizable reduction in pyoverdine in the reference

strain (24% ± 8 and 26% ± 9, respectively) and the clinical isolate (30% ± 8 and 41% ± 9, respectively), Cu-tdda-phen/gentamicin and Ag-tdda-phen/gentamicin were only effective against CF3 (41% ± 9 and 48% ± 7 reduction, respectively).

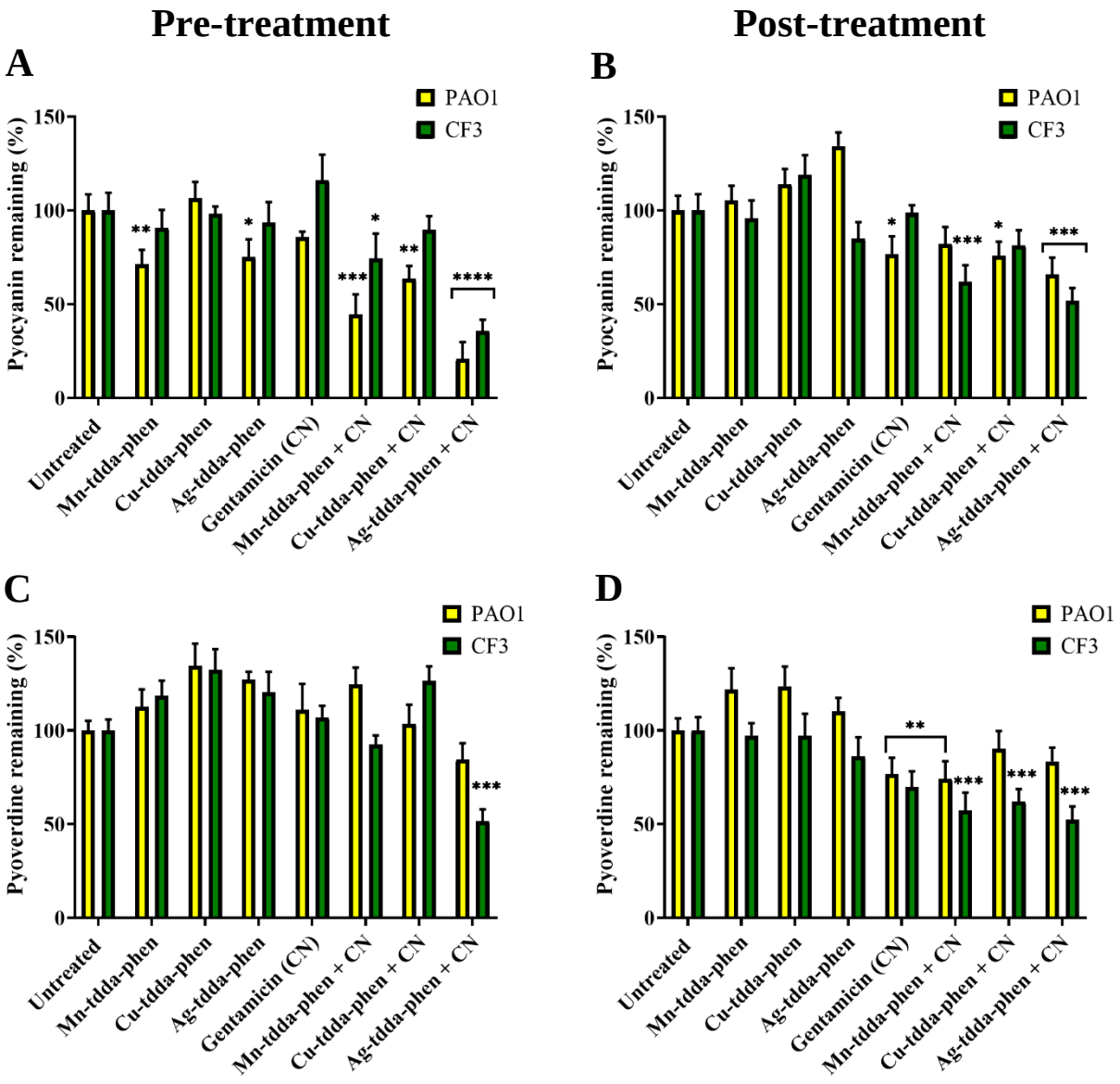

Figure 3.9 Effects of metal-tdda-phen complexes alone, gentamicin alone, and metal-tdda-phen complexes with gentamicin on both the formation of biofilm (pre-treatment) and reduction of established biofilm (post-treatment) of PAO1 and CF3: The percentages of pyocyanin (**A**, **B**) and pyoverdine (**C**, **D**) remaining after treatment (relative to untreated biofilms) are given. (*: $P < 0.05$, **: $P < 0.01$, ***: $P < 0.001$).

In addition to the components of the biofilm, the liquid culture they were grown in was aspirated, and the bacterial cells present were assessed through the plate count method. As presented in **Figure 3.10**, untreated PAO1 had a 7.6×10^8 colony-forming unit (CFU)/mL, while pre-treatment with metal-tdda-phen complexes saw a slight reduction of $7.1–5.2 \times 10^8$ CFU/mL and gentamicin had 3.9×10^8 CFU/mL. Complementing the biofilm component data, the combination of both the metal-tdda-phen complexes with gentamicin saw the greatest reduction of viable cells, with Ag-tdda-phen demonstrating a one-fold reduction to 7.9×10^7 CFU/mL. Pre-treatment of CF3 with gentamicin reduced the viable cells from 7.5×10^8 CFU/mL to 7×10^8 CFU/mL, followed by Cu-tdda-phen (5.9×10^8 CFU/mL), Ag-tdda-phen (5.5×10^8 CFU/mL) and Mn-tdda-phen (5.4×10^8 CFU/mL). Akin to PAO1, metal-tdda-phen/gentamicin reduced viable cells in the culture to 3.3×10^8 CFU/mL–2.2×10^8 CFU/mL. Post-treatment of PAO1 and CF3 had similar trends, with metal-tdda-phen complexes slightly outperforming gentamicin as singular agents. However, the combination of Mn-tdda-phen/gentamicin and Cu-tdda-phen/gentamicin saw a 2-fold reduction in viable cells and Ag-tdda-phen/gentamicin a 3-fold reduction.

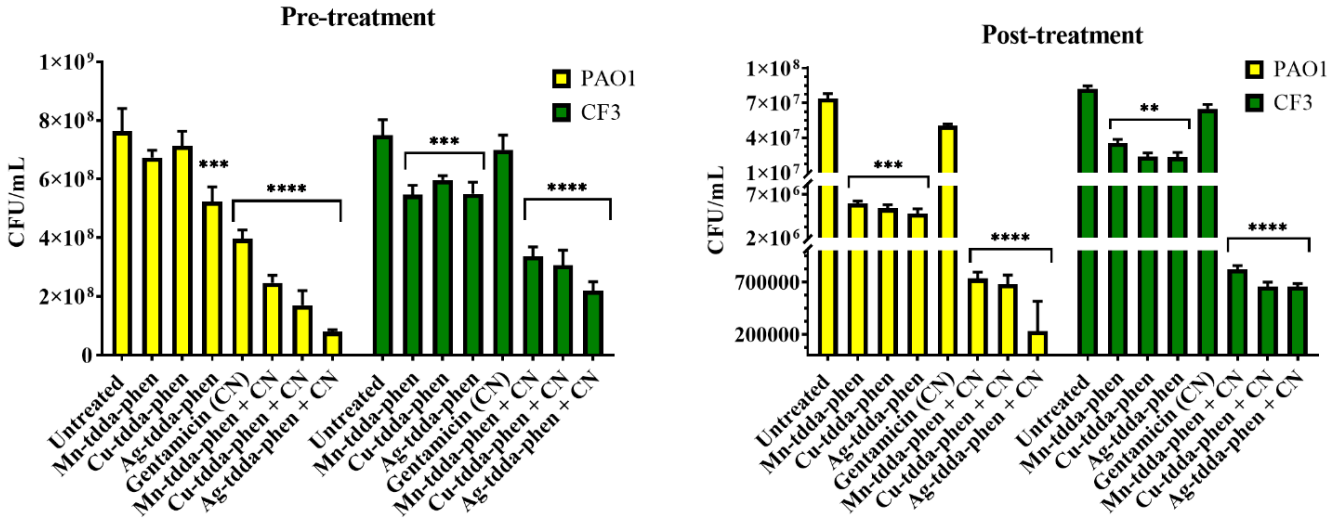

Figure 3.10 Viable cells were measured after pre- and post-exposure to 0.5 × MBIC and 0.5 × MBEC of metal-tdda-phen complexes alone, gentamicin alone, and metal-tdda-phen complexes with gentamicin. The results are the means ± standard errors of the means from three independent experiments, with viable counts done in triplicate. (*: $P < 0.05$, **: $P < 0.01$, ***: $P < 0.001$).

3.4. Discussion

Pseudomonas aeruginosa is the most prevalent pathogen in the lungs of cystic fibrosis (CF) patients and the leading cause of morbidity and mortality (Stefani *et al*., 2017). Ireland has the highest rate of CF per capita in the world, with approximately 7 in every 10,000 people living with the disease, almost three times the average rate in other European countries and the United States (Cystic Fibrosis Ireland, 2018). Conventional antibiotic treatment strategies for *P. aeruginosa* in CF patients are only partially effective and contribute to antibiotic resistance. In addition, *P. aeruginosa* predominantly resides in biofilms in the lungs of CF patients, which are also up to 1000 times more resistant to antibiotic treatment than their planktonic counterparts.

This chapter investigated the antibacterial and anti-biofilm capabilities of copper(II), manganese(II), and silver(I) complexes containing 1,10-phenanthroline (phen) and 3,6,9-trioxaundecanedioate (tdda) ligands against *P. aeruginosa* strains isolated from the lungs of CF patients in Irish hospitals. These metal complexes have previously shown anti-bacterial and anti-fungal capabilities, and including the phen ligand is key to their antimicrobial properties. Furthermore, the tdda dianionic ligand drastically enhances the water solubility of the complex. The results in **Table 2.3** demonstrate the superior potency of the metal-tdda-phen complexes compared to the anti-*P. aeruginosa* activities of the metal-free phen, $tddaH_2$ and the simple copper(II), manganese(II) and silver(I) salts (essentially free metal ions). The antibiotic gentamicin was the most active compound against the reference strains (ATCC 27853 and PAO1). Whereas the efficacy of gentamicin was dampened across the clinical isolates (CF1–CF3), the metal-tdda-phen complexes maintained clinically relevant activity. Taking the mean minimum inhibitory concentration (MIC) for each bacterial strain, the order of planktonic growth inhibition by the metal-tdda-phen complexes was Cu-tdda-phen > Ag-tdda-phen > Mn-tdda-phen.

While the viability profile of the metal complexes within mammalian cells had the same overall cadence, resulting in Mn-tdda-phen having the greatest selectivity index and Cu-tdda-phen demonstrating the worst. Gandra *et al.* (2017) also reported that the Mn(II) complex was exceptionally well tolerated by the mammalian lung cell line, A549, with a concentration capable of reducing cellular viability by 50% (CC_{50}) of 261.67 mg/L validating the observations within this study.

The biofilm lifecycle of *P. aeruginosa* is an important virulence attribute for establishing infections in CF patients. All of the metal-tdda-phen complexes could inhibit biofilm formation (pre-treatment) in terms of both biofilm biomass and cellular viability, outperforming gentamicin across the three clinical isolates. Moreover, all three of the metal-tdda-phen complexes could disrupt the established mature biofilm (post-treatment) of the *P. aeruginosa* strains in a dose-dependent manner. Similar activity has previously been reported by Viganor *et al.* (2016) for the related complex cations, $[Ag(phendione)_2]^{+1}$ and $[Cu(phendione)_3]^{+2}$ (phendione = 1,10-phenanthroline-5,6-dione), against 32 Brazilian clinical isolates of *P. aeruginosa*. Moreover, the same phendione complexes exhibited anti-biofilm action against carbapenemase-producing *Acinetobacter baumannii*, another multidrug-resistant (MDR) Gram-negative bacterium (Ventura *et al*., 2020). Presently, the MIC of Mn-tdda-phen for CF3 was 128 µg/mL (174 µM), and when an established biofilm of this strain is treated at the same concentration, it is reduced by ~79%**.** The MIC of both Cu-tdda-phen and Ag-tdda-phen was 64 µg/mL (86 and 53.2 µM, respectively) for CF3, and the reduction in biofilm biomass after treatment at this concentration was ~70% and ~51%, respectively. These anti-biofilm studies indicated the potential for enhanced anti-biofilm activity by combining the metal-tdda-phen complexes with gentamicin. At the highest concentration of the metal-tdda-phen complexes (64 µg/mL) in combination with gentamicin (32 µg/mL), there was

>90% biofilm removal for CF2 and CF3 and >83% for CF1, and the fractional inhibitory concentration (FIC) index showed a positive synergism for all three metal-tdda-phen complexes in the presence of gentamicin. A clinical study in Ireland on CF *P. aeruginosa* clinical isolates and the same laboratory reference strains (ATCC 27853 and PAO1) showed that tobramycin (aminoglycoside) and ceftazidime (cephalosporin) was the only effective combination to show positive synergism (FIC ≤ 0.5) against a mature biofilm of a single clinical isolate at a concentration of 64 mg/L, *in vitro* (Kapoor and Murphy, 2018). However, as mentioned earlier, the evolving antibiotic resistance is problematic and of concern when considering combinations of established antibiotics for treating *P. aeruginosa* infections in CF patients. Novel therapeutics, where resistance is less likely to be a factor, would be favourable for future clinical interventions.

Since significant activity was evident for the metal-tdda-phen complexes, acting either alone or in combination with gentamicin, against biofilms formed by the PAO1 reference strain and the CF3 clinical isolate, individual components of the biofilm were tested to see if there was a specific molecular target. These targets included exopolysaccharide and extracellular DNA (eDNA), two critical components of the polymeric extracellular matrix (ECM), and the virulence factors, pyocyanin and pyoverdine, found in the ECM. Many *P. aeruginosa* strains can synthesise the three exopolysaccharides, alginate, Psl, and Pel, which play an essential role in biofilm formation and stabilising its structure. Strains isolated from CF patients are commonly found to over-produce alginate, and biofilms of these strains have been observed to have a much higher resistance to aminoglycosides, such as gentamicin, than their isogenic non-mucoid strain (Hentzer *et al*., 2001). Additional studies have also implicated both Psl (Billings *et al*., 2013) and Pel (Colvin *et al*., 2011) in the biofilm-associated tolerance towards aminoglycosides, thus making exopolysaccharides an essential component of the ECM. It is thought that Psl associates

with eDNA through hydrogen bonding to form eDNA–Psl fibres in the centre of pellicles (Wang *et al*., 2015), and cationic Pel cross-links eDNA in the biofilm stalk via ionic interactions (Jennings *et al*., 2015). eDNA is known to chelate divalent metal cations, such as Mg^{2+}, Mn^{2+}, Zn^{2+} and Ca^{2+} (Mulcahy *et al*., 2008), with the latter creating strong electrostatic interactions which give the biofilm integrity (Das *et al*., 2014), and there have been biofilm studies conducted on the use of metal chelators, such as ethylenediaminetetraacetic acid (EDTA). In this context, EDTA alone was found to be 1000-fold more destructive to a PAO1 biofilm than gentamicin, and a combination of EDTA (50 mM) with gentamicin (50 μg/mL) caused a complete reduction of biofilm viability (>99%) and detachment of cells (Banin *et al*., 2006). This chapter demonstrated that the enhanced anti-biofilm activity of metal-tdda-phen/gentamicin combinations was associated with a reduction in both exopolysaccharide and eDNA. It has been widely reported that the treatment of *P. aeruginosa* biofilms with DNase I, an enzyme that cleaves DNA, significantly disrupts biofilms and enhances antibiotic penetration (Tetz *et al*., 2009). As CF sputum is rich in eDNA (<1–20 mg/mL), this is thus a desirable molecular target. The copper(I) complex cation, $[Cu(phen)_2]^+$, in the presence of reducing agents, was the first reported example of a novel artificial metallonuclease possessing potent DNA cleavage capability (Sigman *et al*., 1979). Our group has previously shown that copper(II)-dicarboxylate-phen complexes also display effective nuclease capability, even without added reductant (Kellett *et al*., 2011b). In this context, treating a mature biofilm with Cu-tdda-phen prompted the most significant decrease in eDNA in both the reference and clinical isolates. Our data suggest that the metal-tdda-phen complexes cause biofilm destabilization by interacting with extracellular DNA and exopolysaccharides in the ECM, possibly through Psl. However, further studies will be required to establish the role of Psl and Pel in these interactions. This destabilization could allow the previously

inhibited gentamicin into the biofilm to enhance its cytotoxic action, which the viable cell counts have further supported.

The encouraging results prompt further investigations into the ability of metal-tdda-phen complexes to act on *P. aeruginosa* clinical isolates *in vivo* using larvae of the greater wax moth *Galleria mellonella*.

Chapter 4.

In Vivo evaluation of *Galleria mellonella* larvae response to selected test complexes

Chapter 4 (objective 3) is based on the following paper: ***O'Shaughnessy M****, Piatek M, McCarron P, McCann M, Devereux M, Kavanagh K, Howe O. In vivo activity of metal complexes containing 1,10-phenanthroline and 3,6,9-trioxaundecanedioate ligands against Pseudomonas aeruginosa infection in Galleria mellonella larvae. Biomedicines. 2022; 10(2):222.*

4.1. Introduction

The Gram-negative human pathogen, *P. aeruginosa*, is a noteworthy contributor to elevated AMR prevalence and is frequently isolated from a diverse range of acute, chronic, and biofilm-associated infections. Most strains now present as multidrug-resistant (MDR), which increases morbidity in infected patients, particularly those with cystic fibrosis (CF) (Garcia-Nuñez *et al*., 2017; Jurado-Martín *et al*., 2021). The activity profile of manganese(II), copper(II), and silver(I) complexes incorporating 1,10-phenanthroline (phen) and 3,6,9-trioxaundecanedioate (tdda) were previously presented with effects against *P. aeruginosa* strains of CF patients in **Chapter 3**. The ability to act on *P. aeruginosa* clinical isolates synergistically with gentamicin on mature biofilms prompted the *in vivo* studies, using larvae of the greater wax moth *Galleria mellonella*, reported within.

A critical aspect in evaluating an antibacterial drug is the pre-clinical test for toxicity and effectiveness in suitable animal models. *G. mellonella* larvae are a valuable model for assessing *in vivo* toxicity and mechanism of action studies of novel drugs. Low cost, ease of handling and maintenance are desirable factors for using the larval model. They have a relatively short life cycle (40-60 days) and can survive at 37 °C, which is an important attribute when assessing virulence and treating human pathogens (Browne *et al*., 2014). Therefore, *G. mellonella* has been extensively utilized to assess both pathogens and drug responses, as presented in **Figure 4.1.** Such studies evaluate the pathogenicity of bacterial and fungal pathogens (Kavanagh and Reeves, 2004; Sheehan and Kavanagh, 2019; Sheehan *et al*., 2019), study biofilm formation (Borghi *et al*., 2014), measure the *in vivo* toxicity of novel compounds (Thornton *et al*., 2016; Rochford *et al*., 2018) and determine the *in vivo* efficacy of established (Krezdorn *et al*., 2014; Ignasiak and Maxwell, 2017) and novel antimicrobial agents (McCann *et al*., 2012b; Gandra *et al*., 2020). Moreover,

studies assessing *G. mellonella* and mammalian models have reported a correlation in the results obtained. Jander *et al.* (2000) demonstrated similar virulence patterns in larvae and mice injected with *P. aeruginosa* mutants, and Brennan *et al.* (2002) identified corresponding virulence patterns between *Candida albicans* in the aforementioned models. The generation of comparable data is due to the high degree of structural and functional analogies across human innate immunity and the insect immune response, composed of physical barriers and interconnected cellular and humoral responses (Browne *et al.*, 2013; Sheehan *et al.*, 2018).

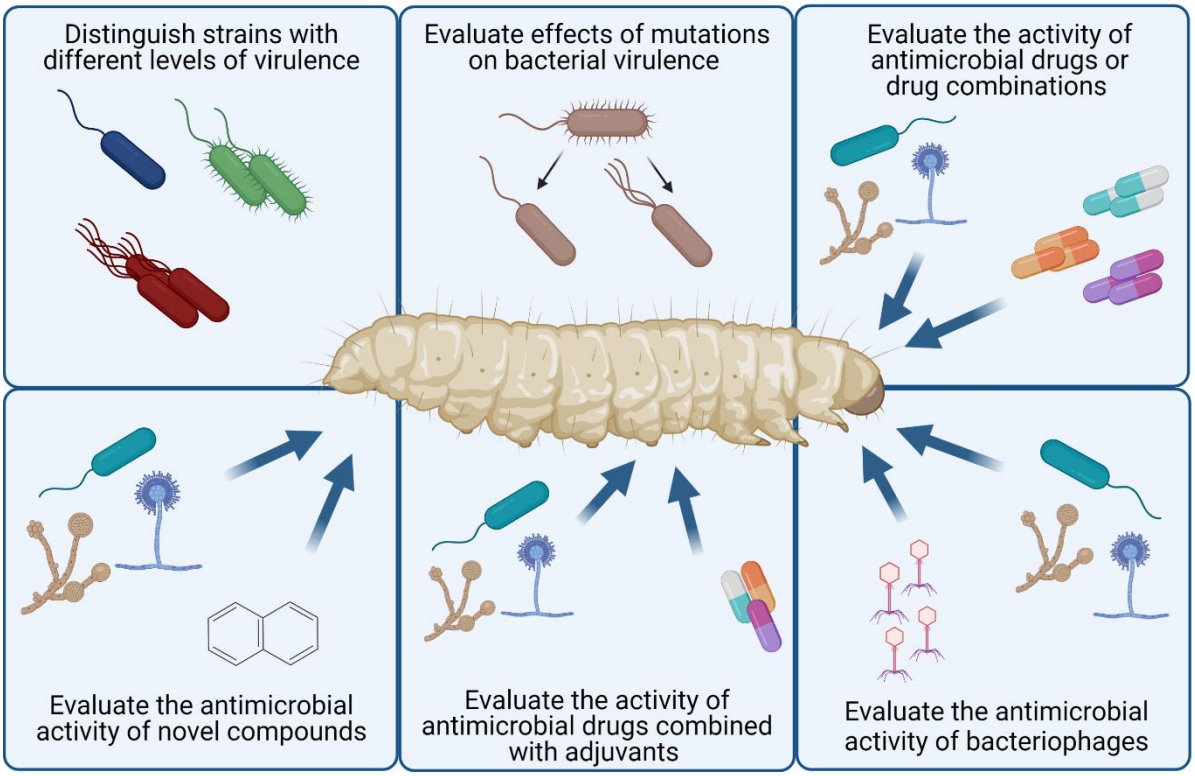

Figure 4.1 Applications of *Galleria mellonella* for pathogen and drug analysis. Adapted from (Kavanagh and Sheehan, 2018; Pereira *et al.*, 2020).

Although the larvae do not have an adaptive immune system, they possess sophisticated systems for non-self-recognition and defence reactions. The hemolymph of *G. mellonella* consists of several hemocyte types, of which plasmatocytes and granular cells are the most common. These cells are similar to human neutrophils and macrophages, involved in phagocytosis and encapsulation, resulting in an oxidation burst (Bergin *et al*., 2005). The humoral response consists of effector molecules such as antimicrobial peptides (AMPs), opsonins, and lytic enzymes that appear in the hemolymph to remove pathogens. In particular, AMPs have been found to destabilise membranes of invading microorganisms (Wu *et al*., 2018) as a mode of action. The humoral system also includes activating the phenoloxidase pathway resulting in melanisation species hydrogen peroxide and superoxide during the pathogen encapsulation (Junqueira *et al*., 2018).

In this chapter, the pathogenicity of laboratory strains and clinical isolates of *P. aeruginosa* using this *in vivo* model of *G. mellonella* and the further therapeutic potential of manganese(II), copper(II), and silver(I) complexes incorporating 1,10-phenanthroline (phen) and 3,6,9-trioxaundecanedioate (tdda) ligands were assessed. Pathogenicity was characterised by the density of hemocytes and bacterial burden in the hemolymph of the larvae at several time points during infection with the clinical strains of *P. aeruginosa*. Simultaneously the ability of the metal-tdda-phen complexes alone and combined with standard antibiotic gentamicin to interfere with the larval immune response was demonstrated. The antibacterial activity of the metal-tdda-phen complexes, alone and combined with gentamicin, against the *P. aeruginosa* laboratory strains and clinical isolates inoculated in *G. mellonella,* are also presented.

4.2. Materials and Methods

4.2.1 *Pseudomonas aeruginosa* strains and culture conditions

P. aeruginosa (CF1, CF2, and CF3) isolated from cystic fibrosis (CF) patients at local Irish hospitals with multidrug-resistant mechanisms (**Table 3.1**) and standard laboratory strains ATCC 27853 and PAO1 were used in this chapter. Bacterial stocks were maintained on nutrient agar (Lab M) plates. Before experiments, a single colony was transferred to nutrient broth (Lab M) and grown at 37 °C and 200 rpm overnight. Bacterial cultures were adjusted by absorbance (OD_{600}), harvested by centrifugation (2000 g), and washed twice with phosphate-buffered saline (PBS) prior to *G. mellonella* inoculation (Desbois and Coote, 2012) to remove secreted virulence factors.

4.2.2 *Galleria mellonella* larvae monitoring

Larvae of the greater wax moth *G. mellonella* (Livefoods Direct Ltd) were stored in wood chippings at 15 °C in darkness to prevent pupation. Larvae weighing 0.25±0.05 g with no cuticle discolouration were selected. Ten healthy larvae per treatment and controls (n = 3) were used per experimental parameter. All experiments were performed independently on three separate occasions.

4.2.3 Test complexes

The metal complexes used for this chapter (**Table 2.1**) were {[Cu(3,6,9-tdda)(phen)$_2$]·$_3$H$_2$O·EtOH}$_n$ (**Cu-tdda-phen**), {[Mn(3,6,9-tdda)(phen)$_2$]·$_3$H$_2$O·EtOH}$_n$ (**Mn-tdda-phen**) and [Ag$_2$(3,6,9-tdda)(phen)$_4$]·EtOH (**Ag-tdda-phen**). In addition, the free ligands, 1,10-phenanthroline (**phen**) and 3,6,9-trioxaundecanedioate (**tdda**), were also assessed. Gentamicin (Sigma-Aldrich) was also incorporated as all three clinical isolates demonstrated resistance to this antibiotic (**Table 3.1**).

4.2.4 *Galleria mellonella* infection studies with *Pseudomonas aeruginosa* strains

4.2.4.1 Bacterial infection of *G. mellonella*

In the pathogenicity studies, ATCC 27853, PAO1, CF1, CF2, and CF3 were investigated by preparing a dilution series ($3x10^0$ to $3x10^5$ CFU/mL) of each isolate, and ten larvae (*n* = 3) were inoculated through the last left pro-leg (as per **Figure 4.2**) into the hemocoel using a Myjector U-100 insulin syringe (Terumo Europe NV) with 20 µL of washed cultures. Undisturbed larvae and larvae inoculated with PBS were utilised as controls. The injected larvae were placed in petri dishes containing wood shavings and were incubated at 37 °C. Mortality, cuticle discolouration and response to touch were recorded 96 h post-injection.

Figure 4.2 The underneath of *G. mellonella* exposing all pro-legs (left). Inoculation of *G. mellonella* into the last left pro-leg (right)

4.2.4.2 Determination of hemocyte density

Hemocyte density was determined after the inoculation of larvae with laboratory strains ATCC 27853 (at $3x10^4$ CFU/mL) and PAO1 (at $3x10^0$ CFU/mL) and clinical isolates, CF1, CF2 (both at $3x10^3$ CFU/mL), and CF3 (at $3x10^0$ CFU/mL). A PBS control and undisturbed larvae were included. Changes in hemocyte density were measured at 0, 2, 4, 6, 12, and 24 h post-inoculation by piercing the back of the anterior end of five larvae (n = 3) with a sterile needle (25 gauge; BD Plastipak). Hemolymph was collected (50 µL) into a pre-chilled tube and diluted in cold PBS containing *N*-phenylthiourea (Sigma-Aldrich) to reduce clotting and prevent melanisation (Kelly and Kavanagh, 2011). Cell density was calculated with a hemocytometer (Neubauer Tiefe) under the microscope.

4.2.4.3 Determination of *G. mellonella* hemolymph burden of *P. aeruginosa*

Groups of five larvae (n = 3) were infected with 20 µL of ATCC 27853 ($3x10^4$ CFU/mL), PAO1 ($3x10^0$ CFU/mL) CF1 ($3x10^3$ CFU/mL), CF2 ($3x10^3$ CFU/mL), and CF3 ($3x10^0$ CFU/mL) into the last left pro-leg (as per **Figure 4.2**) and incubated for 0, 2, 4, 6, 12 and 24 h. After each time point, larval hemolymph (50 µL) was extracted and serially diluted in 450 µL of 0.9% NaCl in an iced tube. Each dilution was plated on *Pseudomonas* isolation agar (Lab M) and colonies were counted after 24 h at 37 °C. Data were expressed as CFU/mL.

4.2.5 *Galleria mellonella* response to metal-tdda-phen complexes +/- gentamicin

4.2.5.1 Toxicity studies

The Cu-tdda-phen, Mn-tdda-phen and Ag-tdda-phen complexes were first tested in *G. mellonella* larvae to determine their toxicity levels. Stock solutions of metal-tdda-phen complexes and gentamicin were diluted in sterile water, and the starting materials, phen and $tddaH_2$, were diluted in methanol (10%). 20 µL were inoculated into the *G. mellonella*

larvae through the last left pro-leg (as per **Figure 4.2**) into the hemocoel using a Myjector U-100 insulin syringe (Terumo Europe NV). Undisturbed larvae, larvae inoculated with water, and larvae inoculated with methanol equivalent to the highest concentration present in the dilutions (10%) acted as experimental controls. The larvae were placed in petri dishes containing wood shavings and incubated at 37 °C for 96 h. Mortality, cuticle discolouration, and touch response were recorded every 12 h post-injection.

Once the toxicity profiles of each metal-tdda-phen complex alone were established, they were individually assessed in combination with gentamicin. The working solutions 500, 200, and 100 µg/mL of the metal-tdda-phen complexes and gentamicin were used in varying permutations by injection (20 µl) into the last left pro-leg (as per **Figure 4.2**). The larvae were placed in petri dishes containing wood shavings and incubated at 37 °C, and mortality, cuticle discolouration and response to touch were recorded every 12 h post-injection.

4.2.5.2 Determination of hemocyte density

Hemocyte densities were measured 2, 6 and 24 h post-inoculation with metal-tdda-phen complexes alone (200 µg/mL and 750 µg/mL) and in combination with gentamicin (200 µg/mL and 750 µg/mL). A PBS control and undisturbed larvae were included. Changes in hemocyte density were measured as previously described.

4.2.5.3 Gene expression of immune-related genes

RNA extraction and quantification, followed by cDNA synthesis, were first carried out on *G. mellonella* larvae inoculated with the metal-tdda-phen complexes alone (750 µg/mL) or in combination with gentamicin (100 µg/mL) prior to real-time PCR for the expression of target immune-related genes. After 2, 6, and 24 h, five larvae were submerged in liquid nitrogen and ground to a fine powder. 1 mL of TRI Reagent (Sigma-

Aldrich) was added for the RNA extraction, and the mixture was transferred to a chilled tube before centrifugation at 2000 g for 2 min. The supernatant was brought to a fresh tube on ice and mixed with 200 µL of chloroform (ACS grade; Sigma-Aldrich), incubated for 3 min at room temperature before centrifuging again at 4 °C for 15 min at 12,000 g. The upper aqueous phase (200 µL) was carefully transferred into a tube, and RNA was precipitated with isopropanol (500 µL) (ACS grade; Sigma-Aldrich). Tubes were then incubated at room temperature for 10 min and centrifuged at 4 °C for 10 min at 12,000 g. The RNA pellet was washed once in 1 mL of 75 % (v/v) ethanol (Sigma-Aldrich), allowed to dry and re-suspended in nuclease-free water. The RNA quantification was measured on a MultiskanTM GO (Thermo Scientific) UV spectrophotometer with the µDrop plate.

cDNA was then synthesized from the extracted RNA of each experimental condition using the cDNA synthesis kit (Quanta Biosciences, USA). Each reaction was placed into the SimpliAmp Thermal Cycler (Applied Biosystems) for 5 min at 22 °C, 30 min at 42 °C, and 5 min at 85 °C, followed by samples being held at 4 °C before the quantitative real-time PCR (qRT-PCR). Primer sets (forward and reverse primer sequences detailed in **Table 4.1**) (Browne, 2014) were obtained from Sigma-Aldrich, and SYBR Green I (KAPA SYBR FAST; Sigma-Aldrich) was used as the reaction probe. The samples were added to the 7500 Fast Real-Time PCR System (Applied Biosystems). Thermal cycling was initiated with a pre-incubation at 95 °C for 5 min, followed by amplification for 45 cycles of 95 °C for 10 s, 60 °C for 10 s and 72 °C for 10 s, melting curve at 95 °C for 5 s, 65 °C for 1 min and 95 °C for 10 s, and cooling at 40 °C for 10 s. The assay was performed in triplicate. The relative gene expression was calculated using the $2^{-\Delta\Delta Ct}$ method.

Gene	Sequence (5'-3')	Fragment size (base pair)
S7e F	ATGTGCCAATGCCCAGTTG	131
S7e R	GTGGCTAGGCTTGGGAAGAAT	
Transferrin F	CCCGAAGATGAACGATCAC	535
Transferrin R	CGAAAGGCCTAGAACGTTTG	
IMPI F	ATTTGTAACGGTGGACACGA	409
IMPI R	CGCAAATTGGTATGCATGG	
Galiomicin F	CCTCTGATTGCAATGCTGAGTG	359
Galiomicin R	GCTGCCAAGTTAGTCAACAGG	
Gallerimycin F	GAAGATCGCTTTCATAGTCGC	175
Gallerimycin R	TACTCCTGCAGTTAGCAATGC	

Table 4.1 Forward and reverse primers for genes related to the immune response of *G. mellonella.*

4.2.6 *Galleria mellonella* response to *Pseudomonas aeruginosa* infection and treatment with metal-tdda-phen complexes +/- gentamicin

4.2.6.1 Treatment of metal-tdda-phen complexes in *G. mellonella* infected with *P. aeruginosa*

To ascertain the *in vivo* activity of metal-tdda-phen complexes alone, larvae were infected with each *P. aeruginosa* isolate ($3x10^0$ CFU/mL for PAO1 and CF3, $3x10^3$ CFU/mL for CF1 and CF2, and $3x10^4$ CFU/mL for ATCC 27853) as described above and then administered with either Cu-tdda-phen, Mn-tdda-phen, Ag-tdda-phen or gentamicin (100-500 μg/mL) 1 h post-infection. Undisturbed larvae and larvae infected with the bacterial strains and PBS (untreated) were included as controls. All larvae were incubated at 37 °C and assessed every 12 h for a total of 96 h for mortality and melanisation.

4.2.6.2 Treatment of metal-tdda-phen complexes + gentamicin in *G. mellonella* infected with *P. aeruginosa*

Similarly to the above, larvae were infected with bacterial strains ($3x10^0$ CFU/mL for PAO1 and CF3, $3x10^3$ CFU/mL for CF1 and CF2, and $3x10^4$ CFU/mL for ATCC 27853) and after 1 h post-inoculation, they were treated with a combination of metal-tdda-phen

complex (100 µg/mL) and gentamicin (100 µg/mL). All larvae were incubated at 37 °C and assessed every 12 h for a total of 96 h.

4.2.7 Statistical analysis

All experiments were performed in triplicate in three independent experimental sets, and the results are presented as the mean ± SE. All statistical analyses were performed with GraphPad Prism 9.0 (GraphPad Software Inc., San Diego, CA, USA). Survival curves of *G. mellonella* larvae experiments were generated using the Kaplan−Meier method. Two-way ANOVA was used to compare the hemocyte densities and gene expression studies.

4.3. Results

4.3.1 Response of *Galleria mellonella* to *Pseudomonas aeruginosa* infection

The effect of infection with *P. aeruginosa* laboratory strains ATCC 27853 and PAO1, and clinical isolates CF1, CF2, and CF3, over a range of 3×10^0 to 3×10^5 CFU/mL, on survival of *G. mellonella* larvae is presented in **Figure 4.3**. Larval survival was affected in an inoculum-dependent manner during a 96 h incubation, with the greater CFU/mL injections causing greater larval death. All infected larvae died at the highest tested concentration (3×10^5 CFU/mL) within a 48 h period. No death was observed in the set of uninfected and PBS-injected larvae used as a control. *G. mellonella* demonstrated the highest tolerance towards laboratory strain ATCC 27853, an inoculum size of 3×10^4 CFU/mL induced mortality rates of 46.7 ± 3.3% after 24 h and 60 ± 3.3%, 63.7 ± 5.7% and 73.3 ± 3.3% over the following days. 3×10^3 CFU/mL produced 26.7 ± 3.3% mortality after 24 h and 55 ± 5% by 96 h. Further dilutions (3×10^2, 3×10^1, 3×10^0 CFU/mL) produced less than 10% mortality over the entire examined time course. Injection with clinical isolates CF1 and CF2 incited similar pathogenicity profiles. At 3×10^4 CFU/mL, 53.3 ± 6.7% of larvae died after 24 h with the injection of CF1, while 46.7 ± 3.3% mortality was observed after infection with CF2. Over 90% of death was recorded after 96 h of injection with either isolate. A ten-fold reduction in inoculum resulted in similar mortality after 24 h (50 ± 3.3% with CF1 and 56.7 ± 3.3% with CF2) with an 80 ± 5.7% mortality for both isolates by the end of the experiment. Injection with lower dilutions (3×10^0; 3×10^1; 3×10^2 CFU/mL) resulted in a 0-26.7 ± 3.3% mortality after 24 h and 0-56.7 ± 6.7% after 96 h. Laboratory strain PAO1 and clinical isolate CF3 were the most virulent to the larvae, with a 20 µL inoculation of 3×10^1 CFU/mL causing complete death after 24 h. This indicated the sensitivity of *G. mellonella* to *P. aeruginosa* infection, which has previously been reported (Andrejko *et al*., 2014; Hill *et al*., 2014;

Beeton *et al.*, 2015). There were significant differences ($P < 0.05$, $P < 0.01$, $P < 0.001$) between the virulence of the examined strains and an inoculum that caused over 50% mortality within 48 h but not 100% mortality within 24 h were chosen for subsequent studies.

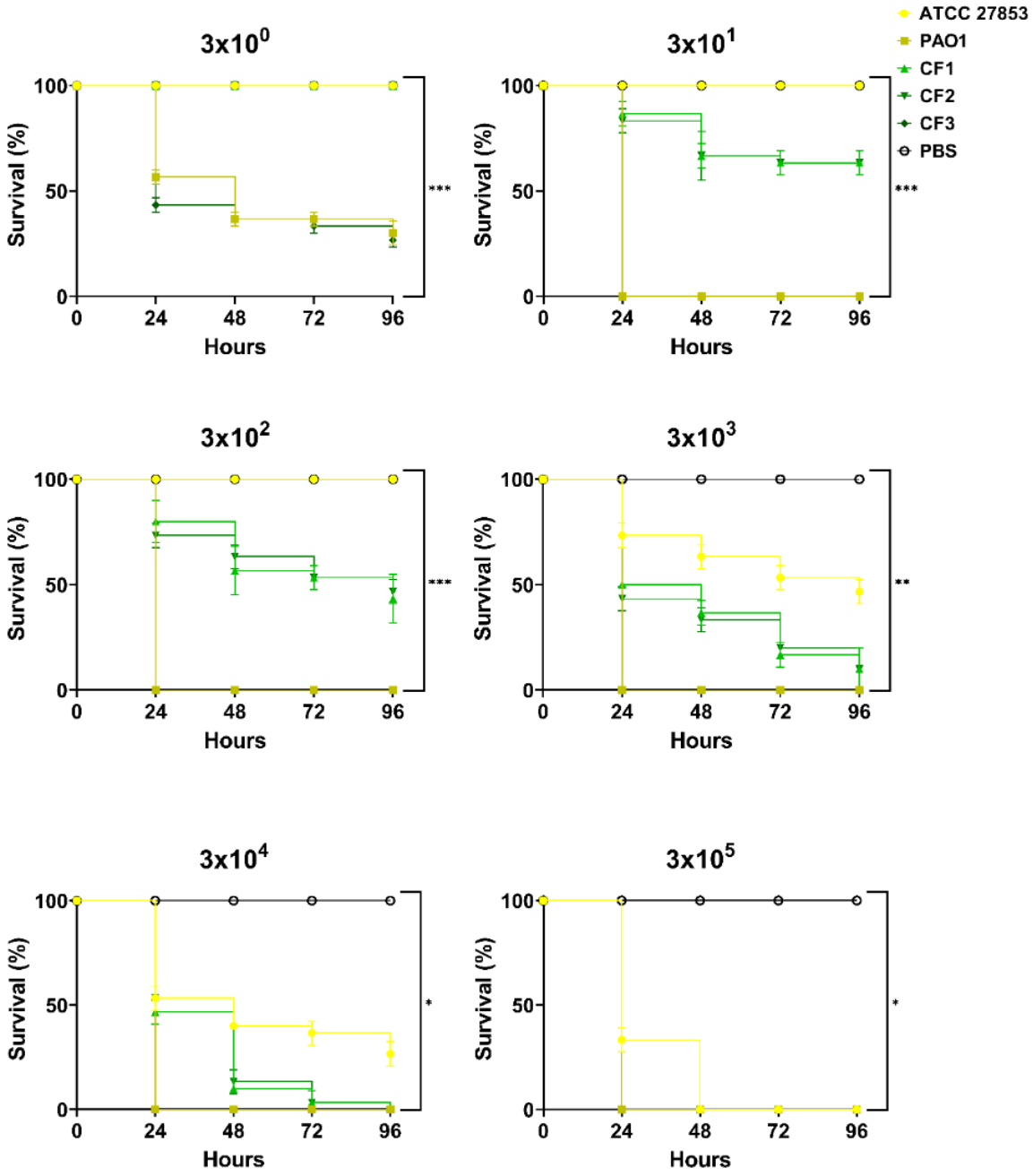

Figure 4.3 Kaplan-Meier survival distributions for each *P. aeruginosa* strain (ATCC 27853, PAO1, CF1, CF2, and CF3) assessed over varying inoculum doses ($3x10^0$ to $3x10^5$ CFU/mL). Significance was assessed through the log-rank (Mantel-Cox) test, and Holm's correction was applied for multiple comparisons (*: $P < 0.05$, **: $P < 0.01$, ***: $P < 0.001$)

4.3.2 Immune response of *Galleria mellonella* to *Pseudomonas aeruginosa* infection

Alterations in the number of circulating immune cells (hemocytes) within *G. mellonella* have been used to indicate the larval immune response to a pathogen (Bergin *et al*., 2003). Drifting hemocytes are the initial responders to an infection, and their density can be enhanced by stimulating those attached to the internal wall of the haemocoel or bound to organs such as fat bodies (Kavanagh and Reeves, 2004). After the mortality studies, alterations in hemocyte density following inoculation with *P. aeruginosa* strains ATCC 27583 (3×10^4 CFU/mL), PAO1 (3×10^0 CFU/mL), CF1 (3×10^3 CFU/mL), CF2 (3×10^3 CFU/mL) and CF3 (3×10^0 CFU/mL) were assessed over a 24 h period (**Figure 4.4.A**). All inoculated larvae had increased levels of hemocytes relative to the initial injection (0 h). With strains PAO1 and CF3, the inocula triggered a statistically significant ($P < 0.001$ and $P < 0.05$, respectively) increase in hemocytes (12.98 ± 0.73 x10^6/mL and 13.86 ± 1.09 x10^6/mL, respectively) after 2 h. ATCC 27853 had a count of 9.69 ± 0.62 x10^6/mL at 2 h while CF1 had 10.93 ± 1.31 x10^6/mL and CF2 had 11.06 ± 1.00 x10^6/mL. Infections with all strains saw a spike in hemocyte populations after 4 h. The greatest response was observed in larvae injected with CF3 (16.17 ± 0.94 x10^6/mL, $P < 0.001$) followed by PAO1 (15.27 ± 1.04 x10^6/mL), CF1 (14.67 ± 0.66 x10^6/mL, $P < 0.05$), CF2 (13.62 ± 0.38 x10^6/mL, $P < 0.01$) and ATCC 27853 (11.64 ± 0.51 x10^6/mL). After 24 h of monitoring, hemocytes populations had decreased but remained elevated compared to their initial levels (0 h). Larvae infected with PAO1 (7.59 ± 0.71 x10^6/mL, $P < 0.01$), CF2 (8.61 ± 0.55 x10^6/mL, $P < 0.05$) and CF3 for 24 h (8.12 ± 1.06 x10^6/mL, $P < 0.05$) showed a significant increase in hemocyte density compared to the controls, ATCC 27853 (8.81 ± 0.57 x10^6/mL, $P > 0.05$) and CF1 (8.51 ± 0.39 x10^6/mL, $P > 0.05$) were not significant.

The infection process was also observed by enumerating *P. aeruginosa* CFU in the hemolymph of the infected larvae. Larvae were infected with ATCC 27853 (3×10^4 CFU/mL), PAO1 (3×10^0 CFU/mL), CF1 (3×10^3 CFU/mL), CF2 (3×10^3 CFU/mL), and CF3 (3×10^0 CFU/mL) and monitored over 24 h (**Figure 4.4.B**). A decrease in viable bacterial cells was observed with initial time points (0 h to 4 h). Bacterial burden in larvae infected with all bacterial strains increased from 4 h and 24 h analysis points, strains ATCC 27853, PAO1, CF1, and CF2 increased to a median value >5 $\log_{10}$ CFU/mL while CF3 increased to a median value >4 $\log_{10}$ CFU/mL.

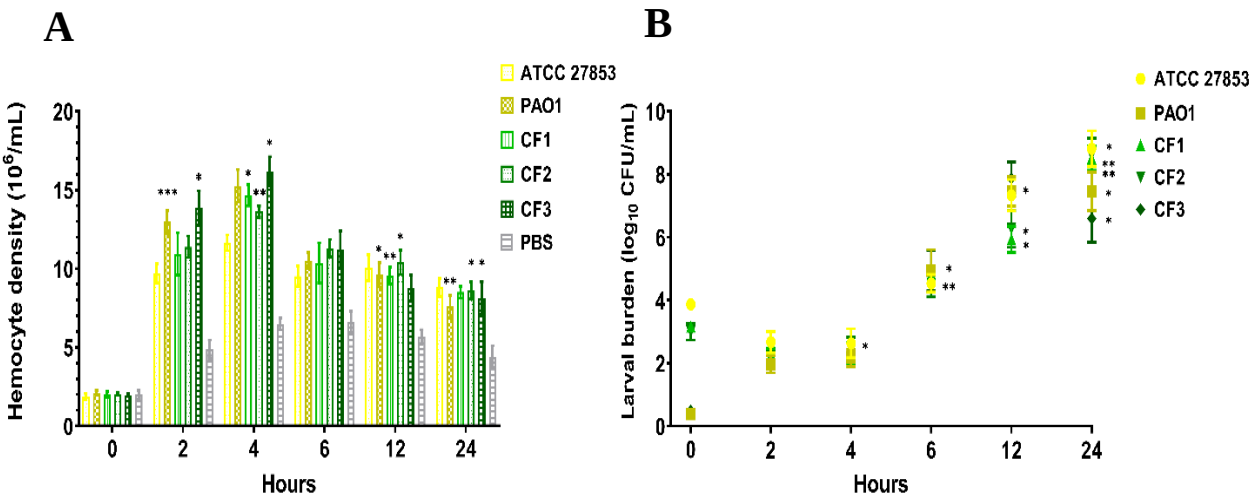

Figure 4.4 Following the inoculation of *G. mellonella* with *P. aeruginosa* strains ATCC 27583 (3×10^4 CFU/mL), PAO1 (3×10^0 CFU/mL), CF1 (3×10^3 CFU/mL), CF2 (3×10^3 CFU/mL) and CF3 (3×10^0 CFU/mL), the (**A**) alteration in circulating hemocyte density and (**B**) bacterial burden, was assessed over a 24 h period. Data are presented as the mean ± SE of the three independent experiments. Statistical analysis was performed by comparing treatments to PBS injected controls at respective time points (*: $P < 0.05$, **: $P < 0.01$, ***: $P < 0.001$).

4.3.3 *Galleria mellonella* response to metal-tdda-phen complexes

G. mellonella larvae were exposed to Mn-tdda-phen, Cu-tdda-phen, Ag-tdda-phen, and gentamicin, and mean mortality (%) was assessed over 72 h (**Table 4.2**). No mortality was recorded after incubation of larvae with solvent (10% methanol), PBS inoculated larvae and larvae that were undisturbed (data not shown) at any time point. However, larvae exposed to the solvent control did demonstrate slight to moderate melanisation, as presented in **Figure 4.5**. All larvae tolerated 2-10 µg/larvae (1.6-13.59 µM) of the metal-tdda-phen complex with no mortality observed over the entire experiment. Similarly, complexes Mn-tdda-phen and Ag-tdda-phen induced no mortality at 15 µg/larvae (20.39 and 12.5 µM, respectively) while doubling the concentration (40.78 and 24.9 µM, respectively) resulted in 6.66 ± 5.77% death for the former and 23.33 ± 5.77% death for the latter, after exposure for 72 h. Cu-tdda-phen was the most toxic to the larvae. A concentration of 15 µg/larvae (20.15 µM) resulted in a mortality rate of 53.33 ± 5.77% after 72 h, and increasing the dose to 30 µg/larvae (40.3 µM) saw complete death of all tested larvae after the same amount of time. It is well known that copper is highly toxic to mammals, and similar studies investigating Cu-phen complexes and their derivatives have also highlighted their lethality towards *G. mellonella* (McCarron *et al*., 2018; Rochford *et al*., 2018). Although lower concentrations of Cu-tdda-phen did not induce mortality, moderate to severe melanisation was observed. In **Chapter 3**, the enhanced toxicity of Cu-tdda-phen towards mammalian cells *in vitro* was also presented. Gandra *et al.* (2020) investigated the toxicity of one copper(II)-phen, seven manganese(II)-phen, and three silver(I)-phen-complexes towards *G. mellonella*, and of this panel Mn-tdda-phen (chelate 8), Cu-tdda-phen (chelate 1) and Ag-tdda-phen (chelate 10) were included. The group also reported the low mortality rate induced in larvae by Mn-tdda-phen (13.33 ± 5.77%) and Ag-tdda-phen (33.33 ± 5.77%) at high concentrations (30 µg/larvae) and

the toxicity of Cu-tdda-phen (100% mortality), corroborating the results obtained in this study.

Test complex	Dose µg/larvae (µM)	Mean Mortality (%) +/- SE over time (h)		
		24 h	48 h	72 h
Mn-tdda-phen	2 µg (2.71 µM)	0±0	0±0	0±0
	4 µg (5.42 µM)	0±0	0±0	0±0
	10 µg (13.59 µM)	0±0	0±0	0±0
	15 µg (20.39 µM)	0±0	0±0	0±0
	30 µg (40.78 µM)	0±0	6.66±5.77	6.66±5.77
Cu-tdda-phen	2 µg (2.68 µM)	0±0	0±0	0±0
	4 µg (5.36 µM)	0±0	0±0	0±0
	10 µg (13.41 µM)	0±0	0±0	0±0
	15 µg (20.15 µM)	23.33±5.77	46.66±5.77	53.33±5.77
	30 µg (40.3 µM)	76.66±5.77	83.33±5.77	100±0
Ag-tdda-phen	2 µg (1.6 µM)	0±0	0±0	0±0
	4 µg (3.3 µM)	0±0	0±0	0±0
	10 µg (8.3 µM)	0±0	0±0	0±0
	15 µg (12.5 µM)	0±0	0±0	0±0
	30 µg (24.9 µM)	3.33±5.77	23.33±5.77	23.33±5.77
Gentamicin	2 µg (3.5 µM)	0±0	0±0	0±0
	4 µg (6.9 µM)	0±0	0±0	0±0
	10 µg (17.4 µM)	0±0	0±0	0±0
	15 µg (26.1 µM)	0±0	0±0	0±0
	30 µg (52.1 µM)	0±0	13.33±5.77	13.33±5.77
Phen	2 µg (11.1µM)	0±0	0±0	0±0
	4 µg (22.2 µM)	0±0	0±0	0±0
	10 µg (55.5 µM)	53.3±5.8	53.3±5.8	53.3±5.8
	15 µg (83.2 µM)	76.7±5.8	76.7±5.8	76.7±5.8
	30 µg (166.5 µM)	100±0	100±0	100±0
tddaH$_2$	2 µg (9 µM)	0±0	0±0	0±0
	4 µg (18 µM)	0±0	0±0	0±0
	10 µg (45 µM)	0±0	0±0	0±0
	15 µg (67.5 µM)	0±0	0±0	0±0
	30 µg (135 µM)	46.7±5.8	46.7±5.8	46.7±5.8

Table 4.2 Mean larval mortality (%) after 24 h, 48 h, and 72 h inoculations with metal-tdda-phen complexes and gentamicin at a concentration range of 2-30 µg/larvae. Data are presented as mean ± SE

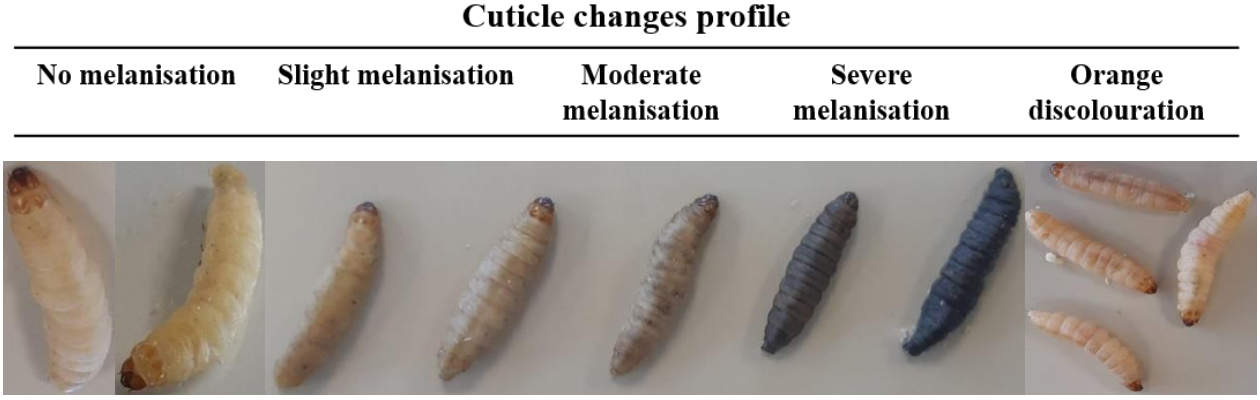

Figure 4.5 *G. mellonella* representing the different levels of melanisation and cuticle discolouration

Injection of the control antibiotic, gentamicin, at 30 µg/larvae (52.1 µM) induced 13.33 ± 5.77% mortality after 48 h. Surviving larvae presented with slight to moderate melanisation; some were slow to respond to stimulation. In addition, the larvae were injected with the metal-tdda-phen complexes starting materials, 3,6,9-trioxaundecanedioate (tdda) and 1,10-phenanthroline (phen), to ensure the recorded effects were not a result of the free ligands alone but the complex itself. The highest dose (30 µg/larvae, 135 µM) of $tddaH_2$ saw 46.7 ± 5.8% of the inoculated larvae perish, while 10 µg/larvae (45 µM) resulted in a mortality of 53.3 ± 5.8% after the initial 24 h. Kellett *et al.* (2011) also demonstrated that *G. mellonella* exposed to high concentrations of phen (5000 and 2000 µg mL^{-1}) had poor tolerance (100% and 90% mortality, respectively). Interestingly the *G. mellonella* larvae that were exposed to lower doses of phen (2-4 µg/larvae, 11.1-22.2 µM), although they survived, showed an orange discolouration of the cuticle post-injection (**Figure 4.5**). It was postulated that the orange discolouration resulted from the phen interfering with the copper-containing enzyme phenoloxidase that drives melanin synthesis (Sheehan *et al*., 2018). To identify whether metal-tdda-phen complexes induced an immunomodulatory effect, larval hemocytes were withdrawn and

counted after exposure to a low (2 µg/larvae) and high (15 µg/larvae) dose that did not induce 100% mortality. At 2 h, both low and high doses prompted similar responses in subjected larvae: Ag-tdda-phen (11.20 ± 0.47 $x10^6$/mL and 12.44 ± 0.54 $x10^6$/mL, respectively), Mn-tdda-phen (7.95 ± 0.37 $x10^6$/mL and 11.43 ± 0.56 $x10^6$/mL, respectively), phen (10.8 ± 0.46 $x10^6$/mL and 8.8 ± 0.24 $x10^6$/mL, respectively) and $tddaH_2$ (7.78 ± 0.34 $x10^6$/mL and 8.30 ± 0.55 $x10^6$/mL, respectively) showed a significant ($P<0.05$) increase compared to the control (**Figure 4.6**). After an extended exposure to 15 µg/larvae to 6 h, Mn-tdda-phen (42.34 ± 0.95 $x10^6$/mL) and Ag-tdda-phen (32.71 ± 0.75 $x10^6$/mL) significantly enhanced hemocyte density that continued to the 24 h time point (135.82 ± 4.29 $x10^6$/mL, 133.14 ± 2.59 $x10^6$/mL, respectively). This demonstrates that at higher concentrations, these metal-tdda-phen complexes induce a priming effect within the insects. There were no hemocytes when phen was assessed at 15 µg/larvae after 24 h, and reduced hemocytes when Cu-tdda-phen (20.66 ± 0.61 $x10^6$/mL) was examined at the same concentration. The toxicity of these compounds to larvae at this concentration could be responsible for this response.

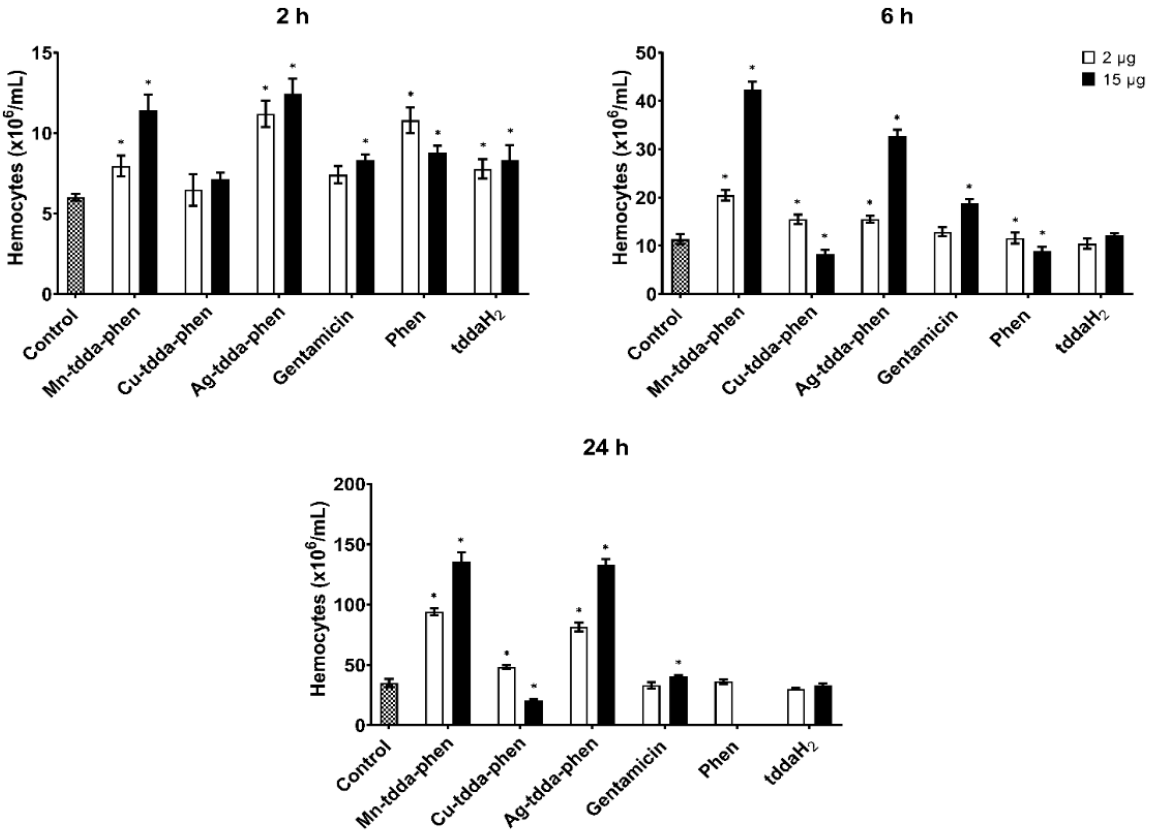

Figure 4.6 Immunomodulation induced by the metal-tdda-phen complexes and gentamicin (2 and 15 µg/larvae) in *G. mellonella* after 2 h, 6 h and 24 h post-injection.

Larvae treated with Mn-tdda-phen, Cu-tdda-phen, Ag-tdda-phen, and gentamicin (15 µg/larvae) were incubated for 2, 6 and 24 h prior to the assessment of immune-related gene expression. *Transferrin* (iron-binding protein), *IMPI* (inducible metalloproteinase inhibitor), *galiomicin* (defensin) and *gallerimycin* (cysteine-rich antifungal peptide) genes were normalised against the expression of *S7e* (reference gene), and larval treatments were compared to the PBS injected control and are presented in **Figure 4.7**. Expression of *transferrin* and *IMPI* encoding genes were significantly ($P < 0.05$) upregulated by Mn-tdda-phen and Ag-tdda-phen across all time points. Time-dependent induction of both genes was observed, reaching the maximum 24 h after injection. This suggests that these metal-tdda-phen complexes initiate an immune response in the larvae.

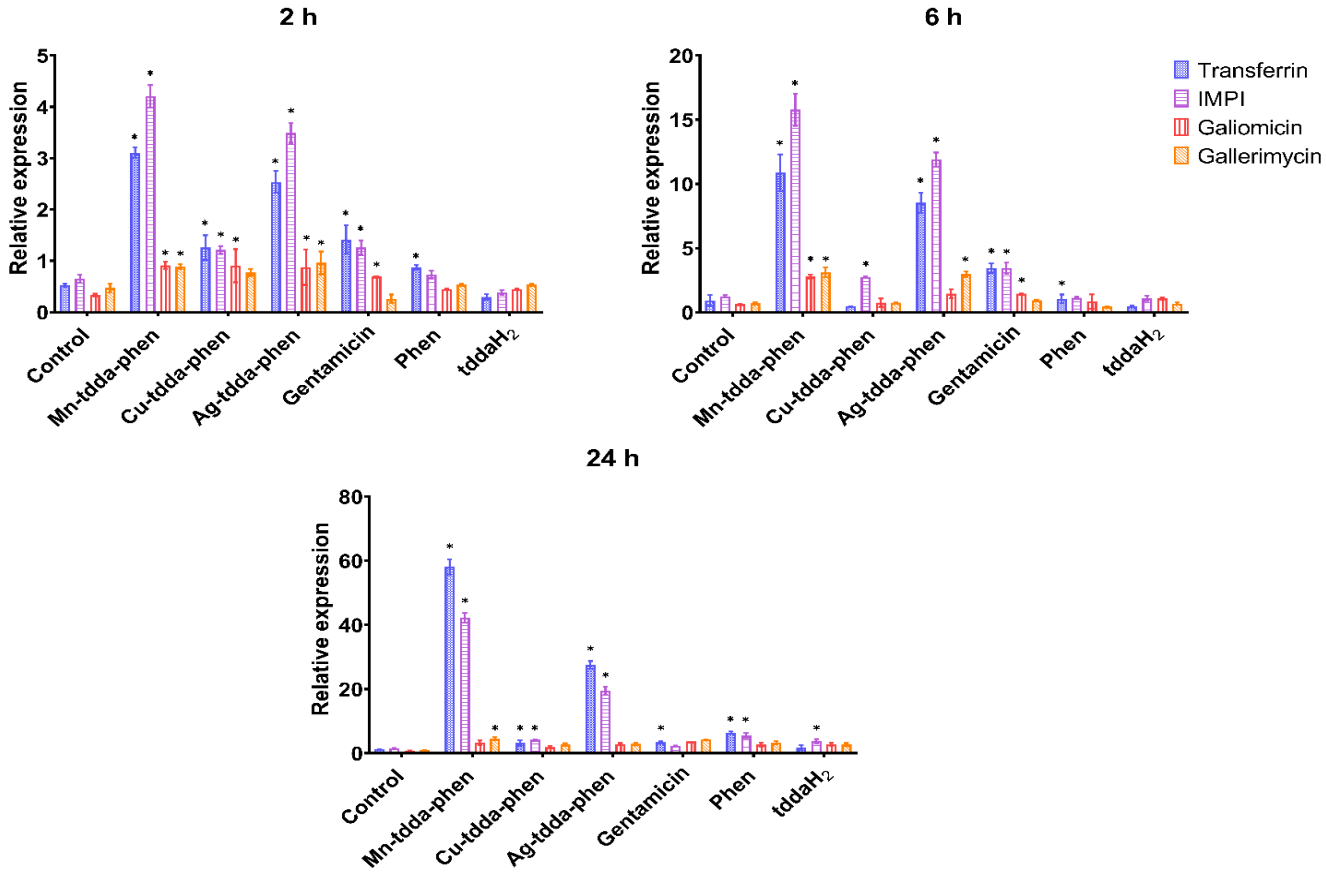

Figure 4.7 Relative expression of genes involved in the immune response of *G. mellonella* when exposed to metal-tdda-phen complexes, gentamicin and phen after 2 h, 6 h and 24 h post-injection. * indicate significant differences to the PBS injected control ($P < 0.05$)

4.3.4 *Galleria mellonella* response to metal-tdda-phen complexes and gentamicin

After toxicity studies of the metal-tdda-phen complexes and gentamicin as single agents, the dual administration of the complexes and antibiotics were assessed within the larval model. The lowest examined concentrations that did not induce mortality (**Figure 4.5**) were examined in varying permutations of 2-10 µg/larvae and observed over three time points (24, 48 and 72 h) (**Figure 4.6**). Overall the combination of agents, even at lower doses, enhanced the toxicity towards the larvae when compared to their toxicity as singular drugs. The highest dose of gentamicin (10 µg/17.4 µM) with Mn-tdda-phen (10

µg/13.59 µM), Cu-tdda-phen (10 µg/13.41 µM) and Ag-tdda-phen (10 µg/8.3 µM) resulted in 86.7, 100 and 93.3 % mortality respectively after 72 h. While the highest dose of gentamicin (10 µg/17.4 µM) with the lowest dose of Mn-tdda-phen (2 µg/2.71 µM) and Ag-tdda-phen (2 µg/1.6 µM) produced mortality rates of 46.7, and 53.3 %, respectively, the combination with Cu-tdda-phen (2 µg/2.68 µM) incited 83% mortality. The lowest concentration of gentamicin (2 µg/2.35 µM) with both Mn-tdda-phen (2 µg/2.71 µM) and Ag-tdda-phen (2 µg/1.6 µM) induced complete survival of all injected larvae and with Cu-tdda-phen (2 µg/3.5 µM), 26.7 % mortality was noted. A high and low and a low and high dose of gentamicin with both Mn-tdda-phen and Ag-tdda-phen exerted a similar toxicity profile in larvae (43.3-53.3 % mortality), suggesting that a combination of agents overstimulate the animal, irrespective of the higher concentration. In contrast, a higher dose of Cu-tdda-phen (10 µg/13.41 µM) with a lower dose of gentamicin (2 µg/2.35 µM) induced elevated mortality (83.3 %) than the reverse (73.3 %), suggesting that Cu-tdda-phen is driving the toxicity towards *G. mellonella.*

Test agents	Dose µg/larvae (µM)	Mean Mortality (%) +/- SE over time (h)		
		24 h	48 h	72 h
Mn-tdda-phen + Gentamicin	2 µg (2.71 µM) + 2µg (3.5 µM)	0±0	0±0	0±0
	4 µg (5.42 µM) + 4 µg (6.9 µM)	20±5.8	20±5.8	20±5.8
	10 µg (13.59 µM) + 10 µg (17.4 µM)	83.3±3.3	86.7±3.3	86.7±3.3
	2 µg (2.71 µM) + 10 µg (17.4 µM)	43.3±3.3	46.7±3.3	46.7±3.3
	10 µg (13.59 µM) + 2 µg (3.5 µM)	46.7±3.3	50.0±5.8	53.3±3.3
Cu-tdda-phen + Gentamicin	2 µg (2.68 µM) + 2µg (3.5 µM)	26.7±3.3	26.7±3.3	26.7±3.3
	4 µg (5.36 µM) + 4 µg (6.9 µM)	70±5.8	73.3±3.3	73.3±3.3
	10 µg (13.41 µM) + 10 µg (17.4 µM)	100±0	100±0	100±0
	2 µg (2.68 µM) + 10 µg (17.4 µM)	63.3±3.3	66.7±3.3	73.3±3.3
	10 µg (13.41 µM) + 2 µg (3.5 µM)	83.3±3.3	83.3±3.3	83.3±3.3
Ag-tdda-phen + Gentamicin	2 µg (1.6 µM) + 2µg (2.5 µM)	0±0	0±0	0±0
	4 µg (3.3 µM) + 4 µg (6.9 µM)	26.7±3.3	33.3±3.3	33.3±5.8
	10 µg (8.3 µM) + 10 µg (17.4 µM)	83.3±3.3	93.3±6.7	93.3±6.7
	2 µg (1.6 µM) + 10 µg (17.4 µM)	43.3±3.3	53.3±3.3	53.3±3.3
	10 µg (8.3 µM) + 2 µg (2.5 µM)	46.7±6.7	50±5.8	53.3±3.3

Table 4.3 Mean larval mortality (%) after 24 h, 48 h and 72 h inoculation of Mn-tdda-phen and gentamicin, Cu-tdda-phen and gentamicin, and Ag-tdda-phen and gentamicin. Data are presented as mean ± SE

To further investigate the combined effect of metal-tdda-phen complexes and gentamicin on the immune system of the larvae, hemocytes were extracted and enumerated (**Figure 4.8**). The combination of Mn-tdda-phen (2 µg (2.71 µM) – 4 µg (5.42 µM)) with gentamicin (2µg (3.5 µM) – 4 µg (6.9 µM)) elicited the greatest hemocyte response at 2 h (7.59 ± 0.38 x10^6/mL and 9.82 ± 0.74 x10^6/mL, respectively), 6 h (20.44 ± 0.61 x10^6/mL and 34.67 ± 1.64 x10^6/mL, respectively), and 24 h (90.61 ± 2.56 x10^6/mL and 93.48 ± 2.04 x10^6/mL, respectively). Administration of Cu-tdda-phen with gentamicin to larvae produced similar hemocyte densities at both low (2 µg (2.71 µM) + 2µg (3.5 µM)) and high doses (4 µg (5.36 µM) + 4 µg (6.9 µM)) at 2 h (6.48 ± 0.57 x10^6/mL and 8.14 ± 1.24

x10^6/mL, respectively) and 6 h (15.44 ± 0.56 x10^6/mL and 18.21 ± 0.52 x10^6/mL, respectively). After 24 h, a hemocyte count of Cu-tdda-phen and gentamicin could not be determined due to the high mortality rate. Unlike the other combinations, Ag-tdda-phen and gentamicin induced a more pronounced hemocyte response at lower concentrations than higher after 2 h (11.20 ± 0.47 x10^6/mL and 10.29 ± 0.59 x10^6/mL, respectively) and 24 h (75.28 ± 2.28 x10^6/mL and 47.92 ± 2.88 x10^6/mL, respectively).

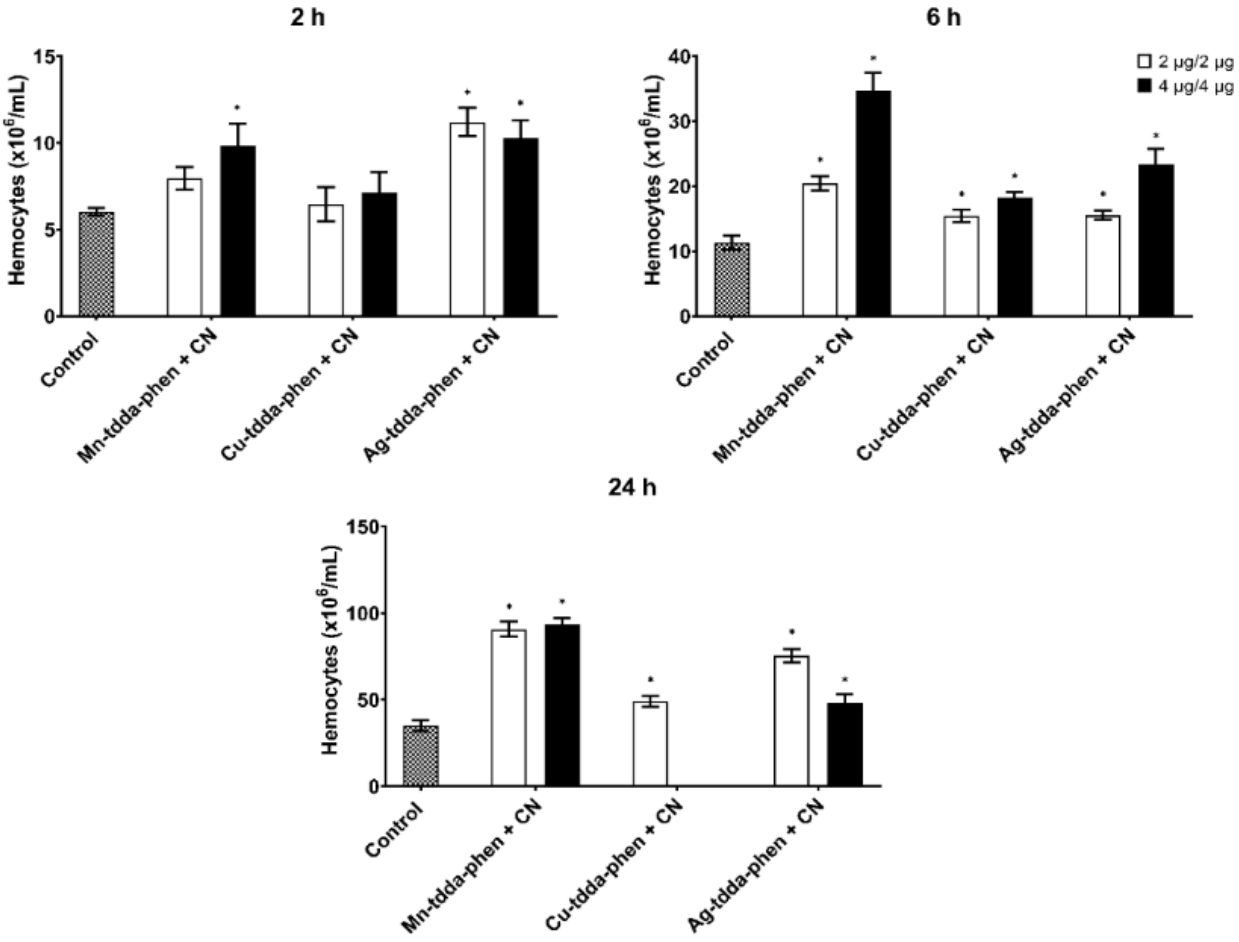

Figure 4.8 Immunomodulation induced by the metal-tdda-phen complexes in combination with gentamicin (CN) (2 µg and 2 µg/larvae, and 4 µg and 4 µg/larvae) in *G. mellonella* after 2 h, 6 h and 24 h post-injection. * indicate significant differences in relation to the PBS injected control ($P < 0.05$)

The expression of *transferrin* (iron-binding protein), *IMPI* (inducible metalloproteinase inhibitor), *galiomicin* (defensin) and *gallerimycin* (cysteine-rich antifungal peptide) genes was assessed after larvae were exposed to a combination of metal-tdda-phen complex (2 µg/larvae) and gentamicin (2 µg/larvae) for 2, 6 and 24 h (**Figure 4.9**). Similar responses were observed to the metal-tdda-phen complexes and gentamicin as single agents (**Figure 4.7**), with significant ($P < 0.05$) upregulation of *transferrin* and *IMPI* encoding genes across all time points.

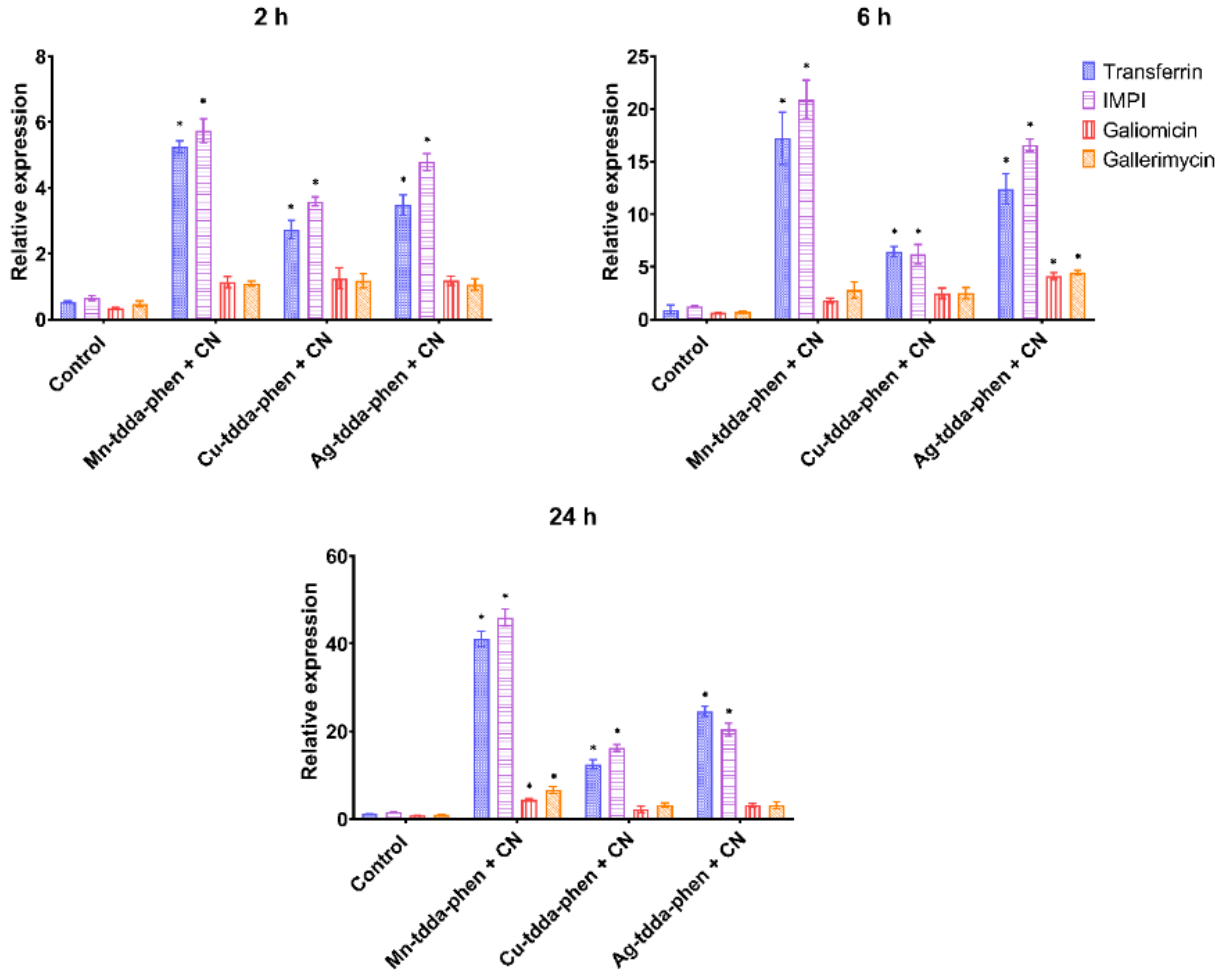

Figure 4.9 Relative expression of genes involved in the immune response of *G. mellonella* when exposed to metal-tdda-phen complexes in combination with gentamicin (CN) after 2 h, 6 h and 24 h post-injection. * indicate significant differences to the PBS control ($P < 0.05$)

4.3.5 Effect of metal-tdda-phen complexes in treating *Pseudomonas aeruginosa* infection in *Galleria mellonella* +/- gentamicin

After screening the bacterial strains in the larval model, an infective dose was determined for each strain. Larvae were inoculated with ATCC 27583 (3×10^4 CFU/mL), PAO1 (3×10^0 CFU/mL), CF1 (3×10^3 CFU/mL), CF2 (3×10^3 CFU/mL) and CF3 (3×10^0 CFU/mL) and subsequently received a single dose of the metal-tdda-phen complexes alone (2-10 µg/larvae) (1.6-13.59 µM), gentamicin (2-10 µg/larvae) (3.5-17.4 µM) alone, or the metal-tdda-phen complex (1 µg/larvae) (831.3 nM-1.36 µM) in combination with gentamicin (1 µg/larvae) (1.74 µM) 1 h post-infection.

The effect of single doses of metal-tdda-phen complexes or gentamicin on survival of *G. mellonella* inoculated with *P. aeruginosa* strains, ATCC 27853 (A-D), PAO1 (E-H), CF1 (I-L), CF2 (M-P), CF3 (R-U), are presented in **Figure 4.10**. Overall, the exposure to a metal-tdda-phen complex increased survival in infected larvae. Gentamicin (10 µg/larvae) (17.4 µM) was the most effective at treating larvae infected with ATCC 27853, which had no mortalities after 96 h when compared to the PBS control (73.33 ± 3.3% mortality). All metal-tdda-phen complexes decreased mortality (26.7-36.7%) at the same concentration and time point. When larvae were inoculated with PAO1, a more virulent strain, mortality increased, except for Cu-tdda-phen treatment. *G. mellonella* presented with a metal-tdda-phen complex or gentamicin increased survival dose-dependently. Larvae administered 10 µg of gentamicin (17.4 µM) had a 23.3 ± 3.3% mortality rate. Those exposed to Mn-tdda-phen (13.59 µM) and Ag-tdda-phen (8.3 µM) at 10 µg/larvae prolonged survival of PAO1 infected larvae. At 48 h, the mortality rate was 26.7 ± 3.3% of larvae presented with Mn-tdda-phen and 40 ± 5.8% of larvae subjected to Ag-tdda-phen, compared to 66.7 ± 6.7% of larvae that received PBS. *G. mellonella,* which encountered 10 µg (13.41 µM) of Cu-tdda-phen, showed a higher mortality rate (70 ±

0%) at 48 h than those given PBS. Due to the toxicity of this complex in larvae, the stress of both seemed to elevate mortality. However, a lower dose of 4 µg/larvae produced a mortality rate of 36.7 ± 3.7 at 48 h. This was expected as Mn-tdda-phen and Ag-tdda-phen presented with lower toxicity towards *G. mellonella* (**Table 4.3**) and induced the immune response (**Figure 4.8**) of the larvae compared to their copper equivalent. As presented in **Table 3.1**, ATCC 27853 and PAO1 were susceptible to gentamicin with MICs of 1 µg/mL (1.7 µM) and 2 µg/mL (3.5 µM), respectively, while all the clinical isolates (MICs of 8 µg/mL (13.9 µM) to over 256 µg/mL (445 µM)), were deemed resistant to the antibiotic. Similarly, in the *G. mellonella* model, the antibiotic efficacy against the clinical isolates decreased compared to the laboratory strains. Larvae infected with CF3, CF2 and CF1 and subsequently treated with the highest dose of gentamicin (10 µg/larvae) (17.4 µM) saw survival recorded at 30 ± 0%, 70 ± 5.8% and 76.7 ± 3.3%, respectively, after 96 h. At the lowest investigated concentrations of metal-tdda-phen complexes (2 µg/larvae) (1.6-2.71 µM), mortality rates were noted at 33.3-43.3% for CF1 and CF2. This activity was not maintained with CF3. However, treatment of metal-tdda-phen complexes extended survival compared to the PBS-treated larvae. After 48 h, larvae treated with Mn-tdda-phen (5.42 µM), Cu-tdda-phen (5.36 µM), and Ag-tdda-phen (3.3 µM) at 4 µg/larvae had mortality rates of 50 ± 0%, 60 ± 5.8% and 53.3 ± 3.3%, respectively, compared to a 66.7 ± 3.3% of larvae that received PBS. Again, this activity profile draws similarities to the result obtained when assessed *in vitro* (**Chapter 3**); metal-tdda-phen complexes were the most active against CF1 and CF2 (with MICs of 8-16 µg/mL); however, a higher concentration was needed to inhibit CF3 (MICs of 64-128 µg/mL).

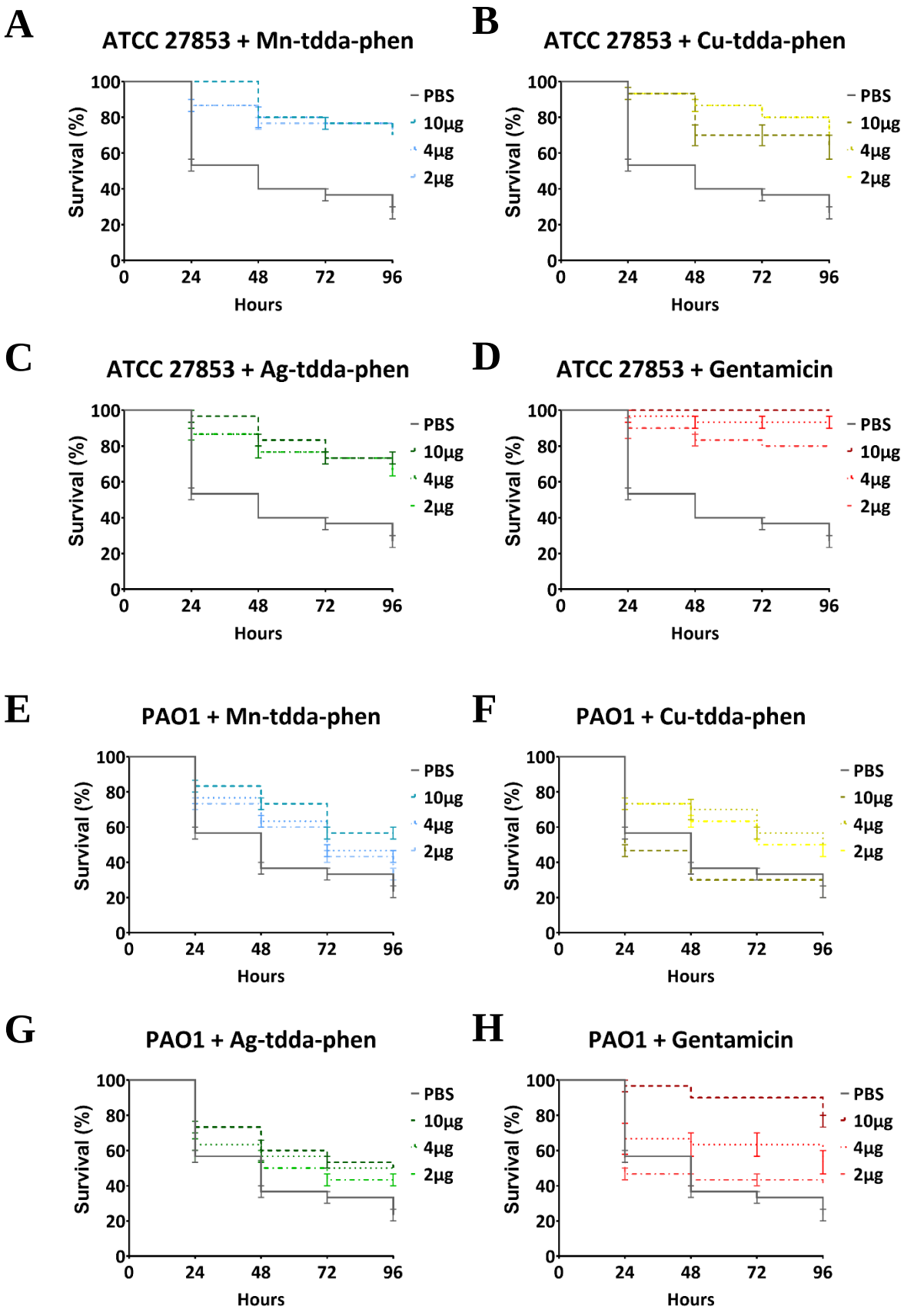
A
ATCC 27853 + Mn-tdda-phen
B
ATCC 27853 + Cu-tdda-phen
C
ATCC 27853 + Ag-tdda-phen
D
ATCC 27853 + Gentamicin
E
PAO1 + Mn-tdda-phen
F
PAO1 + Cu-tdda-phen
G
PAO1 + Ag-tdda-phen
H
PAO1 + Gentamicin
Survival (%)
Hours
PBS
10µg
4µg
2µg
0
20
40
60
80
100
0
24
48
72
96

I

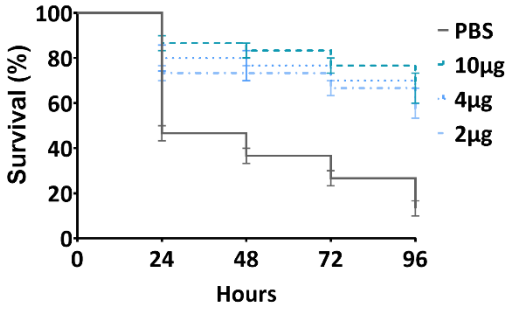
CF1 + Mn-tdda-phen
Survival (%)
100
80
60
40
20
0
0
24
48
72
96
Hours
PBS
10µg
4µg
2µg

J

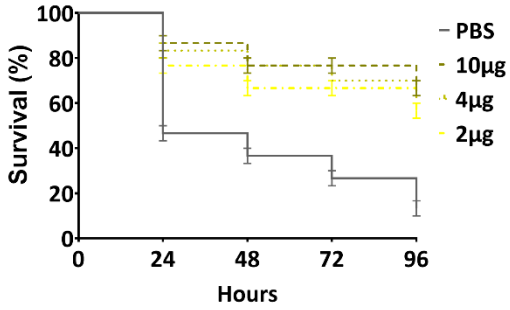
CF1 + Cu-tdda-phen
Survival (%)
100
80
60
40
20
0
0
24
48
72
96
Hours
PBS
10µg
4µg
2µg

K

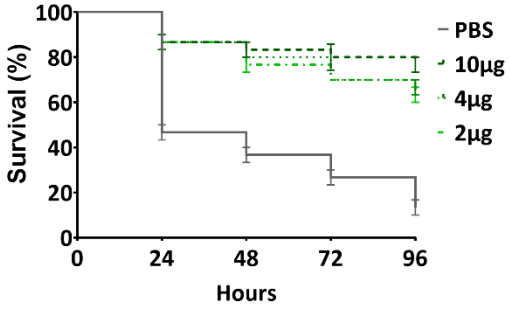
CF1 + Ag-tdda-phen
Survival (%)
100
80
60
40
20
0
0
24
48
72
96
Hours
PBS
10µg
4µg
2µg

L

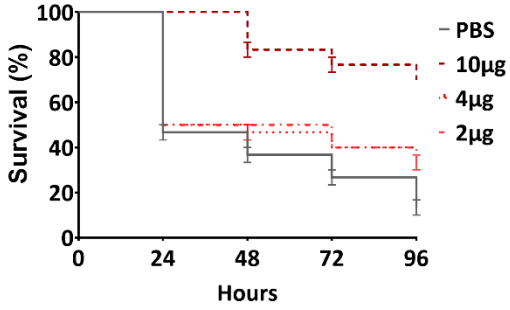
CF1 + Gentamicin
Survival (%)
100
80
60
40
20
0
0
24
48
72
96
Hours
PBS
10µg
4µg
2µg

M

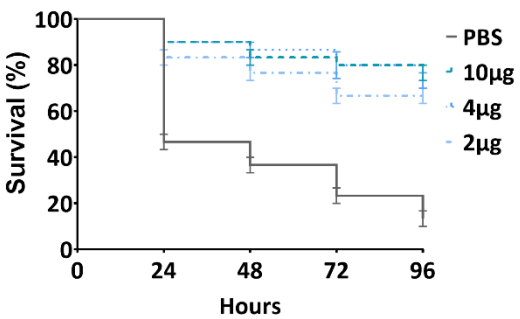
CF2 + Mn-tdda-phen
Survival (%)
100
80
60
40
20
0
0
24
48
72
96
Hours
PBS
10µg
4µg
2µg

N

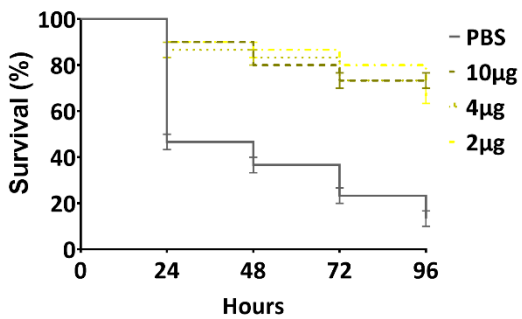
CF2 + Cu-tdda-phen
Survival (%)
100
80
60
40
20
0
0
24
48
72
96
Hours
PBS
10µg
4µg
2µg

O

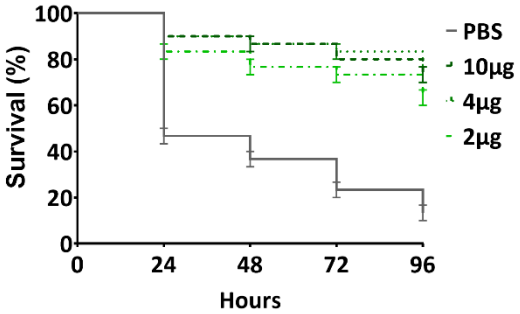
CF2 + Ag-tdda-phen
Survival (%)
100
80
60
40
20
0
0
24
48
72
96
Hours
PBS
10µg
4µg
2µg

P

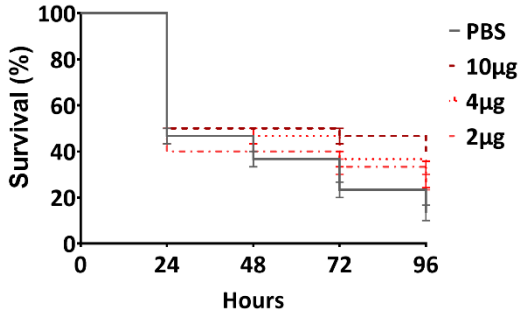
CF2 + Gentamicin
Survival (%)
100
80
60
40
20
0
0
24
48
72
96
Hours
PBS
10µg
4µg
2µg

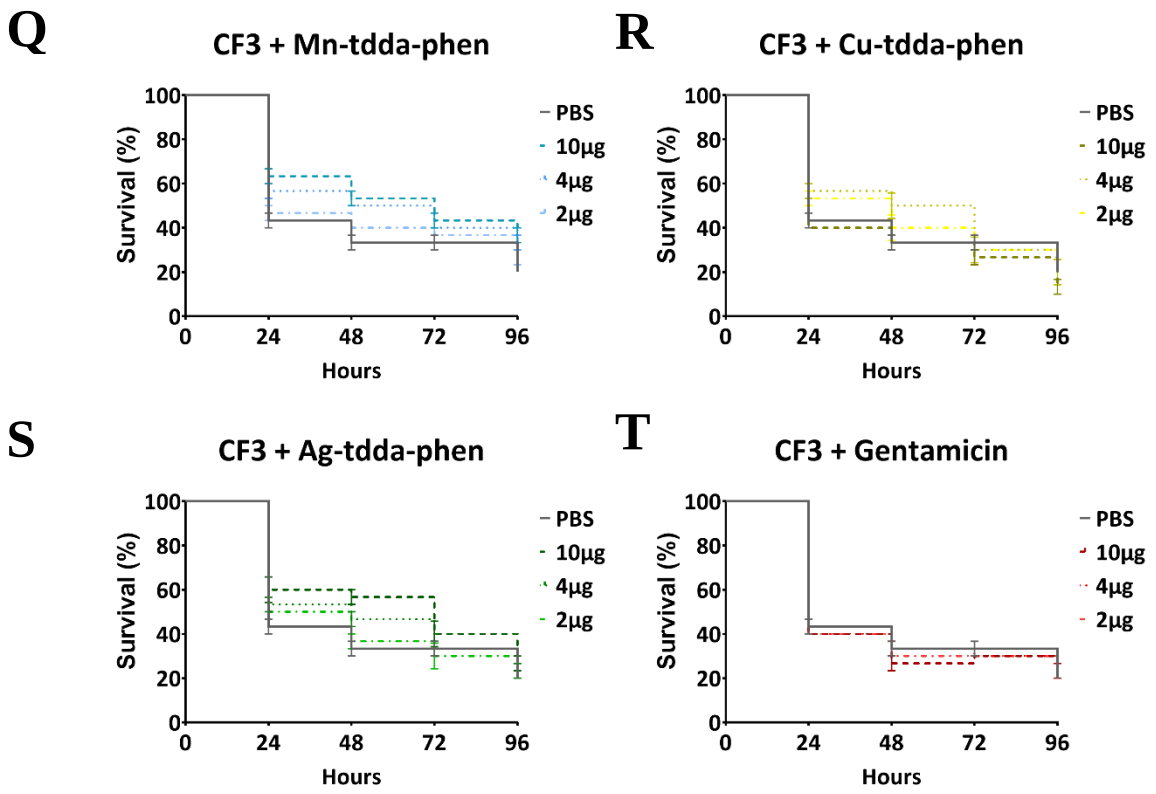

Figure 4.10 Survival (%) of *G. mellonella* inoculated with *P. aeruginosa* strains, ATCC 27853 (**A-D**), PAO1 (**E-H**), CF1 (**I-L**), CF2 (**M-P**), CF3 (**Q-T**) and treated with 2-10 µg/larvae of Mn-tdda-phen (**A,E,I,M,Q**), Cu-tdda-phen (**B,F,J,N,R**), Ag-tdda-phen (**C,G,K,O,S**) and Gentamicin (**D,H,L,P,T**) over 96 h.

To improve therapeutic outcomes, many clinicians recommend dual combinations of antibiotics to increase the likelihood of achieving appropriate therapy for MDR *P. aeruginosa* infections (Bassetti *et al*., 2018). We have also demonstrated synergistic activity against *P. aeruginosa* between all three complexes and gentamicin *in vitro* (**Chapter 3**). The efficacy of metal-tdda-phen complexes in combination with gentamicin was measured in *G. mellonella* larvae infected with ATCC 27583 (3×10^4 CFU/mL), PAO1 (3×10^0 CFU/mL), CF1 (3×10^3 CFU/mL), CF2 (3×10^3 CFU/mL) and CF3 (3×10^0 CFU/mL). A single dose of both Mn-tdda-phen (1.36 µM) and gentamicin (1.74 µM), Cu-tdda-phen (1.34 µM) and gentamicin and Ag-tdda-phen (868.5 nM) and gentamicin at 1 µg/larvae was administered 1 h post-infection and monitored for 96 h (**Figure 4.11** and **Figure 4.12**). Overall, a combination of both drugs outperformed either as a single entity. Of the combinations, larvae that received Mn-tdda-phen and gentamicin and Ag-tdda-phen and gentamicin had the lowest mortality across all strains. Both combinations decreased mortality by 50-53.3%, compared to the PBS-treated larvae, while Cu-tdda-phen and gentamicin decreased mortality by 43.3-50%.

To complement the survival data, the effect of these combinations was also assessed by analysing the larval bacterial burden of *P. aeruginosa* compared to the effect of their constituent mono-therapies and PBS-treated larvae (**Figure 4.11** and **Figure 4.12**). Analysis after 24 h demonstrated that all combinations significantly reduced the bacterial population in the infected larvae. *G. mellonella* infected with ATCC 27853 or PAO1 and subsequently treated with metal-tdda-phen complexes in combination with gentamicin had a 6-7 $\log_{10}$ CFU/mL reduction compared to PBS-treated larvae. The activity was maintained across clinical isolates, CF1-CF3, that had 4-6 $\log_{10}$ CFU/mL in circulating cells that were exposed to both metal-tdda-phen complexes and gentamicin.

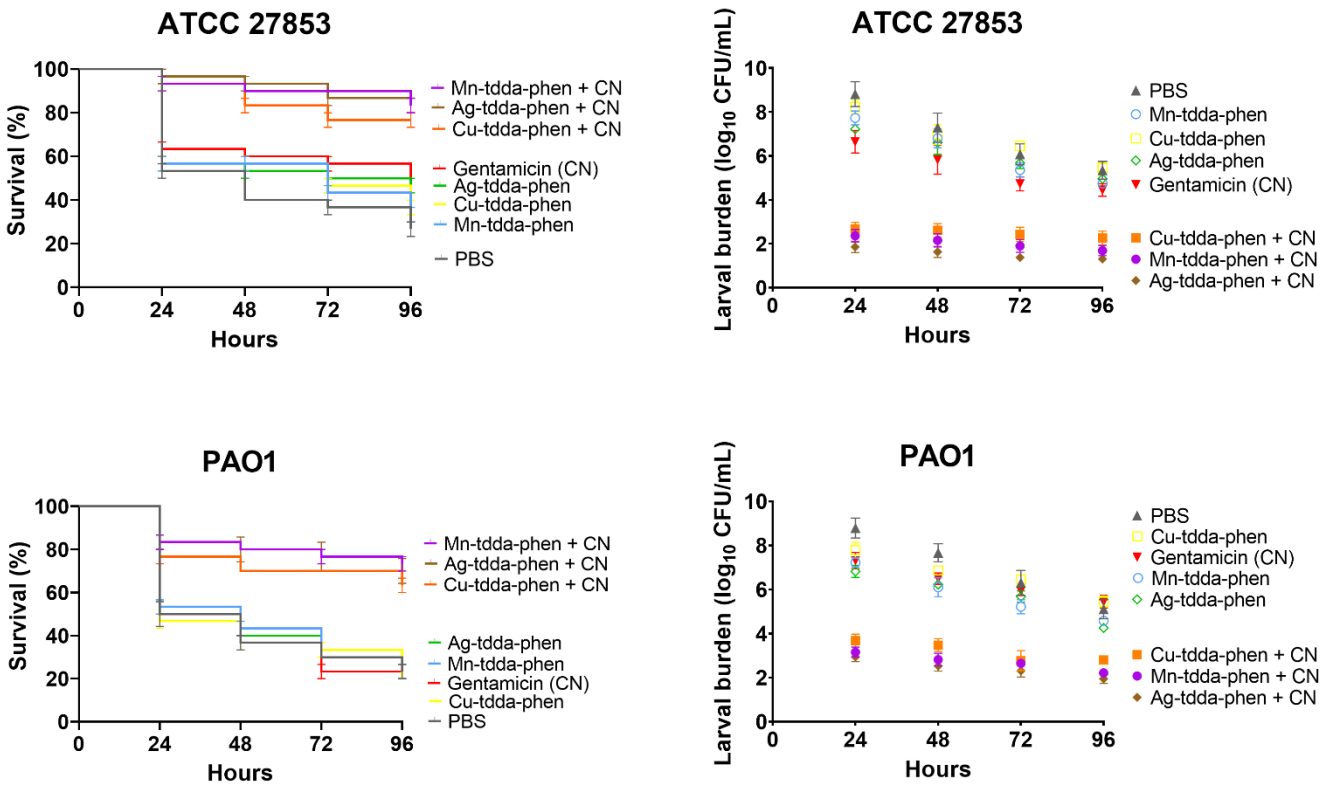

Figure 4.11 Effect of treatment with Mn-tdda-phen, Cu-tdda-phen and Ag-tdda-phen alone (1 µg/larvae) and in combination with gentamicin (CN) (1 µg/larvae) infected with ATCC 27853 and PAO1 on survival (left) and larval bacterial burden (right).

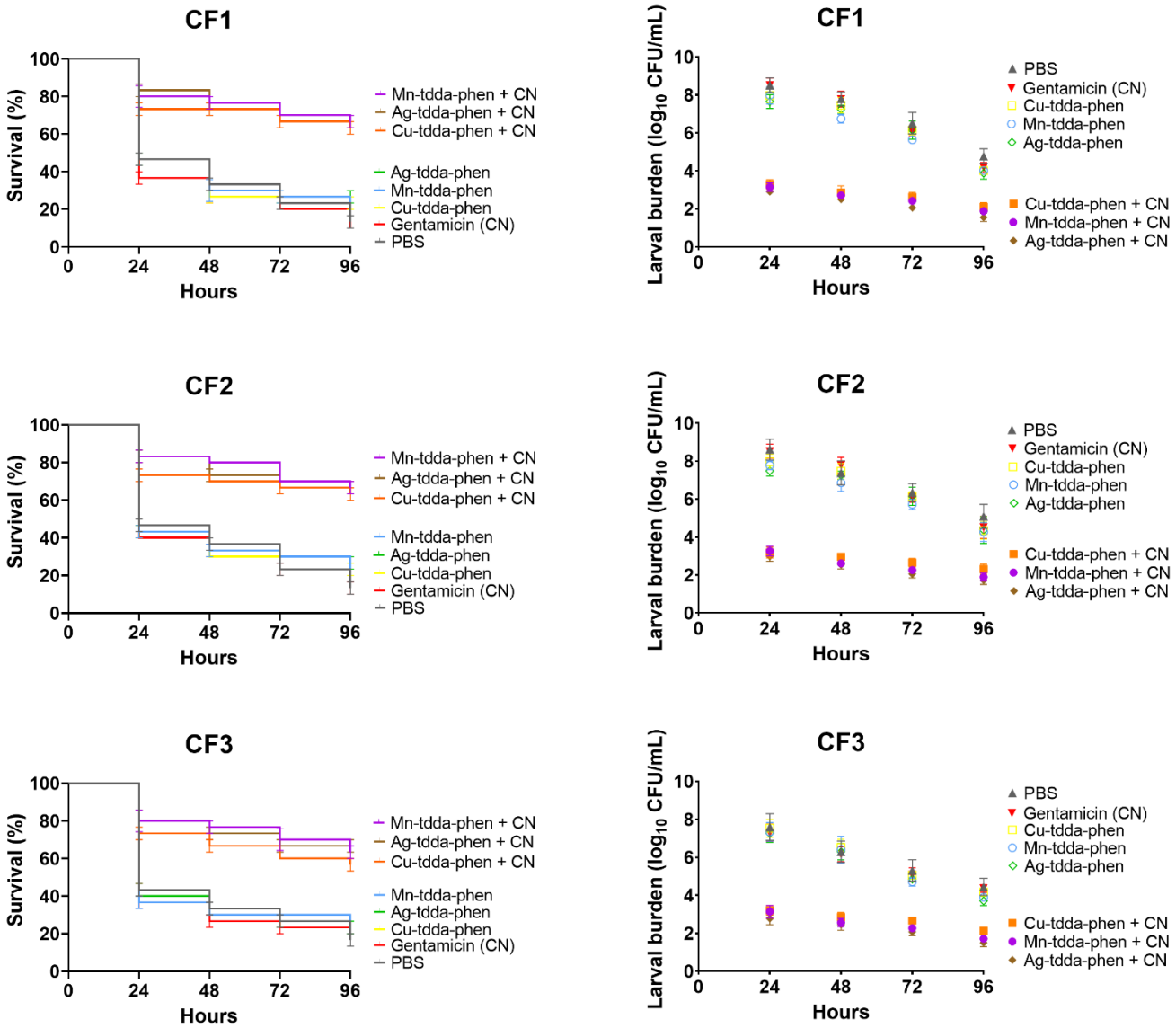

Figure 4.12 Effect of treatment with Mn-tdda-phen, Cu-tdda-phen and Ag-tdda-phen alone (1 µg/larvae) and in combination with gentamicin (CN) (1 µg/larvae) infected with CF1, CF2 and CF3 on survival (left) and larval bacterial burden (right).

4.4. Discussion

P. aeruginosa is a versatile opportunistic pathogen that causes severe clinical complications due to its large genome that harbours an extensive arsenal of virulence factors and antibiotic resistance determinants (Jurado-Martín *et al*., 2021). The bacterium is well reported to swiftly adapt to conditions in the airway with exceptional metabolic flexibility and the ability to evade host immune attacks (Riquelme *et al*., 2020). The presence of *P. aeruginosa* is a particular threat to cystic fibrosis (CF) patients. The deleterious impact that chronic infection has on lung function in CF has been well described and often indicates poor clinical outcomes. *P. aeruginosa* infections are becoming more challenging to treat due to the inherent resistance to many antibiotics, and the number of MDR is increasing worldwide (Pachori *et al*., 2019). Moreover, persistent *P. aeruginosa* infections in CF patients are due to the affinity of bacteria to form a biofilm which is exceedingly more resistant to treatment than their planktonic form (Kovach *et al*., 2017; Ciofu and Tolker-Nielsen, 2019). Thus, the previous chapter (**Chapter 3**) describing metal-tdda-phen complex capabilities against established mature biofilms and synergistic activity with gentamicin warranted the *in vivo* studies to further explore the hypothesis that these complexes could be potential therapeutics for treating *P. aeruginosa* infection as a mono- or combination therapy.

The use of *G. mellonella* larvae as a model to study pathogenicity and virulence, the toxicity of novel complexes and their efficacy as therapies is now well established. Entomopathogenic strains, such as ATCC 27853 and PAO1, and clinical isolates of *P. aeruginosa* are highly virulent in *G. mellonella* with lethal doses ranging from 2 to 100 CFU, killing infected larvae within 24-48 h (Chadwick, 1967; Jander *et al*., 2000; Andrejko *et al*., 2014; Pérez-Gallego *et al*., 2016; Thomaz *et al*., 2020). Similar pathogenicity profiles were observed in this study. For instance, PAO1 and CF3 resulted

in complete larvae death after 24 h at 30 CFU. Mortality assays demonstrated that the metal-tdda-phen complexes are well tolerated by *G. mellonella* up to 10 µg per exposed larvae. At the highest examined concentration (30 µg/larvae), Cu-tdda-phen was highly toxic to the larvae, while Mn-tdda-phen was the least toxic. This was also previously reported within our research group (Gandra *et al*., 2020), demonstrating the reproducibility of this model. *G. mellonella* has been employed to evaluate the toxicity of a range of agents, and the results have shown a strong correlation to those generated utilizing mammalian models. Maguire *et al.* (2016). reported comparable toxicology data (LD_{50}) of food preservatives between insect larvae and rats. Consequently, a mammalian model could tolerate Mn-tdda-phen and Ag-tdda-phen complexes. Furthermore, Mn-tdda-phen demonstrated immunomodulation properties by simulating hemocyte density and immune-related genes, specifically antimicrobial peptides (AMPs), *transferrin* (iron-binding protein) and *IMPI* (inducible metallo-proteinase inhibitor). AMPs have been reported to exert their antimicrobial action through permeabilizing the pathogen membrane and thus their upregulation may aid in the clearing of an infection.

Rapidly increasing antibiotic resistance in already difficult-to-treat pathogens has prompted a variety of studies employing *G. mellonella* larvae to delineate the efficacy of therapies against these problematic bacteria (Tsai *et al*., 2016; Cutuli *et al*., 2019; Piatek *et al*., 2020). Within these studies, the antibiotic susceptibility profiles of the examined microorganisms mirror those established *in vitro*. Moreover, it has been shown that the MICs of anti-pseudomonal drugs in infected larvae correlated with the susceptibilities in patients (Hill *et al*., 2014; Ignasiak and Maxwell, 2017). In **Chapter 3**, the antibacterial capabilities of Mn-tdda-phen, Cu-tdda-phen, and Ag-tdda-phen against *P. aeruginosa* strains originating from CF patients were reported *in vitro*. While gentamicin was the most effective compound against the reference antibiotic-sensitive strains (ATCC 27853

and PAO1), it had reduced efficacy across the resistant clinical isolates (CF1-CF3). However, the metal-tdda-phen complexes maintained clinically relevant activity. Similarities can be seen in the treatment of infected *G. mellonella* larvae. Gentamicin (at the highest tested concentration of 10 μg/larvae) had the greatest potency in treating larvae infected with ATCC 27853 and PAO1, but its activity decreased when administered to larvae infected with the clinical isolates, which had been classified as resistant to the antibiotic (**Chapter 3**). However, mirroring the *in vitro* profiles, the activity of gentamicin diminished across the clinical isolates while the activity of the metal-tdda-phen complexes was preserved.

Although definitive treatment with a single agent would be the ideal scenario, due to the expanding resistance profiles of *P. aeruginosa,* the empirical administration of antibiotic combinations is utilised by clinicians to control pulmonary exacerbations in CF patients. Across published guidelines, the most common combinations are an aminoglycoside or a fluoroquinolone with an anti-pseudomonal β-lactam, which results in a synergistic bactericidal effect (Moreno *et al*., 2021a). Gentamicin is a clinically important aminoglycoside antibiotic. It inhibits protein synthesis by binding with a high affinity to the aminoacyl-tRNA site (A site) within the 30S ribosomal subunit, thereby inhibiting the translation process (Magnet and Blanchard, 2005). This produces truncated proteins, affecting the cell wall composition, which increases membrane permeability and subsequently heightens uptake of the drug (Kohanski *et al*., 2008). However, prolonged treatment with gentamicin can have severe adverse effects, such as nephrotoxicity and ototoxicity, that are thought to be dose-related, with higher concentrations causing a greater chance of toxicity. Metal-based drugs have unique mechanisms of action in comparison to their organic counterparts (Viganor, Howe, *et al.*, 2016a; Claudel, Schwarte and Fromm, 2020; Frei, 2020; Frei *et al.*, 2020; Evans and Kavanagh, 2021;

Wang *et al.*, 2021; Wang and Lippard, 2005; Palermo *et al.*, 2016). Such mechanisms include; ligand exchange or release, ROS generation and catalytic generation of toxic species or depletion of essential substrates (Kohanski *et al*., 2008; Claudel *et al*., 2020). These mechanisms can be multi-modal (Wang *et al*., 2021a) and hugely dependent on the metal centre and attached ligands (Frei *et al*., 2020). In this study, we assessed the combination of the metal-tdda-phen complexes and gentamicin because they demonstrated synergistic activity against *P. aeruginosa* strains in both planktonic (data not shown) and biofilm forms (**Chapter 3**). The combined therapy of metal-tdda-phen and gentamicin in larvae infected with all strains produced an appreciable survival rate than those treated with the individual agents at lower concentrations. Furthermore, the combination dampened the proliferation of bacteria within the larvae, which was elucidated by the more extensive depletion in bacterial burden compared to single treatments. As bacteria adapt to antibiotic treatment, higher doses are required to manage the infection that, as previously mentioned, has been associated with severe adverse effects in patients. The efficacy of the metal-tdda-phen/gentamicin combination at clearing an infection, especially of the resistant clinical isolates, at lower doses is interesting in this regard. Although gentamicin is a bactericidal antibiotic, it is not possible to deduce if the combination is also working in this manner. However, due to the already established antibacterial effects of complex Mn-tdda-phen and its presented capability to induce an immune response through enhancement of hemocytes and immune related genes, it can be postulated that this complex might have several processes for aiding the clearance of an infection.

In conclusion, the data presented here suggest that Mn-tdda-phen and Ag-tdda-phen can clear a *P. aeruginosa* infection at concentrations that are non-toxic toward *G. mellonella* larvae. It is thought to be multi-modal, acting directly on the bacteria and stimulating

cellular and humoral responses that work concomitantly to clear an infection. Although more research is required to understand the mechanisms by which the complexes exert their antibacterial properties, this study has highlighted that substituting the metal centre alters the toxicity level and immunomodulation properties. Combinations of metal-tdda-phen complexes with gentamicin restored the activity of the antibiotic against clinical isolates that were resistant to it, presenting an alternative combination therapeutic approach with greater efficacy.

Chapter 5.

Overall discussion and future perspectives

The rise of antimicrobial resistance (AMR) threatens global health through significant morbidity, mortality, and global economic loss. Currently, in 2022, the coronavirus disease (COVID-19) pandemic caused by severe acute respiratory syndrome coronavirus 2 (SARS-CoV-2) has been one of the most significant challenges of our time and has overwhelmed healthcare systems internationally. Simultaneously, it has highlighted the vulnerability of humanity to a world without adequate treatment for a pathogen. Moreover, the pandemic has exacerbated the existing AMR crisis. There are many avenues to address the now dubbed 'silent pandemic' of AMR and require a global 'One Health' approach. This concept recognises that human, animal and environmental health are all connected and therefore requires a multi-sectorial and transdisciplinary approach from local to global levels to tackle the issue of AMR (Destoumieux-Garzón *et al*., 2018). A common approach is reducing antimicrobial use in agriculture and humans. However, this creates a paradox as the depletion in prescriptions reduces sales and therefore reduces interest from pharmaceutical companies to invest in novel antimicrobial agents. Consequently, the current antibacterial clinical pipeline is inadequate to treat the mounting infections caused by multidrug-resistant pathogens (Butler *et al*., 2022). There is now an increased interest in 'non-traditional' approaches to antibacterial therapy that explore different avenues compared to 'traditional' organic molecules that target pathogens. These agents can prevent or treat bacteria through several modes of action, including directly or indirectly inhibiting growth, inhibiting virulence, inhibiting or removing biofilm, alleviating resistance, restoring the natural gut microbiome, or boosting the immune system to clear or manage their infections (Rex *et al*., 2019; Theuretzbacher and Piddock, 2019; Langendonk *et al*., 2021). Of the 12 new antibacterial agents approved for clinical use since 2017, the WHO reported that only one compound, cefiderocol, meets one of their innovation criteria (absence of known cross-resistance,

new target, a new mode of action, and/or new class) (WHO, 2021) that also has activity against all three critical carbapenem-resistant priority pathogens (**Table 1.3**). Cefiderocol is a siderophore-conjugated cephalosporin that promotes the formation of chelated complexes with ferric iron and facilitates siderophore-like transport across the outer membrane of Gram-negative bacteria using iron transport systems, accumulating in the periplasmic space (Zhanel *et al*., 2019; Wang *et al*., 2022).

Interdisciplinary researchers in biology and inorganic chemistry have been investigating novel metal-bearing drugs and assessing their therapeutic potential to tackle resistance providing a realistic alternative to the 'traditional' antibiotic (Mukherjee and Sadler, 2009; Reece and Marimon, 2019; Claudel *et al*., 2020; Frei *et al*., 2020; Nasiri Sovari and Zobi, 2020; Evans and Kavanagh, 2021). A wealth of research reports the enhanced activity of metals complexed to organic ligands such as 1,10-phenanthroline (phen) (Dwyer *et al*., 1969; McCann *et al*., 2012b; Viganor *et al*., 2015, 2016b; Gandra *et al*., 2017; McCarron *et al*., 2018; Galdino *et al*., 2019; Ahmed *et al*., 2022). The purpose of this research project was to investigate further the antibacterial potential of novel manganese(II)-, silver(I)- and copper(II)-phen complexes.

As presented in **Figure 5.1**, the first objective (**Chapter 2**) was screening a panel of metal complexes incorporating dicarboxylate and 1,10-phenanthroline (phen) ligands against a panel of Gram-positive and Gram-negative WHO priority pathogens that also significantly impact the Irish healthcare system. Metal-complexed phenanthrolines presented an enhanced toxicity profile across examined pathogen panels juxtaposed to their non-phen derivatives and starting materials. The chelates incorporating 3,6,9-trioxaundecanedioate (tdda) and phen (metal-tdda-phen) were the most effective across the broadest range of tested strains and were therefore chosen for additional testing. The three complexes, Cu-tdda-phen, Mn-tdda-phen and Ag-tdda-phen, presented synergistic

activity when co-administered with the antibiotic gentamicin against *S. aureus* and *P. aeruginosa* clinical isolates that were resistant to the prescription drug alone. To elucidate the molecular targets of the metal-tdda-phen complexes in reference, *S. aureus* and *P. aeruginosa* strains were exposed to sub-lethal doses of the three complexes and subsequently whole-genome sequenced (WGS). However, there were complications with *S. aureus* mutant data, discussed in **Section 2.3.4**, mutant *P. aeruginosa* genome presented with changes in proteins involved in cellular respiration, the polyamine biosynthetic pathway, and virulence mechanisms suggestive of the potential mechanisms of action. However, the effect on one pathway could have a knock-on effect on others and more in-depth analysis at a protein level is required to assess exact molecular targets. Even so, these mechanisms suggest a novel mode of action to 'traditional' antibiotics, a criterion on the WHO antibacterial innovation list (WHO, 2021).

The water-soluble metal-tdda-phen complexes presented with good to moderate activity across the bacterial panels and were therefore chosen for subsequent analysis. As they had enhanced activity profiles in *S. aureus* and *P. aeruginosa* strains (**Chapter 2**), a cystic fibrosis (CF) disease model was used further to investigate the potential therapeutic capabilities of the complexes. *S. aureus* is the most prevalent pathogen in the lungs of CF patients in childhood, while *P. aeruginosa* is the most abundant in adulthood (CF Registry of Ireland, 2019). *P. aeruginosa* is an avid biofilm-forming bacterium, and evolving resistance to antibiotics is problematic and of concern when considering the treatment of its infections in CF patients (Beswick *et al*., 2020). Targeting the biofilm and virulence properties has gained considerable attention as an anti-pathogenic strategy; thus, this work offers a significant perspective (Thi *et al*., 2020; Langendonk *et al*., 2021). Moreover, the metal-tdda-phen complexes eluded this potential on a genotypic level from the WGS data.

For the second objective (**Chapter 3**), the metal-tdda-phen complexes were assessed against clinical isolates of *P. aeruginosa* derived from Irish CF patients. The effects of the metal complexes on planktonic growth, biofilm formation, and mature biofilm alone and combined with the prescription antibiotic gentamicin were investigated. Metal-tdda-phen complexes were able to disrupt biofilm, which prompted further investigation into their effect on individual components to potentially decipher elements of their mechanism of action. Metal complexes were able to destabilize the biofilm by interacting with extracellular DNA and exopolysaccharides in the extracellular matrix, possibly through Psl. This destabilization could allow the previously inhibited antibiotic gentamicin into the biofilm to enhance its cytotoxic action and was further supported by the viable cell counts. The potentiating activity of all three metal-tdda-phen complexes with gentamicin is of great interest as this may resensitise the bacteria to concentrations of the antibiotic to which it was previously resistant (Ahmed *et al.*, 2020). This also has excellent potential for treating persister cells, a subpopulation of non-replicating and metabolically quiescent bacteria that become highly tolerant to antibiotics and are very problematic in treating exacerbations in chronic infections (Ciofu and Tolker-Nielsen, 2019). For instance, a new class of glycopolymers includes polycationic poly-N (acetyl, arginyl) glucosamine (PAAG), a polycationic biopolymer currently in Phase I clinical trials in the treatment of CF patients. It has been shown to eradicate *P. aeruginosa* persister cells effectively (Narayanaswamy *et al*., 2018) and improve mucus clearance of the lungs of CF patients by chelation of Ca^{2+} without any harmful effect on tissue (Garcia *et al*., 2022).

Other novel treatment strategies are being trialled and optimized for CF patients, and numerous studies have compared mono- and combination-antibiotic therapies (Anderson *et al*., 1978; Tang *et al*., 2018). Amongst the many alternative therapeutic approaches documented are the guluronate polymer OligoG (derived from alginate), a simple thiol

cysteamine, a novel synthetic peptide, nitric oxide and gallium(III) compounds (Smith *et al*., 2017; Moreno *et al*., 2021b). Ga^{3+} metal ions have been shown to disrupt biofilm formation and protect against *P. aeruginosa* infections *in vitro* in human serum (Bonchi *et al*., 2015), mouse models (Kaneko *et al*., 2007; DeLeon *et al*., 2009) and humans (Goss *et al*., 2018). Moreover, there is a decreased likelihood that *P. aeruginosa* can develop resistance to gallium compared to the classic small-molecule antibiotics (Ross-Gillespie *et al*., 2014). Additional studies showed that co-encapsulation of Ga^{3+} with gentamicin in liposomes was more effective than gentamicin alone for eradicating *P. aeruginosa* in both planktonic and biofilm forms (Halwani *et al*., 2008). There is clearly scope for the development of novel metal complexes, either acting alone or in combination with antibiotics, as a new therapeutic regime for *P. aeruginosa* infections in CF patients.

For the final objective (**Chapter 4**), the anti-pseudomonal activity of metal complexes was further explored within the *in vivo* model of the larvae of *Galleria mellonella*, in combination with gentamicin. Metal-tdda-phen complexes maintained activity against the CF isolates at concentrations that were tolerated by the larvae. The complexes are thought to be multi-modal, acting directly on the bacteria but also through stimulating both the cellular and humoral responses that work concomitantly to clear an infection. The combined therapy of metal-tdda-phen and gentamicin in larvae infected with all strains produced an appreciable increase in survival and dampened proliferation of bacteria within the larvae. This provides an opportunity to streamline the identification and evaluation of novel antimicrobial agents in a valuable preclinical *in vivo* model at a time when there is a desperate need to accelerate the development pipeline. Although promising, a well-validated CF *in vivo* model is still required, such as a cystic fibrosis transmembrane conductance regulator (CFTR) knockout animal, to fully assess the metal-tdda-phen/gentamicin anti-infective therapeutic potential (Semaniakou *et al*., 2019).

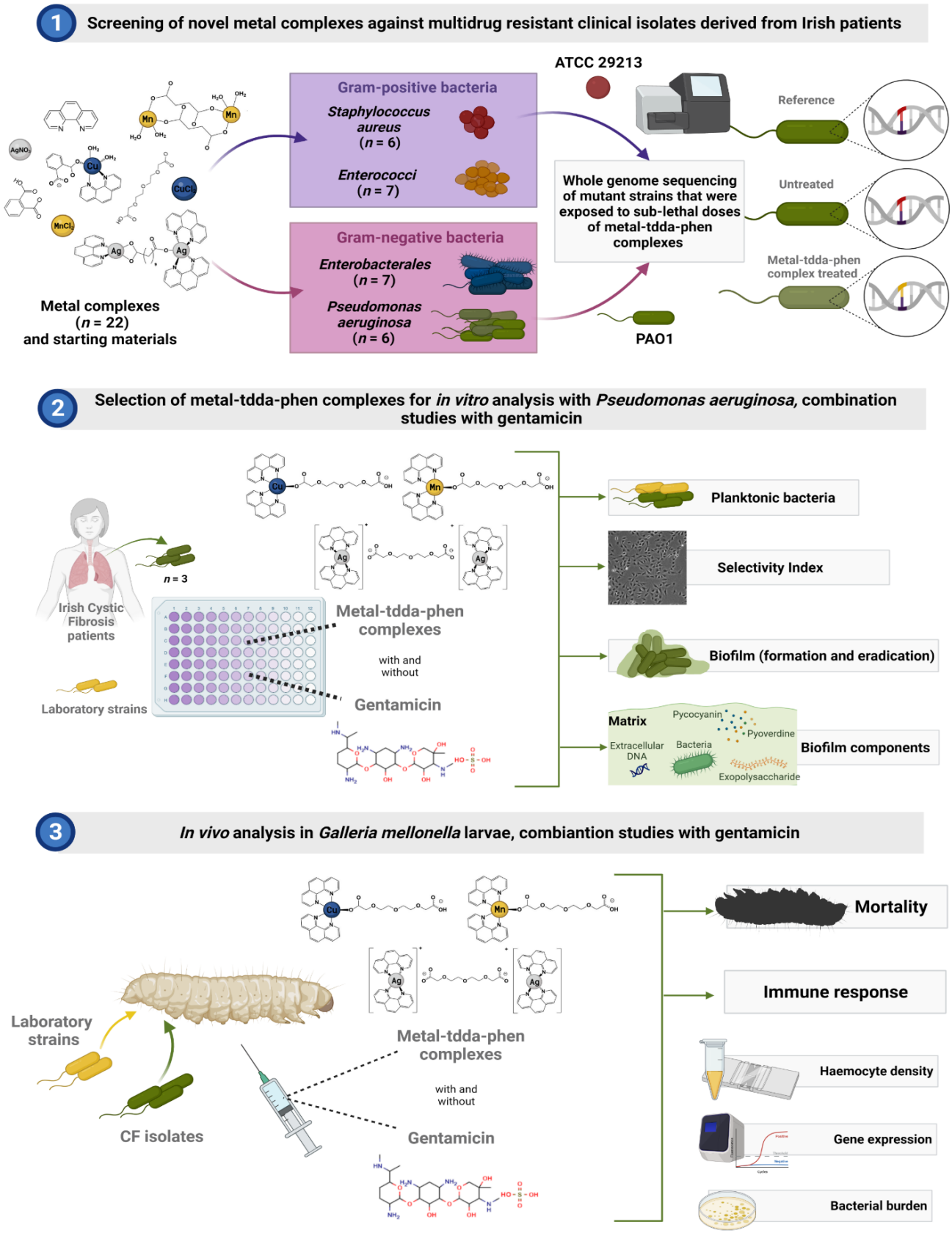

Figure 5.1 A schematic overview of the research presented in this thesis. Steps 1, 2, and 3 (corresponding to chapters 2, 3 and 4) explain the progression of the project from initial screening (step 1) to testing lead complexes in both *in vitro* (step 2) and *in vivo* (step 3) models.

In this body of work, metal-tdda-phen complexes presented activity against clinical isolates of *P. aeruginosa*. Across the inhibitory, WGS, anti-biofilm and *in vivo* data, the activity of the complex was independent of the metal centre. In fact, within the sequencing data, the three complexes had only one common mutation. Although Cu-tdda-phen demonstrated good to moderate activity, the same concentrations were extremely toxic within both an *in vitro* (**Chapter 3**) and *in vivo* model (**Chapter 4**), culminating in a low selectivity index. The copper complex could inhibit the formation of a biofilm and disperse an established biofilm with suggested enhanced activity toward eDNA within the matrix and pyocyanin production to a lesser extent. Therefore, this complex may be better suited for disinfection of implantable medical devices or topical applications. However, it should be noted that the synergistic nature of the anti-biofilm effect with gentamicin allows the use of much lower concentrations of the metal complex and antibiotic than those used individually.

Mn-tdda-phen and Ag-tdda-phen were well tolerated by mammalian cell lines and the *G. mellonella* larvae while maintaining activity, promoting good clinical utility. The manganese derivative was observed to reduce exopolysaccharides in both forming and mature biofilms, enhanced immune response in exposed larvae through elevated haemocytes and antimicrobial peptides, reducing the bacterial load in infected larvae and overall increasing their survival. Ag-tdda-phen also generated the same activity profile but with less efficiency and significantly reduced pyocyanin production when combined with gentamicin. Manganese, like copper, is a trace element and excessive levels in the body can cause poor bone health and neurological symptoms (Evans and Kavanagh, 2021), and chronic exposure may cause infertility (Claudel *et al*., 2020). While silver does not have significant toxic side effects in humans when administered in low doses, chronic

exposure can lead to deposits in the skin, causing skin pigmentation known as argyria (Evans and Kavanagh, 2021).

Although *P. aeruginosa* predominates in the lungs of adolescent CF patients, it does not colonise the airways alone. The interactions within the microbiota of the lungs have been shown to reduce susceptibility to antibiotics and affect patient health. Moreover, the virulence of *P. aeruginosa* is influenced by its co-colonisers in the CF lung microbiome (Reece *et al*., 2021). Their impact on polymicrobial communities should be investigated to garner greater insight into the metal-tdda-phen complexes treatment efficacies of exacerbations in CF patients. Drug development is a complex, expensive, and arduous process. As previously mentioned, pharmaceutical companies are abandoning the investment in antibiotics and instead funding lifetime diseases that require daily medication. A metal drug presented with an anti-virulence activity to dampen the effects of a chronic disorder may appear more lucrative to them. In addition, the potential to resensitise bacteria to an antibiotic such as gentamicin, which regulatory agencies have already approved, may also strengthen the proposal to encourage funding (Skwarczynski *et al*., 2022). To expand the current knowledge highlighted in this thesis elucidating the specific cellular targets of these compounds would further aid their potential clinical development. While the WGS data highlighted the potential mechanisms by which the metal-tdda-phen complexes act, proteomic analysis is required to verify the effects of the mutations on a phenotypic level (Slavin *et al*., 2017; Zielinski *et al*., 2021). In addition, ICP-MS, a sub-cellular fractionation coupled with mass spectrometry, would also be a valuable tool for localising either intact, disassociated or alternative metal-phen complexes within the cell or biofilm (Wang *et al*., 2021a).

In conclusion, this work highlights the therapeutic potential of metal-tdda-phen complexes not only alone but also in combination with gentamicin in both *in vitro* and *in*

vivo models. However, research is still required to understand the pharmacological, toxicological, and pharmacokinetic impacts of the drugs. The data presented in this thesis warrant further investigation into the antimicrobial activities of the metal-tdda-phen complexes.

References

AbuOun, M., Stubberfield, E. J., Duggett, N. A., Kirchner, M., Dormer, L., Nunez-Garcia, J., *et al*. (2017). mcr-1 and mcr-2 variant genes identified in Moraxella species isolated from pigs in Great Britain from 2014 to 2015. *J. Antimicrob. Chemother.* 72, 2745–2749. doi: 10.1093/jac/dkx286.

Acar, J. (1997). Broad- and narrow-spectrum antibiotics: An unhelpful categorization. *Clin. Microbiol. Infect.* 3, 395–396. doi: 10.1111/j.1469-0691.1997.tb00274.x.

Adonizio, A., Kong, K. F., and Mathee, K. (2008). Inhibition of quorum sensing-controlled virulence factor production in *Pseudomonas aeruginosa* by south Florida plant extracts. *Antimicrob. Agents Chemother.* 52, 198–203. doi: 10.1128/AAC.00612-07.

Ahmed, M. A. E. E., Doi, Y., Tian, G., Zhong, L., Shen, C., and Yang, Y. (2020a). Colistin and its role in the Era of antibiotic resistance : an extended review. *Emerg. Microbes Infect.* 9.

Ahmed, M. O., and Baptiste, K. E. (2018). Vancomycin-Resistant Enterococci: A Review of Antimicrobial Resistance Mechanisms and Perspectives of Human and Animal Health. *Microb. Drug Resist.* 24, 590–606. doi: 10.1089/mdr.2017.0147.

Ahmed, M., Rooney, D., McCann, M., Devereux, M., Twamley, B., Galdino, A. C. M., *et al.* (2019). Synthesis and antimicrobial activity of a phenanthroline-isoniazid hybrid ligand and its Ag^{+} and Mn^{2+} complexes. *BioMetals* 32, 671–682. doi: 10.1007/s10534-019-00204-5.

Ahmed, M., Ward, S., McCann, M., Kavanagh, K., Heaney, F., Devereux, M., *et al*. (2022). Synthesis and characterisation of phenanthroline-oxazine ligands and their Ag(I), Mn(II) and Cu(II) complexes and their evaluation as antibacterial agents. *BioMetals* 35, 173–185. doi: 10.1007/s10534-021-00358-1.

Ahmed, S., Sony, S. A., Chowdhury, M. B., Ullah, M. M., Paul, S., and Hossain, T. (2020b).

Retention of antibiotic activity against resistant bacteria harbouring aminoglycoside-N-acetyltransferase enzyme by adjuvants: a combination of in-silico and in-vitro study. *Sci. Rep.* 10, 1–12. doi: 10.1038/s41598-020-76355-0.

Alam, A., Bröms, J. E., Kumar, R., and Sjöstedt, A. (2021). The Role of ClpB in Bacterial Stress Responses and Virulence. *Front. Mol. Biosci.* 8, 283. doi: 10.3389/fmolb.2021.668910.

Aldossary, S. A. (2019). Review on pharmacology of cisplatin: Clinical use, toxicity and mechanism of resistance of cisplatin. *Biomed. Pharmacol. J.* 12, 7–15. doi: 10.13005/bpj/1608.

Alford, M. A., Baghela, A., Yeung, A. T. Y., Pletzer, D., and Hancock, R. E. W. (2020). NtrBC Regulates Invasiveness and Virulence of *Pseudomonas aeruginosa* During High-Density Infection. *Front. Microbiol.* 11, 773. doi: 10.3389/fmicb.2020.00773.

Ambler, R. . (1980). The structure of Beta Lactamases. *Phil. Trans. R. Soc. Lond.* 289, 321–331. doi: 10.1016/0009-2614(94)00453-6.

Anantharajah, A., Mingeot-Leclercq, M. P., and Van Bambeke, F. (2016). Targeting the Type Three Secretion System in *Pseudomonas aeruginosa*. *Trends Pharmacol. Sci.* 37, 734–749. doi: 10.1016/j.tips.2016.05.011.

Anderson, E. T., Young, L. S., and Hewitt, W. L. (1978). Antimicrobial synergism in the therapy of gram-negative rod bacteremia. *Chemotherapy* 24, 45–54. doi: 10.1159/000237759.

Andrejko, M., Zdybicka-Barabas, A., and Cytryńska, M. (2014). Diverse effects of *Galleria mellonella* infection with entomopathogenic and clinical strains of *Pseudomonas aeruginosa*. *J. Invertebr. Pathol.* 115, 14–25. doi: 10.1016/j.jip.2013.10.006.

Angst, D. C., Tepekule, B., Sun, L., Bogos, B., and Bonhoeffer, S. (2021). Comparing treatment strategies to reduce antibiotic resistance in an in vitro epidemiological setting. *Proc. Natl. Acad. Sci. U. S. A.* 118, 1–7. doi: 10.1073/PNAS.2023467118.

Antonoplis, A., Zang, X., Wegner, T., Wender, P. A., and Cegelski, L. (2019). A Vancomycin-Arginine Conjugate Inhibits Growth of Carbapenem-resistant E. coli and Targets Cell-Wall Synthesis Alexandra. *ACS Chem Biol* 14, 2065–2070. doi: 10.1021/acschembio.9b00565.A.

Arakawa, H., Neault, J. F., and Tajmir-Riahi, H. A. (2001). Silver(I) complexes with DNA and RNA studied by fourier transform infrared spectroscopy and capillary electrophoresis. *Biophys. J.* 81, 1580–1587. doi: 10.1016/S0006-3495(01)75812-2.

Arnold, B. J., Huang, I. T., and Hanage, W. P. (2022). Horizontal gene transfer and adaptive evolution in bacteria. *Nat. Rev. Microbiol.* 20, 206–218. doi: 10.1038/s41579-021-00650-4.

Asad, N. R., and Leitao, A. C. (1991). Effects of metal ion chelators on DNA strand breaks and inactivation produced by hydrogen peroxide in Escherichia coli: Detection of iron-independent lesions. *J. Bacteriol.* 173, 2562–2568. doi: 10.1128/jb.173.8.2562-2568.1991.

Ayobami, O., Willrich, N., Reuss, A., Eckmanns, T., and Markwart, R. (2020). The ongoing challenge of vancomycin-resistant Enterococcus faecium and Enterococcus faecalis in Europe: an epidemiological analysis of bloodstream infections. *Emerg. Microbes Infect.* 9, 1180–1193. doi: 10.1080/22221751.2020.1769500.

Baker, S. J., Payne, D. J., Rappuoli, R., and De Gregorio, E. (2018). Technologies to address antimicrobial resistance. *Proc. Natl. Acad. Sci. U. S. A.* 115, 12887–12895. doi: 10.1073/pnas.1717160115.

Banin, E., Brady, K. M., and Greenberg, E. P. (2006). Chelator-induced dispersal and killing of *Pseudomonas aeruginosa* cells in a biofilm. *Appl. Environ. Microbiol.* 72, 2064–2069. doi: 10.1128/AEM.72.3.2064-2069.2006.

Barbosa, C., Mahrt, N., Bunk, J., Graßer, M., Rosenstiel, P., Jansen, G., *et al*. (2021). The Genomic Basis of Rapid Adaptation to Antibiotic Combination Therapy in *Pseudomonas aeruginosa*. *Mol. Biol. Evol.* 38, 449–464. doi: 10.1093/molbev/msaa233.

Barras, F., Aussel, L., and Ezraty, B. (2018). Silver and antibiotic, new facts to an old story. *Antibiotics* 7, 1–10. doi: 10.3390/antibiotics7030079.

Bassetti, M., Merelli, M., Temperoni, C., and Astilean, A. (2013). New antibiotics for bad bugs: Where are we? *Ann. Clin. Microbiol. Antimicrob.* 12, 22. doi: 10.1186/1476-0711-12-22.

Bassetti, M., Vena, A., Croxatto, A., Righi, E., and Guery, B. (2018). How to manage *Pseudomonas aeruginosa* infections. *Drugs Context* 7, 212527. doi: 10.7573/dic.212527.

Beeton, M. L., Aldrich-Wright, J. R., and Bolhuis, A. (2014). The antimicrobial and antibiofilm activities of copper(II) complexes. *J. Inorg. Biochem.* 140, 167–172. doi: 10.1016/j.jinorgbio.2014.07.012.

Beeton, M. L., Alves, D. R., Enright, M. C., and Jenkins, A. T. A. (2015). Assessing phage therapy against *Pseudomonas aeruginosa* using a *Galleria mellonella* infection model. *Int. J. Antimicrob. Agents* 46, 196–200. doi: 10.1016/j.ijantimicag.2015.04.005.

Belluzo, B. S., Abriata, L. A., Giannini, E., Mihovilcevic, D., Dal Peraro, M., and Llarrull, L. I. (2019). An experiment-informed signal transduction model for the role of the Staphylococcus aureus MecR1 protein in β-lactam resistance. *Sci. Rep.* 9, 1–15. doi: 10.1038/s41598-019-55923-z.

Bencini, A., and Lippolis, V. (2010). 1,10-Phenanthroline: A versatile building block for the construction of ligands for various purposes. *Coord. Chem. Rev.* 254, 2096–2180. doi: 10.1016/j.ccr.2010.04.008.

Bennison, D. J., Irving, S. E., and Corrigan, R. M. (2019). GTPases and Prokaryotic Ribosome Assembly. *Cells* 8.

Bergin, D., Brennan, M., and Kavanagh, K. (2003). Fluctuations in haemocyte density and microbial load may be used as indicators of fungal pathogenicity in larvae of *Galleria mellonella*. *Microbes Infect.* 5, 1389–1395. doi: 10.1016/j.micinf.2003.09.019.

Bergin, D., Reeves, E. P., Renwick, J., Wientjes, F. B., and Kavanagh, K. (2005). Superoxide production in *Galleria mellonella* hemocytes: Identification of proteins homologous to the NADPH oxidase complex of human neutrophils. *Infect. Immun.* 73, 4161–4170. doi: 10.1128/IAI.73.7.4161-4170.2005.

Beswick, E., Amich, J., and Gago, S. (2020). Factoring in the complexity of the cystic fibrosis lung to understand *Aspergillus fumigatus* and *Pseudomonas aeruginosa* interactions. *Pathogens* 9, 1–19. doi: 10.3390/pathogens9080639.

Bhagirath, A. Y., Li, Y., Patidar, R., Yerex, K., Ma, X., Kumar, A., *et al*. (2019). Two component regulatory systems and antibiotic resistance in gram-negative pathogens. *Int. J. Mol. Sci.* 20. doi: 10.3390/ijms20071781.

Billings, N., Ramirez Millan, M., Caldara, M., Rusconi, R., Tarasova, Y., Stocker, R., *et al*. (2013). The Extracellular Matrix Component Psl Provides Fast-Acting Antibiotic Defense in *Pseudomonas aeruginosa* Biofilms. *PLoS Pathog.* 9. doi: 10.1371/journal.ppat.1003526.

Blanco-Cabra, N., Paetzold, B., Ferrar, T., Mazzolini, R., Torrents, E., Serrano, L., *et al*. (2020). Characterization of different alginate lyases for dissolving *Pseudomonas aeruginosa* biofilms. *Sci. Rep.* 10, 1–10. doi: 10.1038/s41598-020-66293-2.

Bolhuis, A., and Aldrich-Wright, J. R. (2014). DNA as a target for antimicrobials. *Bioorg. Chem.* 55, 51–59. doi: 10.1016/j.bioorg.2014.03.009.

Bonchi, C., Frangipani, E., Imperi, F., and Visca, P. (2015). Pyoverdine and proteases affect the response of *Pseudomonas aeruginosa* to gallium in human serum. *Antimicrob. Agents Chemother.* 59, 5641–5646. doi: 10.1128/AAC.01097-15.

Borghi, E., Romagnoli, S., Fuchs, B. B., Cirasola, D., Perdoni, F., Tosi, D., *et al*. (2014). Correlation between *Candida albicans* biofilm formation and invasion of the invertebrate host *Galleria mellonella*. *Future Microbiol.* 9, 163–173. doi: 10.2217/fmb.13.159.

Boros, E., Dyson, P. J., and Gasser, G. (2020). Classification of Metal-Based Drugs according to Their Mechanisms of Action. *Chem* 6, 41–60. doi: 10.1016/j.chempr.2019.10.013.

Borovinskaya, M. A., Pai, R. D., Zhang, W., Schuwirth, B. S., Holton, J. M., Hirokawa, G., *et al*. (2007). Structural basis for aminoglycoside inhibition of bacterial ribosome recycling. *Nat. Struct. Mol. Biol.* 14, 727–732. doi: 10.1038/nsmb1271.

Borowiak, M., Fischer, J., Hammerl, J. A., Hendriksen, R. S., Szabo, I., and Malorny, B. (2017). Identification of a novel transposon-associated phosphoethanolamine transferase gene, mcr-5, conferring colistin resistance in d-tartrate fermenting *Salmonella enterica subsp. enterica* serovar Paratyphi B. *J. Antimicrob. Chemother.* 72, 3317–3324. doi: 10.1093/jac/dkx327.

Boucher, H. W., Talbot, G. H., Bradley, J. S., Edwards, J. E., Gilbert, D., Rice, L. B., *et al*. (2009). Bad Bugs, No Drugs: No ESKAPE! An Update from the Infectious Diseases Society of America. *Clin. Infect. Dis.* 48, 1–12. doi: 10.1086/595011.

Brandenburg, K. S., Weaver, A. J., Karna, S. L. R., You, T., Chen, P., Stryk, S. Van, *et al*. (2019). Formation of *Pseudomonas aeruginosa* Biofilms in Full-thickness Scald Burn Wounds in Rats. *Sci. Rep.* 9, 1–12. doi: 10.1038/s41598-019-50003-8.

Braz, V. S., Furlan, J. P. R., Fernandes, A. F. T., and Stehling, E. G. (2016). Mutations in NalC induce MexAB-OprM overexpression resulting in high level of aztreonam resistance in environmental isolates of *Pseudomonas aeruginosa*. *FEMS Microbiol. Lett.* 363, 166. doi: 10.1093/FEMSLE/FNW166.

Brennan, M., Thomas, D. Y., Whiteway, M., and Kavanagh, K. (2002). Correlation between virulence of Candida albicans mutants in mice and *Galleria mellonella* larvae . *FEMS Immunol. Med. Microbiol.* 34, 153–157. doi: 10.1111/j.1574-695x.2002.tb00617.x.

Brown, S., Santa Maria, J. P., and Walker, S. (2013). Wall Teichoic Acids of Gram-Positive Bacteria. *Annu. Rev. Microbiol.* 67, 313–336. doi: 10.1146/annurev-micro-092412-155620.

Browne, N. (2014). An analysis of the cellular and humoral immune responses of *Galleria mellonella* larvae. 1–275. Available at: http://eprints.maynoothuniversity.ie/6186/1/Nialls Thesis Final 2 - Post Viva.pdf [Accessed June 27, 2018].

Browne, N., Heelan, M., and Kavanagh, K. (2013). An analysis of the structural and functional similarities of insect hemocytes and mammalian phagocytes. *Virulence* 4, 597–603. doi: 10.4161/viru.25906.

Browne, N., Surlis, C., and Kavanagh, K. (2014). Thermal and physical stresses induce a short-term immune priming effect in *Galleria mellonella* larvae. *J. Insect Physiol.* 63, 21–26. doi: 10.1016/j.jinsphys.2014.02.006.

Bush, K., Jacoby, G. A., and Medeiros, A. A. (1995). A functional classification scheme for β-lactamases and its correlation with molecular structure. *Antimicrob. Agents Chemother.* 39, 1211–1233. doi: 10.1128/AAC.39.6.1211.

Butler, H. M., Hurse, A., Thursky, E., and Shulman, A. (1969). Bactericidal action of selected phenanthroline chelates and related compounds. *Aust. J. Exp. Biol. Med. Sci.* 47, 541–552. doi: 10.1038/icb.1969.148.

Butler, M. S., Gigante, V., Sati, H., Paulin, S., Al-Sulaiman, L., Rex, J. H., *et al*. (2022). Analysis of the Clinical Pipeline of Treatments for Drug-Resistant Bacterial Infections: Despite Progress, More Action Is Needed. *Antimicrob. Agents Chemother.* 66, 1–39. doi: 10.1128/aac.01991-21.

C Reygaert, W. (2018). An overview of the antimicrobial resistance mechanisms of bacteria. *AIMS Microbiol.* 4, 482–501. doi: 10.3934/microbiol.2018.3.482.

Cabiscol, E., Tamarit, J., and Ros, J. (2000). Oxidative stress in bacteria and protein damage by reactive oxygen species. *Int. Microbiol.* 3, 3–8. doi: 10.2436/im.v3i1.9235.

Cai, Y. ming, and Webb, J. S. (2020). Optimization of nitric oxide donors for investigating biofilm

dispersal response in *Pseudomonas aeruginosa* clinical isolates. *Appl. Microbiol. Biotechnol.* 104, 8859–8869. doi: 10.1007/s00253-020-10859-7.

Cao, Y., Naseri, M., He, Y., Xu, C., Walsh, L. J., and Ziora, Z. M. (2020). Non-antibiotic antimicrobial agents to combat biofilm-forming bacteria. *J. Glob. Antimicrob. Resist.* 21, 445–451. doi: 10.1016/j.jgar.2019.11.012.

Carattoli, A., Villa, L., Feudi, C., Curcio, L., Orsini, S., Luppi, A., *et al*. (2017). Novel plasmid-mediated colistin resistance mcr-4 gene in *Salmonella* and *Escherichia coli*, Italy 2013, Spain and Belgium, 2015 to 2016. *Eurosurveillance* 22. doi: 10.2807/1560-7917.ES.2017.22.31.30589.

Carroll, L. M., Gaballa, A., Guldimann, C., Sullivan, G., Henderson, L. O., and Wiedmann, M. (2019). Identification of novel mobilized colistin resistance gene mcr-9 in a multidrug-resistant, colistin-susceptible *Salmonella enterica serotype typhimurium* isolate. *MBio* 10. doi: 10.1128/mBio.00853-19.

Cassini, A., Högberg, L. D., Plachouras, D., Quattrocchi, A., Hoxha, A., Simonsen, G. S., *et al*. (2019). Attributable deaths and disability-adjusted life-years caused by infections with antibiotic-resistant bacteria in the EU and the European Economic Area in 2015: a population-level modelling analysis. *Lancet Infect. Dis.* 19, 56–66. doi: 10.1016/S1473-3099(18)30605-4.

Cebrián, J., Martínez, V., Hernández, P., Krimer, D. B., Fernández-Nestosa, M. J., and Schvartzman, J. B. (2021). Two-dimensional gel electrophoresis to study the activity of type iia topoisomerases on plasmid replication intermediates. *Biology (Basel).* 10, 1–17. doi: 10.3390/biology10111195.

Centers for Disease Control and Prevention (2019). Antibiotic resistance threats in the United States. *Centers Dis. Control Prev.*, 1–148. doi: CS239559-B.

CF Registry of Ireland (2019). CF Registry of Ireland 2019 Annual Report. 47. Available at:

https://www.cfri.ie/%0Ahttps://www.cfri.ie/docs/annual_reports/CFRI2017.pdf. [Accessed April 25, 2019].

CF Registry of Ireland (2017). CF Registry of Ireland 2017 Annual Report. Available at: https://www.cfri.ie/%0Ahttps://www.cfri.ie/docs/annual_reports/CFRI2017.pdf [Accessed April 25, 2019].

Chadwick, J. S. (1967). Some aspects of immune responses in insects. *In Vitro* 3, 120–128. doi: 10.1007/BF02615927.

Chain, E., Florey, H. W., Adelaide, M. B., Gardner, A. D., Oxfd, D. M., Heatley, N. G., *et al*. (1940). Penicillin As a Chemotherapeutic Agent. *Lancet* 236, 226–228. doi: 10.1016/S0140-6736(01)08728-1.

Chang, E. L., Simmers, C., and Knight, D. A. (2010). Cobalt complexes as antiviral and antibacterial agents. *Pharmaceuticals* 3, 1711–1728. doi: 10.3390/ph3061711.

Chen, F., Moat, J., McFeely, D., Clarkson, G., Hands-Portman, I. J., Furner-Pardoe, J. P., *et al*. (2018). Biguanide Iridium(III) Complexes with Potent Antimicrobial Activity. *J. Med. Chem.* 61, 7330–7344. doi: 10.1021/acs.jmedchem.8b00906.

Chen, H., Du, Y., Xia, Q., Li, Y., Song, S., and Huang, X. (2020). Role of linezolid combination therapy for serious infections: review of the current evidence. *Eur. J. Clin. Microbiol. Infect. Dis.* 39, 1043–1052. doi: 10.1007/s10096-019-03801-x.

Chetana, P. R., Srinatha, B. S., Somashekar, M. N., and Policegoudra, R. S. (2016). Synthesis, spectroscopic characterisation, thermal analysis, DNA interaction and antibacterial activity of copper(I) complexes with N, N′- disubstituted thiourea. *J. Mol. Struct.* 1106, 352–365. doi: 10.1016/j.molstruc.2015.10.010.

Chetri, S., Bhowmik, D., Paul, D., Pandey, P., Chanda, D. D., Chakravarty, A., *et al*. (2019). AcrAB-TolC efflux pump system plays a role in carbapenem non-susceptibility in

Escherichia coli. *BMC Microbiol.* 19, 210. doi: 10.1186/s12866-019-1589-1.

Chiang, W. C., Nilsson, M., Jensen, P. Ø., Høiby, N., Nielsen, T. E., Givskov, M., *et al*. (2013). Extracellular DNA shields against aminoglycosides in *Pseudomonas aeruginosa* biofilms. *Antimicrob. Agents Chemother.* 57, 2352–2361. doi: 10.1128/AAC.00001-13.

Choi, U., and Lee, C. R. (2019). Distinct Roles of Outer Membrane Porins in Antibiotic Resistance and Membrane Integrity in *Escherichia coli*. *Front. Microbiol.* 10, 1–9. doi: 10.3389/fmicb.2019.00953.

Chokshi, A., Sifri, Z., Cennimo, D., and Horng, H. (2019). Global contributors to antibiotic resistance. *J. Glob. Infect. Dis.* 11, 36–42. doi: 10.4103/jgid.jgid_110_18.

Chopra, I., Hesse, L., and O'Neill, A. J. (2002). Exploiting current understanding of antibiotic action for discovery of new drugs. *J. Appl. Microbiol.* 92, 4S-15S. doi: 10.1046/j.1365-2672.92.5s1.13.x.

Christophersen, L., Schwartz, F. A., Lerche, C. J., Svanekjær, T., Kragh, K. N., Laulund, A. S., *et al*. (2020). In vivo demonstration of *Pseudomonas aeruginosa* biofilms as independent pharmacological microcompartments. *J. Cyst. Fibros.* 1, 1–8. doi: 10.1016/j.jcf.2020.01.009.

Chukwudi, C. U. (2016). rRNA Binding Sites and the Molecular Mechanism of Action of the Tetracyclines. *Antimicrob. Agents Chemother*. 60, 4433–4441. doi: 10.1128/AAC.00594-16.Address.

Ciofu, O., and Tolker-Nielsen, T. (2019). Tolerance and resistance of *Pseudomonas aeruginosa* biofilms to antimicrobial agents- How *P. aeruginosa* Can escape antibiotics. *Front. Microbiol.* 10. doi: 10.3389/fmicb.2019.00913.

Ciofu, O., Tolker-Nielsen, T., Jensen, P. Ø., Wang, H., and Høiby, N. (2015). Antimicrobial resistance, respiratory tract infections and role of biofilms in lung infections in cystic fibrosis

patients. *Adv. Drug Deliv. Rev.* 85, 7–23. doi: 10.1016/j.addr.2014.11.017.

Claudel, M., Schwarte, J. V., and Fromm, K. M. (2020). New Antimicrobial Strategies Based on Metal Complexes. *Chemistry (Easton).* 2, 849–899. doi: 10.3390/chemistry2040056.

Coates, A. R. M., Hu, Y., Holt, J., and Yeh, P. (2020). Antibiotic combination therapy against resistant bacterial infections: synergy, rejuvenation and resistance reduction. *Expert Rev. Anti. Infect. Ther.* 18, 5–15. doi: 10.1080/14787210.2020.1705155.

Cocetta, V., Ragazzi, E., and Montopoli, M. (2019). Mitochondrial involvement in cisplatin resistance. *Int. J. Mol. Sci.* 20, 1–17. doi: 10.3390/ijms20143384.

Colclough, A. L., Alav, I., Whittle, E. E., Pugh, H. L., Darby, E. M., Legood, S. W., *et al*. (2020). RND efflux pumps in Gram-negative bacteria; Regulation, structure and role in antibiotic resistance. *Future Microbiol.* 15, 143–157. doi: 10.2217/fmb-2019-0235.

Colvin, K. M., Gordon, V. D., Murakami, K., Borlee, B. R., Wozniak, D. J., Wong, G. C. L., *et al*. (2011). The pel polysaccharide can serve a structural and protective role in the biofilm matrix of *Pseudomonas aeruginosa*. *PLoS Pathog.* 7, e1001264. doi: 10.1371/journal.ppat.1001264.

Correia, S., Poeta, P., Hébraud, M., Capelo, J. L., and Igrejas, G. (2017). Mechanisms of quinolone action and resistance: where do we stand? *J. Med. Microbiol.* 66, 551–559. doi: 10.1099/jmm.0.000475.

Cox, G., and Wright, G. D. (2013). Intrinsic antibiotic resistance: Mechanisms, origins, challenges and solutions. *Int. J. Med. Microbiol.* 303, 287–292. doi: 10.1016/j.ijmm.2013.02.009.

Cutuli, M. A., Petronio Petronio, G., Vergalito, F., Magnifico, I., Pietrangelo, L., Venditti, N., *et al*. (2019). *Galleria mellonella* as a consolidated in vivo model hosts: New developments in antibacterial strategies and novel drug testing. *Virulence* 10, 527–541. doi:

10.1080/21505594.2019.1621649.

Cystic Fibrosis Foundation (2021). Cystic Fibrosis Foundation 2020 Annual Data Report. Available at: https://www.cfireland.ie.

Cystic Fibrosis Ireland (2018). Cystic Fibrosis Ireland Annual Report For 2017. Available at: https://www.cfireland.ie.

D'Atanasio, N., de Joannon, A. C., Sante, L. Di, Mangano, G., Ombrato, R., Vitiello, M., *et al*. (2020). Antibacterial activity of novel dual bacterial DNA type II topoisomerase inhibitors. *PLoS One* 15, 1–21. doi: 10.1371/journal.pone.0228509.

D, A. S. W., Bardin, E., Cameron, L., Edmondson, C. L., Farrant, K. V, Martin, I., *et al*. (2017). Current and future therapies for *Pseudomonas aeruginosa* infection in patients with cystic fibrosis What is CF and why is the CF lung predisposed to *P* . *aeruginosa* infection ? *FEMS Microbiol. Lett.* 364, 121–129.

Dakal, T. C., Kumar, A., Majumdar, R. S., and Yadav, V. (2016). Mechanistic basis of antimicrobial actions of silver nanoparticles. *Front. Microbiol.* 7, 1–17. doi: 10.3389/fmicb.2016.01831.

Dangelo, R. G., Johnson, J. K., Bork, J. T., and Heil, E. L. (2016). Treatment options for extended-spectrum beta-lactamase (ESBL) and AmpC-producing bacteria. *Expert Opin. Pharmacother.* 17, 953–967. doi: 10.1517/14656566.2016.1154538.

Das, T., Sehar, S., Koop, L., Wong, Y. K., Ahmed, S., Siddiqui, K. S., *et al*. (2014). Influence of calcium in extracellular DNA mediated bacterial aggregation and biofilm formation. *PLoS One* 9. doi: 10.1371/journal.pone.0091935.

Dasari, S., Njiki, S., Mbemi, A., Yedjou, C. G., and Tchounwou, P. B. (2022). Pharmacological Effects of Cisplatin Combination with Natural Products in Cancer Chemotherapy. *Int. J. Mol. Sci.* 23, 1–25. doi: 10.3390/ijms23031532.

Dasari, S., and Tchounwou, P. B. (2014). Cisplatin in cancer therapy: Molecular mechanisms of action. *Eur. J. Pharmacol.* 740, 364–378. doi: 10.1016/j.ejphar.2014.07.025.

De la Fuente-Núñez, C., Reffuveille, F., Fernández, L., and Hancock, R. E. W. (2013). Bacterial biofilm development as a multicellular adaptation: Antibiotic resistance and new therapeutic strategies. *Curr. Opin. Microbiol.* 16, 580–589. doi: 10.1016/j.mib.2013.06.013.

De Oliveira, D. M. P., Forde, B. M., Kidd, T. J., Harris, P. N. A., Schembri, M. A., Beatson, S. A., *et al*. (2020). Antimicrobial resistance in ESKAPE pathogens. *Clin. Microbiol. Rev.* 33, 1–49. doi: 10.1128/CMR.00181-19.

DeJarnette, C., Luna-Tapia, A., Estredge, L. R., and Palmer, G. E. (2020). Dihydrofolate Reductase Is a Valid Target for Antifungal Development in the Human Pathogen *Candida albicans* . *mSphere* 5, 1–15. doi: 10.1128/msphere.00374-20.

DeLeon, K., Balldin, F., Watters, C., Hamood, A., Griswold, J., Sreedharan, S., *et al*. (2009). Gallium maltolate treatment eradicates *Pseudomonas aeruginosa* infection in thermally injured mice. *Antimicrob. Agents Chemother.* 53, 1331–1337. doi: 10.1128/AAC.01330-08.

Desbois, A. P., and Coote, P. J. (2012). Utility of greater wax moth larva (*Galleria mellonella*) for evaluating the toxicity and efficacy of new antimicrobial agents. *Advances in Applied Microbiology*, 1st ed. Elsevier Inc. doi: 10.1016/B978-0-12-394805-2.00002-6.

Destoumieux-Garzón, D., Mavingui, P., Boetsch, G., Boissier, J., Darriet, F., Duboz, P., *et al*. (2018). The one health concept: 10 years old and a long road ahead. *Front. Vet. Sci.* 5, 1–13. doi: 10.3389/fvets.2018.00014.

Devereux, M., McCann, M., Cronin, J. F., Ferguson, G., and McKee, V. (1999). Binuclear and polymeric copper(II) dicarboxylate complexes: Syntheses and crystal structures of [Cu2(pda)(Phen)4](ClO4)2.5H 2O.C2H5OH, [Cu2(oda)(Phen)4](ClO4)2.2.67H 2O.C2H5OH. *Polyhedron* 18, 2141–2148. doi: 10.1016/S0277-5387(99)00100-X.

Devereux, M., Mccann, M., Leon, V., Geraghty, M., Mckee, V., and Wikaira, J. (2000). Synthesis and biogical activity of manganese (II) complexes of phtalic and isophtalic acid: X-ray crystal structures of [Mn(ph)(phen)2(H2O)].4H2O, [Mn(phen)2(H2O)2]2(Isoph)2(phen).12H2O and [Mn(isoph)(bipy)]4.2.75bipy. *Met. Based Drugs* 7, 275–288.

Dewachter, L., Fauvart, M., and Michiels, J. (2019). Bacterial Heterogeneity and Antibiotic Survival: Understanding and Combatting Persistence and Heteroresistance. *Mol. Cell* 76, 255–267. doi: 10.1016/j.molcel.2019.09.028.

Di Lorenzo, F., Silipo, A., Bianconi, I., Lore', N. I., Scamporrino, A., Sturiale, L., *et al*. (2015). Persistent cystic fibrosis isolate *Pseudomonas aeruginosa* strain RP73 exhibits an under-acylated LPS structure responsible of its low inflammatory activity. *Mol. Immunol.* 63, 166–175. doi: 10.1016/j.molimm.2014.04.004.

Dik, D. A., Fisher, J. F., and Mobashery, S. (2018). Cell-Wall Recycling of the Gram-Negative Bacteria and the Nexus to Antibiotic Resistance. *Chem. Rev.* 118, 5952–5984. doi: 10.1021/acs.chemrev.8b00277.

Dilda, P. J., and Hogg, P. J. (2007). Arsenical-based cancer drugs. *Cancer Treat. Rev.* 33, 542–564. doi: 10.1016/j.ctrv.2007.05.001.

Dimitrakopoulou, A., Dendrinou-samara, C., Pantazaki, A. A., Raptopoulou, C., Terzis, A., Samaras, E., *et al*. (2007). Interaction of Fe (III) with herbicide-carboxylato ligands . Di- , tri- and tetra-nuclear compounds : Structure , antimicrobial study and DNA interaction. *Inorganica Chim. Acta* 360, 546–556. doi: 10.1016/j.ica.2006.07.102.

Dinos, G. P., Athanassopoulos, C. M., Missiri, D. A., Giannopoulou, P. C., Vlachogiannis, I. A., Papadopoulos, G. E., *et al*. (2016). Chloramphenicol derivatives as antibacterial and anticancer agents: Historic problems and current solutions. *Antibiotics* 5. doi: 10.3390/antibiotics5020020.

Domagk, G. (1935). Ein Beitrag zur Chemotherapie der bakteriellen Infektionen. *Dtsch. Medizinische Wochenschrift* 61, 250–253. doi: 10.1055/s-0028-1129486.

Domínguez, A. V., Algaba, R. A., Canturri, A. M., Villodres, Á. R., and Smani, Y. (2020). Antibacterial activity of colloidal silver against gram-negative and gram-positive bacteria. *Antibiotics* 9, 1–10. doi: 10.3390/antibiotics9010036.

Dos Santos, M. H. B., Da Costa, A. F. E., Santos, G. D. S., Dos Santos, A. L. S., and Nagao, P. E. (2009). Effect of chelating agents on the growth, surface polypeptide synthesis and interaction of *Streptococcus agalactiae* with human epithelial cells. *Mol. Med. Rep.* 2, 81–84. doi: 10.3892/mmr-00000065.

Dubois, M., Gilles, K., Hamilton, J. K., Rebers, P. A., and Smith, F. (1951). A colorimetric method for the determination of sugars. *Nature* 168, 167. doi: 10.1038/168167a0.

Dwyer, D. J., Kohanski, M. A., Hayete, B., and Collins, J. J. (2007). Gyrase inhibitors induce an oxidative damage cellular death pathway in *Escherichia coli*. *Mol. Syst. Biol.* 3, 91. doi: 10.1038/msb4100135.

Dwyer, F. P., Gyarfas, E. C., Rogers, W. P., and Koch, J. H. (1952). Biological activity of complex ions. *Nature* 170, 190–191. doi: 10.1038/170190a0.

Dwyer, F. P., Reid, I. K., Shulman, A., Laycock, G. M., and Dixson, S. (1969). The biological actions of 1,10-phenanthroline and 2,2'-bipyridine hydrochlorides, quaternary salts and metal chelates and related compounds. *Aust J Exp Biol Med* 47, 203–218. doi: 10.1038/icb.1969.21.

ECDC (2022). Antimicrobial resistance surveillance in Europe - *ECDC for WHO*. Available at: https://www.ecdc.europa.eu/sites/default/files/documents/ECDC-WHO-AMR-report.pdf.

Ehrlich, P. (1912). About Salvarsan. *Abhandlungen über Salvarsan* 2, 547–563. Available at: https://www.pei.de/SharedDocs/Downloads/institut/veroeffentlichungen-von-paul-

ehrlich/1906-1914/1912-salvarsan.pdf;jsessionid=B847DD8A600A1F651D79FFF695A6BBE2.1_cid354?__blob=publicationFile&v=1 [Accessed March 8, 2018].

Ehrlich, P., and Bertheim, A. (1912). On the hydrochloric acid 3,3'-diamino-4,4'-dioxyarsenobenzene and its closest relatives. *Rep Ger. Chem Soc* 45, 756–766. Available at: https://www.pei.de/SharedDocs/Downloads/institut/veroeffentlichungen-von-paul-ehrlich/1906-1914/1912-salzsaure-diaminodioxyarsenobenzol-verwandte.pdf;jsessionid=B847DD8A600A1F651D79FFF695A6BBE2.1_cid354?__blob=publicationFile&v=1 [Accessed March 8, 2018].

Elborn, J. S. (2016). Cystic fibrosis. *Lancet* 388, 2519–2531. doi: 10.1016/S0140-6736(16)00576-6.

Elborn, J. S., Bell, S. C., Madge, S. L., Burgel, P. R., Castellani, C., Conway, S., *et al*. (2016). Report of the European respiratory society/European cystic fibrosis society task force on the care of adults with cystic fibrosis. *Eur. Respir. J.* 47, 420–428. doi: 10.1183/13993003.00592-2015.

Epand, R. M., Walker, C., Epand, R. F., and Magarvey, N. A. (2016). Molecular mechanisms of membrane targeting antibiotics. *Biochim. Biophys. Acta - Biomembr.* 1858, 980–987. doi: 10.1016/j.bbamem.2015.10.018.

Essar, D. W., Eberly, L., Hadero, A., and Crawford, I. P. (1990). Identification and characterization of genes for a second anthranilate synthase in *Pseudomonas aeruginosa*: Interchangeability of the two anthranilate synthase and evolutionary implications. *J. Bacteriol.* 172, 884–900. doi: 10.1128/jb.172.2.884-900.1990.

Etebu, E., and Arikekpar, I. (2016). Antibiotics: Classification and mechanisms of action with emphasis on molecular perspectives. *Ijambr* 4, 90–101. Available at: https://pdfs.semanticscholar.org/aebc/840138529c147e54552205bf26ec8aa3ca2e.pdf

[Accessed March 20, 2018].

EUCAST (2000). Terminology relating to methods for the determination of susceptibility of bacteria to antimicrobial agents. *Clin. Microbiol. Infect.* 6, 503–508. doi: 10.1046/J.1469-0691.2000.00149.X.

EUCAST (2017a). Antimicrobial susceptibility testing EUCAST disk diffusion method. *Eucast* 0, 1–22. Available at: www.eucast.org [Accessed June 16, 2017].

EUCAST (2017b). European Committee on Antimicrobial Susceptibility Testing Routine and extended internal quality control as recommended by EUCAST. *Version 7.0*, 0–14. Available at: http://www.eucast.org [Accessed June 20, 2017].

EUCAST (2017c). The European Committee on Antimicrobial Susceptibility Testing. Breakpoint tables for interpretation of MICs and zone diameters. Version 7.1, 2017. http://www.eucast.org. *Break. tables Interpret. MICs Zo. diameters. Version 7.1* 7.1, 0–77. Available at: http://www.eucast.org [Accessed June 20, 2017].

European (2009). Health and Food Safety. *Child. Serv. Parliam. Monit.* 2014, 670. Available at: http://search.ebscohost.com/login.aspx?direct=true&AuthType=ip,url,cookie,uid&db=ehh&AN=44811543&site=ehost-live&scope=site [Accessed April 18, 2018].

Evans, A., and Kavanagh, K. A. (2021). Evaluation of metal-based antimicrobial compounds for the treatment of bacterial pathogens. *J. Med. Microbiol.* 70, 1363. doi: 10.1099/JMM.0.001363.

Fair, R. J., and Tor, Y. (2014). Antibiotics and bacterial resistance in the 21st century. *Perspect. Medicin. Chem.* 6, 25–64. doi: 10.4137/PMC.S14459.

Falkievich, D. B., Martínez Medina, J. J., Alegre, W. S., López Tévez, L. L., Franca, C. A., Ferrer, E. G., *et al*. (2022). Computational studies, antimicrobial activity, inhibition of biofilm production and safety profile of the cadmium complex of 1,10-phenanthroline and

cyanoguanidine. *Appl. Organomet. Chem.*, 1–14. doi: 10.1002/aoc.6695.

Farrell, P. M. (2008). The prevalence of cystic fibrosis in the European Union. *J. Cyst. Fibros.* 7, 450–453. doi: 10.1016/j.jcf.2008.03.007.

Fenker, D. E., Mcdaniel, C. T., Panmanee, W., Panos, R. J., Sorscher, E. J., Sabusap, C., *et al.* (2018). A Comparison between Two Pathophysiologically Different yet Microbiologically Similar Lung Diseases: Cystic Fibrosis and Chronic Obstructive Pulmonary Disease HHS Public Access. *Int J Respir Pulm Med* 5. doi: 10.23937/2378-3516/1410098.

Fernandes, P., Sousa, I., Cunha-Silva, L., Ferreira, M., De Castro, B., Pereira, E. F., *et al*. (2014). Synthesis, characterization and antibacterial studies of a copper(II) lomefloxacin ternary complex. *J. Inorg. Biochem.* 131, 21–29. doi: 10.1016/j.jinorgbio.2013.10.013.

Fernandes, S., Gomes, I. B., Sousa, S. F., and Simões, M. (2022). Antimicrobial Susceptibility of Persister Biofilm Cells of Bacillus cereus and Pseudomonas fluorescens. *Microorganisms* 10, 1–12. doi: 10.3390/microorganisms10010160.

Fernández-Villa, D., Aguilar, M. R., and Rojo, L. (2019). Folic acid antagonists: Antimicrobial and immunomodulating mechanisms and applications. *Int. J. Mol. Sci.* 20, 1–30. doi: 10.3390/ijms20204996.

Fleming, A. (1929). On the antibacterial action of cultures of a penicillium, with special reference to their use in the isolation of B.influenzae. *Br. J. Exp. Pathol.* 10, 226–236. doi: 10.1038/146837a0.

Fleming, A. (1945). AL E X A N D E R F L E M I N G Penicillin. 83–93. Available at: https://www.nobelprize.org/uploads/2018/06/fleming-lecture.pdf [Accessed March 11, 2022].

Fleming, D., Chahin, L., and Rumbaugh, K. (2017). Glycoside hydrolases degrade polymicrobial bacterial biofilms in wounds. *Antimicrob. Agents Chemother.* 61, 1–9. doi:

10.1128/AAC.01998-16.

Flemming, H. C., and Wingender, J. (2010). The biofilm matrix. *Nat. Rev. Microbiol.* 8, 623–633. doi: 10.1038/nrmicro2415.

Flemming, H. C., Wingender, J., Szewzyk, U., Steinberg, P., Rice, S. A., and Kjelleberg, S. (2016). Biofilms: An emergent form of bacterial life. *Nat. Rev. Microbiol.* 14, 563–575. doi: 10.1038/nrmicro.2016.94.

Fonseca, C., Bicker, J., Alves, G., Falcão, A., and Fortuna, A. (2020). Cystic fibrosis: Physiopathology and the latest pharmacological treatments. *Pharmacol. Res.* 162. doi: 10.1016/j.phrs.2020.105267.

Forterre, P., Gribaldo, S., Gadelle, D., and Serre, M. C. (2007). Origin and evolution of DNA topoisomerases. *Biochimie* 89, 427–446. doi: 10.1016/j.biochi.2006.12.009.

Fournier, C., Poirel, L., Despont, S., Kessler, J., and Nordmann, P. (2022). Increasing Trends of Association of 16S rRNA Methylases and Carbapenemases in Enterobacterales Clinical Isolates from Switzerland, 2017–2020. *Microorganisms* 10, 2017–2020. doi: 10.3390/microorganisms10030615.

Frei, A. (2020). Metal complexes, an untapped source of antibiotic potential? *Antibiotics* 9, 90. doi: 10.3390/antibiotics9020090.

Frei, A., Zuegg, J., Elliott, A. G., Baker, M., Braese, S., Brown, C., *et al*. (2020). Metal complexes as a promising source for new antibiotics. *Chem. Sci.* 11, 2627–2639. doi: 10.1039/c9sc06460e.

Friederich, M. W., Timal, S., Powell, C. A., Dallabona, C., Kurolap, A., Palacios-Zambrano, S., *et al*. (2018). Pathogenic variants in glutamyl-tRNAGln amidotransferase subunits cause a lethal mitochondrial cardiomyopathy disorder. *Nat. Commun.* 9, 1–14. doi: 10.1038/s41467-018-06250-w.

Furtado, F. A. C., Asad, N. R., and Leitão, A. C. (1997). Effects of 1,10-phenanthroline and hydrogen peroxide in *Escherichia coli*: Lethal interaction. *Mutat. Res. - DNA Repair* 385, 251–258. doi: 10.1016/S0921-8777(97)00055-4.

Galdino, A. C. M., Branquinha, M. H., Santos, A. L. S., and Viganor, L. (2017). *Pseudomonas aeruginosa* and Its Arsenal of Proteases: Weapons to Battle the Host. doi: 10.1007/978-981-10-6141-7.

Galdino, A. C. M., Viganor, L., De Castro, A. A., Da Cunha, E. F. F., Mello, T. P., Mattos, L. M., *et al*. (2019). Disarming *Pseudomonas aeruginosa* virulence by the inhibitory action of 1,10-phenanthroline-5,6-dione-based compounds: Elastase B (lasB) as a chemotherapeutic target. *Front. Microbiol.* 10. doi: 10.3389/fmicb.2019.01701.

Galdino, A. C. M., Viganor, L., Pereira, M. M., Devereux, M., McCann, M., Branquinha, M. H., *et al*. (2022). Copper(II) and silver(I)-1,10-phenanthroline-5,6-dione complexes interact with double-stranded DNA: further evidence of their apparent multi-modal activity towards *Pseudomonas aeruginosa*. *J. Biol. Inorg. Chem.* 27, 201–213. doi: 10.1007/s00775-021-01922-3.

Gameiro, P., Rodrigues, C., Baptista, T., Sousa, I., and de Castro, B. (2007). Solution studies on binary and ternary complexes of copper(II) with some fluoroquinolones and 1,10-phenanthroline: Antimicrobial activity of ternary metalloantibiotics. *Int. J. Pharm.* 334, 129–136. doi: 10.1016/j.ijpharm.2006.10.035.

Gandra, R. M., Carron, P. M., Fernandes, M. F., Ramos, L. S., Mello, T. P., Aor, A. C., *et al*. (2017). Antifungal potential of copper(II), Manganese(II) and silver(I) 1,10-phenanthroline chelates against multidrug-resistant fungal species forming the *Candida haemulonii* Complex: Impact on the planktonic and biofilm lifestyles. *Front. Microbiol.* 8, 1257. doi: 10.3389/fmicb.2017.01257.

Gandra, R. M., McCarron, P., Viganor, L., Fernandes, M. F., Kavanagh, K., McCann, M., *et al*.

(2020). In vivo Activity of Copper(II), Manganese(II), and Silver(I) 1,10-Phenanthroline Chelates Against *Candida haemulonii* Using the *Galleria mellonella* Model. *Front. Microbiol.* 11, 470. doi: 10.3389/fmicb.2020.00470.

Garcia-Nuñez, M., Marti, S., Puig, C., Perez-Brocal, V., Millares, L., Santos, S., *et al*. (2017). Bronchial microbiome, PA biofilm-forming capacity and exacerbation in severe COPD patients colonized by *P. aeruginosa. Future Microbiol.* 12, 379–392. doi: 10.2217/fmb-2016-0127.

Garcia, B. A., McDaniel, M. S., Loughran, A. J., Johns, J. D., Narayanaswamy, V., Petty, C. F., *et al*. (2022). Poly (acetyl, arginyl) glucosamine disrupts *Pseudomonas aeruginosa* biofilms and enhances bacterial clearance in a rat lung infection model. *Microbiol. (United Kingdom)* 168, 1–12. doi: 10.1099/mic.0.001121.

Garza-Cervantes, J. A., Chávez-Reyes, A., Castillo, E. C., García-Rivas, G., Ortega-Rivera, O. A., Salinas, E., *et al*. (2017). Synergistic antimicrobial effects of silver/transition-metal combinatorial treatments. *Sci. Rep.* 7. doi: 10.1038/s41598-017-01017-7.

Gautam, S. S., KC, R., Leong, K. W., Mac Aogáin, M., and O'Toole, R. F. (2019). A step-by-step beginner. *J. Biol. Methods* 6, e110. doi: 10.14440/jbm.2019.276.

Gebreyohannes, G., Nyerere, A., Bii, C., and Sbhatu, D. B. (2019). Challenges of intervention, treatment, and antibiotic resistance of biofilm-forming microorganisms. *Heliyon* 5, e02192. doi: 10.1016/j.heliyon.2019.e02192.

Gellatly, S. L., and Hancock, R. E. W. (2013). *Pseudomonas aeruginosa*: New insights into pathogenesis and host defenses. *Pathog. Dis.* 67, 159–173. doi: 10.1111/2049-632X.12033.

Geraghty, M., McCann, M., Casey, M. T., Curran, M., Devereux, M., McKee, V., *et al*. (1998). Synthesis and catalytic activity of manganese (II) complexes of pentanedioic acid; X-ray crystal structure of [Mn(phen)2(H20)2][Mn(O2C(CH 2)3CO2)(phen)2H2O] (O2C(CH2)3CO2)·12H 2O(phen=1,10-phenanthroline). *Inorganica Chim. Acta* 277, 257–

262. doi: 10.1016/s0020-1693(97)06160-4.

Gitlin, M. (2016). Lithium side effects and toxicity: prevalence and management strategies. *Int. J. Bipolar Disord.* 4, 27. doi: 10.1186/s40345-016-0068-y.

Gogry, F. A., Siddiqui, M. T., Sultan, I., and Haq, Q. M. R. (2021). Current Update on Intrinsic and Acquired Colistin Resistance Mechanisms in Bacteria. *Front. Med.* 8, 1–19. doi: 10.3389/fmed.2021.677720.

Gordon, O., Slenters, T. V., Brunetto, P. S., Villaruz, A. E., Sturdevant, D. E., Otto, M., *et al*. (2010). Silver coordination polymers for prevention of implant infection: Thiol interaction, impact on respiratory chain enzymes, and hydroxyl radical induction. *Antimicrob. Agents Chemother*. 54, 4208–4218. doi: 10.1128/AAC.01830-09.

Gorle, A. K., Feterl, M., Warner, J. M., Wallace, L., Keene, F. R., and Collins, J. G. (2014). Tri- and tetra-nuclear polypyridyl ruthenium(ii) complexes as antimicrobial agents. *Dalt. Trans.* 43, 16713–16725. doi: 10.1039/c4dt02139h.

Gorle, A. K., Li, X., Primrose, S., Li, F., Feterl, M., Kinobe, R. T., *et al*. (2016). Oligonuclear polypyridylruthenium(II) complexes: Selectivity between bacteria and eukaryotic cells. *J. Antimicrob. Chemother*. 71, 1547–1555. doi: 10.1093/jac/dkw026.

Goss, C. H., Kaneko, Y., Khuu, L., Anderson, G. D., Ravishankar, S., Aitken, M. L., *et al*. (2018). Gallium disrupts bacterial iron metabolism and has therapeutic effects in mice and humans with lung infections. *Sci. Transl. Med.* 10, 1–12. doi: 10.1126/scitranslmed.aat7520.

Gould, K. (2016). Antibiotics: From prehistory to the present day. *J. Antimicrob. Chemother*. 71, 572–575. doi: 10.1093/jac/dkv484.

Granato, M. Q., Gonçalves, D. de S., Seabra, S. H., McCann, M., Devereux, M., dos Santos, A. L. S., *et al*. (2017). 1,10-phenanthroline-5,6-dione-based compounds are effective in disturbing crucial physiological events of Phialophora verrucosa. *Front. Microbiol.* 8, 76.

doi: 10.3389/fmicb.2017.00076.

Granato, M. Q., Mello, T. P., Nascimento, R. S., Pereira, M. D., Rosa, T. L. S. A., Pessolani, M. C. V., *et al*. (2021). Silver(I) and Copper(II) Complexes of 1,10-Phenanthroline-5,6-Dione Against Phialophora verrucosa: A Focus on the Interaction With Human Macrophages and *Galleria mellonella* Larvae. *Front. Microbiol.* 12, 641258. doi: 10.3389/fmicb.2021.641258.

Gruenert, D. C., Willems, M., Cassiman, J. J., and Frizzell, R. A. (2004). Established cell lines used in cystic fibrosis research. *J. Cyst. Fibros.* 3, 191–196. doi: 10.1016/j.jcf.2004.05.040.

Gu, M., and Imlay, J. (2011). The SoxRS response of *Escherichia coli* is directly activated by redox-cycling drugs rather than by superoxide. *Mol Microbiol.* 4, 1136–1150. doi: 10.1111/j.1365-2958.2010.07520.x.The.

Gubaev, A., Weidlich, D., and Klostermeier, D. (2016). DNA gyrase with a single catalytic tyrosine can catalyze DNA supercoiling by a nicking-closing mechanism. *Nucleic Acids Res.* 44, 10354–10366. doi: 10.1093/nar/gkw740.

Guillouzo, A., and Guguen-Guillouzo, C. (2020). Antibiotics-induced oxidative stress. *Curr. Opin. Toxicol.* 20–21, 23–28. doi: 10.1016/j.cotox.2020.03.004.

Gunaydin, G., Gedik, M. E., and Ayan, S. (2021). Photodynamic Therapy for the Treatment and Diagnosis of Cancer–A Review of the Current Clinical Status. *Front. Chem.* 9, 1–26. doi: 10.3389/fchem.2021.686303.

Hachmann, A. B., Sevim, E., Gaballa, A., Popham, D. L., Antelmann, H., and Helmann, J. D. (2011). Reduction in membrane phosphatidylglycerol content leads to daptomycin resistance in *Bacillus subtilis. Antimicrob. Agents Chemother.* 55, 4326–4337. doi: 10.1128/AAC.01819-10.

Hall, S., McDermott, C., Anoopkumar-Dukie, S., McFarland, A. J., Forbes, A., Perkins, A. V., *et*

al. (2016). Cellular effects of pyocyanin, a secreted virulence factor of *Pseudomonas aeruginosa*. *Toxins (Basel).* 8. doi: 10.3390/toxins8080236.

Halwani, M., Yebio, B., Suntres, Z. E., Alipour, M., Azghani, A. O., and Omri, A. (2008). Co-encapsulation of gallium with gentamicin in liposomes enhances antimicrobial activity of gentamicin against *Pseudomonas aeruginosa*. *J. Antimicrob. Chemother.* 62, 1291–1297. doi: 10.1093/jac/dkn422.

Hata, S. (1910). "Experimentelle Grundlage der Chemotherapie der Spirillosen," in *Die experimentelle Chemotherapie der Spirillosen* (Berlin, Heidelberg: Springer Berlin Heidelberg), 1–85. doi: 10.1007/978-3-642-64926-4_1.

Hentzer, M., Teitzel, G. M., Balzer, G. J., Heydorn, A., Givskov, M., and Parsek, M. R. (2001). Alginate Overproduction Affects. *Society* 183, 5395–5401. doi: 10.1128/JB.183.18.5395.

Herisse, M., Duverger, Y., Martin-Verstraete, I., Barras, F., and Ezraty, B. (2017). Silver potentiates aminoglycoside toxicity by enhancing their uptake. *Mol. Microbiol.* 105, 115–126. doi: 10.1111/mmi.13687.

Hernando-Amado, S., Coque, T. M., Baquero, F., and Martínez, J. L. (2020). Antibiotic Resistance: Moving From Individual Health Norms to Social Norms in One Health and Global Health. *Front. Microbiol.* 11. doi: 10.3389/fmicb.2020.01914.

Hill, L., Veli, N., and Coote, P. J. (2014). Evaluation of *Galleria mellonella* larvae for measuring the efficacy and pharmacokinetics of antibiotic therapies against *Pseudomonas aeruginosa* infection. *Int. J. Antimicrob. Agents* 43, 254–261. doi: 10.1016/j.ijantimicag.2013.11.001.

Hoffman, L. R., D'Argenio, D. A., MacCoss, M. J., Zhang, Z., Jones, R. A., and Miller, S. I. (2005). Aminoglycoside antibiotics induce bacterial biofilm formation. *Nature* 436, 1171–1175. doi: 10.1038/nature03912.

Høiby, N. (2017). A short history of microbial biofilms and biofilm infections. *Apmis* 125, 272–

275. doi: 10.1111/apm.12686.

Høiby, N., Ciofu, O., Johansen, H. K., Song, Z. J., Moser, C., Jensen, P. Ø., *et al*. (2011). The clinical impact of bacterial biofilms. *Int. J. Oral Sci.* 3, 55–65. doi: 10.4248/IJOS11026.

Hong, W., Zeng, J., and Xie, J. (2014). Antibiotic drugs targeting bacterial RNAs. *Acta Pharm. Sin. B* 4, 258–265. doi: 10.1016/j.apsb.2014.06.012.

HPSC (2017). Summary of EARS-Net data by pathogen and year. 1–2. Available at: http://www.hpsc.ie/a-z/microbiologyantimicrobialresistance/europeanantimicrobialresistancesurveillancesystemearss/earsssurveillancereports/2016reports/EARS-Net annual-quarterly data summary sheet_website_2016Q4.pdf.

HPSC (2019). Annual epidemiological report: Antimicrobial Resistance in key pathogens causing invasive infections in Ireland, 2018. Available at: http://ecdc.europa.eu/en/healthtopics/echinococcosis /Pages/Annualepidemiologicalreport2016.%0Aaspx.

Hughes, G., and Webber, M. A. (2017). Novel approaches to the treatment of bacterial biofilm infections. *Br. J. Pharmacol.* 174, 2237–2246. doi: 10.1111/bph.13706.

Hunt, R. H. (1991). Treatment of peptic ulcer disease with sucralfate: A review. *Am. J. Med.* 91, S102–S106. doi: 10.1016/0002-9343(91)90459-B.

Hussein, N. H., AL-Kadmy, I. M. S., Taha, B. M., and Hussein, J. D. (2021). Mobilized colistin resistance (mcr) genes from 1 to 10: a comprehensive review. *Mol. Biol. Rep.* 48, 2897–2907. doi: 10.1007/s11033-021-06307-y.

Husseini, R., and Stretton, R. J. (1980). Studies on the antibacterial activity of phanquone: chelating properties in relation to mode of action against Escherichia coli and Staphylococcus aureus. *Microbios* 29, 109–25. Available at:

http://www.ncbi.nlm.nih.gov/pubmed/7022141 [Accessed May 31, 2018].

Hutchings, M., Truman, A., and Wilkinson, B. (2019). Antibiotics: past, present and future. *Curr. Opin. Microbiol.* 51, 72–80. doi: 10.1016/j.mib.2019.10.008.

Ignasiak, K., and Maxwell, A. (2017). *Galleria mellonella* (greater wax moth) larvae as a model for antibiotic susceptibility testing and acute toxicity trials. *BMC Res. Notes* 10, 428. doi: 10.1186/s13104-017-2757-8.

Imlay, J. A. (2008). Cellular Defenses against Superoxide and Hydrogen Peroxide. *Annu. Rev. Biochem.* 77, 755–776. doi: 10.1146/annurev.biochem.77.061606.161055.

Imlay, J. A. (2015). Diagnosing oxidative stress in bacteria: not as easy as you might think. *Curr. Opin. Microbiol.* 24, 124–131. doi: 10.1016/j.mib.2015.01.004.

Impey, R. E., Hawkins, D. A., Sutton, J. M., and Soares da Costa, T. P. (2020). Overcoming intrinsic and acquired resistance mechanisms associated with the cell wall of gram-negative bacteria. *Antibiotics* 9, 1–19. doi: 10.3390/antibiotics9090623.

Irazoki, O., Hernandez, S. B., and Cava, F. (2019). Peptidoglycan muropeptides: Release, perception, and functions as signaling molecules. *Front. Microbiol.* 10. doi: 10.3389/fmicb.2019.00500.

Iredell, J. (2019). Antimicrobial resistance. *Microbiol. Aust.* 40, 55–56. doi: 10.1071/MA19016.

Jander, G., Rahme, L. G., and Ausubel, F. M. (2000). Positive correlation between virulence of *Pseudomonas aeruginosa* mutants in mice and insects. *J. Bacteriol.* 182, 3843–3845. doi: 10.1128/JB.182.13.3843-3845.2000.

Jennings, L. K., Storek, K. M., Ledvina, H. E., Coulon, C., Marmont, L. S., Sadovskaya, I., *et al*. (2015). Pel is a cationic exopolysaccharide that cross-links extracellular DNA in the *Pseudomonas aeruginosa* biofilm matrix. *Proc. Natl. Acad. Sci. U. S. A.* 112, 11353–11358. doi: 10.1073/pnas.1503058112.

Jo, J., Cortez, K. L., Cornell, W. C., Price-Whelan, A., and Dietrich, L. E. P. (2017). An orphan cbb3-type cytochrome oxidase subunit supports *Pseudomonas aeruginosa* biofilm growth and virulence. *Elife* 6. doi: 10.7554/eLife.30205.

Johnstone, T. C., Suntharalingam, K., and Lippard, S. J. (2015). Third row transition metals for the treatment of cancer. *Philos. Trans. R. Soc. A Math. Phys. Eng. Sci.* 373, 20140185–20140185. doi: 10.1098/rsta.2014.0185.

Jung, W. K., Koo, H. C., Kim, K. W., Shin, S., Kim, S. H., and Park, Y. H. (2008). Antibacterial Activity and Mechanism of Action of the Silver Ion in *Staphylococcus aureus* and *Escherichia coli*. *Appl. Environ. Microbiol.* 74, 2171–2178. doi: 10.1128/AEM.02001-07.

Junqueira, J., de Barros, P., Ribeiro, F., Rossoni, R., Scorzoni, L., de Menezes, R., *et al*. (2018). Recent Advances in the Use of *Galleria mellonella* Model to Study Immune Responses against Human Pathogens. *J. Fungi* 4, 128. doi: 10.3390/jof4040128.

Jurado-Martín, I., Sainz-Mejías, M., and McClean, S. (2021). *Pseudomonas aeruginosa*: An audacious pathogen with an adaptable arsenal of virulence factors. *Int. J. Mol. Sci.* 22, 1–37. doi: 10.3390/ijms22063128.

Kadam, S., Shai, S., Shahane, A., and Kaushik, K. S. (2019). Recent advances in non-conventional antimicrobial approaches for chronic wound biofilms: Have we found the "chink in the armor"? *Biomedicines* 7. doi: 10.3390/biomedicines7020035.

Kaneko, Y., Thoendel, M., Olakanmi, O., Britigan, B. E., and Singh, P. K. (2007). The transition metal gallium disrupts *Pseudomonas aeruginosa* iron metabolism and has antimicrobial and antibiofilm activity. *J. Clin. Invest.* 117, 877–888. doi: 10.1172/JCI30783.

Kang, D., Turner, K. E., and Kirienko, N. V. (2018). PqsA promotes pyoverdine production via biofilm formation. *Pathogens* 7. doi: 10.3390/pathogens7010003.

Kapoor, G., Saigal, S., and Elongavan, A. (2017). Action and resistance mechanisms of

antibiotics: A guide for clinicians. *J. Anaesthesiol. Clin. Pharmacol.* 33, 300–305. doi: 10.4103/joacp.JOACP_349_15.

Kapoor, P., and Murphy, P. (2018). Combination antibiotics against *Pseudomonas aeruginosa*, representing common and rare cystic fibrosis strains from different Irish clinics. *Heliyon* 4, e00562. doi: 10.1016/j.heliyon.2018.e00562.

Karaiskos, I., Lagou, S., Pontikis, K., Rapti, V., and Poulakou, G. (2019). The "Old" and the "New" antibiotics for MDR Gram-negative pathogens: For whom, when, and how. *Front. Public Heal.* 7, 1–25. doi: 10.3389/fpubh.2019.00151.

Kasai, T., Suzuki, Y., Kouzuma, A., and Watanabe, K. (2019). Roles of D-lactate dehydrogenases in the anaerobic growth of *Shewanella oneidensis* MR-1 on sugars. *Appl. Environ. Microbiol.* 85. doi: 10.1128/AEM.02668-18.

Kavanagh, K., and Reeves, E. P. (2004). Exploiting the potential of insects for in vivo pathogenicity testing of microbial pathogens. *FEMS Microbiol. Rev.* 28, 101–112. doi: 10.1016/j.femsre.2003.09.002.

Kavanagh, K., and Sheehan, G. (2018). The Use of *Galleria mellonella* Larvae to Identify Novel Antimicrobial Agents against Fungal Species of Medical Interest. *J. Fungi* 4, 113. doi: 10.3390/jof4030113.

Kellett, A., Howe, O., O'Connor, M., McCann, M., Creaven, B. S., McClean, S., *et al*. (2012). Radical-induced DNA damage by cytotoxic square-planar copper(II) complexes incorporating o-phthalate and 1,10-phenanthroline or 2,2′-dipyridyl. *Free Radic. Biol. Med.* 53, 564–576. doi: 10.1016/j.freeradbiomed.2012.05.034.

Kellett, A., O'Connor, M., McCann, M., Howe, O., Casey, A., McCarron, P., *et al*. (2011a). Water-soluble bis(1,10-phenanthroline) octanedioate Cu2+ and Mn2+ complexes with unprecedented nano and picomolar in vitro cytotoxicity: Promising leads for chemotherapeutic drug development. *Medchemcomm* 2, 579–584. doi:

10.1039/c0md00266f.

Kellett, A., O'Connor, M., McCann, M., McNamara, M., Lynch, P., Rosair, G., *et al*. (2011b). Bis-phenanthroline copper(ii) phthalate complexes are potent in vitro antitumour agents with "self-activating" metallo-nuclease and DNA binding properties. *Dalt. Trans.* 40, 1024–1027. doi: 10.1039/c0dt01607a.

Kelly, J., and Kavanagh, K. (2011). Caspofungin primes the immune response of the larvae of *Galleria mellonella* and induces a non-specific antimicrobial response. *J. Med. Microbiol.* 60, 189–196. doi: 10.1099/jmm.0.025494-0.

Kermani, A. A., Macdonald, C. B., Burata, O. E., Ben Koff, B., Koide, A., Denbaum, E., *et al*. (2020). The structural basis of promiscuity in small multidrug resistance transporters. *Nat. Commun.* 11. doi: 10.1038/s41467-020-19820-8.

Khan, M., Stapleton, F., Summers, S., Rice, S. A., and Willcox, M. D. P. (2020). Antibiotic resistance characteristics of *Pseudomonas aeruginosa* isolated from keratitis in Australia and India. *Antibiotics* 9, 1–16. doi: 10.3390/antibiotics9090600.

Kilah, N. L., and Meggers, E. (2012). Sixty years young: The diverse biological activities of metal polypyridyl complexes pioneered by Francis P. Dwyer. *Aust. J. Chem.* 65, 1325–1332. doi: 10.1071/CH12275.

Kim, J., Pitts, B., Stewart, P. S., Camper, A., and Yoon, J. (2008). Comparison of the antimicrobial effects of chlorine, silver ion, and tobramycin on biofilm. *Antimicrob. Agents Chemother*. 52, 1446–1453. doi: 10.1128/AAC.00054-07.

Klasen, H. J. (2000). A historical review of the use of silver in the treatment of burns. II. Renewed interest for silver. *Burns* 26, 131–138. doi: 10.1016/S0305-4179(99)00116-3.

Kohanski, M. A., DePristo, M. A., and Collins, J. J. (2010). Sub-lethal antibiotic treatment leads to multidrug resistance via radical-induced mutagenesis. *Mol. Cell* 37, 311–320. doi:

10.1016/j.earlhumdev.2006.05.022.

Kohanski, M. A., Dwyer, D. J., Hayete, B., Lawrence, C. A., and Collins, J. J. (2007). A Common Mechanism of Cellular Death Induced by Bactericidal Antibiotics. *Cell* 130, 797–810. doi: 10.1016/j.cell.2007.06.049.

Kohanski, M. A., Dwyer, D. J., Wierzbowski, J., Cottarel, G., and Collins, J. J. (2008). Mistranslation of Membrane Proteins and Two-Component System Activation Trigger Antibiotic-Mediated Cell Death. *Cell* 135, 679–690. doi: 10.1016/j.cell.2008.09.038.

Kong, K. F., Schneper, L., and Mathee, K. (2010). Beta-lactam antibiotics: From antibiosis to resistance and bacteriology. *Apmis* 118, 1–36. doi: 10.1111/j.1600-0463.2009.02563.x.

Kostylev, M., Kim, D. Y., Smalley, N. E., Salukhe, I., Peter Greenberg, E., and Dandekar, A. A. (2019). Evolution of the *Pseudomonas aeruginosa* quorum-sensing hierarchy. *Proc. Natl. Acad. Sci. U. S. A.* 116, 7027–7032. doi: 10.1073/pnas.1819796116.

Kovach, K., Davis-Fields, M., Irie, Y., Jain, K., Doorwar, S., Vuong, K., *et al*. (2017). Evolutionary adaptations of biofilms infecting cystic fibrosis lungs promote mechanical toughness by adjusting polysaccharide production. *npj Biofilms Microbiomes* 3, 1–9. doi: 10.1038/s41522-016-0007-9.

Krawczyk, B., Wityk, P., Gałęcka, M., and Michalik, M. (2021). The many faces of enterococcus spp.—commensal, probiotic and opportunistic pathogen. *Microorganisms* 9, 1–20. doi: 10.3390/microorganisms9091900.

Krezdorn, J., Adams, S., and Coote, P. J. (2014). A *Galleria mellonella* infection model reveals double and triple antibiotic combination therapies with enhanced efficacy versus a multidrug-resistant strain of *Pseudomonas aeruginosa*. *J. Med. Microbiol.* 63, 945–955. doi: 10.1099/jmm.0.074245-0.

Kryczka, J., Kryczka, J., Czarnecka-Chrebelska, K. H., and Brzeziańska-Lasota, E. (2021).

Molecular mechanisms of chemoresistance induced by cisplatin in NSCLC cancer therapy. *Int. J. Mol. Sci.* 22. doi: 10.3390/ijms22168885.

Kumar, S. V., Scottwell, S. O., Waugh, E., McAdam, C. J., Hanton, L. R., Brooks, H. J. L., *et al*. (2016). Antimicrobial Properties of Tris(homoleptic) Ruthenium(II) 2-Pyridyl-1,2,3-triazole "click" Complexes against Pathogenic Bacteria, Including Methicillin-Resistant *Staphylococcus aureus* (MRSA). *Inorg. Chem.* 55, 9767–9777. doi: 10.1021/acs.inorgchem.6b01574.

Kusakizako, T., Miyauchi, H., Ishitani, R., and Nureki, O. (2020). Structural biology of the multidrug and toxic compound extrusion superfamily transporters. *Biochim. Biophys. Acta - Biomembr.* 1862, 183154. doi: 10.1016/j.bbamem.2019.183154.

L.S. Santos, A., L. Sodre, C., S. Valle, R., A. Silva, B., A. Abi-chacra, E., V. Silva, L., *et al*. (2012). Antimicrobial Action of Chelating Agents: Repercussions on the Microorganism Development, Virulence and Pathogenesis. *Curr. Med. Chem.* 19, 2715–2737. doi: 10.2174/092986712800609788.

Langendonk, R. F., Neill, D. R., and Fothergill, J. L. (2021). The Building Blocks of Antimicrobial Resistance in *Pseudomonas aeruginosa*: Implications for Current Resistance-Breaking Therapies. *Front. Cell. Infect. Microbiol.* 11, 1–22. doi: 10.3389/fcimb.2021.665759.

Lansbury, L., Lim, B., Baskaran, V., and Lim, W. S. (2020). Co-infections in people with COVID-19: a systematic review and meta-analysis. *J. Infect.* 81, 266–275. doi: 10.1016/j.jinf.2020.05.046.

Lebeaux, D., Ghigo, J.-M., and Beloin, C. (2014). Biofilm-Related Infections: Bridging the Gap between Clinical Management and Fundamental Aspects of Recalcitrance toward Antibiotics. *Microbiol. Mol. Biol. Rev.* 78, 510–543. doi: 10.1128/mmbr.00013-14.

Lee, A. S., De Lencastre, H., Garau, J., Kluytmans, J., Malhotra-Kumar, S., Peschel, A., *et al*.

(2018). Methicillin-resistant Staphylococcus aureus. *Nat. Rev. Dis. Prim.* 4, 1–23. doi: 10.1038/nrdp.2018.33.

Lee, J., Oh, S., Bhattacharya, S., Zhang, Y., Florens, L., Washburn, M. P., *et al*. (2021). The plasticity of the pyruvate dehydrogenase complex confers a labile structure that is associated with its catalytic activity. *PLoS One* 15, e0243489. doi: 10.1371/journal.pone.0243489.

Lee, J., Sands, Z. A., and Biggin, P. C. (2016). A numbering system for MFS transporter proteins. *Front. Mol. Biosci.* 3, 1–13. doi: 10.3389/fmolb.2016.00021.

Lee, J., and Zhang, L. (2014). The hierarchy quorum sensing network in *Pseudomonas aeruginosa*. *Protein Cell* 6, 26–41. doi: 10.1007/s13238-014-0100-x.

Lee, T., Pang, S., Abraham, S., and Coombs, G. W. (2019). Antimicrobial-resistant CC17 Enterococcus faecium: The past, the present and the future. *J. Glob. Antimicrob. Resist.* 16, 36–47. doi: 10.1016/j.jgar.2018.08.016.

Lemire, J. A., Harrison, J. J., and Turner, R. J. (2013). Antimicrobial activity of metals: Mechanisms, molecular targets and applications. *Nat. Rev. Microbiol.* 11, 371–384. doi: 10.1038/nrmicro3028.

Levison, M. E., and Levison, J. H. (2009). Pharmacokinetics and Pharmacodynamics of Antibacterial Agents. *Infect. Dis. Clin. North Am.* 23, 791–815. doi: 10.1016/j.idc.2009.06.008.

Li, F., Collins, J. G., and Keene, F. R. (2015). Ruthenium complexes as antimicrobial agents. *Chem. Soc. Rev.* 44, 2529–2542. doi: 10.1039/c4cs00343h.

Li, F., Feterl, M., Mulyana, Y., Warner, J. M., Collins, J. G., and Keene, F. R. (2012). In vitro susceptibility and cellular uptake for a new class of antimicrobial agents: Dinuclear ruthenium(II) complexes. *J. Antimicrob. Chemother.* 67, 2686–2695. doi: 10.1093/jac/dks291.

Li, F., Feterl, M., Warner, J. M., Keene, F. R., Collins, J. G., and Grant Collins, J. (2013). Dinuclear polypyridylruthenium(II) complexes: Flow cytometry studies of their accumulation in bacteria and the effect on the bacterial membrane. *J. Antimicrob. Chemother*. 68, 2825–2833. doi: 10.1093/jac/dkt279.

Li, F., Harry, E. J., Bottomley, A. L., Edstein, M. D., Birrell, G. W., Woodward, C. E., *et al*. (2014). Dinuclear ruthenium(ii) antimicrobial agents that selectively target polysomes in vivo. *Chem. Sci.* 5, 685–693. doi: 10.1039/c3sc52166d.

Liang, X., Luan, S., Yin, Z., He, M., He, C., Yin, L., *et al*. (2018). Recent advances in the medical use of silver complex. *Eur. J. Med. Chem.* 157, 62–80. doi: 10.1016/j.ejmech.2018.07.057.

Lim, L. M., Ly, N., Anderson, D., Yang, J. C., Macander, L., Jarkowski, A., *et al*. (2010). Resurgence of colistin: A review of resistance, toxicity, pharmacodynamics, and dosing. *Pharmacotherapy* 30, 1279–1291. doi: 10.1592/phco.30.12.1279.

Lima, A. K. C., Elias, C. G. R., Oliveira, S. S. C., Santos-Mallet, J. R., McCann, M., Devereux, M., *et al*. (2021). Anti-Leishmania braziliensis activity of 1,10-phenanthroline-5,6-dione and its Cu(II) and Ag(I) complexes. *Parasitol. Res.* doi: 10.1007/s00436-021-07265-x.

Lin, Y. C., Cornell, W. C., Jo, J., Price-Whelan, A., and Dietrich, L. E. P. (2018). The *Pseudomonas aeruginosa* complement of lactate dehydrogenases enables use of d -and l -lactate and metabolic cross-feeding. *MBio* 9. doi: 10.1128/mBio.00961-18.

Liu, Y. Y., Wang, Y., Walsh, T. R., Yi, L. X., Zhang, R., Spencer, J., *et al*. (2016). Emergence of plasmid-mediated colistin resistance mechanism MCR-1 in animals and human beings in China: A microbiological and molecular biological study. *Lancet Infect. Dis.* 16, 161–168. doi: 10.1016/S1473-3099(15)00424-7.

Loiselle, M., and Anderson, K. W. (2003). The use of cellulase in inhibiting biofilm formation from organisms commonly found on medical implants. *Biofouling* 19, 77–85. doi: 10.1080/0892701021000030142.

López, V., Martínez-Robles, M. L., Hernández, P., Krimer, D. B., and Schvartzman, J. B. (2012). Topo IV is the topoisomerase that knots and unknots sister duplexes during DNA replication. *Nucleic Acids Res.* 40, 3563–3573. doi: 10.1093/nar/gkr1237.

Magiorakos, A. P., Srinivasan, A., Carey, R. B., Carmeli, Y., Falagas, M. E., Giske, C. G., *et al*. (2012). Multidrug-resistant, extensively drug-resistant and pandrug-resistant bacteria: An international expert proposal for interim standard definitions for acquired resistance. *Clin. Microbiol. Infect.* 18, 268–281. doi: 10.1111/j.1469-0691.2011.03570.x.

Magnet, S., and Blanchard, J. S. (2005). Molecular insights into aminoglycoside action and resistance. *Chem. Rev.* 105, 477–497. doi: 10.1021/cr0301088.

Maguire, R., Duggan, O., and Kavanagh, K. (2016). Evaluation of *Galleria mellonella* larvae as an in vivo model for assessing the relative toxicity of food preservative agents. *Cell Biol. Toxicol.* 32, 209–216. doi: 10.1007/s10565-016-9329-x.

Majumdar, R., Barchi, B., Turlapati, S. A., Gagne, M., Minocha, R., Long, S., *et al*. (2016). Glutamate, ornithine, arginine, proline, and polyamine metabolic interactions: The pathway is regulated at the post-transcriptional level. *Front. Plant Sci.* 7, 78. doi: 10.3389/fpls.2016.00078.

Makovník, M., Rejleková, K., Uhrin, I., Mego, M., and Chovanec, M. (2021). Intricacies of Radiographic Assessment in Testicular Germ Cell Tumors. *Front. Oncol.* 10, 1–9. doi: 10.3389/fonc.2020.587523.

Malhotra, S., Hayes, D., and Wozniak, D. J. (2019). Cystic fibrosis and *Pseudomonas aeruginosa*: The host-microbe interface. *Clin. Microbiol. Rev.* 32, 1–46. doi: 10.1128/CMR.00138-18.

Maunders, E., and Welch, M. (2017). Matrix exopolysaccharides; the sticky side of biofilm formation. *FEMS Microbiol. Lett.* 364. doi: 10.1093/femsle/fnx120.

Mazumder, A., Gupta, M., Perrin, D. M., Sigman, D. S., Rabinovitz, M., and Pommier, Y. (1995).

Inhibition of Human Immunodeficiency Virus Type 1 Integrase by a Hydrophobic Cation: The Phenanthroline-Cuprous Complex. *AIDS Res. Hum. Retroviruses* 11, 115–125. doi: 10.1089/aid.1995.11.115.

McCann, M., Casey, M. T., Devereux, M., Curran, M., and Ferguson, G. (1997a). Syntheses, X-ray crystal structures and catalytic activities of the manganese(II) butanedioic acid complexes. *Polyhedron* 16, 2547–2552. doi: 10.1016/S0277-5387(97)00002-8.

McCann, M., Casey, M. T., Devereux, M., Curran, M., and McKee, V. (1997b). Manganese(II) complexes of hexanedioic and heptanedioic acids: X-ray crystal structures of [Mn(O2C(CH2)4CO2)(phen) 2H2O] 7H2O and [Mn(phen)2(H2O)2][Mn(O2C(CH 2)5CO2) (phen)2H2O](O2C(CH2)5CO2). *Polyhedron* 16, 2741–2748. doi: 10.1016/S0277-5387(97)00037-5.

McCann, M., Coyle, B., McKay, S., McCormack, P., Kavanagh, K., Devereux, M., *et al*. (2004). Synthesis and X-ray crystal structure of [Ag(phendio)2]ClO4 (phendio = 1,10-phenanthroline-5,6-dione) and its effects on fungal and mammalian cells. *BioMetals* 17, 635–645. doi: 10.1007/s10534-004-1229-5.

McCann, M., Cronin, J. F., Devereux, M., and Ferguson, G. (1995). Copper(II) complexes of heptanedioic acid (hdaH2) and octanedioic acid (odaH2) : X-ray crystal structures OF [Cu(η2-hda)(phen)2]·11.73H2O and [Cu(η2-oda)(phen)2]·12H2O (phen = 1,10-Phenanthroline). *Polyhedron* 14, 2379–2387. doi: 10.1016/0277-5387(95)00075-4.

McCann, M., Kellett, A., Kavanagh, K., Devereux, M., and L.S. Santos, A. (2012a). Deciphering the Antimicrobial Activity of Phenanthroline Chelators. *Curr. Med. Chem.* 19, 2703–2714. doi: 10.2174/092986712800609733.

McCann, M., Santos, A. L. S., Da Silva, B. A., Romanos, M. T. V., Pyrrho, A. S., Devereux, M., *et al*. (2012b). In vitro and in vivo studies into the biological activities of 1,10-phenanthroline, 1,10-phenanthroline-5,6-dione and its copper(ii) and silver(i) complexes.

Toxicol. Res. (Camb). 1, 47–54. doi: 10.1039/c2tx00010e.

McCann, S., McCann, M., Casey, R. M. T., Devereux, M., McKee, V., McMichael, P., *et al.* (1997c). Manganese(II) complexes of 3,6,9-trioxaundecanedioic acid (3,6,9-tddaH2): X-ray crystal structures of [Mn(3,6,9-tdda) (H2O)2] · 2H2O and {[Mn(3,6,9-tdda)(phen)2 · 3H2O] · EtOH}n. *Polyhedron* 16, 4247–4252. doi: 10.1016/S0277-5387(97)00233-7.

McCarron, P., McCann, M., Devereux, M., Kavanagh, K., Skerry, C., Karakousis, P. C., *et al.* (2018). Unprecedented in vitro antitubercular activitiy of manganese(II) complexes containing 1,10-phenanthroline and dicarboxylate ligands: Increased activity, superior selectivity, and lower toxicity in comparison to their copper(II) analogs. *Front. Microbiol.* 9, 1432. doi: 10.3389/fmicb.2018.01432.

Mccoy, L. S., Xie, Y., and Tor, Y. (2011). Antibiotics that target protein synthesis. *Wiley Interdiscip. Rev. RNA* 2, 209–232. doi: 10.1002/wrna.60.

McDermott, H., Skally, M., O'rourke, J., Humphreys, H., and Fitzgerald-Hughes, D. (2018). Vancomycin-Resistant Enterococci (VRE) in the intensive care unit in a nonoutbreak setting: Identification of potential reservoirs and epidemiological associations between patient and environmental VRE. *Infect. Control Hosp. Epidemiol.* 39, 40–45. doi: 10.1017/ice.2017.248.

McQuillan, J. S., Groenaga Infante, H., Stokes, E., and Shaw, A. M. (2012). Silver nanoparticle enhanced silver ion stress response in Escherichia coli K12. *Nanotoxicology* 6, 857–866. doi: 10.3109/17435390.2011.626532.

Mégraud, F. (2012). The challenge of Helicobacter pylori resistance to antibiotics: The comeback of bismuth-based quadruple therapy. *Therap. Adv. Gastroenterol.* 5, 103–109. doi: 10.1177/1756283X11432492.

Messori, L., and Marcon, G. (2004). Gold complexes in the treatment of rheumatoid arthritis. *Met Ions Biol Syst* 41, 279–304. Available at:

http://www.ncbi.nlm.nih.gov/entrez/query.fcgi?cmd=Retrieve&db=PubMed&dopt=Citation&list_uids=15206120 [Accessed April 12, 2018].

Michel, G. P. F., Durand, E., and Filloux, A. (2007). XphA/XqhA, a Novel GspCD Subunit for Type II Secretion in *Pseudomonas aeruginosa*. *J. Bacteriol.* 189, 3776. doi: 10.1128/JB.00205-07.

Miethke, M., Pieroni, M., Weber, T., Brönstrup, M., Hammann, P., Halby, L., *et al*. (2021). Towards the sustainable discovery and development of new antibiotics. *Nat. Rev. Chem.* 5, 726–749. doi: 10.1038/s41570-021-00313-1.

Millanao, A. R., Mora, A. Y., Villagra, N. A., Bucarey, S. A., and Hidalgo, A. A. (2021). *Biological effects of quinolones: A family of broad-spectrum antimicrobial agents*. doi: 10.3390/molecules26237153.

Minandri, F., Imperi, F., Frangipani, E., Bonchi, C., Visaggio, D., Facchini, M., *et al*. (2016). Role of iron uptake systems in *Pseudomonas aeruginosa* virulence and airway infection. *Infect. Immun.* 84, 2324–2335. doi: 10.1128/IAI.00098-16.

Mjos, K. D., and Orvig, C. (2014). Metallodrugs in medicinal inorganic chemistry. *Chem. Rev.* 114, 4540–4563. doi: 10.1021/cr400460s.

Mmatlia, M., Mbellea, M., and Sekyere, J. O. (2022). Global Epidemiology and Genetic Environment of mcr genes : A One Health Systematic. *medRxiv Prepr.*

Moradali, M. F., Ghods, S., and Rehm, B. H. A. (2017). *Pseudomonas aeruginosa* lifestyle: A paradigm for adaptation, survival, and persistence. *Front. Cell. Infect. Microbiol.* 7, 39. doi: 10.3389/fcimb.2017.00039.

Moreno, R. M. G., García-Clemente, M., Diab-Cáceres, L., Martínez-Vergara, A., Martínez-García, M. Á., and Gómez-Punter, R. M. (2021a). Treatment of pulmonary disease of cystic fibrosis: A comprehensive review. *Antibiotics* 10, 486. doi: 10.3390/antibiotics10050486.

Moreno, R. M. G., García-Clemente, M., Diab-Cáceres, L., Martínez-Vergara, A., Martínez-García, M. Á., and Gómez-Punter, R. M. (2021b). *Treatment of pulmonary disease of cystic fibrosis: A comprehensive review*. doi: 10.3390/antibiotics10050486.

Mosaei, H., and Zenkin, N. (2020). Inhibition of RNA Polymerase by Rifampicin and Rifamycin-Like Molecules. *EcoSal Plus* 9, 1–16. doi: 10.1128/ecosalplus.esp-0017-2019.

Mukherjee, A., and Sadler, P. J. (2009). "Metals in Medicine: Therapeutic Agents," in *Wiley Encyclopedia of Chemical Biology*, 1–47. doi: 10.1002/9780470048672.wecb333.

Mulcahy, H., Charron-Mazenod, L., and Lewenza, S. (2008). Extracellular DNA chelates cations and induces antibiotic resistance in *Pseudomonas aeruginosa* biofilms. *PLoS Pathog.* 4. doi: 10.1371/journal.ppat.1000213.

Munita, J. M., and Arias, C. A. (2016). Mechanisms of Antibiotic Resistance. *Microbiol. Spectr.* 4. doi: 10.1128/microbiolspec.VMBF-0016-2015.

Murray, C. J., Ikuta, K. S., Sharara, F., Swetschinski, L., Robles Aguilar, G., Gray, A., *et al*. (2022). Global burden of bacterial antimicrobial resistance in 2019: a systematic analysis. *Lancet* 6736. doi: 10.1016/s0140-6736(21)02724-0.

Najafpour, G. D. (2007). "Production of Antibiotics," in *Biochemical Engineering and Biotechnology* (Elsevier), 263–279. doi: 10.1016/b978-044452845-2/50011-2.

Nanayakkara, A. K., Boucher, H. W., Fowler, V. G., Jezek, A., Outterson, K., and Greenberg, D. E. (2021). Antibiotic resistance in the patient with cancer: Escalating challenges and paths forward. *CA. Cancer J. Clin.* 71, 488–504. doi: 10.3322/CAAC.21697.

Narayanaswamy, V. P., Keagy, L. L., Duris, K., Wiesmann, W., Loughran, A. J., Townsend, S. M., *et al*. (2018). Novel glycopolymer eradicates antibiotic- and CCCP-induced persister cells in *Pseudomonas aeruginosa*. *Front. Microbiol.* 9, 1–12. doi: 10.3389/fmicb.2018.01724.

Nasiri Sovari, S., and Zobi, F. (2020). Recent Studies on the Antimicrobial Activity of Transition Metal Complexes of Groups 6–12. *Chemistry (Easton).* 2, 418–452. doi: 10.3390/chemistry2020026.

Neill, J. O. ' (2014). Antimicrobial Resistance: Tackling a crisis for the health and wealth of nations The Review on Antimicrobial Resistance Chaired. Available at: https://amr-review.org/sites/default/files/AMR Review Paper - Tackling a crisis for the health and wealth of nations_1.pdf [Accessed February 12, 2018].

Ng, N. S., Leverett, P., Hibbs, D. E., Yang, Q., Bulanadi, J. C., Jie Wu, M., *et al*. (2013). The antimicrobial properties of some copper(ii) and platinum(ii) 1,10-phenanthroline complexes. *Dalt. Trans.* 42, 3196–3209. doi: 10.1039/c2dt32392c.

Ng, N. S., Wu, M. J., and Aldrich-Wright, J. R. (2018). The cytotoxicity of some phenanthroline-based antimicrobial copper(II) and ruthenium(II) complexes. *J. Inorg. Biochem.* 180, 61–68. doi: 10.1016/j.jinorgbio.2017.11.022.

Ng, N. S., Wu, M. J., Jones, C. E., and Aldrich-Wright, J. R. (2016). The antimicrobial efficacy and DNA binding activity of some copper(II) complexes of 3,4,7,8-tetramethyl-1,10-phenanthroline, 4,7-diphenyl-1,10-phenanthroline and 1,2-diaminocyclohexane. *J. Inorg. Biochem.* 162, 62–72. doi: 10.1016/J.JINORGBIO.2016.06.006.

Nieder, C., Pawinski, A., and Andratschke, N. H. (2013). Combined radio- and chemotherapy for non-small cell lung cancer: Systematic review of landmark studies based on acquired citations. *Front. Oncol.* 3 JUL, 1–6. doi: 10.3389/fonc.2013.00176.

Niederman, M. S., Baron, R. M., Bouadma, L., Calandra, T., Daneman, N., DeWaele, J., *et al.* (2021). Initial antimicrobial management of sepsis. *Crit. Care* 25, 1–11. doi: 10.1186/s13054-021-03736-w.

Nobili, S., Mini, E., Landini, I., Gabbiani, C., Casini, A., and Messori, L. (2009). Gold compounds as anticancer agents: chemistry, cellular pharmacology, and preclinical studies. *Med. Res.*

Rev. 30, 550–580. doi: 10.1002/med.20168.

Odds, F. C. (2003). Synergy, antagonism, and what the chequerboard puts between them. *J. Antimicrob. Chemother*. 52, 1–1. doi: 10.1093/jac/dkg301.

Okuda, S., Sherman, D. J., Silhavy, T. J., Ruiz, N., and Kahne, D. (2016). Lipopolysaccharide transport and assembly at the outer membrane: The PEZ model. *Nat. Rev. Microbiol.* 14, 337–345. doi: 10.1038/nrmicro.2016.25.

Olademehin, O. P., Kim, S. J., and Shuford, K. L. (2021). Molecular Dynamics Simulation of Atomic Interactions in the Vancomycin Binding Site. *ACS Omega* 6, 775–785. doi: 10.1021/acsomega.0c05353.

Orelle, C., Mathieu, K., and Jault, J. M. (2019). *Multidrug ABC transporters in bacteria*. doi: 10.1016/j.resmic.2019.06.001.

Pachori, P., Gothalwal, R., and Gandhi, P. (2019). Emergence of antibiotic resistance *Pseudomonas aeruginosa* in intensive care unit; a critical review. *Genes Dis.* 6, 109–119. doi: 10.1016/j.gendis.2019.04.001.

Páez, P. L., Bazán, C. M., Bongiovanni, M. E., Toneatto, J., Albesa, I., Becerra, M. C., *et al*. (2013). Oxidative stress and antimicrobial activity of chromium(iii) and ruthenium(II) complexes on *Staphylococcus aureus* and *Escherichia coli*. *Biomed Res. Int.* 2013. doi: 10.1155/2013/906912.

Palermo, G., Magistrato, A., Riedel, T., von Erlach, T., Davey, C. A., Dyson, P. J., *et al*. (2016). Fighting Cancer with Transition Metal Complexes: From Naked DNA to Protein and Chromatin Targeting Strategies. *ChemMedChem*, 1199–1210. doi: 10.1002/cmdc.201500478.

Panáček, A., Smékalová, M., Večeřová, R., Bogdanová, K., Röderová, M., Kolář, M., *et al*. (2016). Silver nanoparticles strongly enhance and restore bactericidal activity of inactive

antibiotics against multiresistant Enterobacteriaceae. *Colloids Surfaces B Biointerfaces* 142, 392–399. doi: 10.1016/j.colsurfb.2016.03.007.

Pancu, D. F., Scurtu, A., Macasoi, I. G., Marti, D., Mioc, M., Soica, C., *et al*. (2021). Antibiotics: Conventional therapy and natural compounds with antibacterial activity-a pharmaco-toxicological screening. *Antibiotics* 10. doi: 10.3390/antibiotics10040401.

Pang, Z., Raudonis, R., Glick, B. R., Lin, T. J., and Cheng, Z. (2019). Antibiotic resistance in *Pseudomonas aeruginosa*: mechanisms and alternative therapeutic strategies. *Biotechnol. Adv.* 37, 177–192. doi: 10.1016/j.biotechadv.2018.11.013.

Papadia, P., Margiotta, N., Bergamo, A., Sava, G., and Natile, G. (2005). Platinum(II) complexes with antitumoral/antiviral aromatic heterocycles: Effect of glutathione upon in vitro cell growth inhibition. *J. Med. Chem.* 48, 3364–3371. doi: 10.1021/jm0500471.

Parnham, M. J., Haber, V. E., Giamarellos-Bourboulis, E. J., Perletti, G., Verleden, G. M., and Vos, R. (2014). Azithromycin: Mechanisms of action and their relevance for clinical applications. *Pharmacol. Ther.* 143, 225–245. doi: 10.1016/j.pharmthera.2014.03.003.

Peeters, E., Nelis, H. J., and Coenye, T. (2008). Comparison of multiple methods for quantification of microbial biofilms grown in microtiter plates. *J. Microbiol. Methods* 72, 157–165. doi: 10.1016/j.mimet.2007.11.010.

Pelfrene, E., Botgros, R., and Cavaleri, M. (2021). Antimicrobial multidrug resistance in the era of COVID-19: a forgotten plight? *Antimicrob. Resist. Infect. Control* 10, 21. doi: 10.1186/s13756-021-00893-z.

Pena, R. T., Blasco, L., Ambroa, A., González-Pedrajo, B., Fernández-García, L., López, M., *et al*. (2019). Relationship between quorum sensing and secretion systems. *Front. Microbiol.* 10, 1100. doi: 10.3389/fmicb.2019.01100.

Pereira, M. F., Rossi, C. C., Da Silva, G. C., Rosa, J. N., and Bazzolli, D. M. S. (2020). *Galleria*

mellonella as an infection model: An in-depth look at why it works and practical considerations for successful application. *Pathog. Dis.* 78, 1–15. doi: 10.1093/femspd/ftaa056.

Pérez-Gallego, M., Torrens, G., Castillo-Vera, J., Moya, B., Zamorano, L., Cabot, G., *et al*. (2016). Impact of AmpC derepression on fitness and virulence: the mechanism or the pathway? *MBio* 7. doi: 10.1128/mBio.01783-16.

Périchon, B., and Courvalin, P. (2009). VanA-type vancomycin-resistant *Staphylococcus aureus*. *Antimicrob. Agents Chemother.* 53, 4580–4587. doi: 10.1128/AAC.00346-09.

Peterson, E., and Kaur, P. (2018). Antibiotic resistance mechanisms in bacteria: Relationships between resistance determinants of antibiotic producers, environmental bacteria, and clinical pathogens. *Front. Microbiol.* 9, 1–21. doi: 10.3389/fmicb.2018.02928.

Piatek, M., Sheehan, G., and Kavanagh, K. (2020). Utilising *Galleria mellonella* larvae for studying in vivo activity of conventional and novel antimicrobial agents. *Pathog. Dis.* 78. doi: 10.1093/femspd/ftaa059.

Piddock, L. J. V. (2016). Reflecting on the final report of the O'Neill Review on Antimicrobial Resistance. *Lancet Infect. Dis.* 16, 767–768. doi: 10.1016/S1473-3099(16)30127-X.

Polikanov, Y. S., Aleksashin, N. A., Beckert, B., and Wilson, D. N. (2018). The mechanisms of action of ribosome-targeting peptide antibiotics. *Front. Mol. Biosci.* 5, 1–21. doi: 10.3389/fmolb.2018.00048.

Psomas, G., and Kessissoglou, D. P. (2013). Quinolones and non-steroidal anti-inflammatory drugs interacting with copper(ii), nickel(ii), cobalt(ii) and zinc(ii): Structural features, biological evaluation and perspectives. *Dalt. Trans.* 42, 6252–6276. doi: 10.1039/c3dt50268f.

Qu, J., Cai, Z., Liu, Y., Duan, X., Han, S., Liu, J., *et al*. (2021). Persistent Bacterial Coinfection

of a COVID-19 Patient Caused by a Genetically Adapted *Pseudomonas aeruginosa* Chronic Colonizer. *Front. Cell. Infect. Microbiol.* 11, 1–12. doi: 10.3389/fcimb.2021.641920.

Rabin, N., Zheng, Y., Opoku-Temeng, C., Du, Y., Bonsu, E., and Sintim, H. O. (2015). Biofilm formation mechanisms and targets for developing antibiofilm agents. *Future Med. Chem.* 7, 493–512. doi: 10.4155/fmc.15.6.

Raman, N., Dhaveethu Raja, J., and Sakthivel, A. (2007). Synthesis, spectral characterization of Schiff base transition metal complexes: DNA cleavage and antimicrobial activity studies. *J. Chem. Sci.* 119, 303–310. doi: 10.1007/s12039-007-0041-5.

Raman, N., and Raja, S. J. (2007). DNA cleavage, structural elucidation and anti-microbial studies of three novel mixed ligand Schiff base complexes of copper(II). *J. Serbian Chem. Soc.* 72, 983–992. doi: 10.2298/JSC0710983R.

Ramírez-Estrada, S., Borgatta, B., and Rello, J. (2016). *Pseudomonas aeruginosa* ventilator-associated pneumonia management. *Infect. Drug Resist.* 9, 7–18. doi: 10.2147/IDR.S50669.

Ramirez, M. S., and Tolmasky, M. E. (2010). Aminoglycoside modifying enzymes. *Drug Resist. Updat.* 13, 151–171. doi: 10.1016/j.drup.2010.08.003.

Rasamiravaka, T., Labtani, Q., Duez, P., and El Jaziri, M. (2015). The Formation of Biofilms by *Pseudomonas aeruginosa* : A Review of the Natural and Synthetic Compounds Interfering with Control Mechanisms . *Biomed Res. Int.* 2015, 1–17. doi: 10.1155/2015/759348.

Reddel, R., Ohnuki, Y., Ke, Y., Gerwin, B. I., Lechner, J. F., and Harris, C. C. (1993). Development of Tumorigenicity in Simian Virus 40-immortalized Human Bronchial Epithelial Cell Lines. *Cancer Res.* 53, 985–991.

Reece, E., de Almeida Bettio, P. H., and Renwick, J. (2021). Polymicrobial interactions in the cystic fibrosis airway microbiome impact the antimicrobial susceptibility of *Pseudomonas aeruginosa*. *Antibiotics* 10. doi: 10.3390/antibiotics10070827.

Reece, E., Segurado, R., Jackson, A., McClean, S., Renwick, J., and Greally, P. (2017). Co-colonisation with *Aspergillus fumigatus* and *Pseudomonas aeruginosa* is associated with poorer health in cystic fibrosis patients: An Irish registry analysis. *BMC Pulm. Med.* 17, 70. doi: 10.1186/s12890-017-0416-4.

Reece, G. K., and Marimon, J. C. (2019). *Chapter 1 - Enhancing the Therapeutic Potential of Platinumbased Anticancer Agents by Incorporating Clinically Approved Drugs as Ligands*. , eds. A. Casini, A. Vessières, and S. Meier-Menches The Royal Society of Chemistry.

Rex, J. H., Fernandez Lynch, H., Cohen, I. G., Darrow, J. J., and Outterson, K. (2019). Designing development programs for non-traditional antibacterial agents. *Nat. Commun.* 10. doi: 10.1038/s41467-019-11303-9.

Rice, L. B. (2008). Federal Funding for the Study of Antimicrobial Resistance in Nosocomial Pathogens: No ESKAPE. *J. Infect. Dis.* 197, 1079–1081. doi: 10.1086/533452.

Rice, L. B. (2012). Mechanisms of resistance and clinical relevance of resistance to β-lactams, glycopeptides, and fluoroquinolones. *Mayo Clin. Proc.* 87, 198–208. doi: 10.1016/j.mayocp.2011.12.003.

Riquelme, S. A., Liimatta, K., Wong Fok Lung, T., Fields, B., Ahn, D., Chen, D., *et al*. (2020). *Pseudomonas aeruginosa* Utilizes Host-Derived Itaconate to Redirect Its Metabolism to Promote Biofilm Formation. *Cell Metab.* 31, 1091-1106.e6. doi: 10.1016/j.cmet.2020.04.017.

Rochford, G., Molphy, Z., Browne, N., Surlis, C., Devereux, M., McCann, M., *et al*. (2018). In-vivo evaluation of the response of *Galleria mellonella* larvae to novel copper(II) phenanthroline-phenazine complexes. *J. Inorg. Biochem.* 186, 135–146. doi: 10.1016/j.jinorgbio.2018.05.020.

Rochford, G., Molphy, Z., Kavanagh, K., McCann, M., Devereux, M., Kellett, A., *et al*. (2020). Cu(ii) phenanthroline-phenazine complexes dysregulate mitochondrial function and

stimulate apoptosis. *Metallomics* 12, 65–78. doi: 10.1039/c9mt00187e.

Rodnina, M. V. (2018). Translation in prokaryotes. *Cold Spring Harb. Perspect. Biol.* 10, 1–21. doi: 10.1101/cshperspect.a032664.

Rolo, J., Worning, P., Boye Nielsen, J., Sobral, R., Bowden, R., Bouchami, O., *et al*. (2017). Evidence for the evolutionary steps leading to mecA-mediated β-lactam resistance in staphylococci. *PLoS Genet.* 13, 1–22. doi: 10.1371/journal.pgen.1006674.

Rommens, J. M., Iannuzzi, M. C., Kerem, B., Drumm, M. L., Melmer, G., Dean, M., *et al*. (1989). Identification of the Cystic Fibrosis Gene: Chromosome Walking and Jumping. *Science (80-.).* 122, 1059–1065.

Rosenberg, B., Van Camp, L., and Krigas, T. (1965). Inhibition of cell division in Escherichia coli by electrolysis products from a platinum electrode. *Nature* 205, 698–699. doi: 10.1038/205698a0.

Rosenberg, B., Vancamp, L., Trosko, J. E., and Mansour, V. H. (1969). Platinum Compounds: a New Class of Potent Antitumour Agents. *Nature* 222, 385–386. doi: 10.1038/222385a0.

Ross-Gillespie, A., Weigert, M., Brown, S. P., and Kümmerli, R. (2014). Gallium-mediated siderophore quenching as an evolutionarily robust antibacterial treatment. *Evol. Med. Public Heal.* 2014, 18–29. doi: 10.1093/emph/eou003.

RubenMorones-Ramirez, J., Winkler, J. A., Spina, C. S., Collins, J. J., Morones-Ramirez, J. R., Winkler, J. A., *et al*. (2013). Silver Enhances Antibiotic Activity Against Gram-negative Bacteria. *Sci Transl Med.* 5, 1–21. doi: 10.1126/scitranslmed.3006276.Silver.

Ruh, E., Zakka, J., Hoti, K., Fekrat, A., Guler, E., Gazi, U., *et al*. (2019). Extended-spectrum β-lactamase, plasmid-mediated AmpC β-lactamase, fluoroquinolone resistance, and decreased susceptibility to carbapenems in Enterobacteriaceae: Fecal carriage rates and associated risk factors in the community of Northern Cyprus. *Antimicrob. Resist. Infect. Control* 8, 1–10.

doi: 10.1186/s13756-019-0548-9.

Sabin, N. S., Calliope, A. S., Simpson, S. V., Arima, H., Ito, H., Nishimura, T., *et al*. (2020). Implications of human activities for (re)emerging infectious diseases, including COVID-19. *J. Physiol. Anthropol.* 39, 1–12. doi: 10.1186/s40101-020-00239-5.

Sader, H. S., Castanheira, M., Duncan, L. R., and Flamm, R. K. (2018). Antimicrobial Susceptibility of Enterobacteriaceae and *Pseudomonas aeruginosa* Isolates from United States Medical Centers Stratified by Infection Type: Results from the International Network for Optimal Resistance Monitoring (INFORM) Surveillance Program,. *Diagn. Microbiol. Infect. Dis.* 92, 69–74. doi: 10.1016/j.diagmicrobio.2018.04.012.

Sammes, P. G., and Yahioglu, G. (1994). 1,10-Phenanthroline: A versatile ligand. *Chem. Soc. Rev.* 23, 327–334. doi: 10.1039/CS9942300327.

Sarges, E. D. S. N. F., Rodrigues, Y. C., Furlaneto, I. P., de Melo, M. V. H., Brabo, G. L. da C., Lopes, K. C. M., *et al*. (2020). *Pseudomonas aeruginosa* type iii secretion system virulotypes and their association with clinical features of cystic fibrosis patients. *Infect. Drug Resist.* 13, 3771–3781. doi: 10.2147/IDR.S273759.

Saulou-Bérion, C., Gonzalez, I., Enjalbert, B., Audinot, J. N., Fourquaux, I., Jamme, F., *et al*. (2015). Escherichia coli under ionic silver stress: An integrative approach to explore transcriptional, physiological and biochemical responses. *PLoS One* 10, 1–25. doi: 10.1371/journal.pone.0145748.

Schramm, F. D., Schroeder, K., and Jonas, K. (2019). Protein aggregation in bacteria. *FEMS Microbiol. Rev.* 44, 54–72. doi: 10.1093/femsre/fuz026.

Scoffone, V. C., Trespidi, G., Barbieri, G., Irudal, S., Perrin, E., and Buroni, S. (2021). Role of rnd efflux pumps in drug resistance of cystic fibrosis pathogens. *Antibiotics* 10, 1–25. doi: 10.3390/antibiotics10070863.

Sekula, B., and Dauter, Z. (2019). Structural study of agmatine iminohydrolase from Medicago truncatula, the second enzyme of the agmatine route of putrescine biosynthesis in plants. *Front. Plant Sci.* 10, 320. doi: 10.3389/fpls.2019.00320.

Semaniakou, A., Croll, R. P., and Chappe, V. (2019). Animal models in the pathophysiology of cystic fibrosis. *Front. Pharmacol.* 9, 1–16. doi: 10.3389/fphar.2018.01475.

Seo, S. Y., Kim, Y. J., and Park, K. Y. (2019). Increasing Polyamine Contents Enhances the Stress Tolerance via Reinforcement of Antioxidative Properties. *Front. Plant Sci.* 10, 1331. doi: 10.3389/fpls.2019.01331.

Seviour, T., Derlon, N., Dueholm, M. S., Flemming, H. C., Girbal-Neuhauser, E., Horn, H., *et al*. (2019). Extracellular polymeric substances of biofilms: Suffering from an identity crisis. *Water Res.* 151, 1–7. doi: 10.1016/j.watres.2018.11.020.

Shaheen, A., Tariq, A., Iqbal, M., Mirza, O., Haque, A., Walz, T., *et al*. (2021). Mutational Diversity in the Quinolone Resistance-Determining Regions of Type-II Topoisomerases of Salmonella Serovars. *Antibiotics* 10, 1–26. doi: 10.3390/antibiotics10121455.

Sharma, D., Misba, L., and Khan, A. U. (2019). Antibiotics versus biofilm: An emerging battleground in microbial communities. *Antimicrob. Resist. Infect. Control* 8. doi: 10.1186/s13756-019-0533-3.

She, P., Zhou, L., Li, S., Liu, Y., Xu, L., Chen, L., *et al*. (2019). Synergistic microbicidal effect of auranofin and antibiotics against planktonic and biofilm-encased S. aureus and E. faecalis. *Front. Microbiol.* 10, 2453. doi: 10.3389/fmicb.2019.02453.

Sheehan, G., Dixon, A., and Kavanagh, K. (2019). Utilization of *Galleria mellonella* larvae to characterize the development of *Staphylococcus aureus* infection. *Microbiol. (United Kingdom)* 165, 863–875. doi: 10.1099/mic.0.000813.

Sheehan, G., Garvey, A., Croke, M., and Kavanagh, K. (2018). Innate humoral immune defences

in mammals and insects: The same, with differences? *Virulence* 9, 1625–1639. doi: 10.1080/21505594.2018.1526531.

Sheehan, G., and Kavanagh, K. (2019). Proteomic analysis of the responses of *Candida albicans* during infection of *Galleria mellonella* larvae. *J. Fungi* 5, 7. doi: 10.3390/jof5010007.

Shivakumar, L., Shivaprasad, K., and Revanasiddappa, H. D. (2013). SODs, DNA binding and cleavage studies of new Mn(III) complexes with 2-((3-(benzyloxy)pyridin-2-ylimino)methyl)phenol. *Spectrochim. Acta - Part A Mol. Biomol. Spectrosc.* 107, 203–212. doi: 10.1016/j.saa.2013.01.025.

Shulman, A., and White, D. O. (1973). Virostatic activity of 1,10-phenanthroline transition metal chelates: A structure-activity analysis. *Chem. Biol. Interact.* 6, 407–413. doi: 10.1016/0009-2797(73)90060-4.

Sigman, D. S., Graham, D. R., D'Aurora, V., and Stern, A. M. (1979). Oxygen-dependent Cleavage of DNA by the 1,10-Phenantroline Cuprous Complex. *J. Biol. Chem.* 254, 12269–12272.

Silhavy, T. J., Kahne, D., and Walker, S. (2010). The bacterial cell envelope. *Cold Spring Harb. Perspect. Biol.* 2, a000414. doi: 10.1101/cshperspect.a000414.

Silver, L. L. (2011). Challenges of antibacterial discovery. *Clin. Microbiol. Rev.* 24, 71–109. doi: 10.1128/CMR.00030-10.

Skogman, M. E., Vuorela, P. M., and Fallarero, A. (2012). Combining biofilm matrix measurements with biomass and viability assays in susceptibility assessments of antimicrobials against Staphylococcus aureus biofilms. *J. Antibiot. (Tokyo).* 65, 453–459. doi: 10.1038/ja.2012.49.

Skwarczynski, M., Bashiri, S., Yuan, Y., Ziora, Z. M., Nabil, O., Masuda, K., *et al*. (2022). Antimicrobial Activity Enhancers: Towards Smart Delivery of Antimicrobial Agents.

Antibiotics 11, 412. doi: 10.3390/antibiotics11030412.

Slavin, Y. N., Asnis, J., Häfeli, U. O., and Bach, H. (2017). Metal nanoparticles: Understanding the mechanisms behind antibacterial activity. *J. Nanobiotechnology* 15, 1–20. doi: 10.1186/s12951-017-0308-z.

Smoleński, P., Jaros, S. W., Pettinari, C., Lupidi, G., Quassinti, L., Bramucci, M., *et al*. (2013). New water-soluble polypyridine silver(i) derivatives of 1,3,5-triaza-7-phosphaadamantane (PTA) with significant antimicrobial and antiproliferative activities. *Dalt. Trans.* 42, 6572–6581. doi: 10.1039/c3dt33026e.

Sousa, I., Claro, V., Pereira, J. L., Amaral, A. L., Cunha-Silva, L., De Castro, B., *et al*. (2012). Synthesis, characterization and antibacterial studies of a copper(II) levofloxacin ternary complex. *J. Inorg. Biochem.* 110, 64–71. doi: 10.1016/j.jinorgbio.2012.02.003.

Speziale, P., Arciola, C. R., and Pietrocola, G. (2019). Fibronectin and Its Role in Human Infective Diseases. *Cells* 8. doi: 10.3390/cells8121516.

Stacy, A., McNally, L., Darch, S. E., Brown, S. P., and Whiteley, M. (2016). The biogeography of polymicrobial infection. *Nat. Rev. Microbiol.* 14, 93–105. doi: 10.1038/nrmicro.2015.8.

Stefani, S., Campana, S., Cariani, L., Carnovale, V., Colombo, C., Lleo, M. M., *et al*. (2017). Relevance of multidrug-resistant *Pseudomonas aeruginosa* infections in cystic fibrosis. *Int. J. Med. Microbiol.* 307, 353–362. doi: 10.1016/j.ijmm.2017.07.004.

Steitz, T. A., and Moore, P. B. (2003). RNA, the first macromolecular catalyst: The ribosome is a ribozyme. *Trends Biochem. Sci.* 28, 411–418. doi: 10.1016/S0968-0004(03)00169-5.

Suay-García, B., and Pérez-Gracia, M. T. (2019). Present and future of carbapenem-resistant Enterobacteriaceae (CRE) infections. *Antibiotics* 8. doi: 10.3390/antibiotics8030122.

Tabassum, S., Asim, A., Arjmand, F., Afzal, M., and Bagchi, V. (2012). Synthesis and characterization of copper(II) and zinc(II)-based potential chemotherapeutic compounds:

Their biological evaluation viz. DNA binding profile, cleavage and antimicrobial activity. *Eur. J. Med. Chem.* 58, 308–316. doi: 10.1016/j.ejmech.2012.09.051.

Tacconelli, E., Carrara, E., Savoldi, A., Harbarth, S., Mendelson, M., Monnet, D. L., *et al*. (2018). Discovery, research, and development of new antibiotics: the WHO priority list of antibiotic-resistant bacteria and tuberculosis. *Lancet Infect. Dis.* 18, 318–327. doi: 10.1016/S1473-3099(17)30753-3.

Tang, S. Y., Zhang, S. W., Wu, J. D., Wu, F., Zhang, J., Dong, J. T., *et al*. (2018). Comparison of mono- and combination antibiotic therapy for the treatment of *Pseudomonas aeruginosa* bacteraemia: A cumulative meta-analysis of cohort studies. *Exp. Ther. Med.* 15, 2418–2428. doi: 10.3892/etm.2018.5727.

Tao, Y., Zhou, K., Xie, L., Xu, Y., Han, L., Ni, Y., *et al*. (2020). Emerging coexistence of three PMQR genes on a multiple resistance plasmid with a new surrounding genetic structure of qnrS2 in E. coli in China. *Antimicrob. Resist. Infect. Control* 9, 1–8. doi: 10.1186/s13756-020-00711-y.

Tay, C. X., Quah, S. Y., Lui, J. N., Yu, V. S. H., and Tan, K. S. (2015). Matrix metalloproteinase inhibitor as an antimicrobial agent to eradicate Enterococcus faecalis biofilm. *J. Endod.* 41, 858–863. doi: 10.1016/j.joen.2015.01.032.

Tchounwou, P. B., Dasari, S., Noubissi, F. K., Ray, P., and Kumar, S. (2021). Advances in our understanding of the molecular mechanisms of action of cisplatin in cancer therapy. *J. Exp. Pharmacol.* 13, 303–328. doi: 10.2147/JEP.S267383.

Testa, R., Cantón, R., Giani, T., Morosini, M. I., Nichols, W. W., Seifert, H., *et al*. (2015). In vitro activity of ceftazidime, ceftaroline and aztreonam alone and in combination with avibactam against European Gram-negative and Gram-positive clinical isolates. *Int. J. Antimicrob. Agents* 45, 641–646. doi: 10.1016/j.ijantimicag.2014.12.033.

Tetz, G. V., Artemenko, N. K., and Tetz, V. V. (2009). Effect of DNase and antibiotics on biofilm

characteristics. *Antimicrob. Agents Chemother*. 53, 1204–1209. doi: 10.1128/AAC.00471-08.

The European Centre for Disease Prevention and Control (2019). Antimicrobial Resistance Tackling the Burden in the European Union Briefing note for EU/EEA countries Contents. 1–30. Available at: https://www.oecd.org/health/health-systems/AMR-Tackling-the-Burden-in-the-EU-OECD-ECDC-Briefing-Note-2019.pdf [Accessed March 10, 2020].

Theuretzbacher, U. (2020). Dual-mechanism antibiotics. *Nat. Microbiol.* 5, 984–985. doi: 10.1038/s41564-020-0767-0.

Theuretzbacher, U., Gottwalt, S., Beyer, P., Butler, M., Czaplewski, L., Lienhardt, C., *et al.* (2019). Analysis of the clinical antibacterial and antituberculosis pipeline. *Lancet Infect. Dis.* 19, e40–e50. doi: 10.1016/S1473-3099(18)30513-9.

Theuretzbacher, U., and Piddock, L. J. V. (2019). Non-traditional Antibacterial Therapeutic Options and Challenges. *Cell Host Microbe* 26, 61–72. doi: 10.1016/j.chom.2019.06.004.

Thi, M. T. T., Wibowo, D., and Rehm, B. H. A. (2020). *Pseudomonas aeruginosa* biofilms. *Int. J. Mol. Sci.* 21, 1–25. doi: 10.3390/ijms21228671.

Thomaz, L., Gustavo de Almeida, L., Silva, F. R. O., Cortez, M., Taborda, C. P., and Spira, B. (2020). In vivo Activity of Silver Nanoparticles Against *Pseudomonas aeruginosa* Infection in *Galleria mellonella*. *Front. Microbiol.* 11, 582107. doi: 10.3389/fmicb.2020.582107.

Thornton, L., Dixit, V., Assad, L. O. N., Ribeiro, T. P., Queiroz, D. D., Kellett, A., *et al*. (2016). Water-soluble and photo-stable silver(I) dicarboxylate complexes containing 1,10-phenanthroline ligands: Antimicrobial and anticancer chemotherapeutic potential, DNA interactions and antioxidant activity. *J. Inorg. Biochem.* 159, 120–132. doi: 10.1016/j.jinorgbio.2016.02.024.

Tong, S. Y. C., Davis, J. S., Eichenberger, E., Holland, T. L., and Fowler, V. G. (2015).

Staphylococcus aureus infections: Epidemiology, pathophysiology, clinical manifestations, and management. *Clin. Microbiol. Rev.* 28, 603–661. doi: 10.1128/CMR.00134-14.

Tooke, C. L., Hinchliffe, P., Bragginton, E. C., Colenso, C. K., Hirvonen, V. H. A., Takebayashi, Y., *et al*. (2019). β-Lactamases and β-Lactamase Inhibitors in the 21st Century. *J. Mol. Biol.* 431, 3472–3500. doi: 10.1016/j.jmb.2019.04.002.

Tribedi, P., and Sil, A. K. (2014). Cell surface hydrophobicity: A key component in the degradation of polyethylene succinate by Pseudomonas sp. AKS2. *J. Appl. Microbiol.* 116, 295–303. doi: 10.1111/jam.12375.

Tsai, C. J. Y., Loh, J. M. S., and Proft, T. (2016). *Galleria mellonella* infection models for the study of bacterial diseases and for antimicrobial drug testing. *Virulence* 7, 214–229. doi: 10.1080/21505594.2015.1135289.

Tuon, F. F., Dantas, L. R., Suss, P. H., and Tasca Ribeiro, V. S. (2022). Pathogenesis of the *Pseudomonas aeruginosa* Biofilm: A Review. *Pathogens* 11. doi: 10.3390/pathogens11030300.

Turian, G. (1951). Tuberculostatic action of o-phenanthroline. *Schweiz. Z. Pathol. Bakteriol.* 14, 338–44.

Turner, M. R. J. (2021). Antimicrobial metals. *Heal. Med.* Available at: https://researchfeatures.com/antimicrobial-metals-recycled-weapon-bacteria/

U.S. Food and Drug Administration (2018). U S Food and Drug Administration Home Page. doi: 1-888-INFO-FDA.

Ude, Z., Flothkötter, N., Sheehan, G., Brennan, M., Kavanagh, K., and Marmion, C. J. (2021). Multi-targeted metallo-ciprofloxacin derivatives rationally designed and developed to overcome antimicrobial resistance. *Int. J. Antimicrob. Agents* 58, 106449. doi: 10.1016/j.ijantimicag.2021.106449.

Ude, Z., Kavanagh, K., Twamley, B., Pour, M., Gathergood, N., Kellett, A., *et al*. (2019). A new class of prophylactic metallo-antibiotic possessing potent anti-cancer and anti-microbial properties. *Dalt. Trans.* 48, 8578–8593. doi: 10.1039/c9dt00250b.

Ullah, H., and Ali, S. (2017). "Classification of Anti-Bacterial Agents and Their Functions," in *Antibacterial Agents* (InTech). doi: 10.5772/intechopen.68695.

UniProt hemE - Uroporphyrinogen decarboxylase - *Pseudomonas aeruginosa* (strain ATCC 15692 / DSM 22644 / CIP 104116 / JCM 14847 / LMG 12228 / 1C / PRS 101 / PAO1) - hemE gene & amp; protein. Available at: https://www.uniprot.org/uniprot/P00282%0Ahttps://www.uniprot.org/uniprot/P95458 [Accessed February 8, 2022].

Valentini, M., and Filloux, A. (2016). Biofilms and Cyclic di-GMP (c-di-GMP) Signaling: Lessons from *Pseudomonas aeruginosa* and Other Bacteria. *J. Biol. Chem.* 291, 12547–12555. doi: 10.1074/JBC.R115.711507.

Valentini, M., Gonzalez, D., Mavridou, D. A., and Filloux, A. (2018). Lifestyle transitions and adaptive pathogenesis of *Pseudomonas aeruginosa*. *Curr. Opin. Microbiol.* 41, 15–20. doi: 10.1016/j.mib.2017.11.006.

Van Acker, H., and Coenye, T. (2017). The Role of Reactive Oxygen Species in Antibiotic-Mediated Killing of Bacteria. *Trends Microbiol.* 25, 456–466. doi: 10.1016/j.tim.2016.12.008.

Van den Bossche, S., De Broe, E., Coenye, T., Van Braeckel, E., and Crabbé, A. (2021). The cystic fibrosis lung microenvironment alters antibiotic activity: Causes and effects. *Eur. Respir. Rev.* 30. doi: 10.1183/16000617.0055-2021.

Vargas Rigo, G., Petro-Silveira, B., Devereux, M., McCann, M., Souza Dos Santos, A. L., and Tasca, T. (2019). Anti-Trichomonas vaginalis activity of 1,10-phenanthroline-5,6-dione-based metallodrugs and synergistic effect with metronidazole. *Parasitology* 146, 1179–

1183. doi: 10.1017/S003118201800152X.

Veerachamy, S., Yarlagadda, T., Manivasagam, G., and Yarlagadda, P. K. (2014). Bacterial adherence and biofilm formation on medical implants: A review. *Proc. Inst. Mech. Eng. Part H J. Eng. Med.* 228, 1083–1099. doi: 10.1177/0954411914556137.

Ventura, R. F., Galdino, A. C. M., Viganor, L., Schuenck, R. P., Devereux, M., McCann, M., *et al*. (2020). Antimicrobial action of 1,10-phenanthroline-based compounds on carbapenemase-producing Acinetobacter baumannii clinical strains: efficacy against planktonic- and biofilm-growing cells. *Brazilian J. Microbiol.* 51, 1703–1710. doi: 10.1007/s42770-020-00351-9.

Vestby, L. K., Grønseth, T., Simm, R., and Nesse, L. L. (2020). Bacterial biofilm and its role in the pathogenesis of disease. *Antibiotics* 9. doi: 10.3390/antibiotics9020059.

Vianez Peregrino, I., Ferreira Ventura, R., Borghi, M., Pinto Schuenck, R., Devereux, M., McCann, M., *et al*. (2021). Antibacterial activity and carbapenem re-sensitizing ability of 1,10-phenanthroline-5,6-dione and its metal complexes against KPC-producing Klebsiella pneumoniae clinical strains. *Lett. Appl. Microbiol.* 73, 139–148. doi: 10.1111/lam.13485.

Viganor, L., Galdino, A. C. M., Nunes, A. P. F., Santos, K. R. N., Branquinha, M. H., Devereux, M., *et al*. (2016a). Anti-*Pseudomonas aeruginosa* activity of 1,10-phenanthroline-based drugs against both planktonic- and biofilm-growing cells. *J. Antimicrob. Chemother*. 71, 128–134. doi: 10.1093/jac/dkv292.

Viganor, L., Howe, O., McCarron, P., McCann, M., and Devereux, M. (2016b). The Antibacterial Activity of Metal Complexes Containing 1,10- phenanthroline: Potential as Alternative Therapeutics in the Era of Antibiotic Resistance. *Curr. Top. Med. Chem.* 17, 1280–1302. doi: 10.2174/1568026616666161003143333.

Viganor, L., Howe, O., McCarron, P., McCann, M., and Devereux, M. (2016c). The Antibacterial Activity of Metal Complexes Containing 1,10- phenanthroline: Potential as Alternative

Therapeutics in the Era of Antibiotic Resistance. *Curr. Top. Med. Chem.* 17, 1280–1302. doi: 10.2174/1568026616666161003143333.

Viganor, L., Skerry, C., McCann, M., and Devereux, M. (2015). Tuberculosis: An Inorganic Medicinal Chemistry Perspective. *Curr. Med. Chem.* 22, 2199–2224. doi: 10.2174/0929867322666150408112357.

Vos, S. M., Tretter, E. M., Schmidt, B. H., and Berger, J. M. (2011). All tangled up: How cells direct, manage and exploit topoisomerase function. *Nat. Rev. Mol. Cell Biol.* 12, 827–841. doi: 10.1038/nrm3228.

Walkty, A., Lagace-Wiens, P., Adam, H., Baxter, M., Karlowsky, J., Mulvey, M. R., *et al*. (2017). Antimicrobial susceptibility of 2906 *Pseudomonas aeruginosa* clinical isolates obtained from patients in Canadian hospitals over a period of 8 years: Results of the Canadian Ward surveillance study (CANWARD), 2008–2015. *Diagn. Microbiol. Infect. Dis.* 87, 60–63. doi: 10.1016/j.diagmicrobio.2016.10.003.

Wang, C., Chen, W., Xia, A., Zhang, R., Huang, Y., Yang, S., *et al*. (2019a). Carbon Starvation Induces the Expression of PprB-Regulated Genes in *Pseudomonas aeruginosa*. *Appl. Environ. Microbiol.* 85. doi: 10.1128/aem.01705-19.

Wang, C., Yang, D., Wang, Y., and Ni, W. (2022). Cefiderocol for the Treatment of Multidrug-Resistant Gram-Negative Bacteria: A Systematic Review of Currently Available Evidence. *Front. Pharmacol.* 13, 1–13. doi: 10.3389/fphar.2022.896971.

Wang, D., and Lippard, S. J. (2005). Cellular processing of platinum anticancer drugs. *Nat. Rev. Drug Discov.* 4, 307–320. doi: 10.1038/nrd1691.

Wang, H., Wang, M., Xu, X., Gao, P., Xu, Z., Zhang, Q., *et al*. (2021a). Multi-target mode of action of silver against Staphylococcus aureus endows it with capability to combat antibiotic resistance. *Nat. Commun.* 12, 1–16. doi: 10.1038/s41467-021-23659-y.

Wang, H., Yan, A., Liu, Z., Yang, X., Xu, Z., Wang, Y., *et al*. (2019b). Deciphering molecular mechanism of silver by integrated omic approaches enables enhancing its antimicrobial efficacy in E. coli. *PLOS Biol.* 17, e3000292. doi: 10.1371/JOURNAL.PBIO.3000292.

Wang, R., Van Dorp, L., Shaw, L. P., Bradley, P., Wang, Q., Wang, X., *et al*. (2018a). The global distribution and spread of the mobilized colistin resistance gene mcr-1. *Nat. Commun.* 9, 1–9. doi: 10.1038/s41467-018-03205-z.

Wang, S., König, G., Roth, H. J., Fouché, M., Rodde, S., and Riniker, S. (2021b). Effect of Flexibility, Lipophilicity, and the Location of Polar Residues on the Passive Membrane Permeability of a Series of Cyclic Decapeptides. *J. Med. Chem.* 64, 12761–12773. doi: 10.1021/acs.jmedchem.1c00775.

Wang, S., Liu, X., Liu, H., Zhang, L., Guo, Y., Yu, S., *et al*. (2015). The exopolysaccharide Psl-eDNA interaction enables the formation of a biofilm skeleton in *Pseudomonas aeruginosa*. *Environ. Microbiol. Rep.* 7, 330–340. doi: 10.1111/1758-2229.12252.

Wang, X., Wang, Y., Zhou, Y., Li, J., Yin, W., Wang, S., *et al*. (2018b). Emergence of a novel mobile colistin resistance gene, mcr-8, in NDM-producing Klebsiella pneumoniae article. *Emerg. Microbes Infect.* 7, 1–9. doi: 10.1038/s41426-018-0124-z.

Wang, X., and Zhao, X. (2009). Contribution of oxidative damage to antimicrobial lethality. *Antimicrob. Agents Chemother.* 53, 1395–402. doi: 10.1128/AAC.01087-08.

Wang, Y., Tian, G. B., Zhang, R., Shen, Y., Tyrrell, J. M., Huang, X., *et al*. (2017). Prevalence, risk factors, outcomes, and molecular epidemiology of mcr-1-positive Enterobacteriaceae in patients and healthy adults from China: an epidemiological and clinical study. *Lancet Infect. Dis.* 17, 390–399. doi: 10.1016/S1473-3099(16)30527-8.

Wax, P. M. (1995). Elixirs, diluents, and the passage of the 1938 federal food, drug and cosmetic act. *Ann. Intern. Med.* 122, 456–461. doi: 10.7326/0003-4819-122-6-199503150-00009.

Weber, D. K., Sani, M. A., Downton, M. T., Separovic, F., Keene, F. R., and Collins, J. G. (2016). Membrane Insertion of a Dinuclear Polypyridylruthenium(II) Complex Revealed by Solid-State NMR and Molecular Dynamics Simulation: Implications for Selective Antibacterial Activity. *J. Am. Chem. Soc.* 138, 15267–15277. doi: 10.1021/jacs.6b09996.

Werner, G., Coque, T. M., Franz, C. M. A. P., Grohmann, E., Hegstad, K., Jensen, L., *et al*. (2013). Antibiotic resistant enterococci-Tales of a drug resistance gene trafficker. *Int. J. Med. Microbiol.* 303, 360–379. doi: 10.1016/j.ijmm.2013.03.001.

WHO (2017). Prioritization of pathogens to guide discovery, research and development of new antibiotics for drug resistant bacterial infections, including tuberculosis. *Essent. Med. Heal. Prod.*, 88. doi: WHO reference number: WHO/EMP/IAU/2017.12.

WHO (2019). Tuberculosis. *World Heal. Organ.*, 1–10. Available at: https://www.who.int/news-room/fact-sheets/detail/tuberculosis [Accessed March 10, 2020].

WHO (2021). *2020 Antibacterial Agents in Clinical and Preclinical Development*. Available at: https://www.who.int/publications/i/item/9789240021303.

Woodworth, B. A., Tamashiro, E., Bhargave, G., Cohen, N. A., and Palmer, J. N. (2008). An in vitro model of *Pseudomonas aeruginosa* biofilms on viable airway epithelial cell monolayers. *Am. J. Rhinol.* 22, 235–238. doi: 10.2500/ajr.2008.22.3178.

Wu, J., and Xi, C. (2009). Evaluation of different methods for extracting extracellular DNA from the biofilm matrix. *Appl. Environ. Microbiol.* 75, 5390–5. doi: 10.1128/AEM.00400-09.

Wu, Q., Patočka, J., and Kuča, K. (2018). Insect antimicrobial peptides, a mini review. *Toxins (Basel).* 10. doi: 10.3390/toxins10110461.

Xavier, B. B., Lammens, C., Ruhal, R., Malhotra-Kumar, S., Butaye, P., Goossens, H., *et al*. (2016). Identification of a novel plasmid-mediated colistinresistance gene, mcr-2, in Escherichia coli, Belgium, june 2016. *Eurosurveillance* 21, 30280. doi: 10.2807/1560-

7917.ES.2016.21.27.30280.

Yan, S., and Wu, G. (2019). Can Biofilm Be Reversed Through Quorum Sensing in *Pseudomonas aeruginosa*? *Front. Microbiol.* 10, 1–9. doi: 10.3389/fmicb.2019.01582.

Yang, Y. Q., Li, Y. X., Lei, C. W., Zhang, A. Y., and Wang, H. N. (2018). Novel plasmid-mediated colistin resistance gene mcr-7.1 in Klebsiella pneumoniae. *J. Antimicrob. Chemother*. 73, 1791–1795. doi: 10.1093/jac/dky111.

Yin, W., Li, H., Shen, Y., Liu, Z., Wang, S., Shen, Z., *et al*. (2017). Novel plasmid-mediated colistin resistance gene mcr-3 in Escherichia coli. *MBio* 8, 1–2. doi: 10.1128/mBio.00543-17.

Yushchuk, O., Binda, E., and Marinelli, F. (2020). Glycopeptide Antibiotic Resistance Genes: Distribution and Function in the Producer Actinomycetes. *Front. Microbiol.* 11. doi: 10.3389/fmicb.2020.01173.

Zandi, T. A., and Townsend, C. A. (2021). Competing off-loading mechanisms of meropenem from an L,D-transpeptidase reduce antibiotic effectiveness. *Proc. Natl. Acad. Sci. U. S. A.* 118, 1–7. doi: 10.1073/pnas.2008610118.

Zgurskaya, H. I., López, C. A., and Gnanakaran, S. (2016). Permeability Barrier of Gram-Negative Cell Envelopes and Approaches to Bypass It. *ACS Infect. Dis.* 1, 512–522. doi: 10.1021/acsinfecdis.5b00097.

Zhanel, G. G., Golden, A. R., Zelenitsky, S., Wiebe, K., Lawrence, C. K., Adam, H. J., *et al*. (2019). Cefiderocol: A Siderophore Cephalosporin with Activity Against Carbapenem-Resistant and Multidrug-Resistant Gram-Negative Bacilli. *Drugs* 79, 271–289. doi: 10.1007/s40265-019-1055-2.

Zhanel, G. G., Love, R., Adam, H., Golden, A., Zelenitsky, S., Schweizer, F., *et al*. (2015). Tedizolid: A novel oxazolidinone with potent activity against multidrug-resistant gram-

positive pathogens. *Drugs* 75, 253–270. doi: 10.1007/s40265-015-0352-7.

Zhang, K., Li, X., Yu, C., and Wang, Y. (2020). Promising Therapeutic Strategies Against Microbial Biofilm Challenges. *Front. Cell. Infect. Microbiol.* 10. doi: 10.3389/fcimb.2020.00359.

Zielinski, J. M., Luke, J. J., Guglietta, S., and Krieg, C. (2021). High Throughput Multi-Omics Approaches for Clinical Trial Evaluation and Drug Discovery. *Front. Immunol.* 12, 1–10. doi: 10.3389/fimmu.2021.590742.

Zipper, H. (2003). Mechanisms underlying the impact of humic acids on DNA quantification by SYBR Green I and consequences for the analysis of soils and aquatic sediments. *Nucleic Acids Res.* 31, 39e – 39. doi: 10.1093/nar/gng039.

Zoroddu, M. A., Zanetti, S., Pogni, R., and Basosi, R. (1996). An electron spin resonance study and antimicrobial activity of copper(II)-phenanthroline complexes. *J. Inorg. Biochem.* 63, 291–300. doi: 10.1016/0162-0134(96)00015-3.

Zou, L., Wang, J., Gao, Y., Ren, X., Rottenberg, M. E., Lu, J., *et al*. (2018). Synergistic antibacterial activity of silver with antibiotics correlating with the upregulation of the ROS production. *Sci. Rep.* 8. doi: 10.1038/s41598-018-29313-w.

Appendices

6.1.1 MICs and MBCs of metal complexes and controls against *Staphylococcus aureus* panel

Compounds	*Staphylococcus aureus*											
	ATCC 29213		MRSA1		MRSA2		MRSA3		MRSA4		MRSA5	
	MIC	MBC	MIC	MBC	MIC	MBC	MIC	MBC	MIC	MBC	MIC	MBC
Antibiotic controls												
Ciprofloxacin	0.5	1	>256	-	>256	-	>256	-	>256	-	>256	
Gentamicin	1	4	64	256	128	>256	1	4	1	4	1	4
Copper(II) complexes												
Cu-ph-phen	1	64	32	128	32	128	32	128	32	128	32	128
Cu-oda	>256	-	>256	-	>256	-	>256	-	>256	-	>256	-
Cu-oda-phen	1	64	16	128	16	128	16	128	16	128	16	128
Cu_2-oda-phen	1	64	16	128	16	128	16	128	8	128	16	128
Cu-tdda	>256	-	>256	-	>256	-	>256	-	>256	-	>256	-
Cu-tdda-phen	1	4	8	32	8	32	8	32	4	32	8	32
Manganese(II) complexes												
Mn-bda	>256	-	>256	-	>256	-	>256	-	>256	-	>256	-
Mn-bda-phen	32	256	128	>256	128	>256	128	>256	128	>256	128	>256
Mn-pda	>256	-	>256	-	>256	-	>256	-	>256	-	>256	-
Mn-pda-phen	4	16	32	256	32	256	16	128	8	128	16	128
Mn-hxda	>256	-	>256	-	>256	-	>256	-	>256	-	>256	-
Mn-hxda-phen	4	16	128	>256	128	>256	128	>256	128	>256	128	>256
Mn-hpda	>256	-	>256	-	>256	-	>256	-	>256	-	>256	-
Mn-hpda-phen	>256	-	>256	-	>256	-	>256	-	>256	-	>256	-
Mn-oda	>256	-	>256	-	>256	-	>256	-	>256	-	>256	-
Mn-oda-phen	32	128	64	256	128	>256	128	>256	128	>256	128	>256
Mn-tdda	>256	-	>256	-	>256	-	>256	-	>256	-	>256	-
Mn-tdda-phen	1	32	1	64	8	128	8	128	8	128	8	128
Silver(I) complexes												
Ag-udda	32	128	32	128	32	128	32	128	32	64	32	128
Ag-udda-phen	16	64	16	64	16	64	16	64	16	64	16	64
Ag-tdda	32	64	32	64	32	128	32	64	32	64	32	64
Ag-tdda-phen	4	32	8	32	8	64	8	32	8	32	8	32
Controls												
$CuCl_2$	>256	-	>256	-	>256	-	>256	-	>256	-	>256	-
$MnCl_2$	>256	-	>256	-	>256	-	>256	-	>256	-	>256	-
$AgNO_3$	4	16	16	128	16	64	16	64	16	64	16	64
Phen	64	>256	128	>256	128	>256	128	>256	128	>256	128	>256

Table A.9 Minimal inhibitory concentration (MIC) and minimal bactericidal concentration (MBC) values obtained for *Staphylococcus aureus* sub-panel exposed to novel metal complexes and their controls using the broth micro-dilution assay. Values are presented as µg/mL.

6.1.2 MICs and MBCs of metal complexes and controls against *Enterococcus* spp panel

Compounds	*Enterococcus faecalis* and *Enterococcus faecium*													
	ATCC 29212		VRE1		VRE2		VRE3		VRE4		VRE5		VRE6	
	MIC	MBC	MIC	MBC	MIC	MBC	MIC	MBC	MIC	MBC	MIC	MBC	MIC	MBC
Antibiotic controls														
Ciprofloxacin	1	2	>256	-	>256	-	>256	-	>256	-	>256	-	>256	-
Gentamicin	8	32	>256	-	>256	-	>256	-	>256	-	>256	-	>256	-
Copper(II) complexes														
Cu-ph-phen	32	128	256	>256	256	>256	256	>256	128	>256	256	>256	256	>256
Cu-oda	>256	-	>256	-	>256	-	>256	-	>256	-	>256	-	>256	-
Cu-oda-phen	16	128	256	>256	32	256	128	>256	128	>256	128	>256	256	>256
Cu_2-oda-phen	64	128	256	>256	256	>256	256	>256	128	>256	256	>256	256	>256
Cu-tdda	>256	-	>256	-	>256	-	>256	-	>256	-	>256	-	>256	-
Cu-tdda-phen	16	32	64	128	16	32	64	128	64	128	64	128	64	128
Manganese(II) complexes														
Mn-bda	>256	-	>256	-	>256	-	>256	-	>256	-	>256	-	>256	-
Mn-bda-phen	>256	-	>256	-	>256	-	>256	-	>256	-	>256	-	>256	-
Mn-pda	>256	-	>256	-	>256	-	>256	-	>256	-	>256	-	>256	-
Mn-pda-phen	32	64	>256	-	>256	-	>256	-	>256	-	>256	-	>256	-
Mn-hxda	>256	-	>256	-	>256	-	>256	-	>256	-	>256	-	>256	-
Mn-hxda-phen	>256	-	>256	-	>256	-	>256	-	>256	-	>256	-	>256	-
Mn-hpda	>256	-	>256	-	>256	-	>256	-	>256	-	>256	-	>256	-
Mn-hpda-phen	>256	-	>256	-	>256	-	>256	-	>256	-	>256	-	>256	-
Mn-oda	>256	-	>256	-	>256	-	>256	-	>256	-	>256	-	>256	-
Mn-oda-phen	32	128	>256	-	>256	-	>256	-	>256	-	>256	-	>256	-
Mn-tdda	>256	-	>256	-	>256	-	>256	-	>256	-	>256	-	>256	-
Mn-tdda-phen	16	32	64	>256	32	128	64	>256	32	>256	32	>256	32	>256
Silver(I) complexes														
Ag-udda	32	128	32	128	32	128	32	128	32	128	32	128	32	128
Ag-udda-phen	8	32	16	64	16	64	16	64	16	64	16	64	16	64
Ag-tdda	32	64	32	128	32	128	32	128	32	128	32	128	32	128
Ag-tdda-phen	8	32	16	64	16	64	16	64	16	64	16	64	16	64
Controls														
$CuCl_2$	>256	-	>256	-	>256	-	>256	-	>256	-	>256	-	>256	-
$MnCl_2$	>256	-	>256	-	>256	-	>256	-	>256	-	>256	-	>256	-
$AgNO_3$	4	16	4	128	4	128	4	128	4	128	4	128	4	128
Phen	64	>256	128	>256	128	>256	128	>256	128	>256	128	>256	128	>256

Table A.10 Minimal inhibitory concentration (MIC) and minimal bactericidal concentration (MBC) values obtained for *Enterococcus* sub-panel exposed to novel metal complexes and their controls using the broth micro-dilution assay. Values are presented as µg/mL.

6.1.3 MICs and MBCs of metal complexes and controls against resistant *Enterobacterales* panel

Compounds	*Enterobacterales strains*													
	ATCC 25922		ATCC 10031		ATCC 700603		ESBL1		MBL1		ATCC BAA1705		KPC1	
	MIC	MBC	MIC	MBC	MIC	MBC	MIC	MBC	MIC	MBC	MIC	MBC	MIC	MBC
Antibiotic controls														
Meropenem	0.03	0.12	1	4	1	4	2	8	>256	-	128	>256	>256	-
Gentamicin	0.5	1	16	64	16	64	>256	-	>256	-	2	8	>256	-
Copper(II) complexes														
Cu-ph-phen	>256	-	>256	-	>256	-	>256	-	>256	-	>256	-	>256	-
Cu-oda	>256	-	>256	-	>256	-	>256	-	>256	-	>256	-	>256	-
Cu-oda-phen	64	>256	64	>256	128	>256	128	>256	128	>256	256	>256	>256	-
Cu_2-oda-phen	64	>256	64	>256	128	>256	128	>256	128	>256	256	>256	>256	-
Cu-tdda	>256	-	>256	-	>256	-	>256	-	>256	-	>256	-	>256	-
Cu-tdda-phen	16	32	32	64	32	64	64	256	16	256	64	256	>256	-
Manganese(II) complexes														
Mn-bda	>256	-	>256	-	>256	-	>256	-	>256	-	>256	-	>256	-
Mn-bda-phen	32	64	128	>256	>256	-	>256	-	>256	-	>256	-	>256	-
Mn-pda	>256	-	>256	-	>256	-	>256	-	>256	-	>256	-	>256	-
Mn-pda-phen	32	64	128	>256	>256	-	>256	-	>256	-	>256	-	>256	-
Mn-hxda	>256	-	>256	-	>256	-	>256	-	>256	-	>256	-	>256	-
Mn-hxda-phen	32	64	128	>256	>256	-	>256	-	>256	-	>256	-	>256	-
Mn-hpda	>256	-	>256	-	>256	-	>256	-	>256	-	>256	-	>256	-
Mn-hpda-phen	>256	-	>256	-	>256	-	>256	-	>256	-	>256	-	>256	-
Mn-oda	>256	-	>256	-	>256	-	>256	-	>256	-	>256	-	>256	-
Mn-oda-phen	64	>256	>256	-	>256	-	>256	-	128	>256	>256	-	>256	-
Mn-tdda	128	>256	>256	-	>256	-	>256	-	>256	-	>256	-	>256	-
Mn-tdda-phen	16	32	32	128	128	>256	64	128	32	128	64	128	128	>256
Silver(I) complexes														
Ag-udda	16	32	32	64	64	128	64	128	32	128	16	128	32	128
Ag-udda-phen	16	32	64	128	32	64	16	64	32	>256	32	>256	64	>256
Ag-tdda	16	64	64	256	64	128	64	128	64	128	64	128	64	128
Ag-tdda-phen	8	32	16		32	64	16	64	32	64	64	128	64	128
Controls														
$AgNO_3$	16	32	16	32	32	128	32	128	32	128	16	128	32	256
$CuCl_2$	>256	-	>256	-	>256	-	>256	-	>256	-	>256	-	>256	-
$MnCl_2$	>256	-	>256	-	>256	-	>256	-	>256	-	>256	-	>256	-
Phen	64	>256	64	>256	64	>256	128	>256	64	128	128	>256	128	>256

Table A.11 Minimal inhibitory concentration (MIC) and minimal bactericidal concentration (MBC) values obtained for *Enterobacterales* sub-panel exposed to novel metal complexes and their controls using the broth micro-dilution assay. Values are presented as μg/mL.

6.1.4 MICs and MBCs of metal complexes and controls against *Pseudomonas aeruginosa* panel

Compounds	*Pseudomonas aeruginosa*											
	ATCC 27853		PAO1		PA1		PA2		PA3		PA4	
	MIC	MBC	MIC	MBC	MIC	MBC	MIC	MBC	MIC	MBC	MIC	MBC
Antibiotic controls												
Meropenem	0.5	2	1	4	2	8	>256	-	4	16	256	>256
Gentamicin	1	4	2	8	16	128	>256	-	>256	-	>256	-
Copper(II) complexes												
Cu-ph-phen	>256	-	>256	-	>256	-	>256	-	>256	-	>256	-
Cu-oda	>256	-	>256	-	>256	-	>256	-	>256	-	>256	-
Cu-oda-phen	64	>256	64	>256	128	>256	128	>256	128	>256	256	>256
Cu_2-oda-phen	64	>256	64	>256	128	>256	128	>256	128	>256	256	>256
Cu-tdda	>256	-	128	256	>256	-	>256	-	>256	-	>256	-
Cu-tdda-phen	16	32	32	64	32	64	64	256	16	256	64	256
Manganese(II) complexes												
Mn-bda	>256	-	>256	-	>256	-	>256	-	>256	-	>256	-
Mn-bda-phen	>256	-	>256	-	>256	-	>256	-	>256	-	>256	-
Mn-pda	>256	-	>256	-	>256	-	>256	-	>256	-	>256	-
Mn-pda-phen	>256	-	>256	-	>256	-	>256	-	>256	-	>256	-
Mn-hxda	>256	-	>256	-	>256	-	>256	-	>256	-	>256	-
Mn-hxda-phen	>256	-	>256	-	>256	-	>256	-	>256	-	>256	-
Mn-hpda	>256	-	>256	-	>256	-	>256	-	>256	-	>256	-
Mn-hpda-phen	>256	-	>256	-	>256	-	>256	-	>256	-	>256	-
Mn-oda	>256	-	>256	-	>256	-	>256	-	>256	-	>256	-
Mn-oda-phen	64	128	64	128	128	>256	>256	-	128	>256	>256	-
Mn-tdda	64	128	>256	-	128	>256	>256	-	128	>256	>256	-
Mn-tdda-phen	16	32	32	64	32	64	64	128	32	128	64	256
Silver(I) complexes												
Ag-udda	64	128	32	256	128	256	256	>256	128	256	>256	-
Ag-udda-phen	16	32	32	64	32	128	16	64	32	128	32	128
Ag-tdda	128	256	128	256	128	256	256	>256	256	>256	>256	-
Ag-tdda-phen	8	32	32	64	8	32	32	64	32	64	64	128
Controls												
$CuCl_2$	>256	-	>256	-	>256	-	>256	-	>256	-	>256	-
$MnCl_2$	>256	-	>256	-	>256	-	>256	-	>256	-	>256	-
$AgNO_3$	16	32	256		16	64	64	128	32	128	128	>256
Phen	64	>256	64	>256	64	>256	128	>256	128	>256	128	>256

Table A.12 Minimal inhibitory concentration (MIC) and minimal bactericidal concentration (MBC) values obtained for *Pseudomonas aeruginosa* sub-panel exposed to novel metal complexes and their controls using the broth micro-dilution assay. Values are presented as μg/mL.

6.1.5 FICs of metal-phen complexes with antibiotics against *Staphylococcus aureus*

Antibiotic	Metal complex	Isolate	FIC		
			Metal complex	Antibiotic	Index
Ciprofloxacin	Cu-tdda-phen	MRSA1	1.00	0.02	1.02
		MRSA2	1.00	0.02	1.02
	Mn-tdda-phen	MRSA1	1.00	0.00	1.00
		MRSA2	1.00	0.02	1.02
	Ag-tdda-phen	MRSA1	1.00	0.02	1.02
		MRSA2	1.00	0.02	1.02
Gentamicin	Cu-tdda-phen	MRSA1	0.03	0.00	0.04
		MRSA2	0.13	0.01	0.13
	Mn-tdda-phen	MRSA1	0.25	0.00	0.25
		MRSA2	0.06	0.00	0.07
	Ag-tdda-phen	MRSA1	0.03	0.00	0.04
		MRSA2	0.06	0.00	0.07

Table A.13 The fractional inhibitory concentration (FIC) and the FIC index (FIC_I) for metal-tdda-phen complexes against a selection of methicillin-resistant *Staphylococcus aureus* isolates

6.1.6 FICs of metal-phen complexes with antibiotics against *Enterococci* isolates

Antibiotic	Metal complex	Isolate	FIC		
			Metal complex	Antibiotic	Index
Vancomycin	Cu-tdda-phen	VRE1	1.00	0.06	1.06
		VRE6	1.00	0.06	1.06
	Mn-tdda-phen	VRE1	1.00	0.06	1.06
		VRE6	1.00	0.03	1.03
	Ag-tdda-phen	VRE1	1.00	0.02	1.02
		VRE6	1.00	0.02	1.02
Linezolid	Cu-tdda-phen	VRE1	1.00	0.06	1.06
		VRE6	1.00	0.06	1.06
	Mn-tdda-phen	VRE1	1.00	0.06	1.06
		VRE6	1.00	0.03	1.03
	Ag-tdda-phen	VRE1	1.00	0.02	1.02
		VRE6	1.00	0.02	1.02

Table A.14 The fractional inhibitory concentration (FIC) and the FIC index (FIC_I) for metal-tdda-phen complexes against a selection of vancomycin-resistant *Enterococci* isolates

6.1.7 FICs of metal-phen complexes with antibiotics against *Enterobacterales*

Antibiotic	Metal complex	Isolate	FIC		
			Metal complex	Antibiotic	Index
Ceftazidime	Cu-tdda-phen	ATCC 700603	1.00	0.13	1.13
		ESBL1	1.00	0.13	1.13
		MBL1	1.00	0.03	1.03
		ATCC BAA1705	1.00	0.13	1.13
		KPC1	1.00	0.50	1.50
	Mn-tdda-phen	ATCC 700603	1.00	0.25	1.25
		ESBL1	1.00	0.13	1.13
		MBL1	1.00	0.06	1.06
		ATCC BAA1705	1.00	0.13	1.13
		KPC1	1.00	0.13	1.13
	Ag-tdda-phen	ATCC 700603	0.50	0.06	0.56
		ESBL1	1.00	0.03	1.03
		MBL1	0.50	0.03	0.53
		ATCC BAA1705	0.50	0.06	0.56
		KPC1	1.00	0.13	1.13
Gentamicin	Cu-tdda-phen	ATCC 700603	0.50	1.00	1.50
		ESBL1	0.50	0.06	0.56
	Mn-tdda-phen	ATCC 700603	0.25	1.00	1.25
		ESBL1	0.50	0.06	0.56
	Ag-tdda-phen	ATCC 700603	0.50	1.00	1.50
		ESBL1	0.50	0.02	0.52
Meropenem	Cu-tdda-phen	MBL1	1.00	0.03	1.03
		ATCC BAA1705	1.00	0.50	1.50
		KPC1	1.00	0.50	1.50
	Mn-tdda-phen	MBL1	1.00	0.06	1.06
		ATCC BAA1705	1.00	0.50	1.50
		KPC1	1.00	0.13	1.13
	Ag-tdda-phen	MBL1	1.00	0.06	1.06
		ATCC BAA1705	1.00	0.50	1.50
		KPC1	1.00	0.13	1.13

Table A.15 The fractional inhibitory concentration (FIC) and the FIC index (FIC_I) for metal-tdda-phen complexes against a selection of resistant *Enterobacterales* isolates

6.1.8 FICs of metal-phen complexes with antibiotics against *Pseudomonas aeruginosa*

Antibiotic	Metal complex	Isolate	FIC		
			Metal complex	Antibiotic	Index
Meropenem	Cu-tdda-phen	PA2	1.00	0.13	1.13
		PA4	1.00	0.25	1.25
	Mn-tdda-phen	PA2	1.00	0.13	1.13
		PA4	1.00	0.25	1.25
	Ag-tdda-phen	PA2	1.00	0.06	1.06
		PA4	1.00	0.25	1.25
Gentamicin	Cu-tdda-phen	PA2	0.06	0.01	0.07
		PA4	0.06	0.01	0.07
	Mn-tdda-phen	PA2	0.06	0.01	0.07
		PA4	0.06	0.01	0.07
	Ag-tdda-phen	PA2	0.01	0.00	0.01
		PA4	0.00	0.00	0.00

Table A.16 The fractional inhibitory concentration (FIC) and the FIC index (FIC_I) for metal-tdda-phen complexes against a selection of resistant *Pseudomonas aeruginosa* isolate